U.S. Department
of Transportation
**National Highway
Traffic Safety
Administration**

DOT HS 808 280

September 1994

Final Report

Evaluation of the TAD-50M Thorax

Technical Report Documentation Page

1. Report No.	2. Government Accession No.	3. Recipient's Catalog No.
DOT HS 808 280		

4. Title and Subtitle	5. Report Date
Evaluation of the TAD-50M Thorax	September 1994
	6. Performing Organization Code: NRD-21
	8. Performing Organization Report No.: VRTC-82-0229
7. Author(s): Alena V. Hagedorn and Howard B. Pritz	
9. Performing Organization Name and Address: National Highway Traffic Safety Administration, Vehicle Research and Test Center, P.O. Box 37, East Liberty, Ohio 43319	10. Work Unit No. (TRAIS)
	11. Contract or Grant No.
	13. Type of Report and Period Covered: FINAL
12. Sponsoring Agency Name and Address: National Highway Traffic Safety Administration, 400 Seventh Street, S.W., Washington, D.C. 20590	14. Sponsoring Agency Code

15. Supplementary Notes

The authors wish to recognize Kathleen Klinich for her editorial assistance.

16. Abstract

This report describes the laboratory evaluation of an advanced ATD (Anthropomorphic Test Device) thorax system, denoted TAD-50M (Trauma Assessment Device, 50th percentile male), which has been integrated with Hybrid III lower and upper extremity, neck, and head components for testing. The evaluation program consisted of pendulum, quasi-static thorax compression, and sled tests in a variety of restraint environments, including air bag, two-point belt/knee bolster, and three-point belt systems. TAD-50M thorax instrumentation included four internal thoracic displacement measurement assemblies and two externally mounted chest bands. Baseline sled tests using the Hybrid III ATD were also conducted and are reported.

17. Key Words	18. Distribution Statement
ATD Thorax TAD-50M Prototype Dummy Three-point Belt System Crash Test Dummies	Document is available to the public from the National Technical Information Service, Springfield, VA 22161

19. Security Classif. (of this report)	20. Security Classif. (of this page)	21. No. of Pages	22. Price
Unclassified	Unclassified	123	

METRIC CONVERSION FACTORS

Approximate Conversions to Metric Measures

Symbol	When You Know	Multiply by	To Find	Symbol
		LENGTH		
in	inches	*2.5	centimeters	cm
ft	feet	30	centimeters	cm
yd	yards	0.9	meters	m
mi	miles	1.6	kilometers	km
		AREA		
in^2	square inches	6.5	square centimeters	cm^2
ft^2	square feet	0.09	square meters	m^2
yd^2	square yards	0.8	square meters	m^2
mi^2	square miles	2.6	square kilometers	km^2
	acres	0.4	hectares	ha
		MASS (weight)		
oz	ounces	28	grams	g
lb	pounds	0.45	kilograms	kg
	short tons (2000 lb)	0.9	tonnes	t
		VOLUME		
tsp	teaspoons	5	milliliters	ml
Tbsp	tablespoons	15	milliliters	ml
fl oz	fluid ounces	30	milliliters	ml
c	cups	0.24	liters	l
pt	pints	0.47	liters	l
qt	quarts	0.95	liters	l
gal	gallons	3.8	liters	l
ft^3	cubic feet	0.03	cubic meters	m^3
yd^3	cubic yards	0.76	cubic meters	m^3
		TEMPERATURE (exact)		
°F	Fahrenheit temperature	5/9 (after subtracting 32)	Celsius temperature	°C

*1 in = 2.54 (exactly). For other exact conversions and more detailed tables, see NBS Misc. Publ. 286, Units of Weights and Measures, Price $2.25, SD Catalog No. C13.10:286.

Approximate Conversions from Metric Measures

Symbol	When You Know	Multiply by	To Find	Symbol
		LENGTH		
mm	millimeters	0.04	inches	in
cm	centimeters	0.4	inches	in
m	meters	3.3	feet	ft
m	meters	1.1	yards	yd
km	kilometers	0.6	miles	mi
		AREA		
cm^2	square centimeters	0.16	square inches	in^2
m^2	square meters	1.2	square yards	yd^2
km^2	square kilometers	0.4	square miles	mi^2
ha	hectares (10,000 m^2)	2.6	acres	
		MASS (weight)		
g	grams	0.035	ounces	oz
kg	kilograms	2.2	pounds	lb
t	tonnes (1000 kg)	1.1	short tons	
		VOLUME		
ml	milliliters	0.03	fluid ounces	fl oz
l	liters	2.1	pints	pt
l	liters	1.06	quarts	qt
l	liters	0.26	gallons	gal
m^3	cubic meters	35	cubic feet	ft^3
m^3	cubic meters	1.3	cubic yards	yd^3
		TEMPERATURE (exact)		
°C	Celsius temperature	9/5 (then add 32)	Fahrenheit temperature	°F

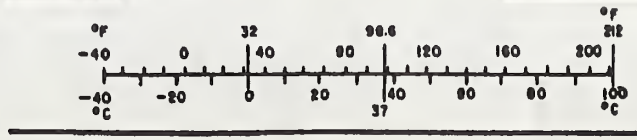

TABLE OF CONTENTS

Section **Page**

TECHNICAL REPORT DOCUMENTATION PAGE i

METRIC CONVERSION FACTORS ii

LIST OF FIGURES iv

LIST OF TABLES vi

TECHNICAL SUMMARY vii

INTRODUCTION 1

PROTOTYPE DESCRIPTION 1

SCOPE OF TEST PROGRAM 4

QUASI-STATIC TESTS 4

PENDULUM TESTS 5

SLED TESTS 7

RESULTS AND DISCUSSION 11

- 48 KPH TAD Tests 18
- 48 KPH TAD Oblique Tests 28
- 48 KPH HYBRID III Tests 42
- 56 KPH TAD Tests 47

MHD MEASUREMENTS 48

CONCLUSIONS 54

REFERENCES 55

APPENDIX A -- Sled Test Accelerations and Velocities . . . . . A

APPENDIX B -- TAD Chest Band Plots: Selected Examples . . . . . B

APPENDIX C -- TAD Sled Test MHD Plots (All Tests) C

LIST OF FIGURES

Page

Figure 1. TAD Thorax 2
Figure 2. TAD Thorax 2
Figure 3. TAD Spinal Axis Coordinate System 3
Figure 4. TAD Double Gimballed Stringpot Assembly 3
Figure 5. TAD Compression Axes for Pendulum Impact Tests 6
Figure 6. TAD Pre and Post Sled Test Pendulum Impacts - 4.3 m/s Mid Sternum 6
Figure 7. TAD Pre and Post Sled Test Pendulum Impacts - 6.7 m/s Mid Sternum 6
Figure 8. Lower Ribcage Axis of Compression for TAD Pendulum Impacts 7
Figure 9. TAD Pre and Post Sled Test Pendulum Impacts - 4.3 m/s Lower Ribcage 7
Figure 10. Sled Buck Rotation for Oblique Configuration Tests 8
Figure 11. Chest Band Used in Sled Test Series 9
Figure 12. Chest Band Configuration for TAD Sled Tests 10
Figure 13. Horizontal Cross Section of Hybrid III Thorax 10
Figure 14. TAD and Hybrid III Deflection Sensor Locations 11
Figure 15. Frangible Abdomen From Test 472, a Three-Point Belt/Air Bag Test 14
Figure 16. Frangible Abdomen From Test 476, a Three-Point Belt Test 14
Figure 17. Frangible Abdomen From Test 477, a Two-Point Belt/Knee Bolster Test 15
Figure 18. Frangible Abdomen From Test 478, a Lap Belt/Air Bag Test 15
Figure 19. TAD Chest Resultant Acceleration For Five Frontal Sled Tests at 48 Kph 17
Figure 20. Chest Resultant Accelerations For TAD And Hybrid III For Lap Belt/Air Bag Tests at 48 Kph 17
Figure 21. Chest Resultant Accelerations For TAD And Hybrid III For Three-Point Belt Tests at 48 Kph 17
Figure 22. Steering Wheel From Test 474, a TAD Air Bag Test at 48 Kph 19
Figure 23. TAD Test 474, Air Bag, 48 Kph Test - X Deflection 19
Figure 24. TAD Test 474, Air Bag, 48 Kph Test - Y Deflection 20
Figure 25. TAD Test 474, Air Bag, 48 Kph Test - Z Deflection 20
Figure 26. TAD Test 478 Air Bag/Lap Belt, 48 Kph - Sternal Sensors (Top View) 22
Figure 27. TAD Test 489 Air Bag/Lap Belt, 48 Kph - Lower Sensors (top View) 22
Figure 28. TAD Test 478 Lap Belt/Air Bag, 48 Kph - X Deflection 22
Figure 29. TAD Test 478 Lap Belt/Air Bag, 48 Kph - Y Deflection 23
Figure 30. TAD Test 478 Lap Belt/Air Bag, 48 Kph - Z Deflection 23
Figure 31. TAD Test 478, Air Bag/Lap Belt, 48 Kph - Right Side Sensors (Side View) 24
Figure 32. TAD Test 475 Three-Point Belt, 48 Kph - Sternal Sensors (Top View) 25
Figure 33. TAD Test 475 Three-Point Belt, 48 Kph - Lower Sensors (Top View) 25
Figure 34. TAD Test 475 Three-Point Belt, 48 Kph - X Deflection 25
Figure 35. TAD Test 475 Three-Point Belt, 48 Kph - Y Deflection 26
Figure 36. TAD Test 475 Three-Point Belt, 48 Kph - Z Deflection 26
Figure 37. TAD Test 475, Three-Point Belt, 48 Kph - Right Side Sensors (Side View) 27
Figure 38. TAD Test 475, Three-Point Belt, 48 Kph - Left Side Sensors (Side View) 27
Figure 39. TAD Test 472 Three-Point Belt/Air Bag, 48 Kph - Sternal Sensors (Top View) 29
Figure 40. TAD Test 472 Three-Point Belt/Air Bag, 48 Kph - Lower Sensors (Top View) 29

LIST OF FIGURES
(Continued)

Page

Figure 41. TAD Test 472, Three-Point Belt/Air Bag, 48 Kph - Right Side Sensors (Side View) 30
Figure 42. TAD Test 472, Three-Point Belt, 48 Kph - Right Side Sensors (Side View) 30
Figure 43. TAD Test 472 Three-Point Belt/Air Bag, 48 Kph - X Deflection 31
Figure 44. TAD Test 472 Three-Point Belt/Air Bag, 48 Kph - Y Deflection 31
Figure 45. TAD Test 472 Three-Point Belt/Air Bag, 48 Kph - Z Deflection 31
Figure 46. TAD Three-Point Belt Shoulder Belt Force With and Without Air Bag 32
Figure 47. TAD Test 477 Two-Point Belt/Knee Bolster, 48 Kph - Sternal Sensors (Top View) . . 32
Figure 48. TAD Test 477 Two-Point Belt/Knee Bolster, 48 Kph - Lower Sensors (Top View) . . 32
Figure 49. TAD Test 477 Two-Point Belt/Knee Bolster, 48 Kph - X Deflection 33
Figure 50. TAD Test 477 Two-Point Belt/Knee Bolster, 48 Kph - Y Deflection 33
Figure 51. TAD Test 477 Two-Point Belt/Knee Bolster, 48 Kph - Z Deflection 33
Figure 52. TAD Test 477, Passenger Two-Point Belt/Knee Bolster, 48 Kph - Right Side Sensors (Side View) 34
Figure 53. TAD Test 477, Passenger Two-Point Belt/Knee Bolster, 48 Kph - Left Side Sensors (Side View) 34
Figure 54. TAD Test 482, Three-Point Belt/Air Bag, Oblique, 48 Kph - Sternal Sensors (Top View) 35
Figure 55. TAD Test 482, Three-Point Belt/Air Bag, Oblique, 48 Kph - Lower Sensors (Top View) 35
Figure 56. TAD Test 482, Three-Point Belt/Air Bag, Oblique, 48 Kph - Right Side Sensors (Side View) 36
Figure 57. TAD Test 482, Three-Point Belt/Air Bag, Oblique, 48 Kph - Left Side Sensors (Side View) 36
Figure 58. TAD Test 482, Three-Point Belt/Air Bag, Oblique, 48 Kph - X Deflection 37
Figure 59. TAD Test 482, Three-Point Belt/Air Bag, Oblique, 48 Kph - Y Deflection 37
Figure 60. TAD Test 482, Three-Point Belt/Air Bag, Oblique, 48 Kph - Z Deflection 38
Figure 61. TAD Test 483, Three-Point Belt, Oblique, 48 Kph - Sternal Sensors (Top View) . . 38
Figure 62. TAD Test 483, Three-Point Belt, Oblique, 48 Kph - Lower Sensors (Top View) . . . 39
Figure 63. TAD Test 483, Three-Point Belt, Oblique, 48 Kph - Right Side Sensors (Side View) 39
Figure 64. TAD Test 483, Three-Point Belt, Oblique, 48 Kph - Left Side Sensors (Side View) . 40
Figure 65. TAD Test 483, Three-Point Belt, Oblique, 48 Kph - X Deflection 40
Figure 66. TAD Test 483, Three-Point Belt, Oblique, 48 Kph - Y Deflection 41
Figure 67. TAD Test 483, Three-Point Belt, Oblique, 48 Kph - Z Deflection 41
Figure 68. Hybrid III Test 485 Air Bag/Lap Belt, 48 Kph - Upper Sensors (Top View) 44
Figure 69. Hybrid III Test 485 Air Bag/Lap Belt, 48 Kph - Lower Sensors (Top View) 44
Figure 70. Hybrid III Test 486 Three-Point Belt, 48 Kph - Upper Sensors (Top View) 45
Figure 71. Hybrid III Test 486 Three-Point Belt, 48 Kph - Lower Sensors (Top View) 45
Figure 72. Head and T1 Excursions for TAD Test 475, a Three-point Belt, 48 Kph Test 46
Figure 73. Head and T1 Excursions for Hybrid III Test 486, a Three-point Belt, 48 Kph Test . . 46
Figure 74. TAD Three-Point Belt Sled Velocities for 48 and 56 kph Tests 47
Figure 75. TAD Three-Point Belt Shoulder Forces for 48 and 56 kph Tests 48

LIST OF FIGURES
(Continued)

Page

Figure 76. MHD "Stick Figure" Interpretation 49
Figure 77. Stick Figure for TAD Test 472, a Three-Point Belt/Air Bag, 48 Kph Test 51
Figure 78. Stick Figure for TAD Test 475, a Three-Point Belt, 48 Kph Test 51
Figure 79. Stick Figure for TAD Test 475, a Lap Belt/Air Bag, 48 Kph Test 51
Figure 80. Pelvis Angles as Derived From MHD Analysis 52
Figure 81. Lumbar Angles as Derived From MHD Analysis 52
Figure 82. Thoracic Angles as Derived From MHD Angles 53
Figure 83. Lumbar Bending as Derived From MHD Analysis 53
Figure 84. Thoracic Bending as Derived From MHD Analysis 54

LIST OF TABLES

Page

TABLE 1 -- TAD-50M and Hybrid III Sled Test Matrix 5

TABLE 2 -- TAD-50M and Hybrid III Sled Test Instrumentation 9

TABLE 3 -- TAD and Hybrid III Sled Test Maximum Measurements 13

Department of Transportation
National Highway Traffic Safety Administration

TECHNICAL SUMMARY

Report Title:	Date:
Evaluation of the TAD-50M Thorax	June 1994
Report Author(s):	
Alena V. Hagedorn and Howard B. Pritz	

This report describes the laboratory evaluation of an Advanced ATD thorax system, denoted TAD-50M (Trauma Assessment Device, 50th percentile male), which has been integrated with Hybrid III lower and upper extremity, neck and head components for testing. The evaluation included pendulum impact tests to the mid sternum and lower ribcage at 4.3 m/s and at the mid sternum at 6.7 m/s. Results of these tests reveal that the TAD-50M thorax meets the pendulum corridors at the sternum at 6.7 m/s and at the lower ribcage at 4.3 m/s. The thorax falls somewhat short of the 4.3 m/s corridor at the mid sternum. Further evaluation included quasi-static thoracic compression tests to verify the displacement of the TAD's ribs using the TAD's internal double gimballed stringpot assemblies. The focus of the evaluation was a series of twelve sled tests in a variety of restraint environments, including air bag, two-point belt/knee bolster, and three-point belt systems. Tests were conducted in both the frontal and oblique configurations at 48 kph and 56 kph. TAD-50M thorax instrumentation included four internal thoracic displacement measurement assemblies, angular motion sensors (magnetohydrodynamic sensors [MHD]) mounted on the spine, and two externally mounted chest bands. Results from the thoracic displacement assemblies indicate that the TAD thorax system appears to be capable of discriminating the degree of concentration of restraint loading, the degree of symmetry of restraint loading, and the intensity of local loading to the sternal region and lower ribcage. Results from the MHD's located on the spine provided information regarding the effect of various restraint systems on the articulated spine. Chest band results are also reported for the various restraints examined. Baseline sled tests using the Hybrid III ATD were also conducted and are reported for comparison with the TAD-50M results. The durability of the TAD-50M thorax was displayed by the minimal calibration shift for the prototype thorax after 37 transfer pendulum tests and 12 full-scale sled tests.

INTRODUCTION

This test program represents the first extensive performance evaluation of the TAD-50M design. The results of this evaluation were first reported by Hagedorn, et al. (1) and will be described in further detail in this report. The test protocol was designed to evaluate overall prototype performance in a wide variety of restraint environments, and to assess durability and practicality of the new design.

The broad goal of the TAD-50M thorax system development effort was the creation of an ATD thoracic structure which could offer more informed assessment of thoracic injury potential for vehicle occupants restrained by belts and air bags. A specific goal was the development of a thoracic test device which could reliably assess performance of combined belt/air bag restraint systems.

These goals were approached in the thorax design by implementing new ribcage, spinal, and abdominal anthropometry, by attempting emulation of human structural interaction between thoracic regions, by paying close attention to local dynamic impact response requirements, and by incorporating more comprehensive internal instrumentation.

PROTOTYPE DESCRIPTION

The TAD-50M thorax system (hereafter referred to as the "TAD") shown in Figures 1 and 2 is described in detail in reference (2); thus, only a design overview will be provided.

A primary goal of the development effort was to create an ATD thoracic structure which responded in a realistic way to both distributed and concentrated loads typical of air bag and belt restraint systems, respectively. Toward this end, the design includes the following general features:

- Realistic vehicle-seated posture and anthropometry, including representation of upper and lower ribcage geometry important to torso belt interaction.

- Biofidelic impact response at both the sternum and lower ribcage locations.

Figure 1. TAD Thorax

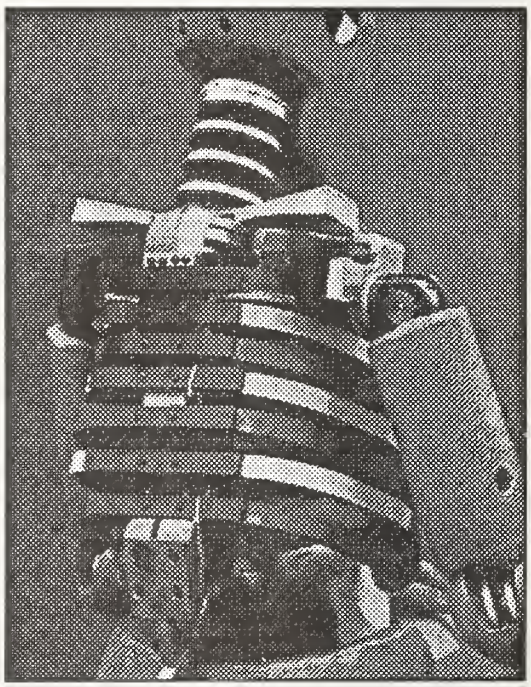

Figure 2. TAD Thorax

- Improved regional stiffness and inter-regional coupling behavior.
- Representation of the clavicle (to provide human-like upper belt load path).
- A new shoulder assembly with more realistic kinematic and dynamic behavior.
- Introduction of a non-rigid, articulated thoracic spine.

Instrumentation supplied with the prototype included:

- Three-dimensional thoracic displacement measurement assemblies at four sites on the anterior ribcage -- bilaterally at the sternum and at lower ribcage locations.
- Y-axis angular velocity/position sensors on the upper and lower thoracic spine segments, in addition to the pelvis, for computing planar spinal kinematics.
- A frangible abdominal insert, to detect belt or steering wheel rim intrusion.

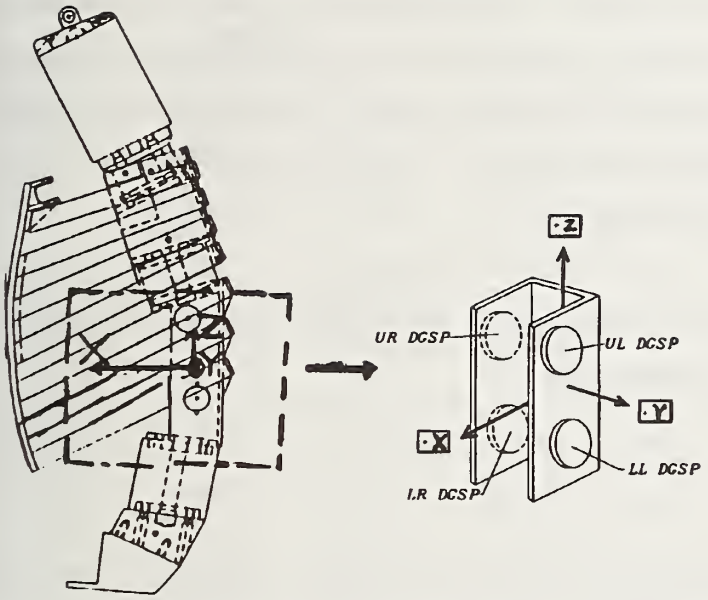

Figure 3. TAD Spinal Axis Coordinate System

The reference coordinate system for the TAD is the spinal axis system. A sketch of this coordinate system appears in Figure 3. This coordinate system originates at the lower thoracic spine segment. The positive x-axis, which lies perpendicular to the front surface of the lower spine, points forward; positive y is to the left, and positive z is upward. The coordinate system follows the right hand rule sign convention for rotations about x, y, and z.

The construction and installation of a typical displacement measurement assembly, called a double-gimballed stringpot (DGSP), is shown schematically in Figure 4. Four such assemblies are installed in the thorax. Two bilateral assemblies originate at the spine and extend to the sternum, attaching on each side at a distance of 3.8 cm from the mid-sagittal plane, at the human anatomical equivalent location of rib 4/5 interspace. The other two bilateral assemblies originate at the spine and extend to the lower ribcage, attaching at a distance of 8.3 cm on either side of the mid-sagittal plane, at the human anatomical equivalent location of rib 8. (These rib numbers refer to the standard numbering scheme for human ribs and do not correspond with the ATD rib numbers; the TAD prototype has only seven ribs. See Figures 1 and 2.)

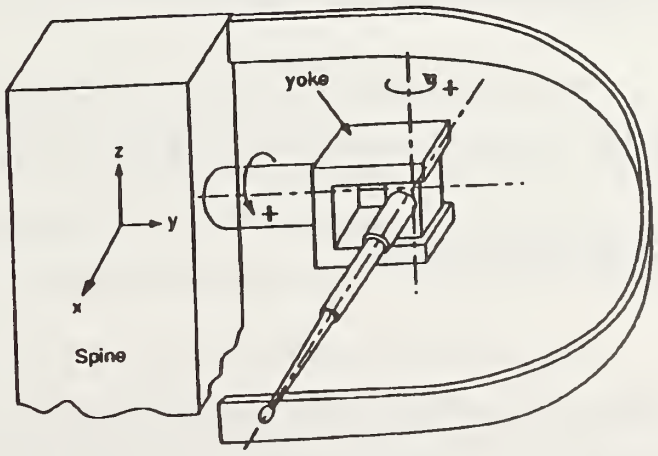

Figure 4. TAD Double Gimballed Stringpot Assembly

Each DGSP assembly consists of a telescoping joystick connected front to back, with joystick length continuously monitored by a string potentiometer. Each telescoping joystick is mounted to the TAD lower thoracic spine segment via a double gimbal, with potentiometer measurement of rotational displacement of both gimbals. Thus, each DGSP assembly captures the three-dimensional motion of its anterior attachment point relative to its lower thoracic spine attachment. Dedicated software interprets the stringpot and rotary potentiometer outputs as changes in x, y, and z displacement of the anterior attachment point relative to the spinal coordinate system.

A description of additional instrumentation installed on the prototype TAD and the Hybrid III during the testing and evaluation will be provided below.

SCOPE OF TEST PROGRAM

Tests conducted to evaluate the performance of the TAD thorax system consisted of 21 quasi-static thoracic compression tests, 37 transfer pendulum tests, and 12 full-scale sled tests. The full sled test series conducted, including baseline Hybrid III tests, is shown in Table 1. The emphasis of the sled test series was to determine the sensitivity of the TAD to various restraint environments as well as to assess the durability of the thorax system design.

The following sections will discuss TAD-50M quasi-static, pendulum, and sled test results from the TAD. Hybrid III sled test data is included for reference and general comparison.

QUASI-STATIC TESTS

This section briefly describes the quasi-static tests performed primarily to validate the thoracic deflection instrumentation and the accompanying software. These tests employed a tensile testing machine (Instron). The thorax was placed in a fixture that held the spine in place, allowing the machine's compression head to depress the ribs. Tests were performed with rectangular (5.1 cm x 10.2 cm) and circular (15.3 cm diameter) compression heads. Physical measurements were obtained locating the x, y, and z displacement of the thorax from initial position to a final position after approximately 51 mm of compression. These measurements were then compared to those calculated by the TAD chest deflection processing routine. Results of the quasi-static tests revealed the instrumentation accuracy to be within approximately 2 mm of actual values in the x, y, and z directions.

TABLE 1 – TAD-50M and Hybrid III Sled Test Matrix					
Dummy	Test Number	Position	Speed	Direction	Restraint
TAD-50M Torso	472-473	Driver	48 kph (30 mph)	Frontal	3-pt. belt/air bag
	474	Driver	48 kph (30 mph)	Frontal	Air bag
	475-476	Driver	48 kph (30 mph)	Frontal	3-pt. belt
	477	Passenger	48 kph (30 mph)	Frontal	2-pt. belt/knee bolster
	478	Driver	48 kph (30 mph)	Frontal	Lap belt/air bag
	479	Driver	56 kph (35 mph)	Frontal	3-pt. belt/air bag
	480	Driver	56 kph (35 mph)	Frontal	Lap belt/air bag
	481	Driver	56 kph (35 mph)	Frontal	3-pt. belt
	482	Driver	48 kph (30 mph)	Oblique	3-pt. belt/air bag
	483	Driver	48 kph (30 mph)	Oblique	3-pt. belt
Hybrid III Stringpot Thorax	485	Driver	48 kph (30 mph)	Frontal	Lap belt/air bag
	486	Driver	48 kph (30 mph)	Frontal	3-pt. belt
	487	Passenger	48 kph (30 mph)	Frontal	2-pt. belt/knee bolster

PENDULUM TESTS

The TAD-50M thorax was tested on a linear pendulum using a 23.2 kg, 152 mm diameter rigid impactor. An accelerometer mounted to the impactor ram permitted computation of a force-deflection curve for the thorax. Tests were conducted at both the mid sternum and lower ribcage at 4.3 m/s, and at the mid sternum at 6.7 m/s.

For mid sternum pendulum impacts, the TAD thorax was positioned so the x-axis (Figure 5) was horizontal. This placed the x-axis for sternal deflection computations coincident with the axis of pendulum-to-thorax impact (the axis of compression), and allowed direct comparison of TAD-50M thorax force-deflection data with the Kroell (3,4) pendulum force-deflection corridors.

Figures 6 and 7 show the force-deflection response of the upper thorax at 4.3 and 6.7 m/s respectively for tests run before and after the sled test series. The deflection results are taken from the upper right deflection assembly, and are calculated along the x-axis of compression,

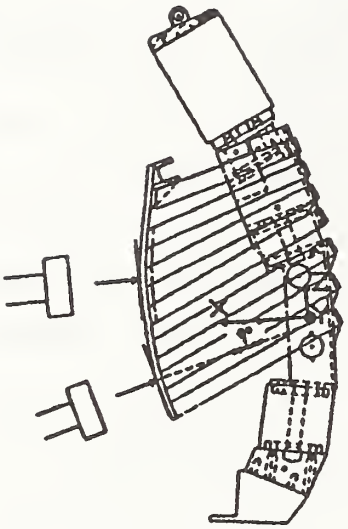

Figure 5. TAD Compression Axes for Pendulum Impact Tests

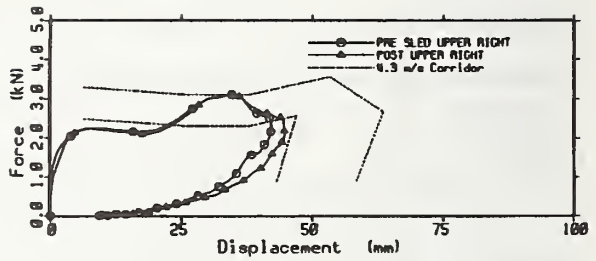

Figure 6. TAD Pre and Post Sled Test Pendulum Impacts - 4.3 m/s Mid Sternum

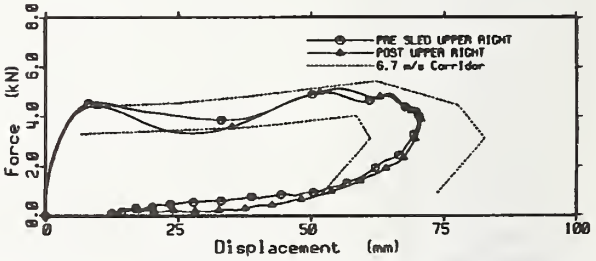

Figure 7. TAD Pre and Post Sled Test Pendulum Impacts - 6.7 m/s Mid Sternum

which is coincident with the x-axis described previously (Figure 5). The upper left displacement measurement assembly showed similar deflections. The dashed line corridors in these plots represent the target corridor derived by Neathery (5) from the Kroell data base for each velocity. These plots show that the thorax response falls just short of the desired corridor for the 4.3 m/s impacts. This response is similar to that seen in the Hybrid III (6). However, the response lies within the corridor for the 6.7 m/s impacts.

Thoracic durability is also implied by the congruence of post- and pre-test results. These plots show little shift for tests run before and after the series of 70 tests (37 pendulum impact, 21 quasi-static compression, and 12 sled tests) conducted using the torso. The thorax was designed to sustain 50 to 100 impact exposures (7); the thorax response exhibited after the test series indicates its ability to meet design goals. In addition, no apparent degradation of the rib damping material occurred after the 70 tests, further indicating durability.

Impacts were also performed at the lower left ribcage at 4.3 m/s. At the lower ribcage locations, the impact was directed along a line 9° downward from the x axis (Figure 5) and 12° outward from the x axis (Figure 8). Therefore, x deflections from pendulum impacts to the lower ribcage were calculated along this rotated x-axis of compression to allow comparison with the provisional corridor developed from cadaver tests as described by Schneider et al. (2). Figure 9 shows the force-deflection plots for these tests performed before and after the sled test series. The "point" on the force deflection curve, which occurred at approximately 60 mm deflection and over 3000 N of force, resulted from the impactor face contacting the support which holds the frangible abdomen. Upon contact with this support, force increased and deflection remained relatively constant. Except for this artifactual event, the curve fits well into the corridor. This contact did not occur in the pre-test, likely due to a slight difference in the initial positioning of the dummy.

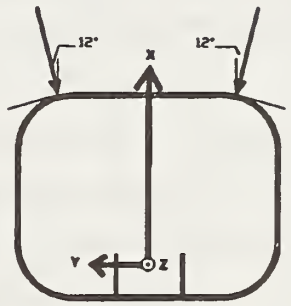

Figure 8. Lower Ribcage Axis of Compression for TAD Pendulum Impacts

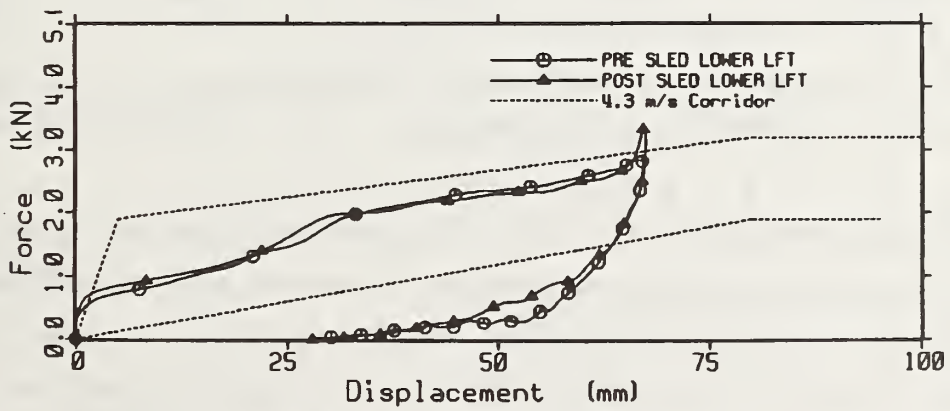

Figure 9. TAD Pre and Post Sled Test Pendulum Impacts - 4.3 m/s Lower Ribcage

SLED TESTS

Sled tests were performed with both the TAD-50M and Hybrid III. The test buck represented a "generic" vehicle capable of configuration in a variety of restraint conditions: driver three-point belt, driver air bag, driver combination three-point belt/air bag, and passenger two-point belt/knee bolster.

The intent was to evaluate the TAD dummy in a variety of repeatable vehicle configurations, rather than to specifically model one particular vehicle type. Complete measured data for all 15 sled tests is available from the NHTSA Biomechanics Database.

The 48 kph sled pulse was based on an average of twenty-five 48 kph barrier crash test pulses using mid-size cars. To account for the 6 kph rebound velocity, tests were actually performed at a velocity of 54 kph, with a peak acceleration of 23 G's. In a similar manner, the 56 kph sled test pulse was based on an average of twenty-five 56 kph barrier crash test pulses. Tests were therefore performed with a change of velocity of 63 kph (which includes rebound velocity) and 25 G's maximum acceleration. Samples of sled accelerations and velocities at each severity are contained in Appendix A. Table 1 lists the full array of tests conducted. Tests with an "oblique" direction were set up with the test buck rotated 15° clockwise when viewed from the top (Figure 10). This allowed more direct loading of the shoulder belt into the sternum (when compared to a counterclockwise rotation) when the dummy was seated in the driver position.

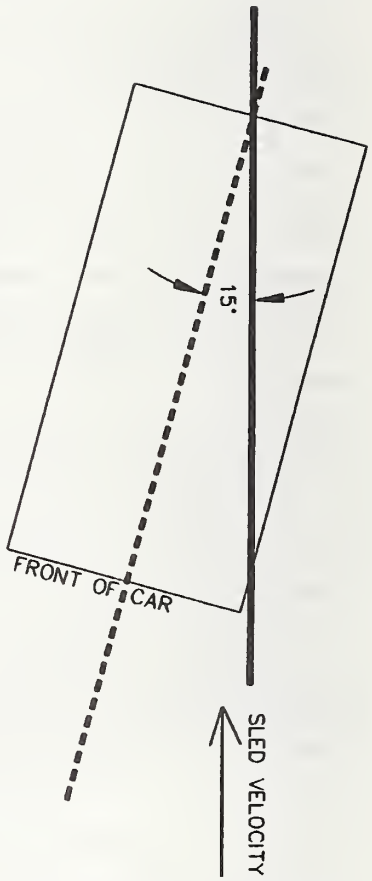

Figure 10. Sled Buck Rotation for Oblique Configuration Tests

A listing of the transducers used in both the TAD and Hybrid III sled tests appears in Table 2. In addition to the standard transducers, chest bands (8) were placed externally around the thorax of each dummy at the levels of the upper and lower ribcage. Each chest band consists of a series of strain gages mounted along a metal band and covered with a urethane coating (Figure 11). These strain gages detect the curvature of the band at their locations along the thorax circumference. Using these curvatures, along with the relative locations and spacings of the gages along the periphery, a cross-sectional shape of the thorax during compression can be constructed. In this test series, each chest band had 24 active gages. The highest density of gages (with regard to spacing) was concentrated in the center of the band where the gages were spaced approximately 2.5 cm apart (see Figure 11). When the bands were wrapped around the thorax, this region corresponded to the frontal portion of the dummy where the most deflection was likely to occur. Gages around the sides and back of the dummy were spaced approximately 5 cm from one another, since large deflections were less likely to occur in these areas

TABLE 2 -- TAD-50M and Hybrid III Sled Test Instrumentation			
Instrumentation	TAD-50M	Hybrid III	SAE Filter Class
4 DGSP Thoracic Deflection Assemblies	X		180
8 Thoracic Deflection Stringpots		X	180
2 24-Gage Chest Bands	X	X	180
Triaxial Head Accelerometers	X	X	1000
Triaxial Pelvis Accelerometers	X	X	1000
Triaxial Chest Accelerometers	X	X	180
3 MHD Spine Angular Velocity Sensors	X		1000
Femur Load Cells	X		600
Triaxial Upper Neck Load Cell	X		1000
Standard Chest Potentiometer		X	180
Safety Belt Load Cells	X	X	60

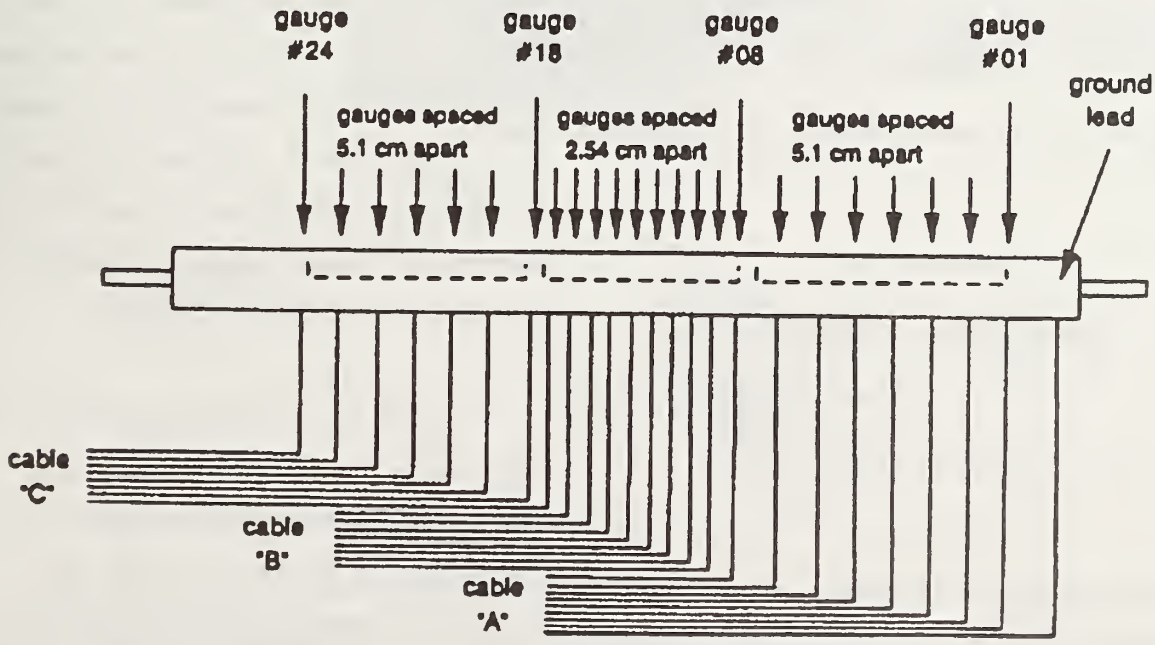

Figure 11. Chest Band Used in Sled Test Series

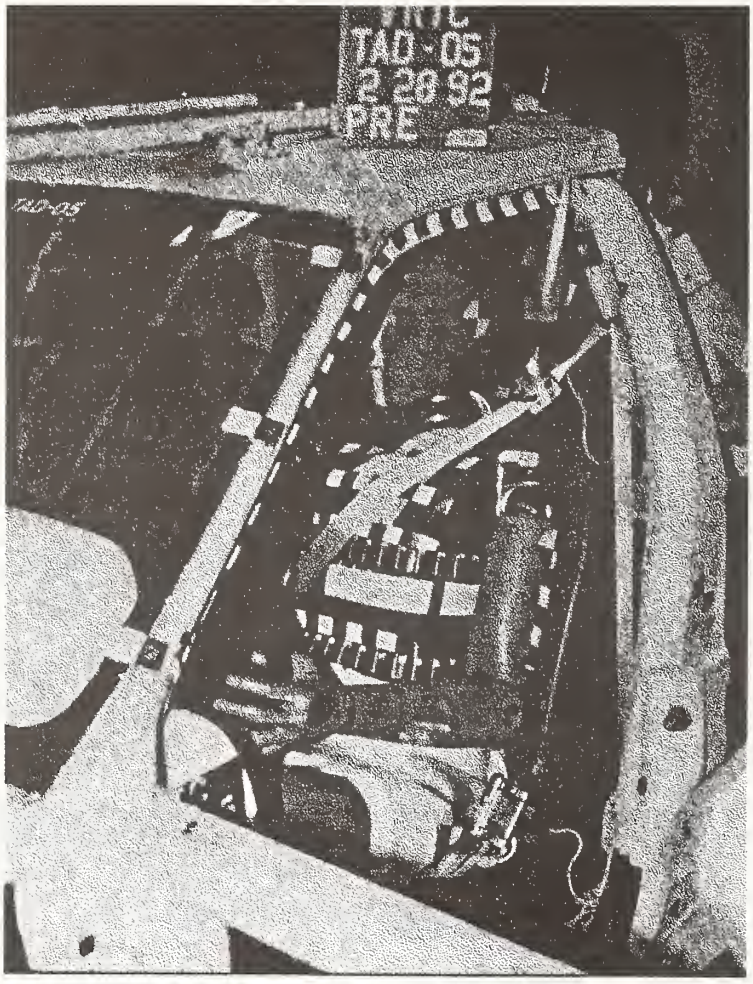

Figure 12. Chest Band Configuration for TAD Sled Tests

during frontal testing. The two chest bands were wrapped around the TAD thorax jacket and placed over the deflection assemblies on the front of the dummy. Figure 12 illustrates the positioning of the chest bands on the TAD.

Previous research (8,9) has shown that the best chest contours are measured when using a 40-gage chest band with gages evenly spaced every 2.54 cm. However, channel limitations prevented use of chest bands with this many gages. In addition, several tests lost gages or had wiring problems, which compromised the chest band data even further. Examples of irregular chest contours for one sled test caused by the low number of gages appear in Appendix B. Because the accuracy of the chest bands was affected by insufficient data channels and damaged gages, the remaining plots have not been included in this report.

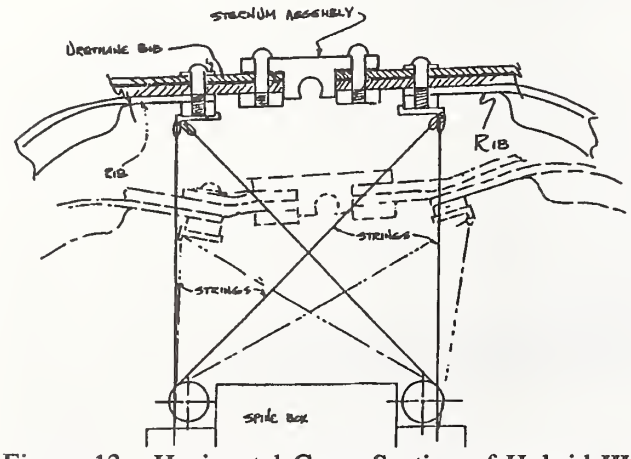

Figure 13. Horizontal Cross Section of Hybrid III Thorax

In addition to the standard Hybrid III chest potentiometer, a series of string pots was incorporated into the Hybrid III chest using a configuration described by Pritz (10). As illustrated in Figure 13, four of the string pots are connected directly between the sternum and spine box at the first and sixth ribs, and the other four are "crossover" string pots. A computer program calculates both the X- and Y- displacements of the rib attachment points.

RESULTS AND DISCUSSION

Directly comparing chest deflection patterns between TAD and Hybrid III proves difficult because of differing measurement locations (Figure 14), and TAD's measurement capabilities in the z direction. As Figure 14 displays, locations of measured deflections between the TAD and Hybrid III are not the same. Any direct comparison, say between the upper left measurement locations, would show differences partly caused by different measurement locations and partly caused by different dummy characteristics. Isolating differences from each cause would be impossible. Therefore, this report will focus on the performance of the TAD thorax in various restraint configurations, in particular the air bag/lap belt, three-point belt, three-point belt/air bag, and two-point belt/knee bolster configurations, rather than attempt detailed comparison to the Hybrid III. However, the tests did reveal general performance characteristics of each dummy which will be discussed.

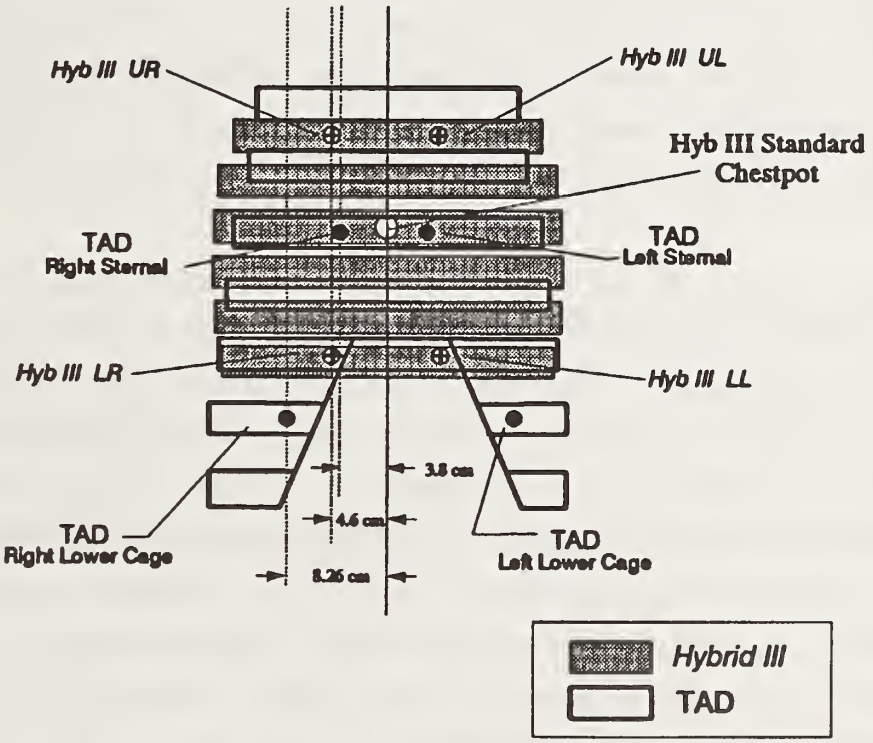

Figure 14. TAD and Hybrid III Deflection Sensor Locations

Although Figure 14 appears to illustrate that the TAD sternal sensors might be comparable to the Hybrid III chestpot, differences exist between the two dummies at these points. Since the TAD sternum is made of a urethane material similar to that of the Hybrid III chest bib, it is flexible between the right and left sternal sensors. Therefore, the measurements from the left and right sensors are not necessarily indicative of the deflection between them. However, an average of the left and right sensors would serve as a rough estimate of the mid-sternum deflection. In comparison, the Hybrid III sternum consists of a

rigid plate whose deflection is measured at the center of the plate. Chest deflection for the Hybrid III in the driver lap belt/air bag configuration (test 485) was 40 mm. An average of the sternal sensors for the TAD in the same configuration (test 478) was also 40 mm. This average was obtained using the maximum left and right sternal deflections for the TAD (Table 3). These peaks may have occurred at different times, but their average represents the worst case deflection. Similarly, in the driver three-point belt configuration, Hybrid III chest deflection was 43 mm (test 475), while TAD averaged 32 mm (test 486).

The frangible abdominal inserts used in the TAD sled tests are designed to detect seat belt intrusion into the abdomen. This behavior is characterized by "crushing" of the points of the abdominal insert. In many cases, the abdominal insert crush patterns proved difficult to interpret because of additional dents and crushing caused by lower ribcage intrusion. In particular, the ribcage seems responsible for severing off the points of the insert. It is likely that ribcage interference had some influence on the Z-deflections measured by the TAD thorax, especially at the lower ribcage. Although the upper and lower ribs are designed to move somewhat independently, the contact of the lower ribs with the frangible abdomen could also affect the Z-movement of the upper ribs to a lesser extent.

Photos of the frangible abdomen from each type of test configuration appear in Figures 15 - 18. In the three-point belt/air bag test shown in Figure 15, the points are severed off and whole, indicating ribcage intrusion into the abdomen. Figure 16, which depicts the insert from a three-point belt test, suggests seat belt intrusion since the crush occurs on the underside of the points of the abdomen. The small dents on the top result from minor ribcage interference. In Figure 17, when viewing the condition of the abdomen in the two-point belt passenger test, the underside crush patterns do not appear since no lap belt was available to intrude into the abdomen. For this case, the left abdomen point broke off, indicating contact by the left ribcage. The last photo in Figure 18 shows the insert for a lap belt/air bag test. This particular test shows how interpreting results of multiple loading patterns can be difficult. Most likely, both belt and ribcage intrusion occurred.

Peak results for the TAD and Hybrid III sled tests appear in Table 3. The data from test 487, the Hybrid III with 2-point belt/knee bolster, are not included because the belt failed during the test. In test 480, the head data are omitted because the steering column attachment failed, causing irregularities in the data. Deflections quoted in the tables are peak values, and generally do not coincide in time. All TAD sled test sternal and lower ribcage deflections are calculated relative to the x, y, and z axes (the spinal axis system) shown in Figure 3 with the sign conventions previously given.

TABLE 3. TAD and Hybrid III Sled Test Maximum Measurements

	TAD 48 kph Tests									TAD 56 kph Tests				Hybrid III 48 kph Tests	
Test Number	472	473	474	475	476	477	478	482	483	479	480*	481		485	486
Configuration	Driver 3 Point Belt With Air Bag	Driver 3 Point Belt With Air Bag	Driver Air Bag	Driver 3 Point Belt	Driver 3 Point Belt	Passenger 2 Point Belt/Knee Bolster	Driver Lap Belt /Air Bag	Driver 3 Point/ Air Bag Oblique	Driver 3 Point Belt Oblique	Driver 3 Point Belt With Air Bag	Driver Lap Belt /Air Bag	Driver 3 Point Belt		Driver Lap Belt /Air Bag	Driver 3 Point Belt
HIC	639	646	373	1413**	1273**	994	400	2223	1237**	762	----	1745**		392	1169**
Max Head Result (G)	66	64	56	166	157	92	62	425	173	76	----	205		59	209
Max Chest Result (G)	51	53	71	56	51	52	48	53	51	61	62	59		46	50
Lap Belt Inboard Force (N)	----	----	----	----	----	----	7212	----	----	----	8022	----		8926	----
Lap Belt Outboard Force (N)	6086	7251	----	8691	7972	----	7751	8025	8515	8441	8440	8546		9451	9346
Shoulder Belt Inboard Force (N)	----	----	----	----	----	11040	----	----	----	----	----	----		----	----
Shoulder Belt Outboard Force (N)	8002	8232	----	8902	8659	7234	----	7875	8853	8598	----	9428		----	8803
Chest Pot (mm)	----	----	----	----	----	----	----	----	----	----	----	----		40	43
Maximum Deflections															
Right Sternum X	-49	-51	-56	-48	-48	-24	-45	-44	-38	-49	-31	-51	UR Defl X (mm)	-47	-50
Left Sternum X	-15	-18	-58	-15	-14	-69	-34	-14	-8	-14	-25	-15	UL Defl X (mm)	-39	-30
Right Lower Cage X	-33	-39	16	-37	-38	13	9	-31	-19	-35	13	-37	LR Defl X (mm)	-29	-45
Left Lower Cage X	10	12	-6	13	14	-57	11	12	13	14	12	13	LL Defl X (mm)	-19	-13
Right Sternum Y	23	28	-4	32	32	-25	7	25	32	33	-5	35	UR Defl Y (mm)	-3	-8
Left Sternum Y	17	21	6	25	20	-33	9	17	11	22	4	21	UL Defl Y (mm)	9	11
Right Lower Cage Y	34	35	11	37	36	-14	7	37	15	39	5	41	LR Defl Y (mm)	-3	6
Left Lower Cage Y	11	12	-8	11	10	-67	-9	11	19	14	-9	12	LL Defl Y (mm)	9	-4
Right Sternum Z	-6	-17	-13	-18	-15	-30	30	-21	-13	-17	22	-20	UR Defl Z (mm)	----	----
Left Sternum Z	-13	-10	-13	10	13	-31	28	-13	13	13	23	13	UL Defl Z (mm)	----	----
Right Lower Cage Z	12	10	13	17	20	-19	29	11	17	17	36	16	LR Defl Z (mm)	----	----
Left Lower Cage Z	8	12	-9	12	17	-14	24	16	22	20	37	14	LL Defl Z (mm)	----	----

*Steering Column attachment failure
**Indicates head contact with steering wheel

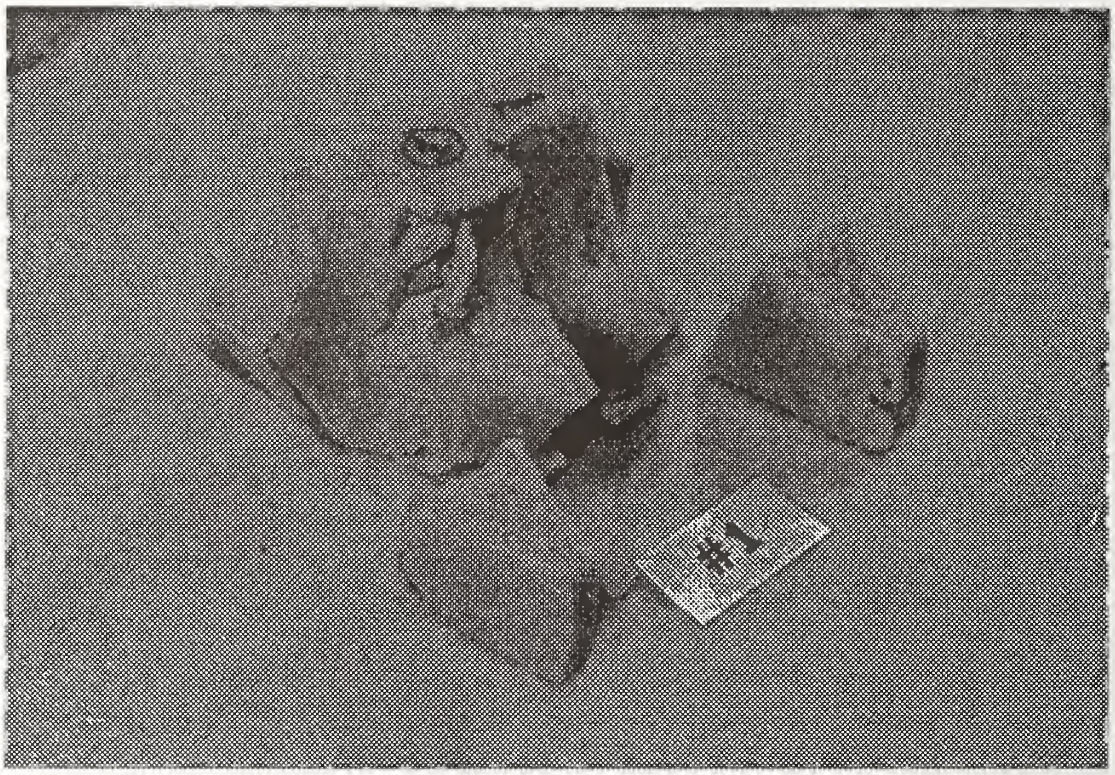

Figure 15. Frangible Abdomen From Test 472, a Three-Point Belt/Air Bag Test

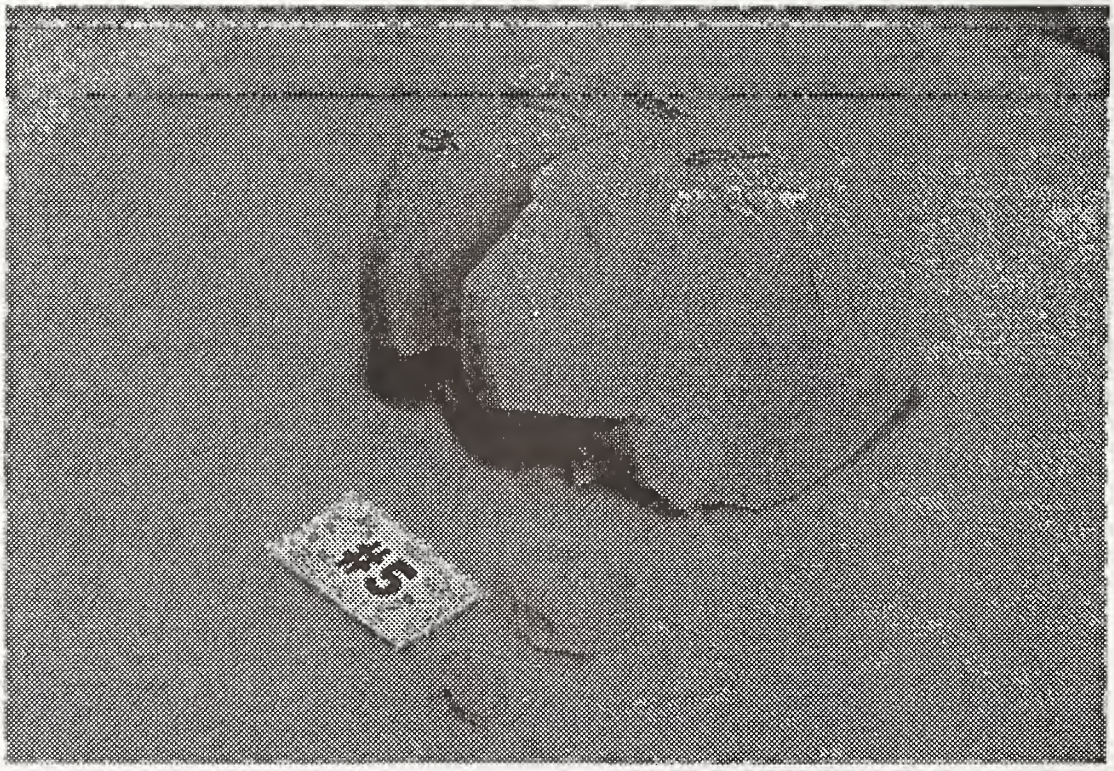

Figure 16. Frangible Abdomen From Test 476, a Three-Point Belt Test

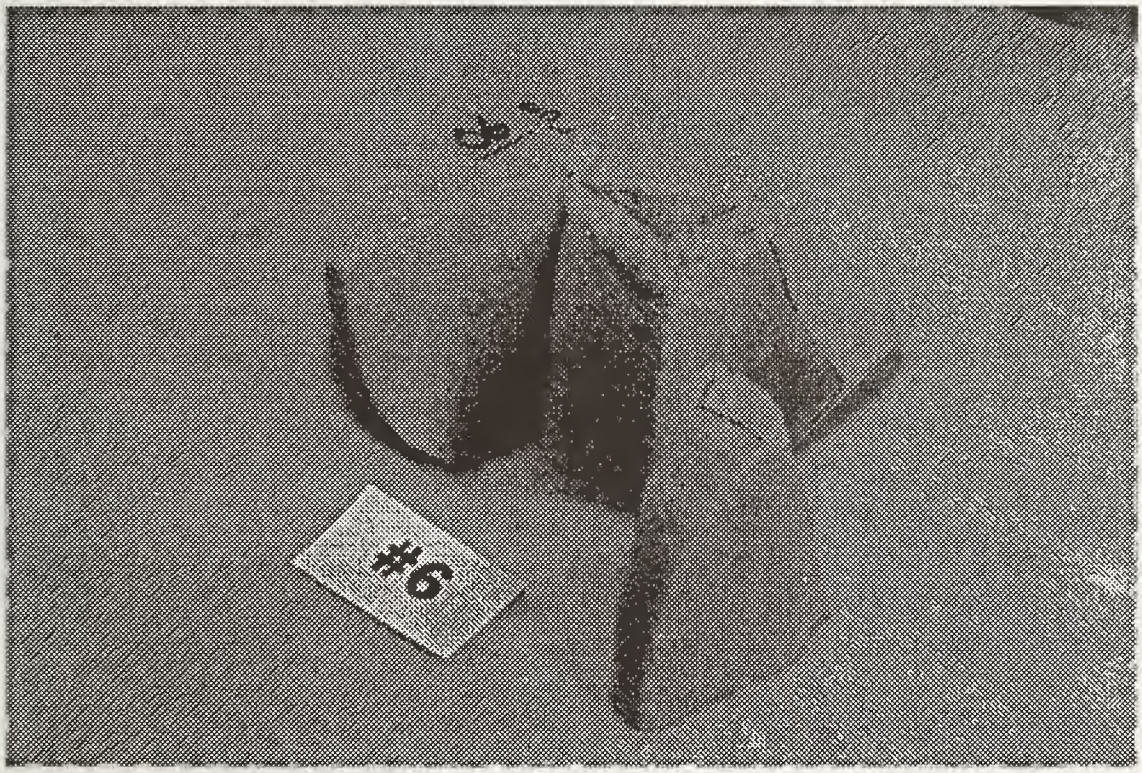

Figure 17. Frangible Abdomen From Test 477, a Two-Point Belt/Knee Bolster Test

Figure 18. Frangible Abdomen From Test 478, a Lap Belt/Air Bag Test

Table 3 reveals that both the TAD and Hybrid III HIC's exceed 1000 in all three-point belt tests (without air bags) conducted in this study. The largest HIC (2223) occurred in the three-point belt/air bag test at 48-kph in the oblique configuration. HIC's were below 1000 in all other test conditions. Test 477, the passenger side TAD two-point belt/knee bolster test, was 994, only slightly below the 1000 level. When looking at belt load trends shown in Table 3, the belt loads with the TAD generally are less than those with the Hybrid III, particularly for the lap belt. This may occur because of the TAD's more compliant abdominal structure.

The highest peak resultant chest G's occurred in TAD test 474, an air bag test at 48-kph without belt restraint (Figure 19 and Table 3). Figure 19 reveals that chest acceleration signals from the TAD thorax design did not exhibit excessive noise. Peak chest G's were similar between the TAD and Hybrid III in the 48-kph and lap belt/air bag tests and three-point belt (Figures 20 and 21), but TAD was slightly higher by 2 to 6 G's.

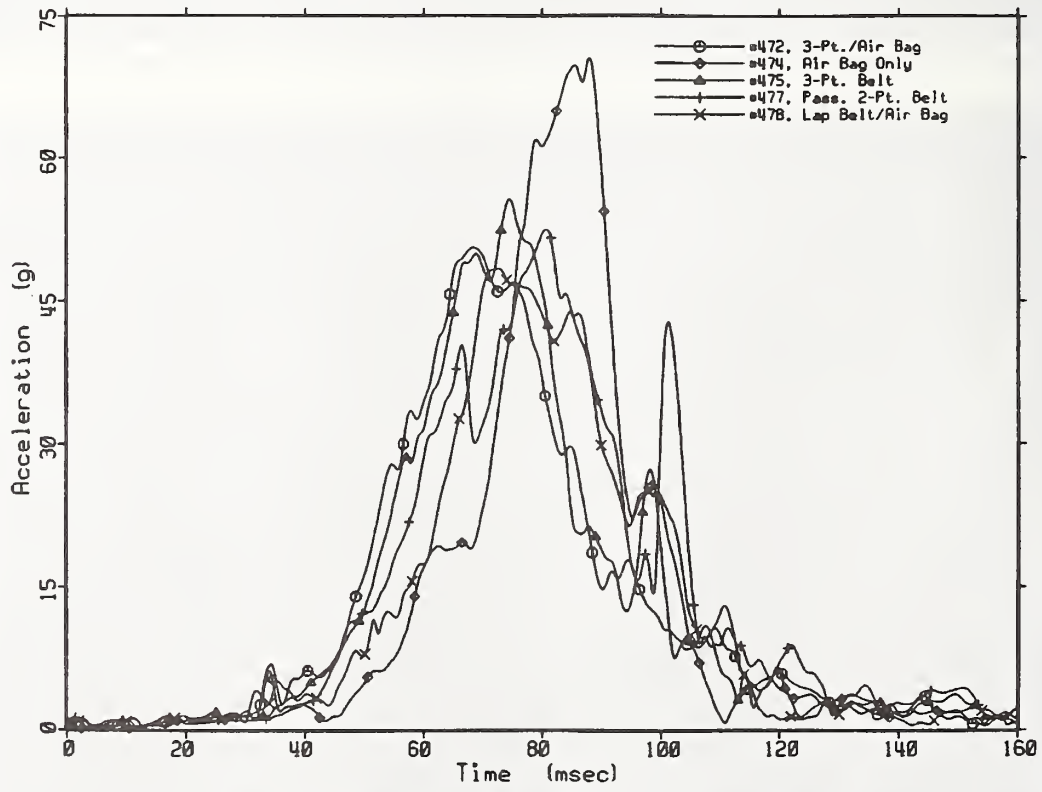

Figure 19. TAD Chest Resultant Acceleration For Five Frontal Sled Tests at 48 Kph

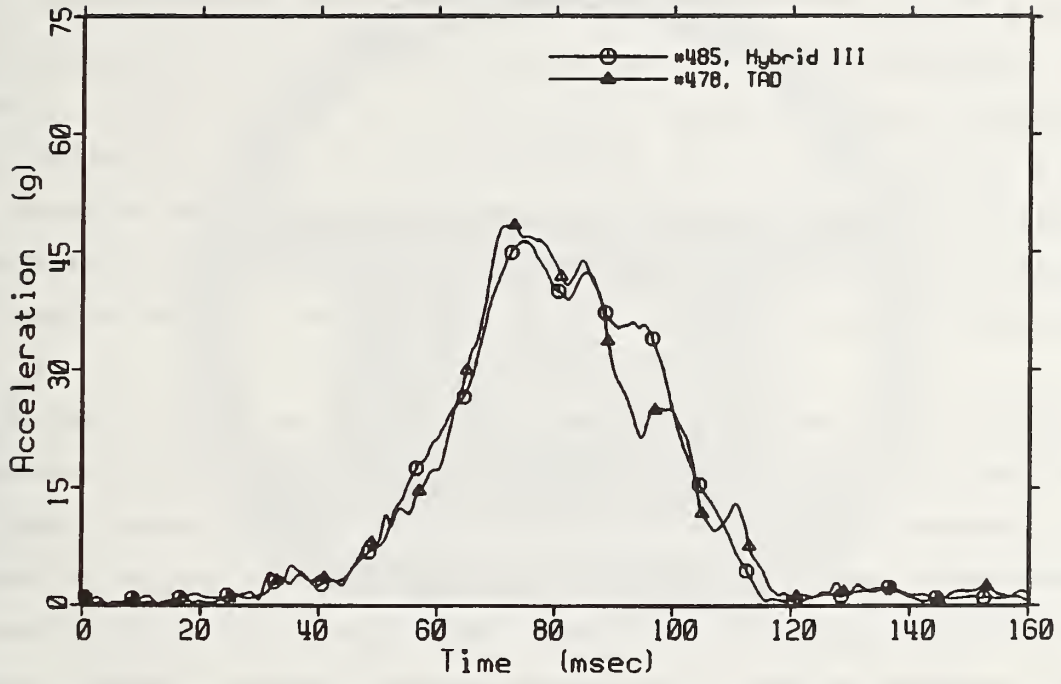

Figure 20. Chest Resultant Accelerations For TAD And Hybrid III For Lap Belt/Air Bag Tests at 48 Kph

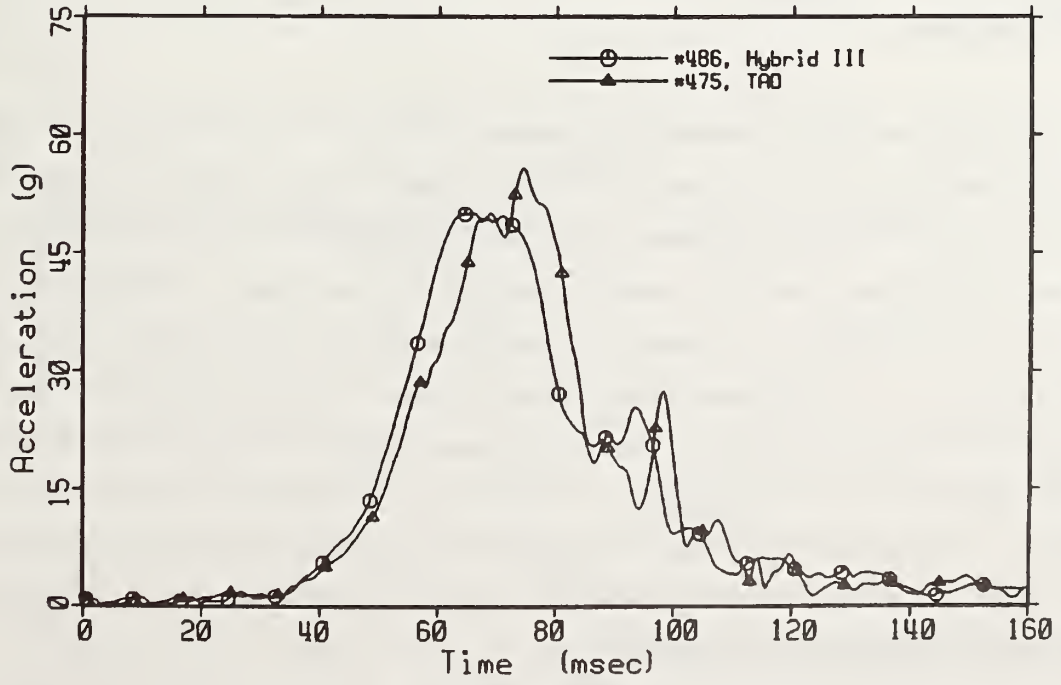

Figure 21. Chest Resultant Accelerations For TAD And Hybrid III For Three-Point Belt Tests at 48 Kph

The peak deflections at each measurement point also appear in Table 3. However, a method for depicting the deflection patterns has been developed, and will be described before beginning detailed analysis of each test. To visualize the movement of the ribcage in the x,y plane, plots were created using the x and y deflection time histories from the right and left sternal and right and left lower ribcage sensors. Examples appear later in this report in Figures 26 and 27. These plots represent the motion of the sternal or lower ribcage sensors, as viewed from the top. The horizontal axis represents the baseline at which the sensors are initially positioned. Movement of the sensor above this axis represents an expansion of the ribcage, while deflection below this line corresponds to chest compression. Dotted lines connecting the left and right sensor locations at various time intervals are provided to illustrate time sequence, but do not represent the shape of the sternum between sensor attachment locations.

Similar plots were obtained in the x,z plane for tests of interest; an example appears in Figure 31. For these plots, the vertical axis indicates the initial x position of each of the upper and lower right sensors. Movement to the right of this line indicates (positive x) ribcage expansion, while leftward movement signifies (negative) x compression. The horizontal lines at both the upper and lower sensor locations indicates the initial z position of the sensor. Sensor movement above each line indicates upward (positive) z movement, and below the line, negative, downward movement. These plots illustrate the ability of the upper and lower ribcage to move separately in the x and z directions, rather than to be constrained to move as a unit. Plots for both the left and right side sensors are given.

48 KPH TAD Tests

The 48 kph tests will be discussed first, beginning with test 474, the TAD air bag test without seat belt. The air bag fire time was at 18 msec for all tests utilizing air bags. Table 3 reveals that the largest x-deflections, up to 58 mm at the sternum, occur in this test configuration. Film analysis shows that the lower portion of the wheel contacts the dummy's chest near the sternal sensors. The large steering wheel deformation shown in Figure 22 corresponds with the high x-deflections at the sternum. Deflection time histories for the x, y, and z movement of each deflection sensor are given in Figures 23 -25 and follow the sign conventions noted in Figure 3. The sternum sensors experience large inward deflections, while the lower ribcage sensors move outward on the right side and slightly inward and outward on the left (Figure 23). The y-deflection plot (Figure 24) indicates slight movement (less than 10 mm) of the ribs laterally. Figure 25 reveals that initially the whole ribcage moves slightly downward. At approximately 70 msec, the lower ribcage is pushed upward.

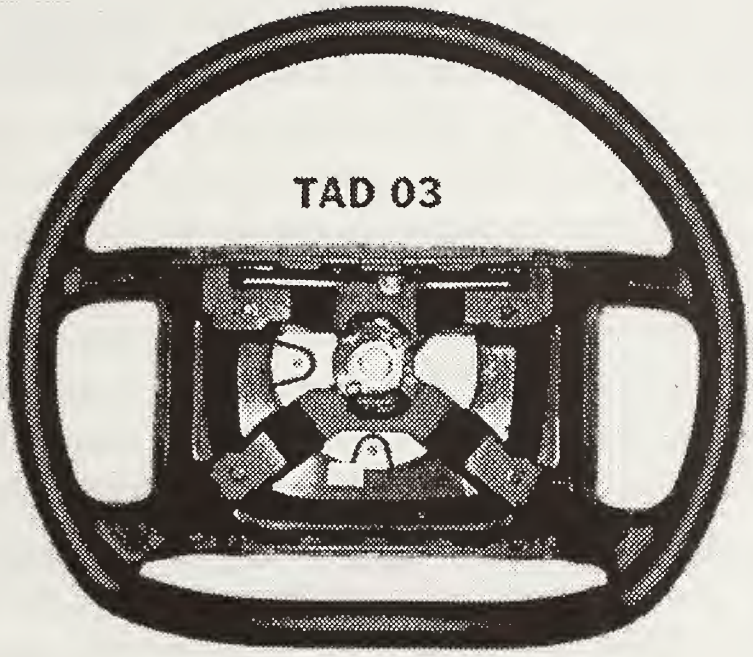

Figure 22. Steering Wheel From Test 474, a TAD Air Bag Test at 48 Kph

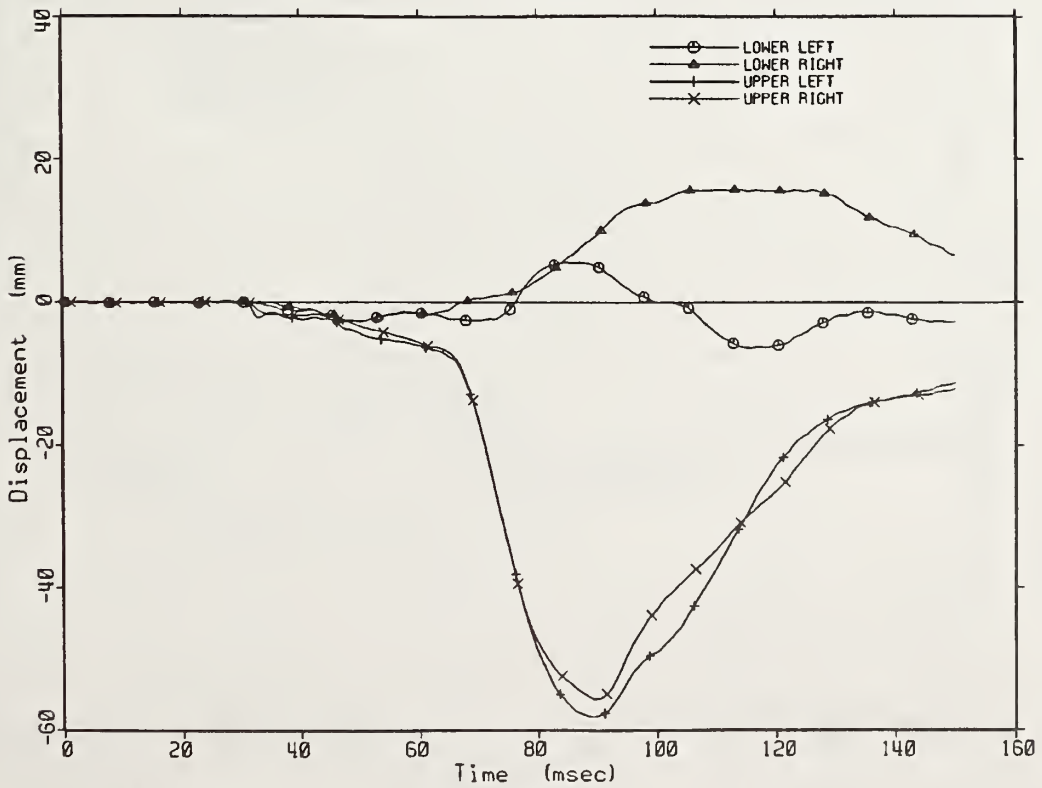

Figure 23. TAD Test 474, Air Bag, 48 Kph Test - X Deflection

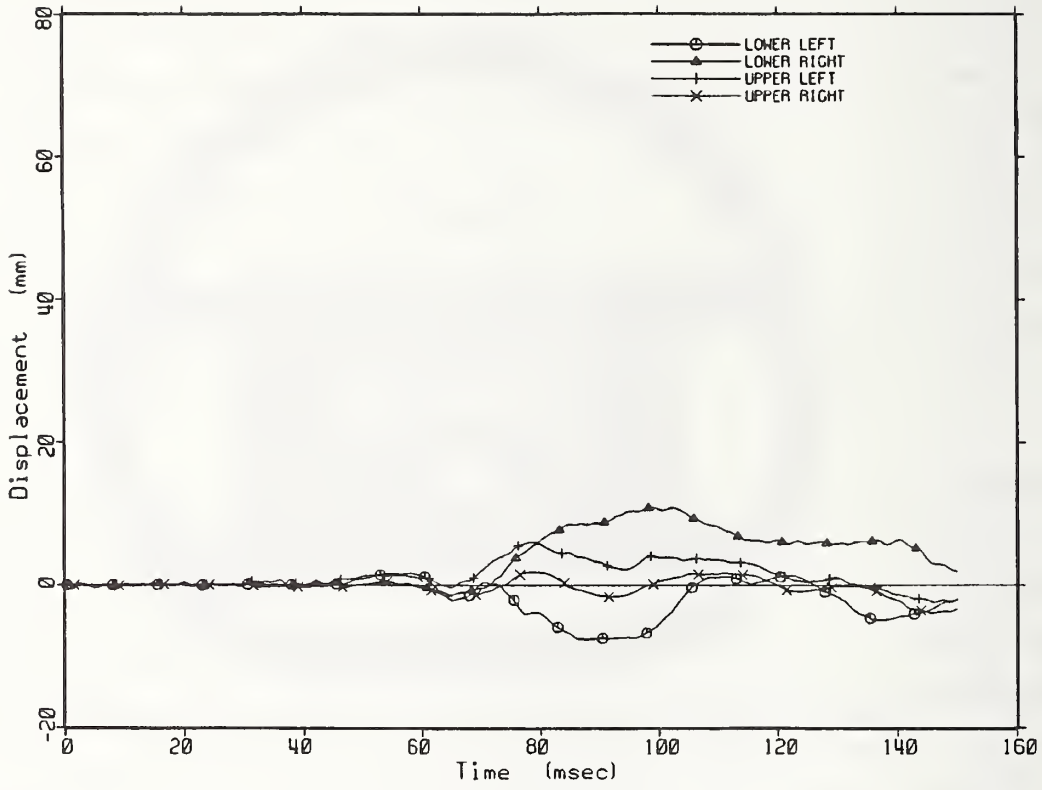

Figure 24. TAD Test 474, Air Bag, 48 Kph Test - Y Deflection

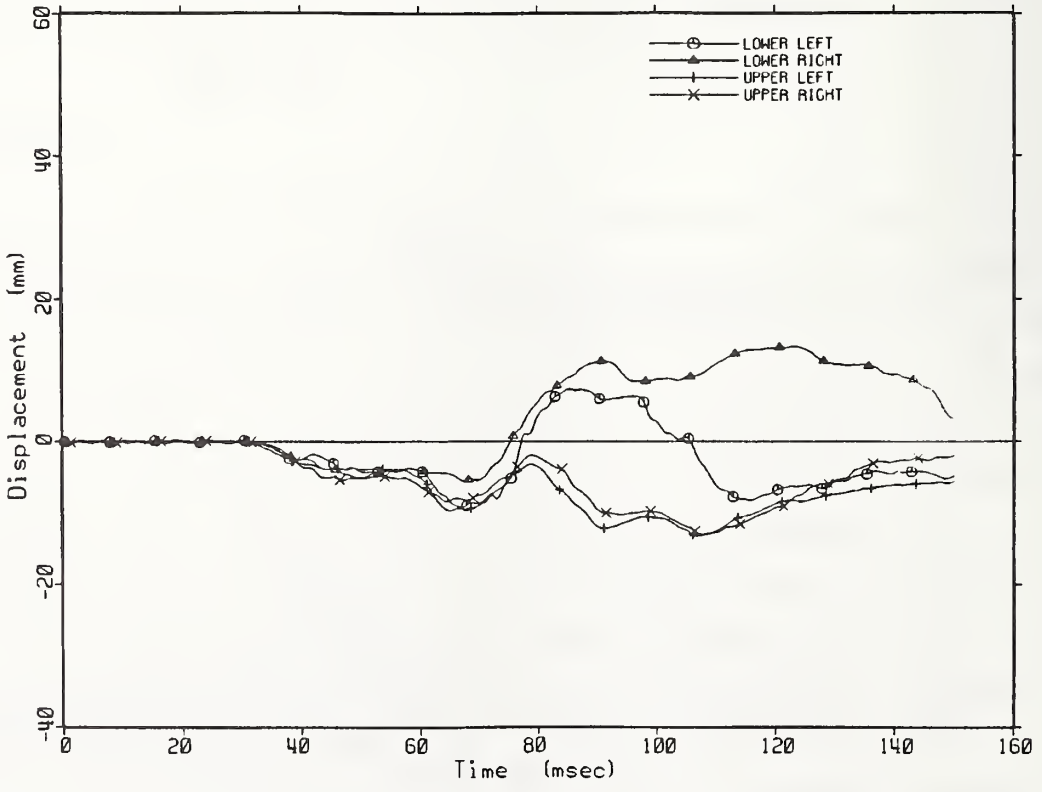

Figure 25. TAD Test 474, Air Bag, 48 Kph Test - Z Deflection

In test 478, the TAD lap belt/ air bag test, the x,y plane plots for the sternal deflections (Figure 26) reveal an inward uniform movement of the thorax. The lower ribcage moves slightly outward (Figure 27). Figures 28 - 30 show the deflection time histories for test 478. The x deflection plots (Figure 28) also demonstrate that the sternum is being pushed inward while the lower ribcage moves outward. The flat portion of the traces for the lower ribcage sensors, beginning at roughly 60 msec, may indicate that the lower sensors have reached their expansion stroke limit, which is approximately 10 to 15 mm. The x,z plane plot for the right side of the TAD (Figure 31) also suggests the possibility of reaching the expansion limit at the lower ribcage. As pictured in Figure 29, y-deflections of the entire anterior ribcage are small (less than 9 mm). The z plots (Figure 30) and the x-z plane plot (Figure 31) show that the anterior ribcage exhibits rather uniform upward z-deflection of 24-30 mm until approximately 70 msec, then the upper ribcage moves downward while the lower ribcage remains pushed up. This may result from the TAD's mid-thoracic articulation segment coupled with the contact of the lower ribcage with the frangible abdomen; the upper and lower ribs can move separately rather than being constrained to act as a unit.

Tests 475 and 476 represent baseline three-point belt exposures. Figures 32 and 33 show the x,y plane plots for the sternum and lower ribcage for test 475. Results for test 476 were similar. Both the upper and lower ribs compress more on the right side than on the left. This result corresponds with the shoulder belt path crossing close to the right sternal deflection assembly attachment. This result also illustrates that the right and left sternum are largely decoupled in the x direction. Figures 34 - 36 show the deflection time histories for the three-point belt configuration. Confirming the x,y plane plots, the x deflections in Figure 34 show the majority of compression occurring on the right side. At the lower ribcage locations, the right side x-deflection (under the belt path) averaged 38 mm compression, while the left side exhibited x-deflection of 14 mm expansion. The y deflection plots suggest that the seat belt pulled the thorax to the left. This behavior is most noticeable on the thorax's lower right side. Y-deflection at the right averaged 37 mm, much greater than lower left y-deflection of 11 mm. Thus, the right lower ribcage appears to move independently of the left lower ribcage. The z deflection plots (Figure 36) reveal that all but the lower left deflection sensors initially move downward. This is visualized in the x-z plane plots for test 475 (Figures 37 and 38). At approximately 80 msec, the lower left sensor begins to move downward, while the lower right assembly follows an upward path, suggesting rotation about the x axis.

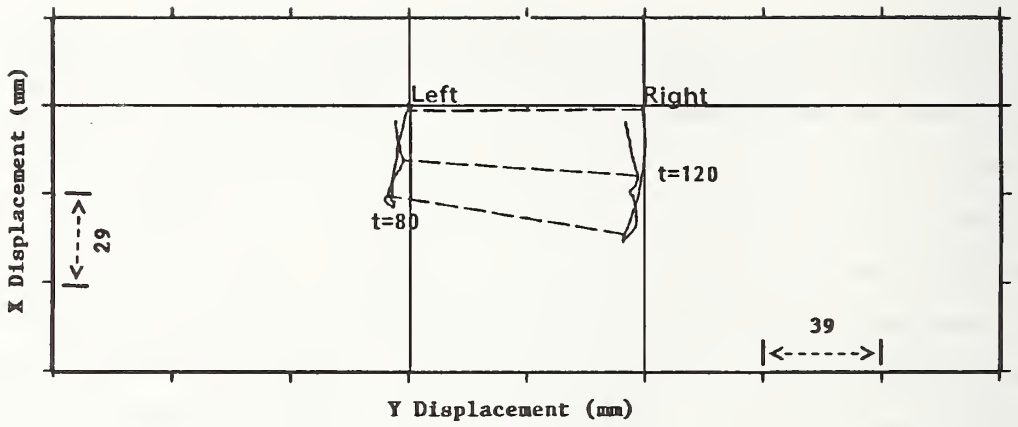

Figure 26. TAD Test 478 Air Bag/Lap Belt, 48 Kph - Sternal Sensors (Top View)

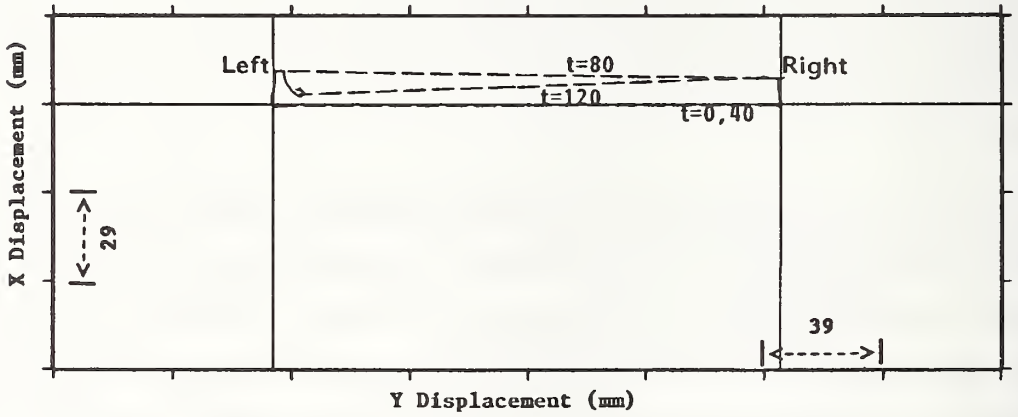

Figure 27. TAD Test 478 Air Bag/Lap Belt, 48 Kph - Lower Sensors (top View)

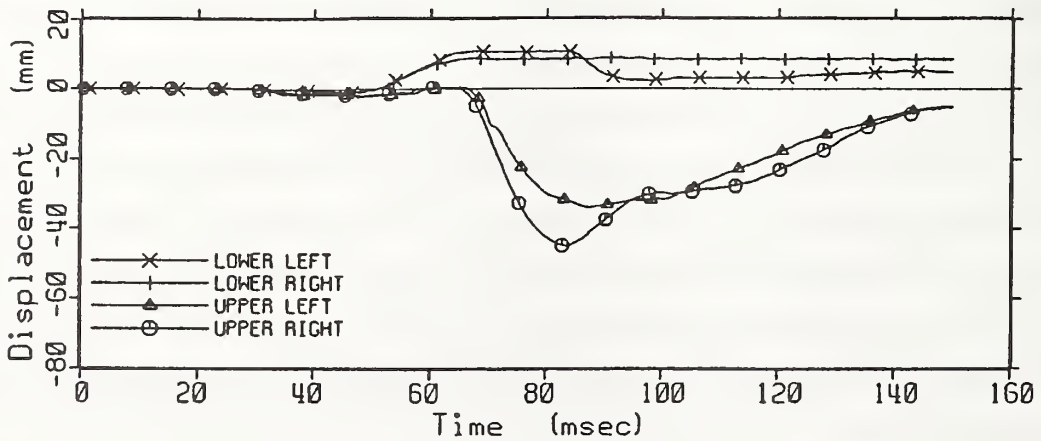

Figure 28. TAD Test 478 Lap Belt/Air Bag, 48 Kph - X Deflection

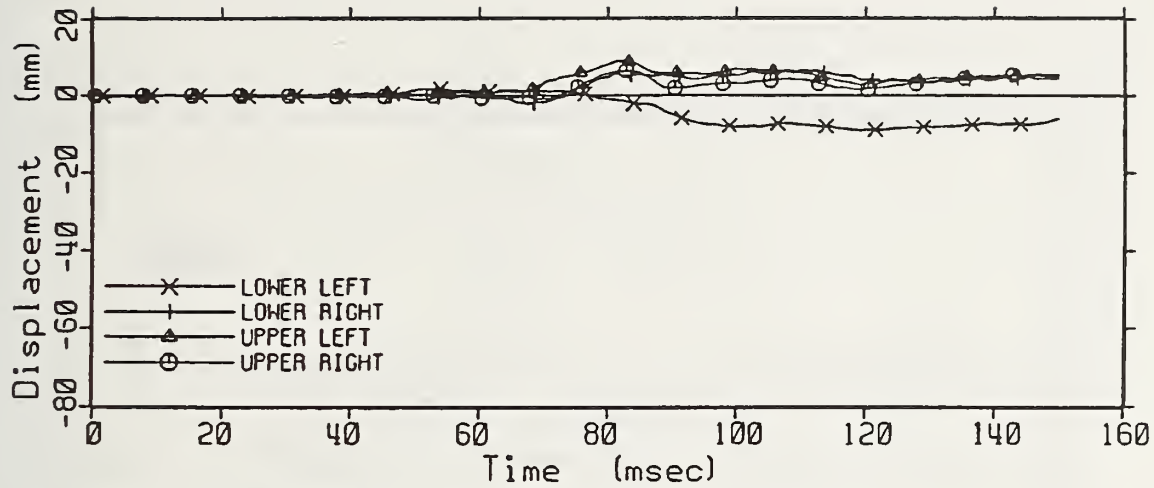

Figure 29. TAD Test 478 Lap Belt/Air Bag, 48 Kph - Y Deflection

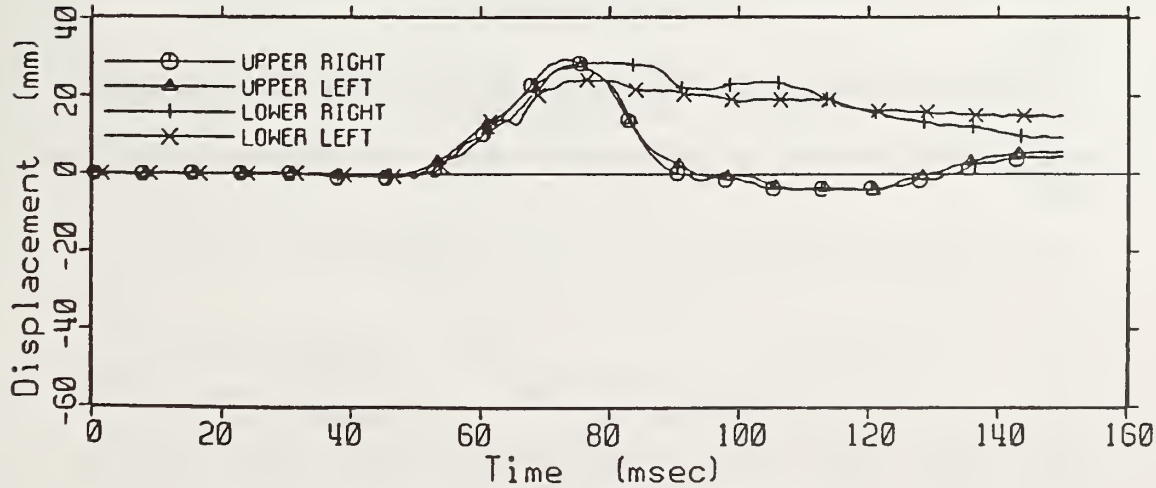

Figure 30. TAD Test 478 Lap Belt/Air Bag, 48 Kph - Z Deflection

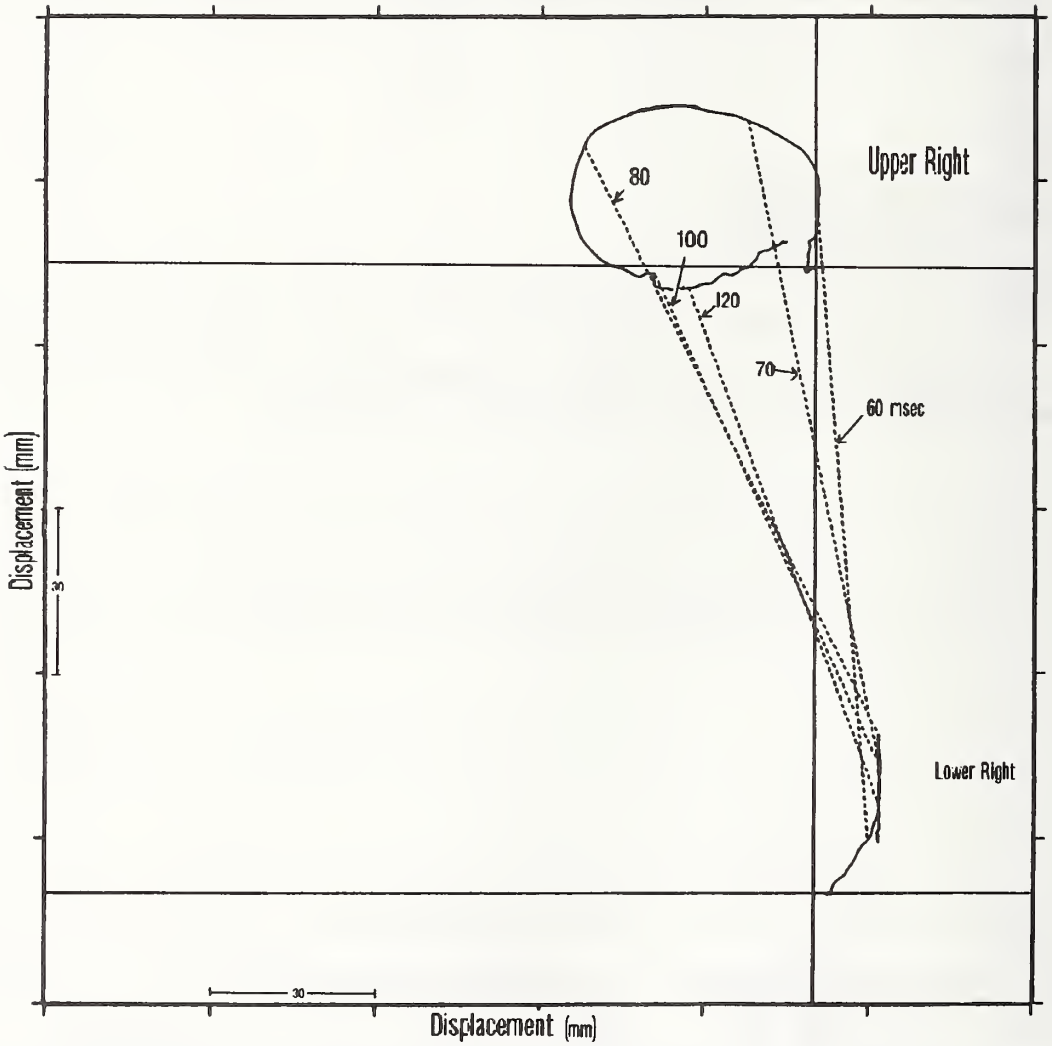

Figure 31. TAD Test 478, Air Bag/Lap Belt, 48 Kph - Right Side Sensors (Right Side View)

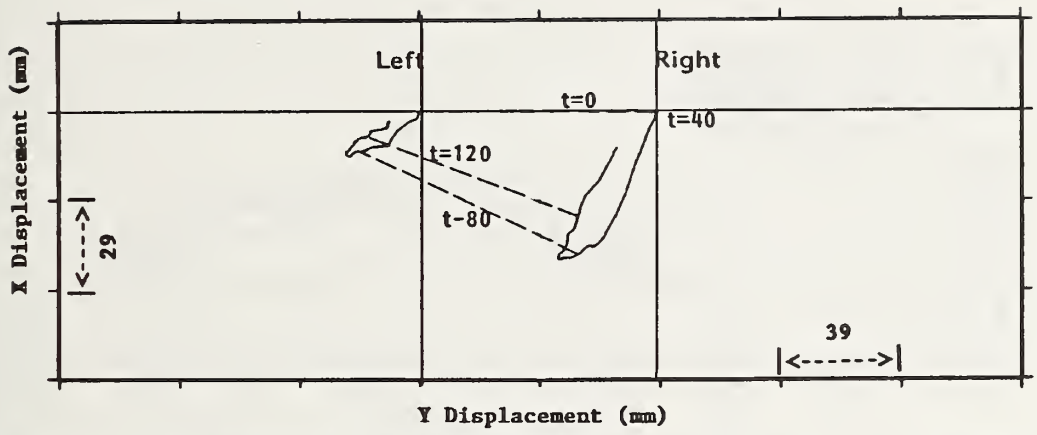

Figure 32. TAD Test 475 Three-Point Belt, 48 Kph - Sternal Sensors (Top View)

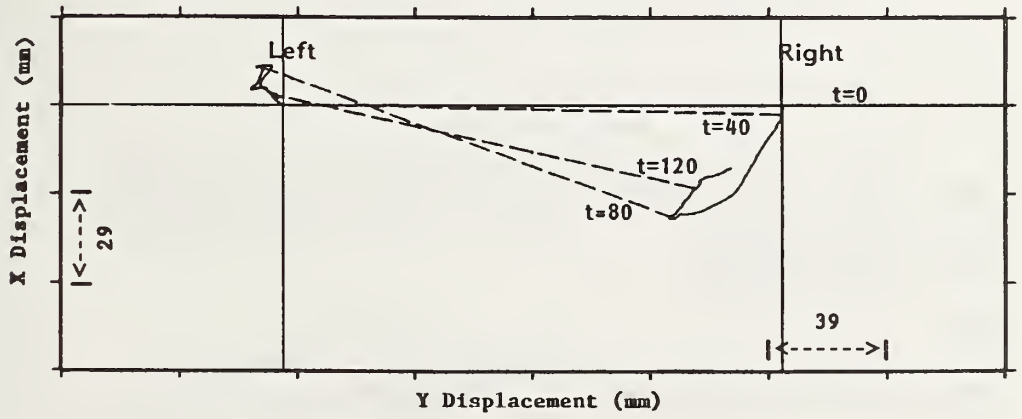

Figure 33. TAD Test 475 Three-Point Belt, 48 Kph - Lower Sensors (Top View)

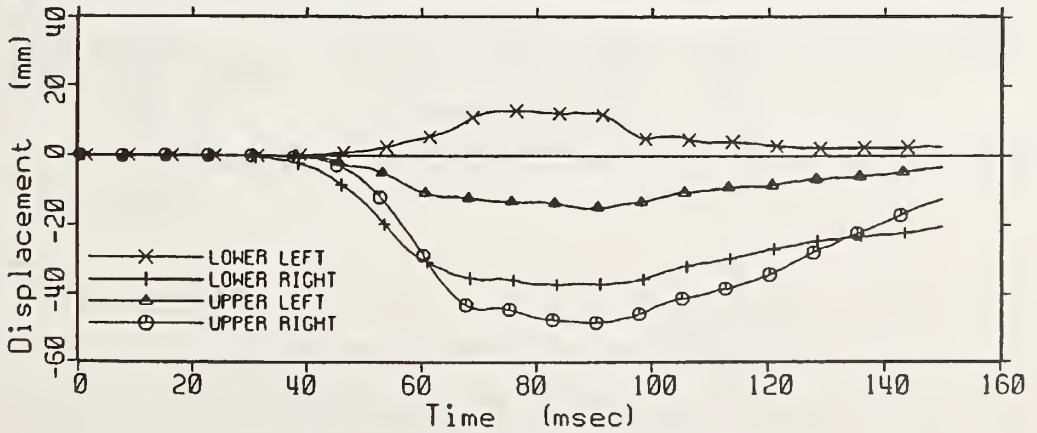

Figure 34. TAD Test 475 Three-Point Belt, 48 Kph - X Deflection

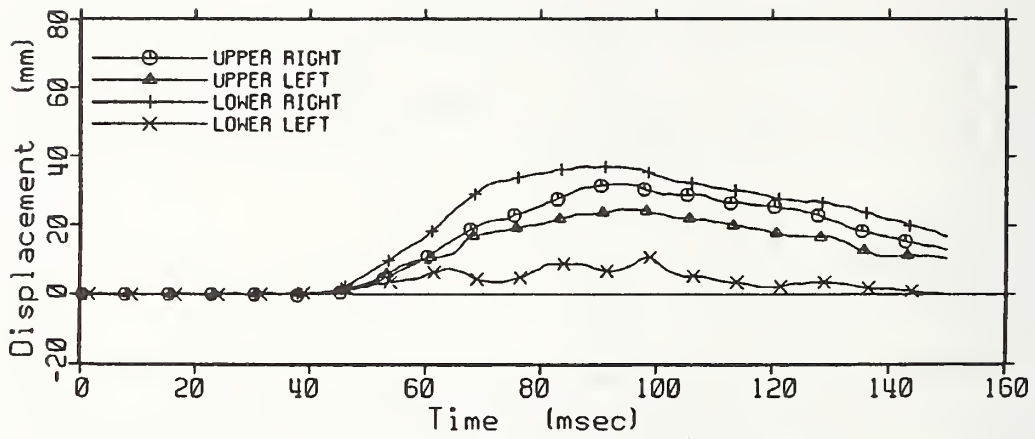

Figure 35. TAD Test 475 Three-Point Belt, 48 Kph - Y Deflection

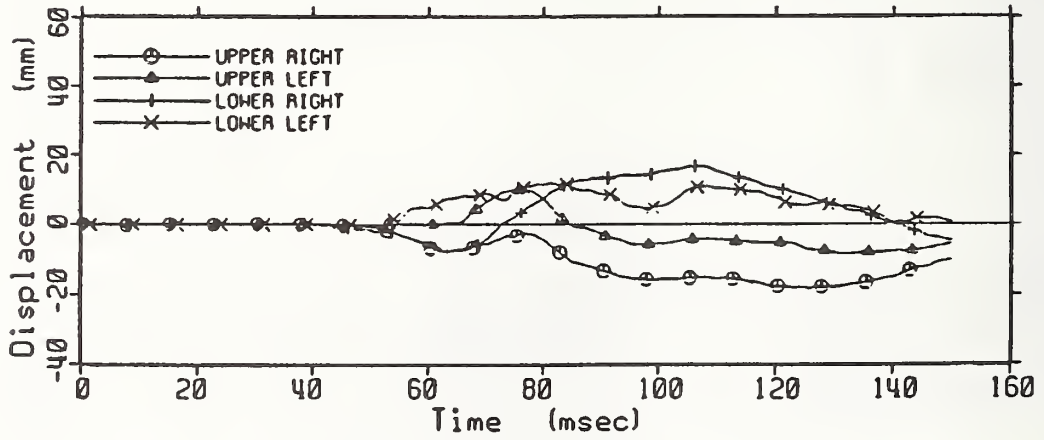

Figure 36. TAD Test 475 Three-Point Belt, 48 Kph - Z Deflection

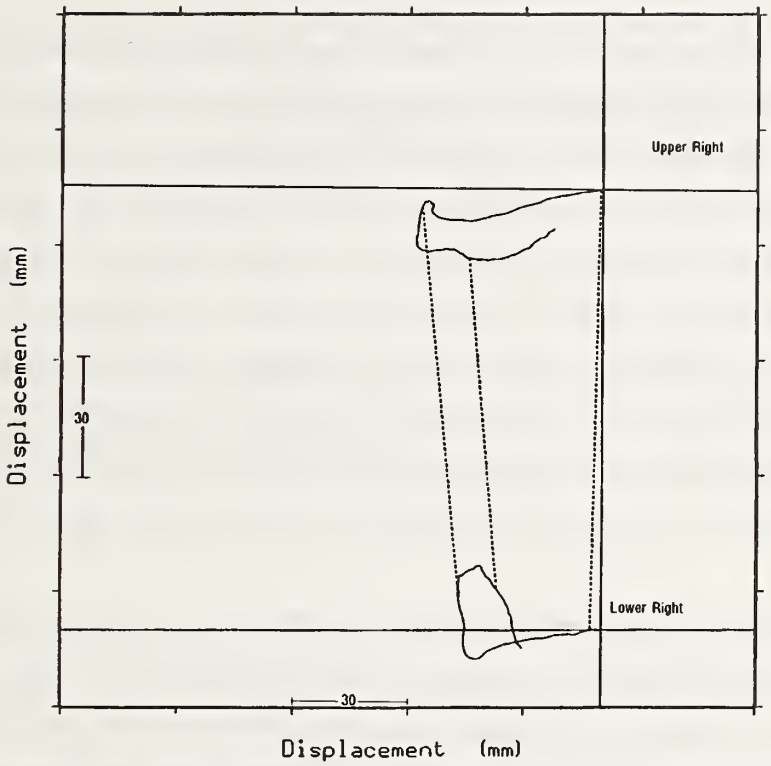

Figure 37. TAD Test 475, Three-Point Belt, 48 Kph - Right Side Sensors (Side View)

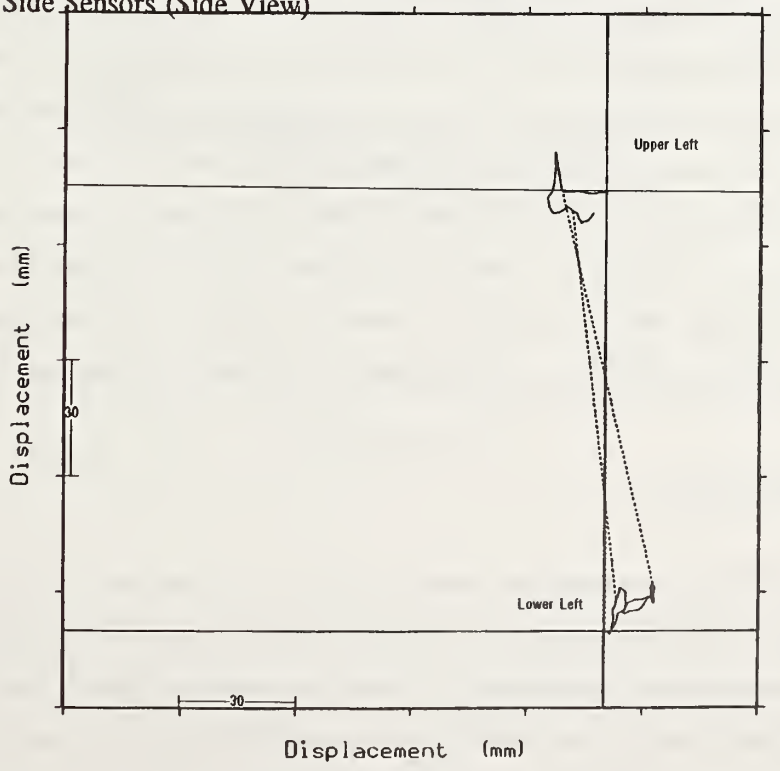

Figure 38. TAD Test 475, Three-Point Belt, 48 Kph - Left Side Sensors (Side View)

Figures 39 - 45 show the x,y and x,z plane plots, and deflection time histories for test 472, a three-point belt/air bag test. When compared to the three-point belt test (475) cited above, the responses appear very similar. The shoulder belt force time histories for both tests are shown in Figure 46. This plot displays identical belt forces until approximately 75 msec. At that point, the shoulder belt force in the air bag/ three-point belt configuration is somewhat lower (approximately 10%) than the belt only test. Since this test includes an air bag plus a three-point belt restraint, one might expect more of a difference in chest compression or belt loads. However, this did not happen. In general, the three-point belt system appears to dominate overall restraint performance in tests 472/473, suggesting that the belt was too stiff or that the bag was too late to allow the torso to benefit from the air bag. Under this circumstance, the TAD-50M thorax did not detect benefit from addition of the air bag and responded accordingly.

In the passenger two-point belt/knee-bolster test (test 477), a unique deflection pattern was also evident. Figures 47 and 48 show the x,y plane plots for the sternal and lower ribcage deflection sensors, respectively. The maximum sternal deflection was seen on the left, which agrees with the shoulder belt location left of mid sternum. The deflections in this test are larger than any other tests in the series. The peak x-compression of 69 mm was the largest x-deflection value recorded in the test series at the sternum. At the lower left ribcage, under the belt path for this test, the x-deflection of 57 mm compression was also the largest recorded at this location. The time histories for the two-point belt test (Figures 49 - 51) further illustrate the inward (x) deflection of the chest, especially on the left side. The y deflection time histories reveal significant lateral motion (up to 67 mm) of the ribcage towards the right side. The z deflection plot (Figure 51) and the x,z plane plots (Figures 52 and 53) indicate that the left side of the ribcage is pulled downward while the right side is pushed up slightly and is then pushed downward. This test exhibits approximately twice the z-deflection seen in the three-point belt tests 475/476.

48 KPH TAD Oblique Tests

Two tests (482,483) were performed with the TAD on the driver's side in an oblique configuration (Figure 10). Test 482 used a three-point seat belt with air bag while test 483 had only a three-point belt. Figures 54 - 60 illustrate the x,y plane plots, x,z plane plots, and time history plots for test 482. These plots illustrate that the dummy behaves with an air bag and three-point belt in much the same manner as in test 483 (Figures 61 - 67), a three-point belt test. The magnitude of the x movement in the sternal

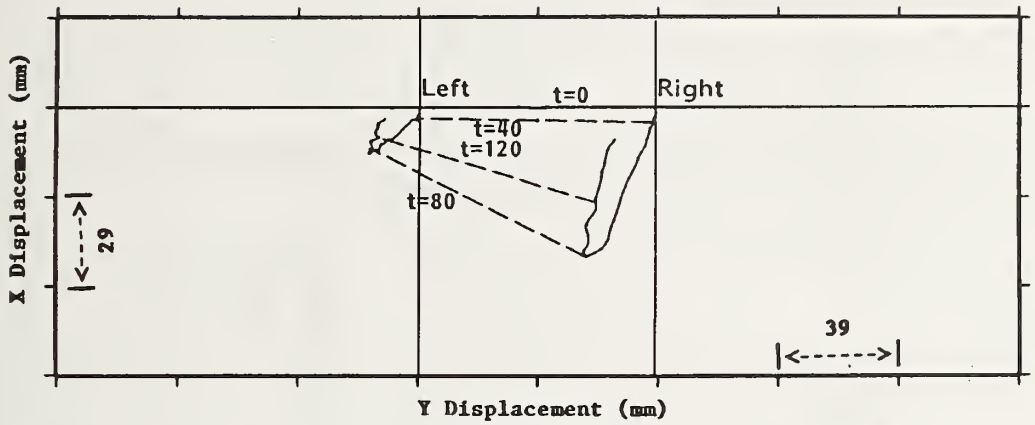

Figure 39. TAD Test 472 Three-Point Belt/Air Bag, 48 Kph - Sternal Sensors (Top View)

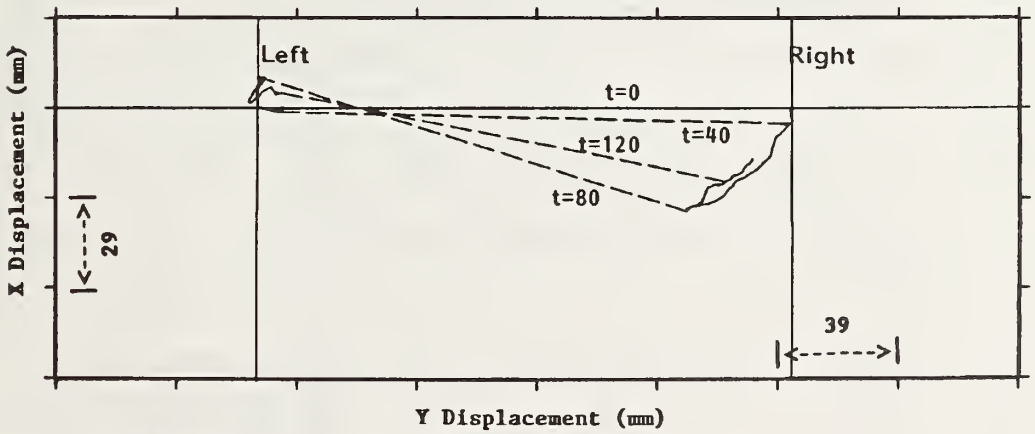

Figure 40. TAD Test 472 Three-Point Belt/Air Bag, 48 Kph - Lower Sensors (Top View)

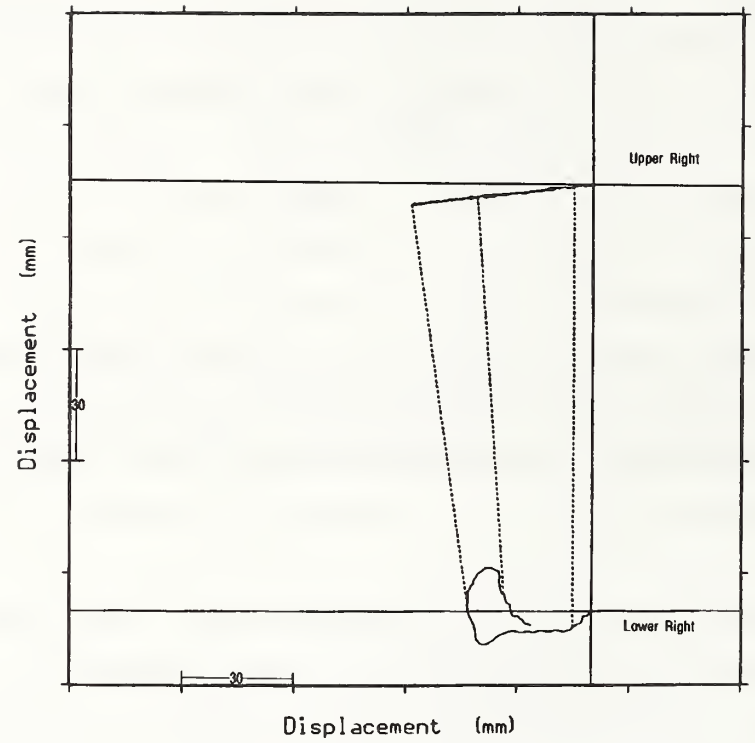

Figure 41. TAD Test 472, Three-Point Belt/Air Bag, 48 Kph - Right Side Sensors (Side View)

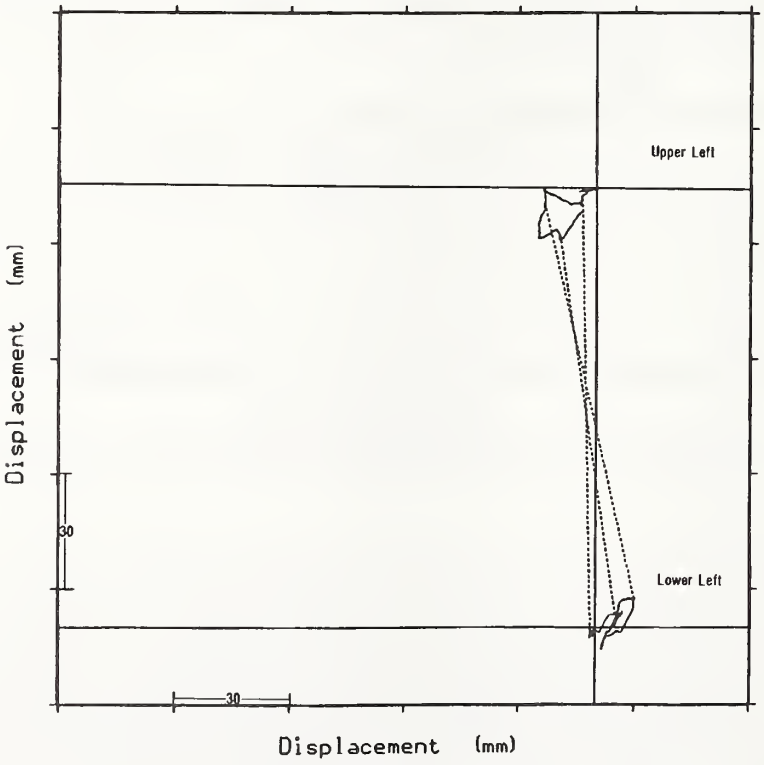

Figure 42. TAD Test 472, Three-Point Belt, 48 Kph - Left Side Sensors (Side View)

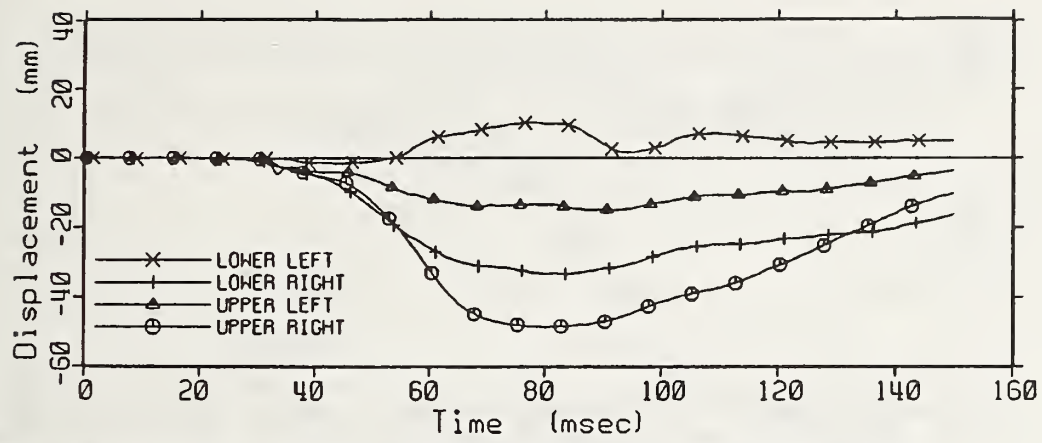

Figure 43. TAD Test 472 Three-Point Belt/Air Bag, 48 Kph - X Deflection

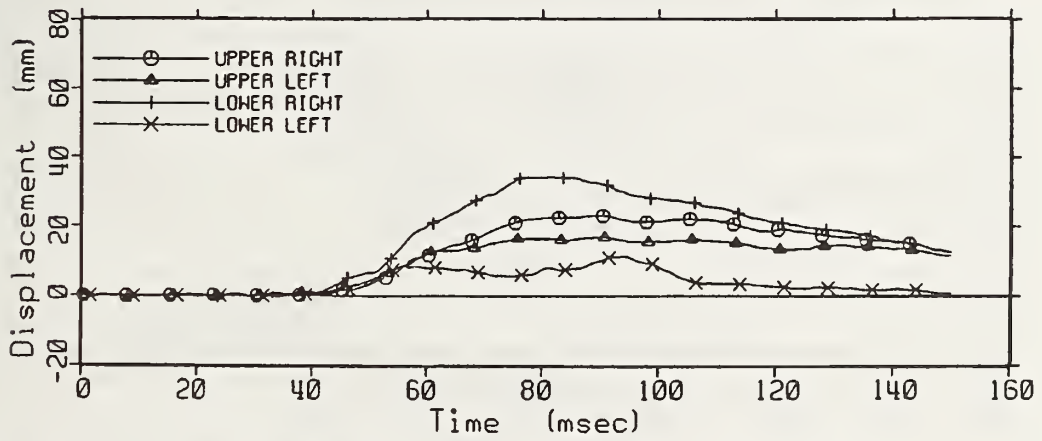

Figure 44. TAD Test 472 Three-Point Belt/Air Bag, 48 Kph - Y Deflection

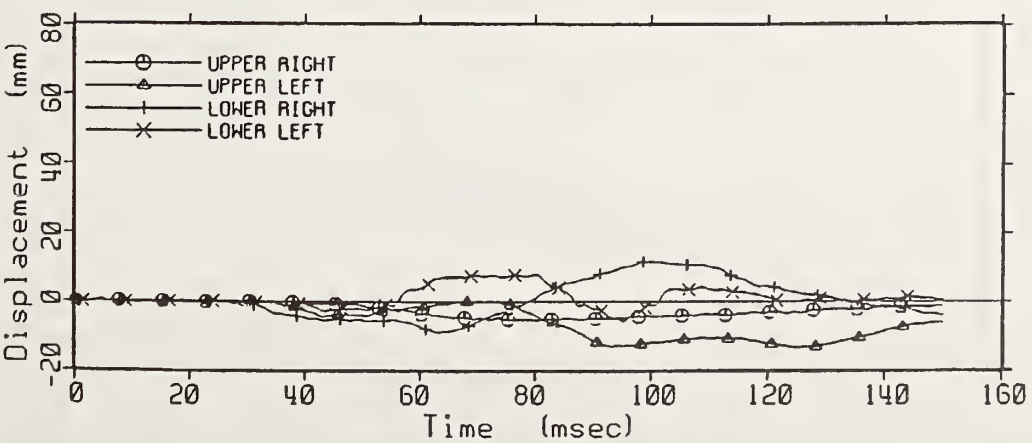

Figure 45. TAD Test 472 Three-Point Belt/Air Bag, 48 Kph - Z Deflection

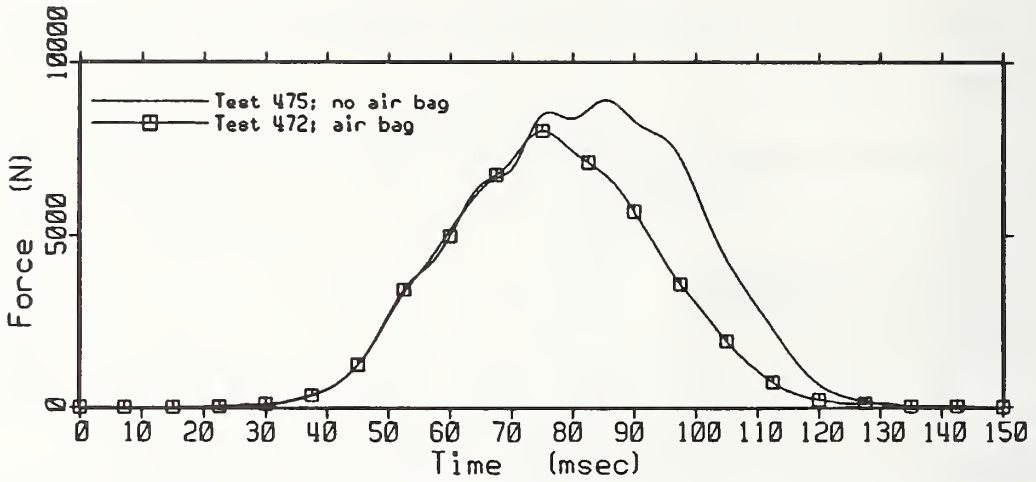

Figure 46. TAD Three-Point Belt Shoulder Belt Force With and Without Air Bag

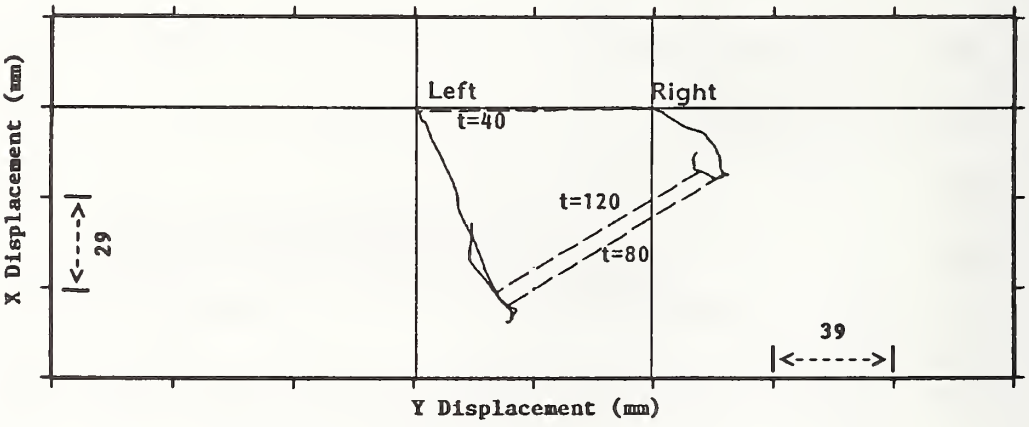

Figure 47. TAD Test 477 Two-Point Belt/Knee Bolster, 48 Kph - Sternal Sensors (Top View)

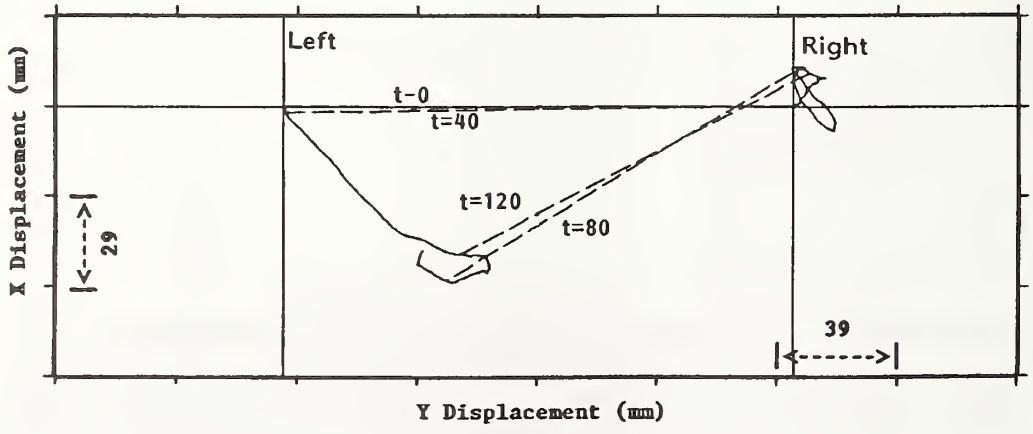

Figure 48. TAD Test 477 Two-Point Belt/Knee Bolster, 48 Kph - Lower Sensors (Top View)

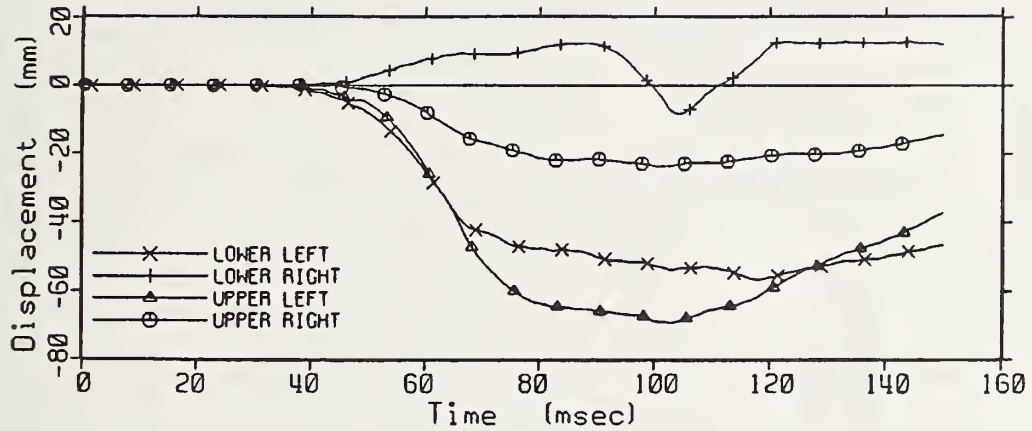

Figure 49. TAD Test 477 Two-Point Belt/Knee Bolster, 48 Kph - X Deflection

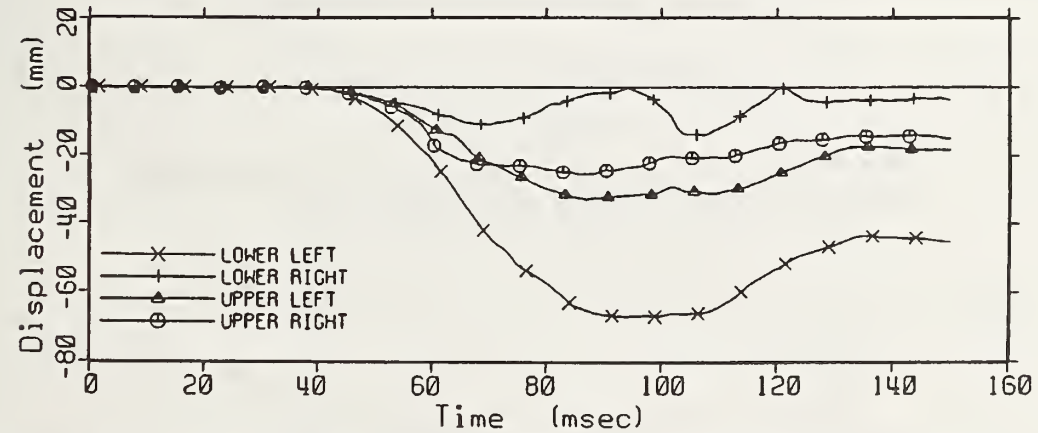

Figure 50. TAD Test 477 Two-Point Belt/Knee Bolster, 48 Kph - Y Deflection

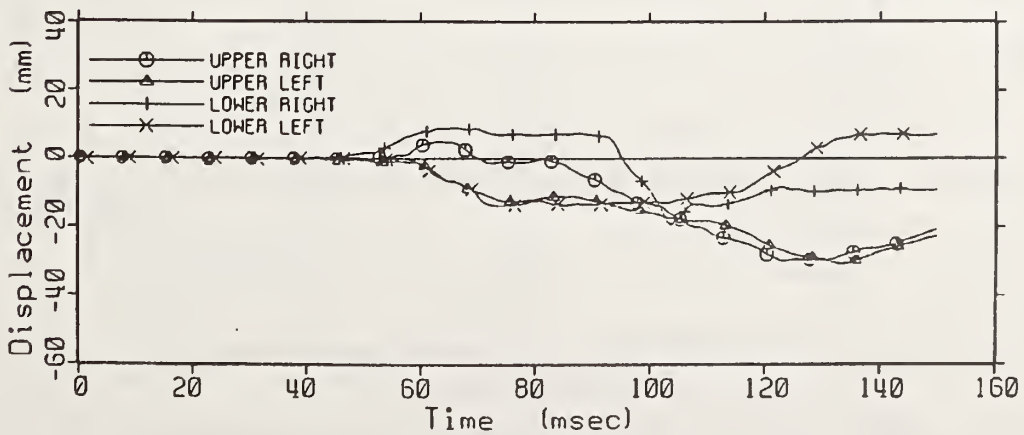

Figure 51. TAD Test 477 Two-Point Belt/Knee Bolster, 48 Kph - Z Deflection

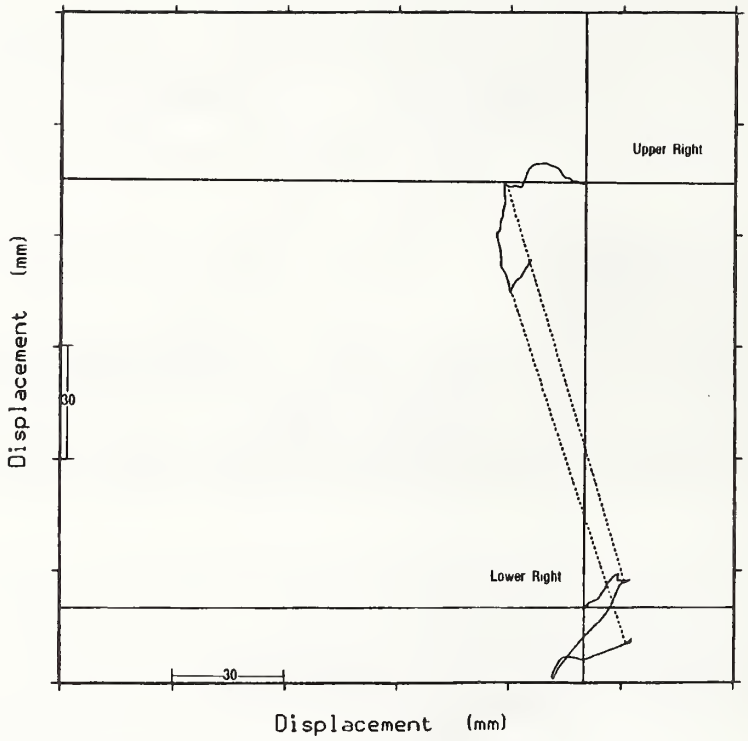

Figure 52. TAD Test 477, Passenger Two-Point Belt/Knee Bolster, 48 Kph - Right Side Sensors (Side View)

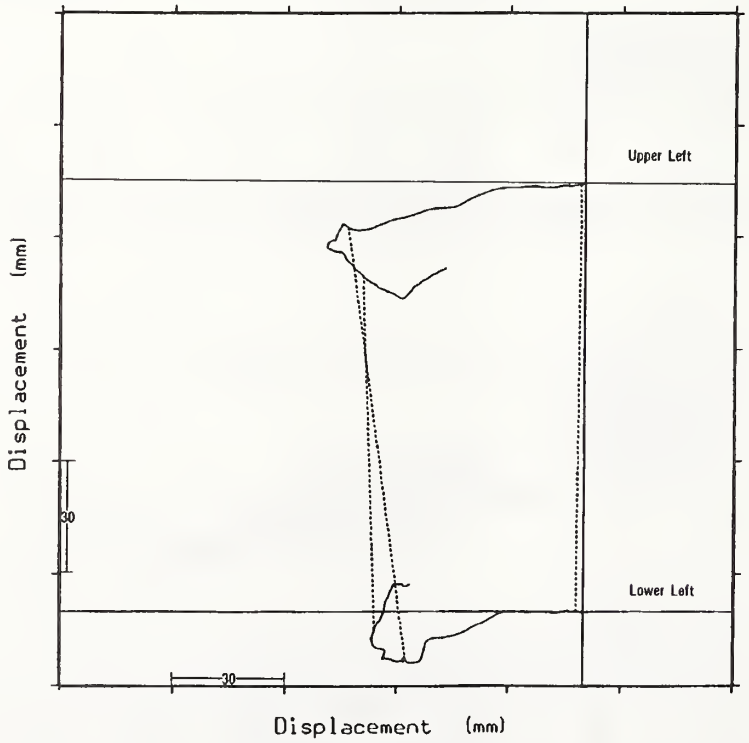

Figure 53. TAD Test 477, Passenger Two-Point Belt/Knee Bolster, 48 Kph - Left Side Sensors (Side View)

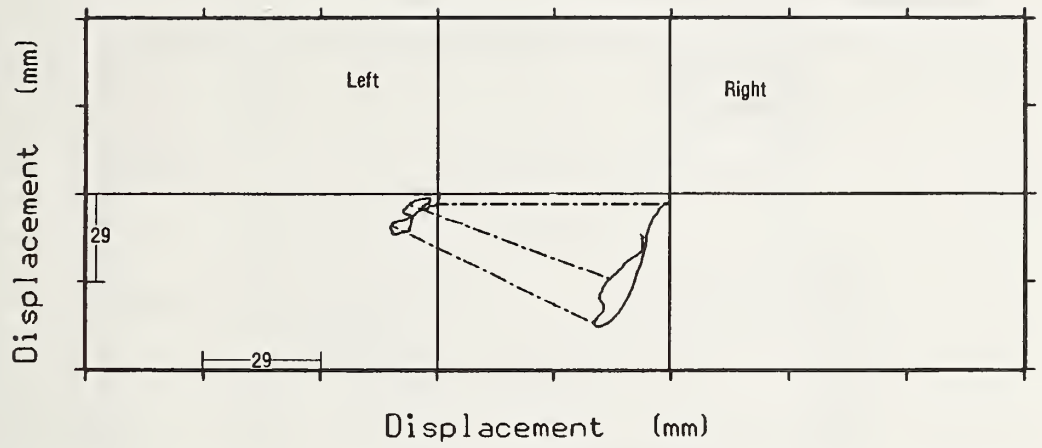

Figure 54. TAD Test 482, Three-Point Belt/Air Bag, Oblique, 48 Kph - Sternal Sensors (Top View)

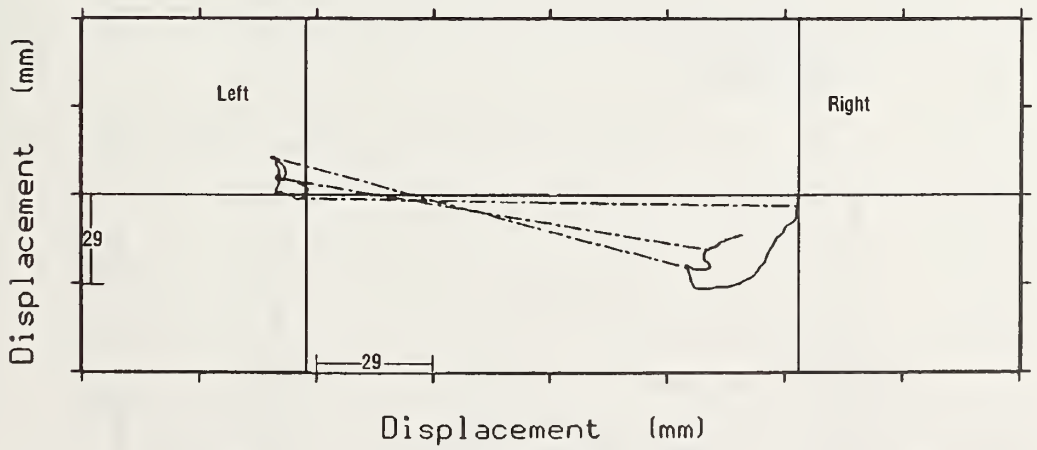

Figure 55. TAD Test 482, Three-Point Belt/Air Bag, Oblique, 48 Kph - Lower Sensors (Top View)

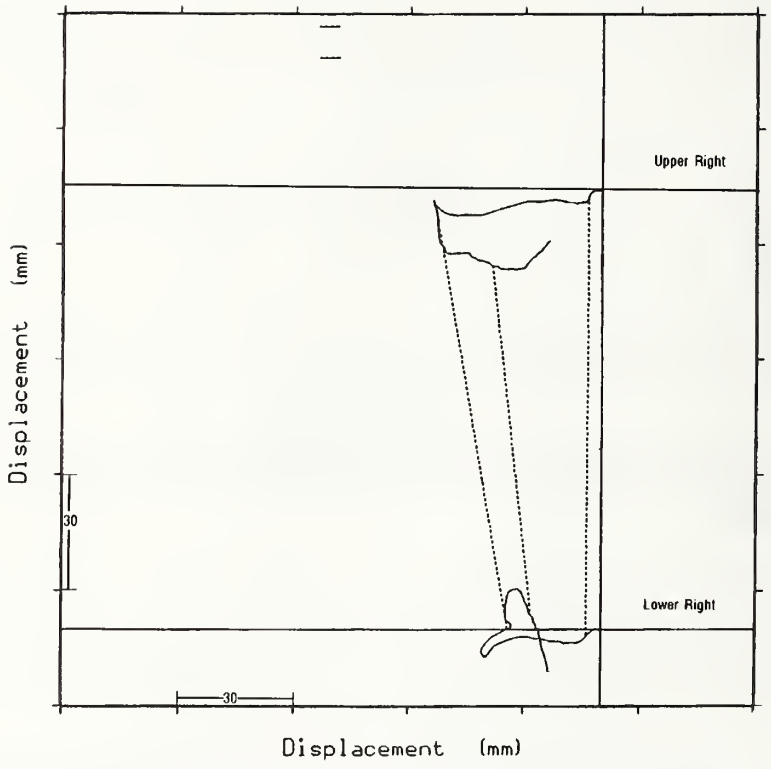

Figure 56. TAD Test 482, Three-Point Belt/Air Bag, Oblique, 48 Kph - Right Side Sensors (Side View)

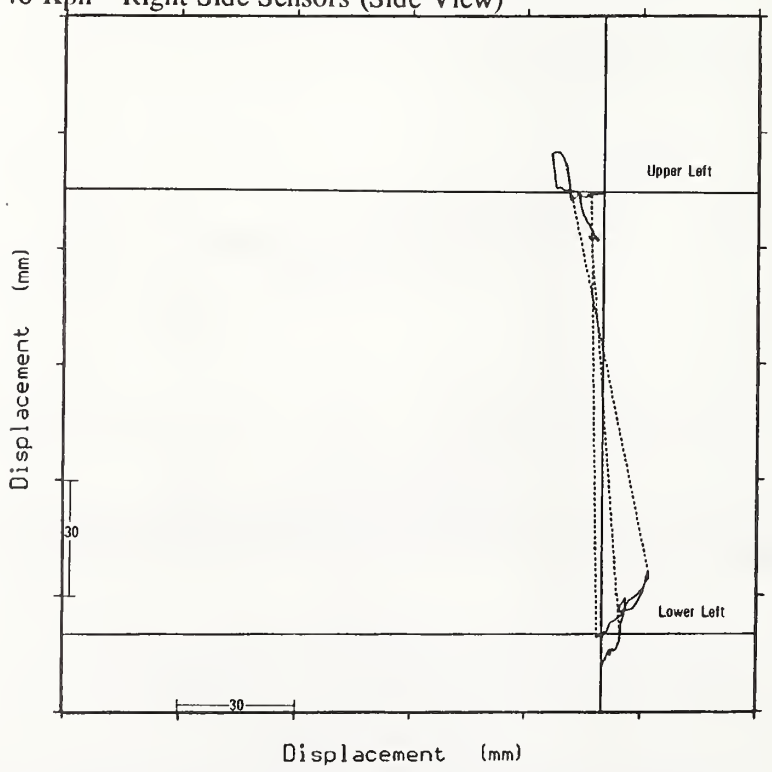

Figure 57. TAD Test 482, Three-Point Belt/Air Bag, Oblique, 48 Kph - Left Side Sensors (Side View)

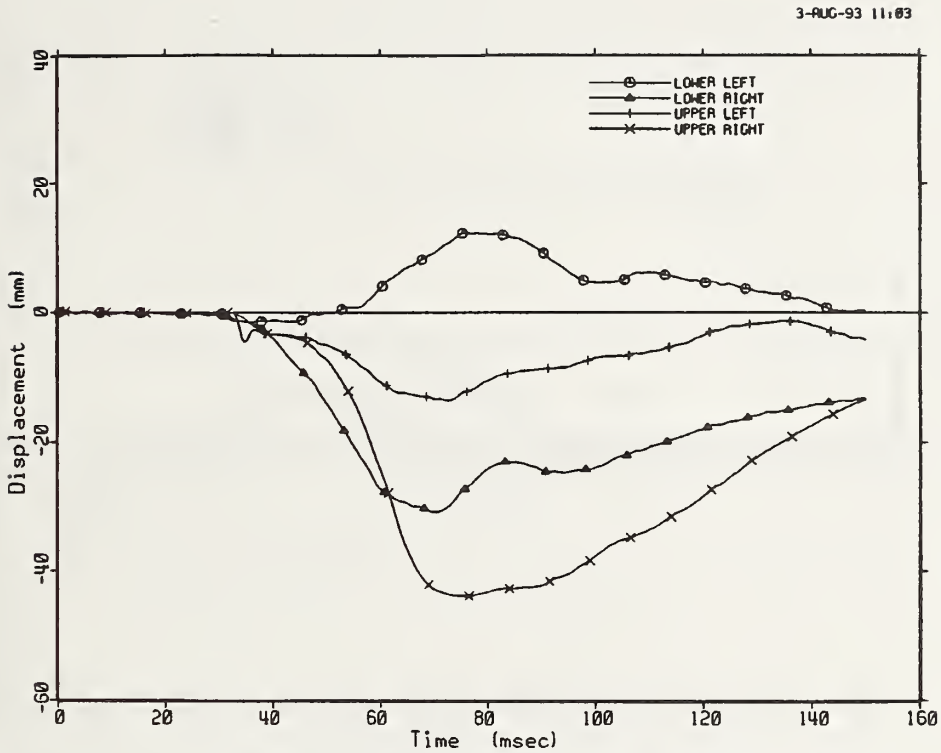

Figure 58. TAD Test 482, Three-Point Belt/Air Bag, Oblique, 48 Kph - X Deflection

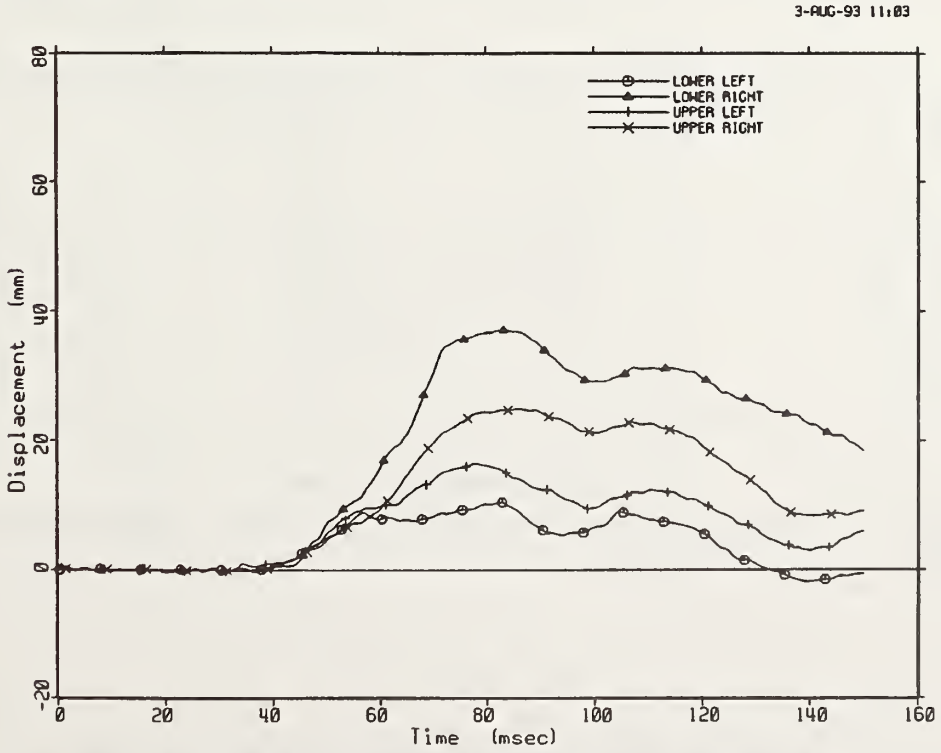

Figure 59. TAD Test 482, Three-Point Belt/Air Bag, Oblique, 48 Kph - Y Deflection

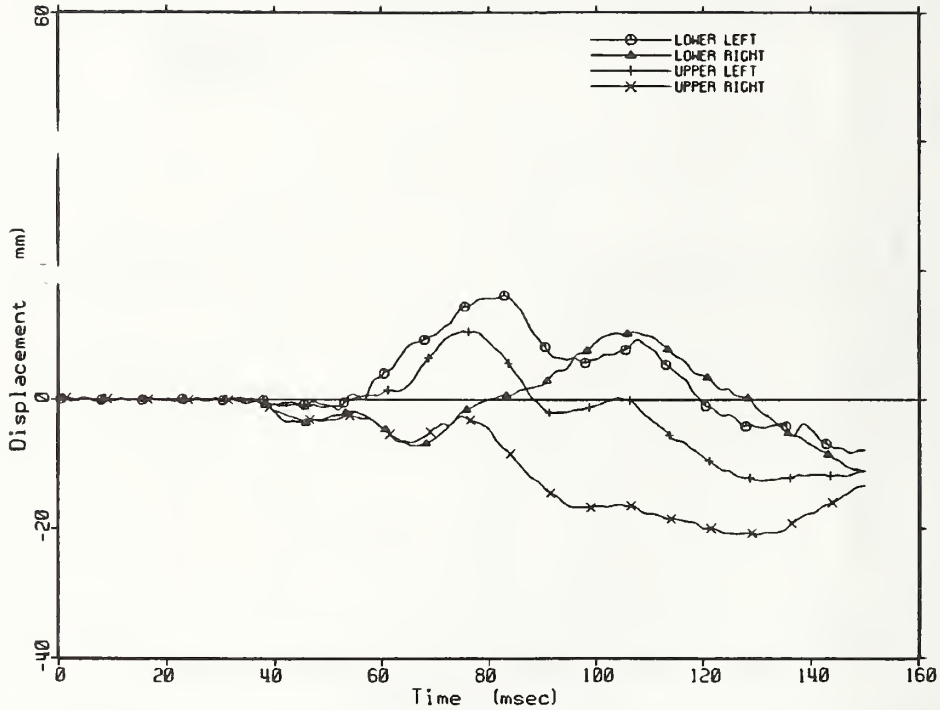

Figure 60. TAD Test 482, Three-Point Belt/Air Bag, Oblique, 48 Kph - Z Deflection

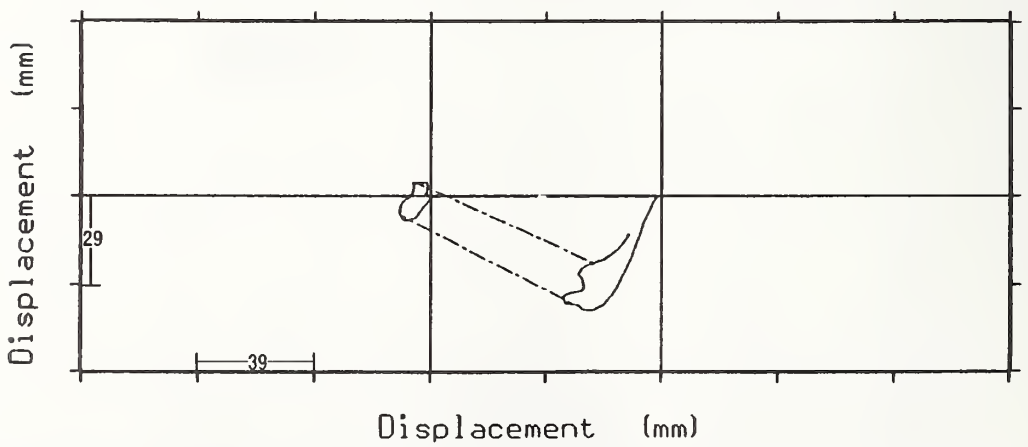

Figure 61. TAD Test 483, Three-Point Belt, Oblique, 48 Kph - Sternal Sensors (Top View)

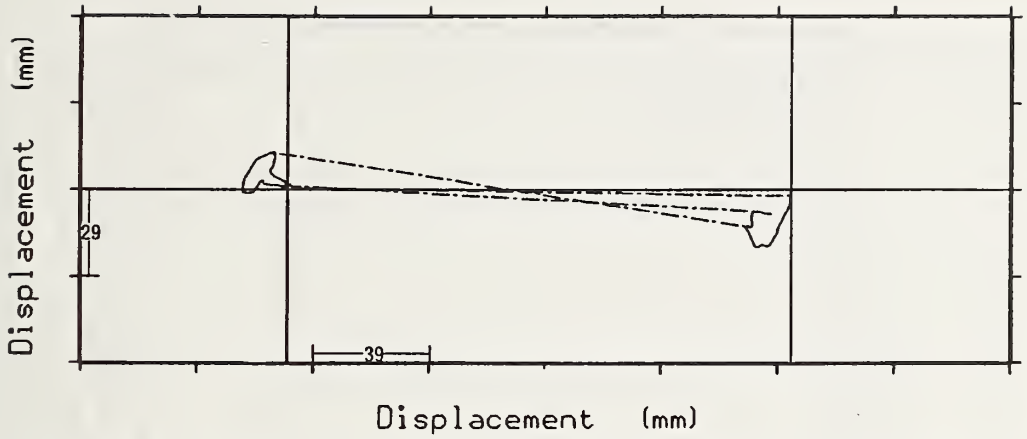

Figure 62. TAD Test 483, Three-Point Belt, Oblique, 48 Kph - Lower Sensors (Top View)

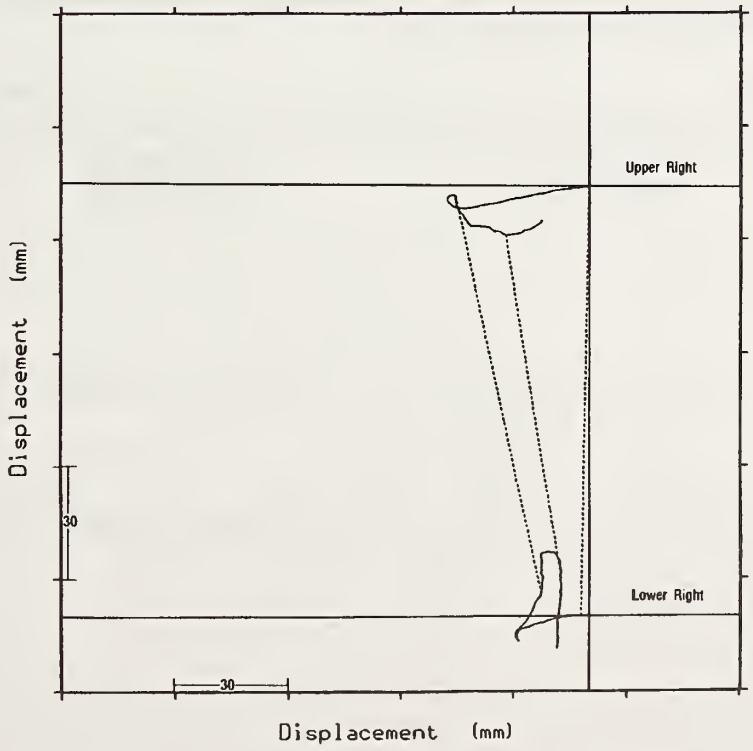

Figure 63. TAD Test 483, Three-Point Belt, Oblique, 48 Kph - Right Side Sensors (Side View)

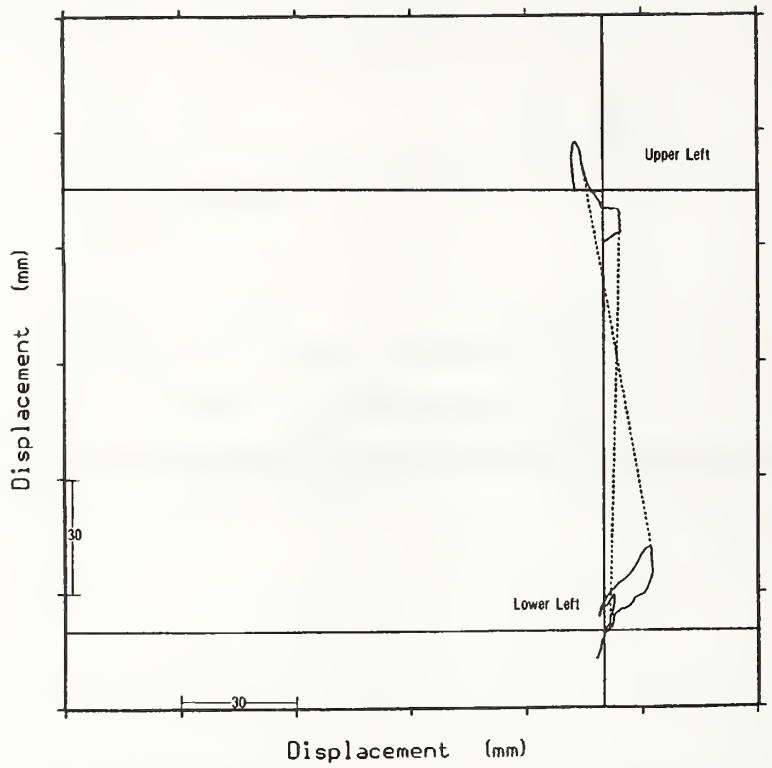

Figure 64. TAD Test 483, Three-Point Belt, Oblique, 48 Kph - Left Side Sensors (Side View)

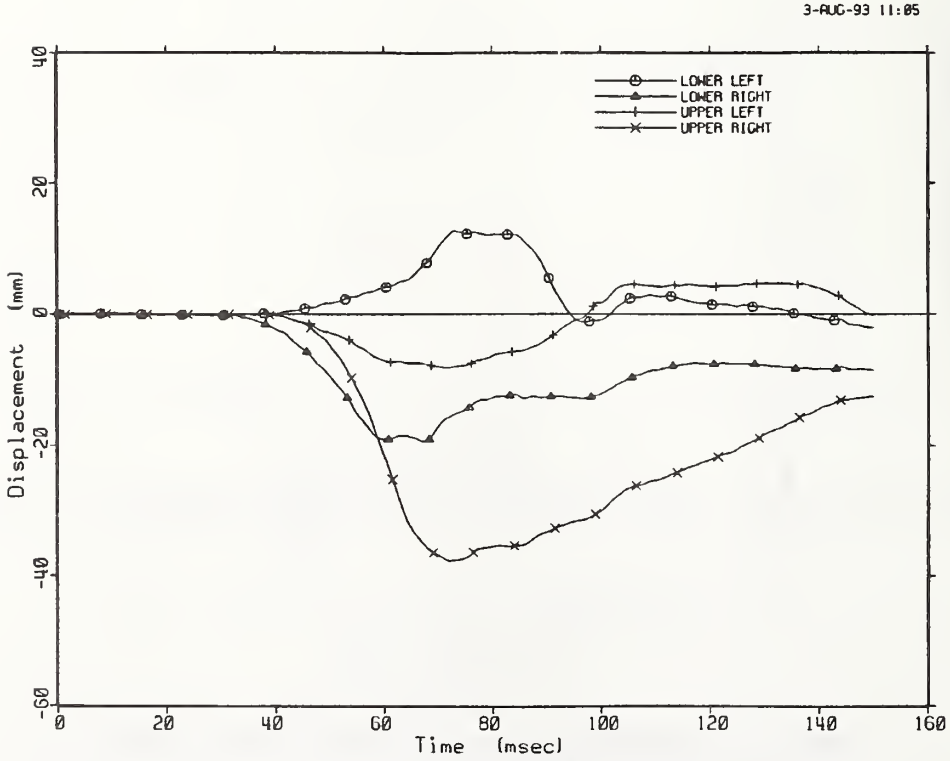

Figure 65. TAD Test 483, Three-Point Belt, Oblique, 48 Kph - X Deflection

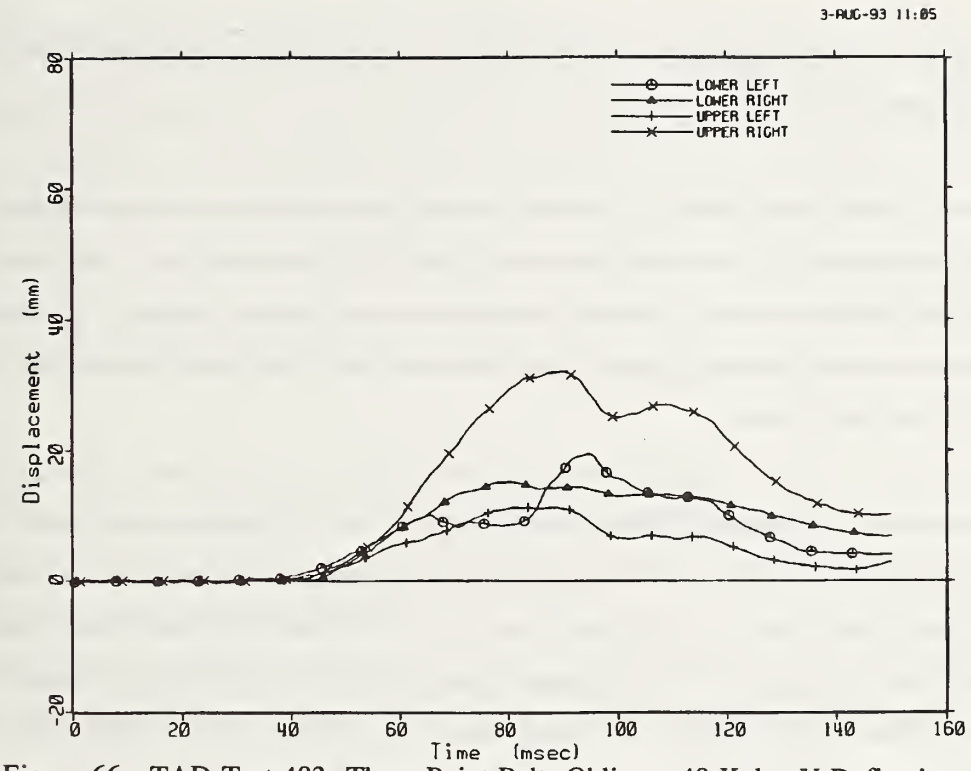

Figure 66. TAD Test 483, Three-Point Belt, Oblique, 48 Kph - Y Deflection

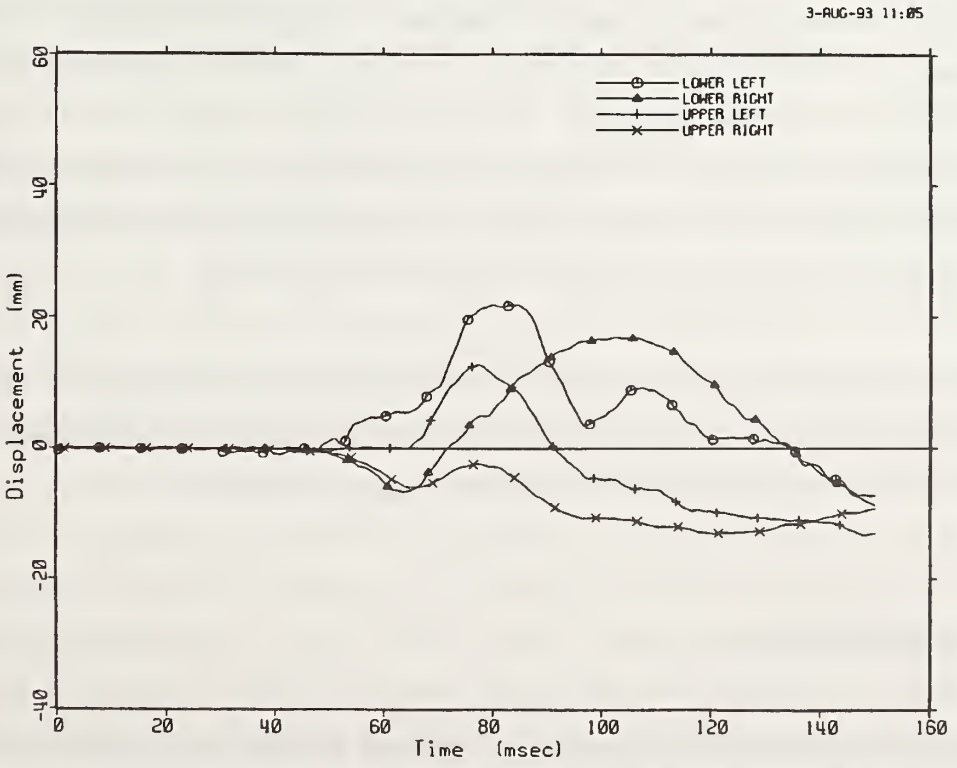

Figure 67. TAD Test 483, Three-Point Belt, Oblique, 48 Kph - Z Deflection

sensors and in the lower right sensors are slightly higher in test 482 (Figures 54 and 55) when compared to test 483 (Figures 61 and 62).

When compared to one another, results from these tests maintain a relationship similar to those seen in the frontal tests 472 (three-point belt/air bag) and 475 (three-point belt). The frontal tests were similar with and without air bags because the belt dominates the restraint system. The seat belt/air bag system does not seem optimized to take advantage of the air bag's distributed loading. This phenomenon also occurs in the oblique tests.

A comparison between the TAD response in the oblique configuration to the frontal for the three-point belt air bag tests (472, frontal and 482, oblique) can be most easily seen by reviewing the x,y and x,z plane plots for each test. The x,y plane plots for test 472 (Figures 39 and 40) appear very similar to those from test 482 (Figures 54 and 55) except that test 482 reveals slightly more lateral movement than its frontal counterpart. This is to be expected since the oblique sled test would solicit more lateral response.

The x,z plane plots (Figures 42 and 57) display comparable responses for the left side, as the sternal sensors move inward and the lower sensors move out. However, the oblique test shows more upward (z) deflection than the frontal test. On the right side, the oblique test also demonstrates an upward followed by a downward movement of the right sternum (in the z direction), while the frontal test reveals little change in the z direction. Finally, x compression in the oblique test is reduced slightly, possibly because the dummy was offset from the direction of deceleration.

Comparing frontal test 475 with oblique test 483 (three-point belt tests), the frontal test displays more x compression and inward lateral motion of both the sternal and lower right ribcage in the frontal test (Figures 32 and 33) compared to the oblique test (Figures 61 and 62).

48 KPH HYBRID III Tests

Plots similar to the TAD x,y plots can be displayed for Hybrid III results, since the stringpot thorax provides a method of determining the x and y coordinates of the ends of the stringpot attachment

points. As explained previously, although deflection magnitudes from each dummy cannot be directly compared because of differences in sensor attachments, a general comparison of the performance of the two dummies is possible. Sternal deflection results from test 485 (Figure 68), the Hybrid III air bag/lap belt configuration, reveal a sternal deflection pattern similar to that of the TAD in the same restraint (Figure 26). The chest compresses rather uniformly in the x direction with little y movement apparent. At the lower ribcage however, the TAD exhibits expansion (Figure 27) while the Hybrid III experiences compression (Figure 69). Both dummies exhibit small y deflections in the air bag/lap belt configuration.

X,y plots of the three-point belt test (486) for the Hybrid III (Figures 70 and 71) indicate the same type of deflection pattern as seen in the TAD test 475 (Figures 32 and 33). As expected in this configuration, the thorax compresses more on the right than on the left. However, the TAD exhibits a bigger difference in the right/left deflections than the Hybrid III. As seen in Figure 32, the angle subtended by the line connecting the left and right sensors and the horizontal is approximately 25 degrees in the TAD sternal deflection, while the same angle is only about 15 degrees in the Hybrid III upper sensors (Figure 70). In addition, the Hybrid III exhibits a smaller y deflection than does the TAD, evident at both the sternum and lower ribcage. The Hybrid III experiences only compression at the lower ribcage (Figure 71) while the TAD reveals a compression on the right and expansion on the left at the lower ribcage (Figure 33).

Figures 72 and 73 show the head and T1 excursions for the TAD and the Hybrid III in the three-point belt configuration at 48-kph (tests 475 and 486, respectively). In Figure 72, for example, the head excursion is depicted in the upper curve, which begins at the origin (0,0). The origin represents the initial position of the head. The circular symbols indicate the head position relative to the initial position every 10 msec. Steering wheel contact location is noted by the three vertical triangles. Similarly, the lower curve represents T1 location relative to the head location every 10 msec. In comparing Figures 72 and 73, the TAD's head and T1 location travel approximately 8 cm farther (from their initial positions) than the Hybrid III under similar test conditions. This may be partially attributed to the additional compliance of the TAD thorax and the contribution of TAD's articulated spine. However, head excursion dissimilarities may be due, for the most part, to differences in initial clearances between the TAD dummy and the steering wheels rather than compliance of the TAD thorax. The initial postures (including head position) of both dummies relative to the steering wheel indicated that the Hybrid III's

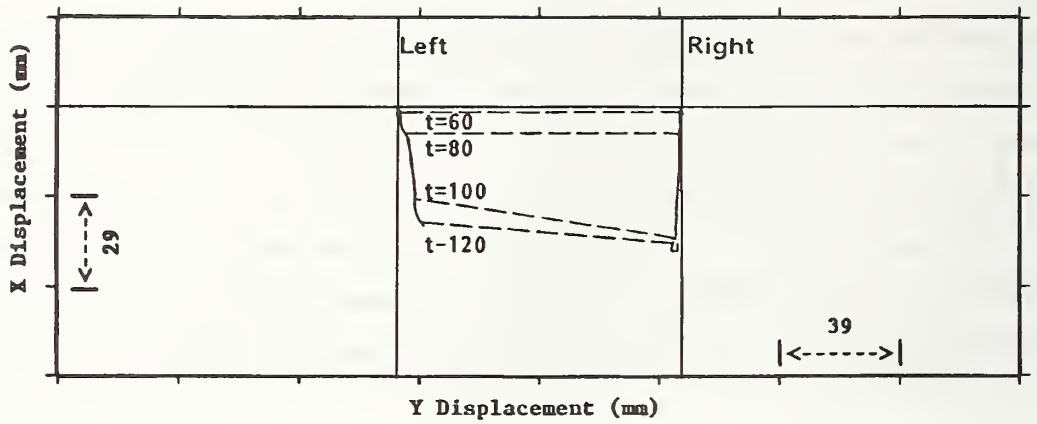

Figure 68. Hybrid III Test 485 Air Bag/Lap Belt, 48 Kph - Upper Sensors (Top View)

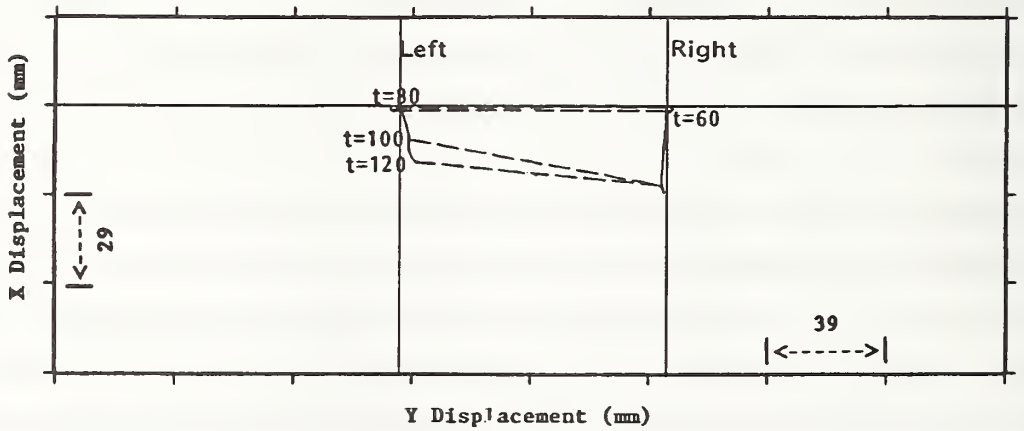

Figure 69. Hybrid III Test 485 Air Bag/Lap Belt, 48 Kph - Lower Sensors (Top View)

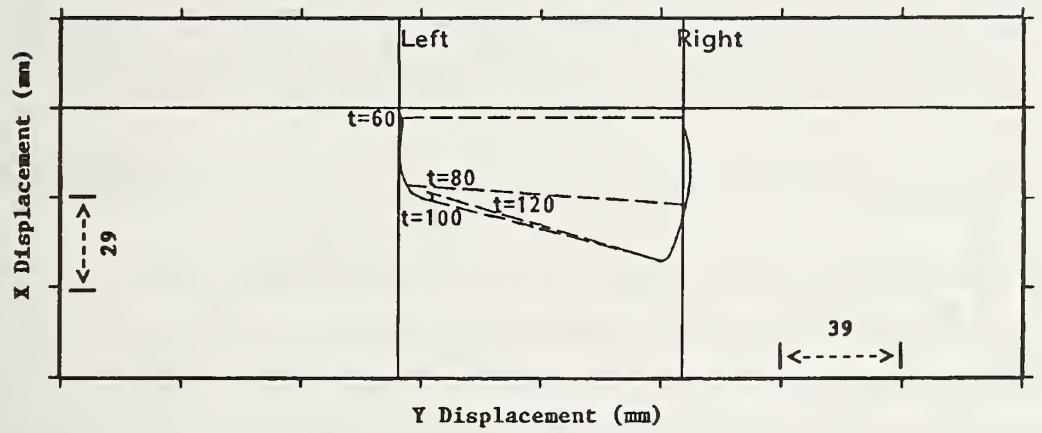

Figure 70. Hybrid III Test 486 Three-Point Belt, 48 Kph - Upper Sensors (Top View)

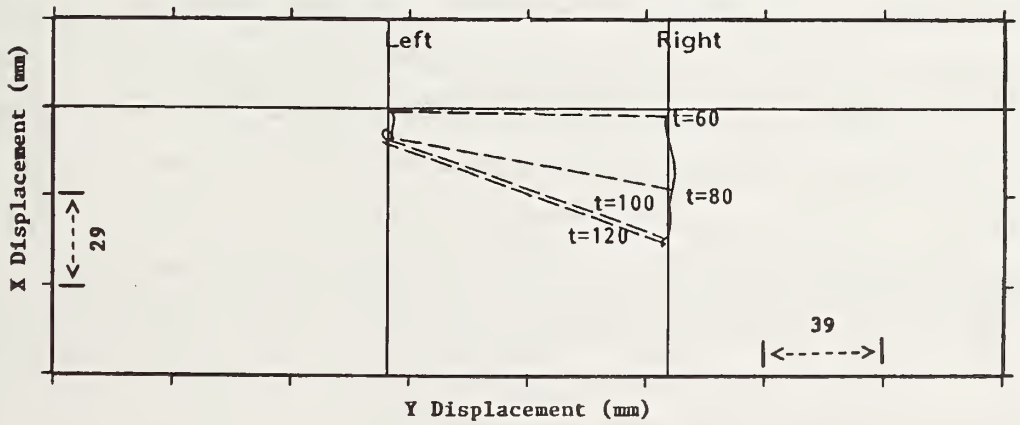

Figure 71. Hybrid III Test 486 Three-Point Belt, 48 Kph - Lower Sensors (Top View)

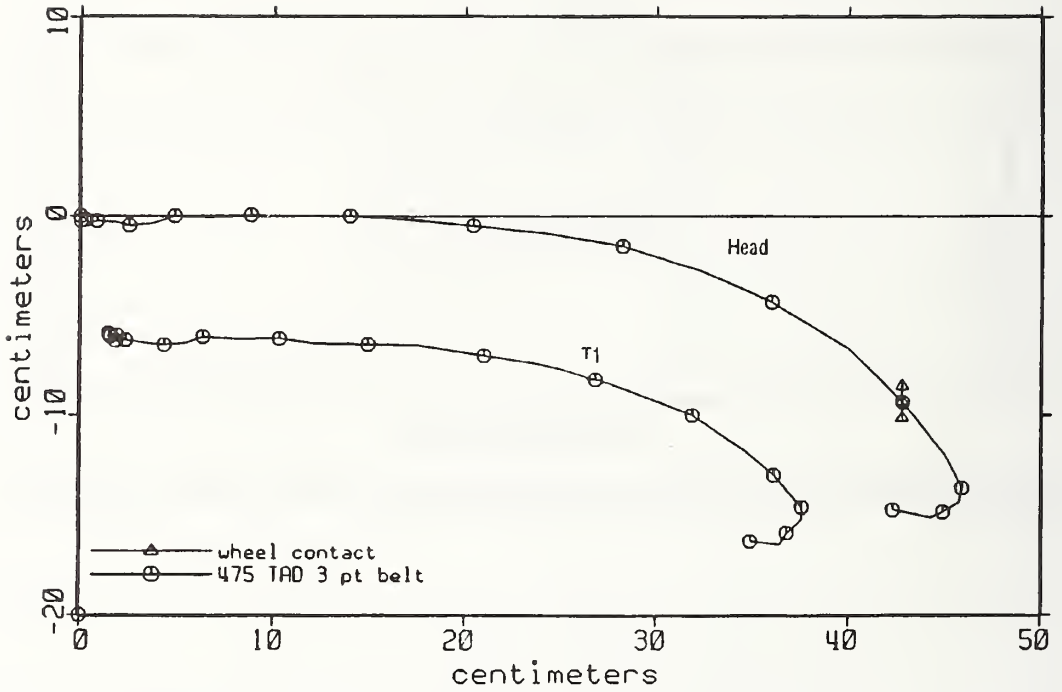

Figure 72. Head and T1 Excursions for TAD Test 475, a Three-Point Belt, 48 Kph Test

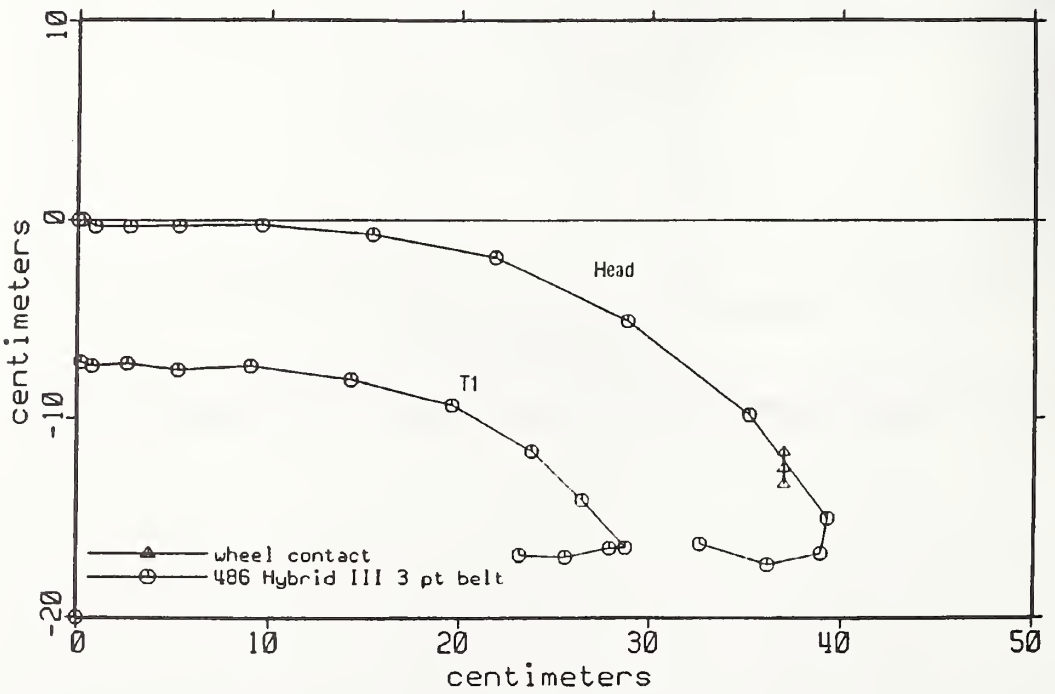

Figure 73. Head and T1 Excursions for Hybrid III Test 486, a Three-Point Belt, 48 Kph Test

head was approximately 8 cm forward of the TAD's head position prior to each test. Therefore, wheel contact effectively controlled and limited the maximum head excursion for each dummy.

56 KPH TAD Tests

Test 481, a 56-kph, three-point belt test, can be compared with tests 475/476 conducted at lower speed. Upon contact with the steering wheel, somewhat higher chest g's and higher head resultant accelerations are noted, but little change occurs in thorax x, y, and z deflection measurements. However, measured lap belt and shoulder belt peak loads are only slightly higher (5-7%) than those measured in tests 475/476.

Similar circumstances were noted when comparing the three-point belt/air bag test at 48 kph (tests 472/473) to the 56 kph test in the same configuration (test 479). The dummy response to the higher velocity was not significantly different from results at the lower velocity.

Comparing test pulses (Appendix A) from the 48 kph and 56 kph tests helps establish the reason why minimal change occurred between the two configurations run at different velocities. Figure 74 shows sled velocity for the two pulses. They are nearly identical up to 80 msec. The differences in impact severity, as seen by the TAD, were small up to the time of maximum deflection. Therefore, the results of the 48 and 54 kph tests do not differ significantly. Further evidence can be seen in the shoulder belt force plots for tests 475 and 481 (Figure 75). The belt forces appear only slightly higher in the 56 kph test when compared to the 48 kph test. This situation is not typical of all sled tests conducted at these two different velocities, but may be considered unique to this sled test series.

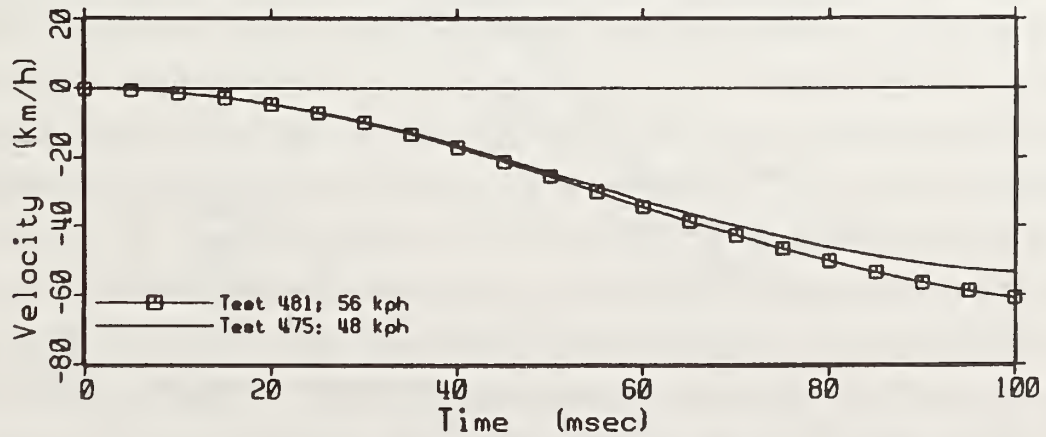

Figure 74. TAD Three-Point Belt Sled Velocities for 48 and 56 kph Tests

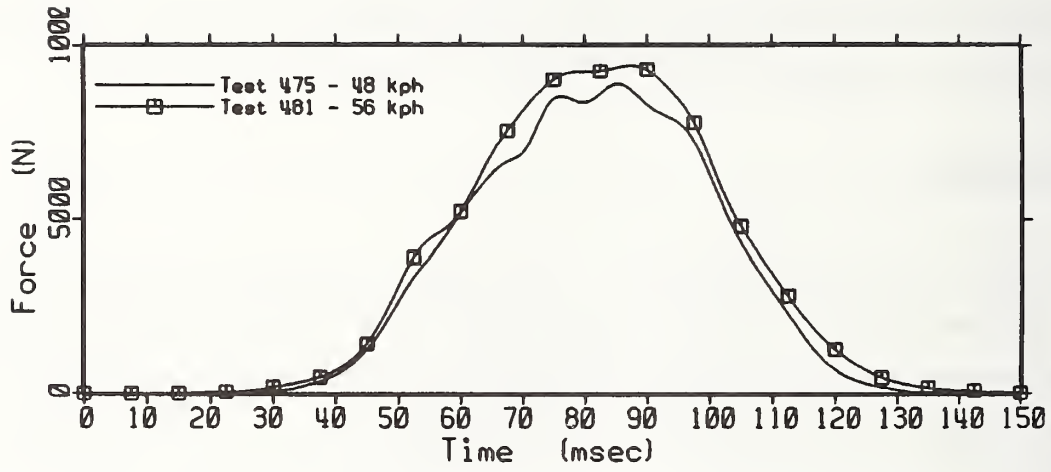

Figure 75. TAD Three-Point Belt Shoulder Forces for 48 and 56 kph Tests

Finally, test 480, a lap belt/air bag test, offers an interesting comparison because a failure in the steering column attachment resulted in column stroke that did not occur in the other tests. Under this condition, sternal x-deflections were significantly reduced. Consistent with results of test 478, test 480 demonstrated very small y-deflections, typical of air bag loading in this test series, and uniform upward z-deflections of the anterior ribcage.

MHD MEASUREMENTS

Other data contained in this report include spinal position plots calculated from the magnetohydrodynamic (MHD) angular motion sensors located at the upper, middle, and lower (pelvic) regions of the TAD spine. Since this spine has flexible articulations at the thoracic and lumbar areas, a "stick figure" plot of the spine during an acceleration event can be created by integrating the angular velocities to obtain angular displacement. Rigid links connect the flexible articulations. Figure 76 shows the initial distance between the rigid links and the angles relative to the vertical created by connecting these links (17°, 2°, and -43° for the upper thoracic, lower thoracic, and pelvic links, respectively). These angles were obtained from the TAD seated as in a sternal impact test. For sled tests, it was assumed that the seat back angle (-23°) was equal to the lower thoracic spine link angle, since the lower spine lies along the seat back. Treating the links in Figure 76 as a rigid structure and rotating the lower spine rearward by -25°, one obtains the new angles for sled test seating. The angles for the pelvic, lower thoracic, and upper thoracic links then become -68° (22° from horizontal), -23°, and -8°, respectively.

The negative angles indicate that the spine is leaning backwards. The H-point was used as the pivot or "ground" for the figures, so the trajectory is drawn relative to the H-point. Therefore, the trajectory does not include any movement of the pelvis relative to the seat. If the path of the H-point had been included, the differences between tests would not have shown up as clearly.

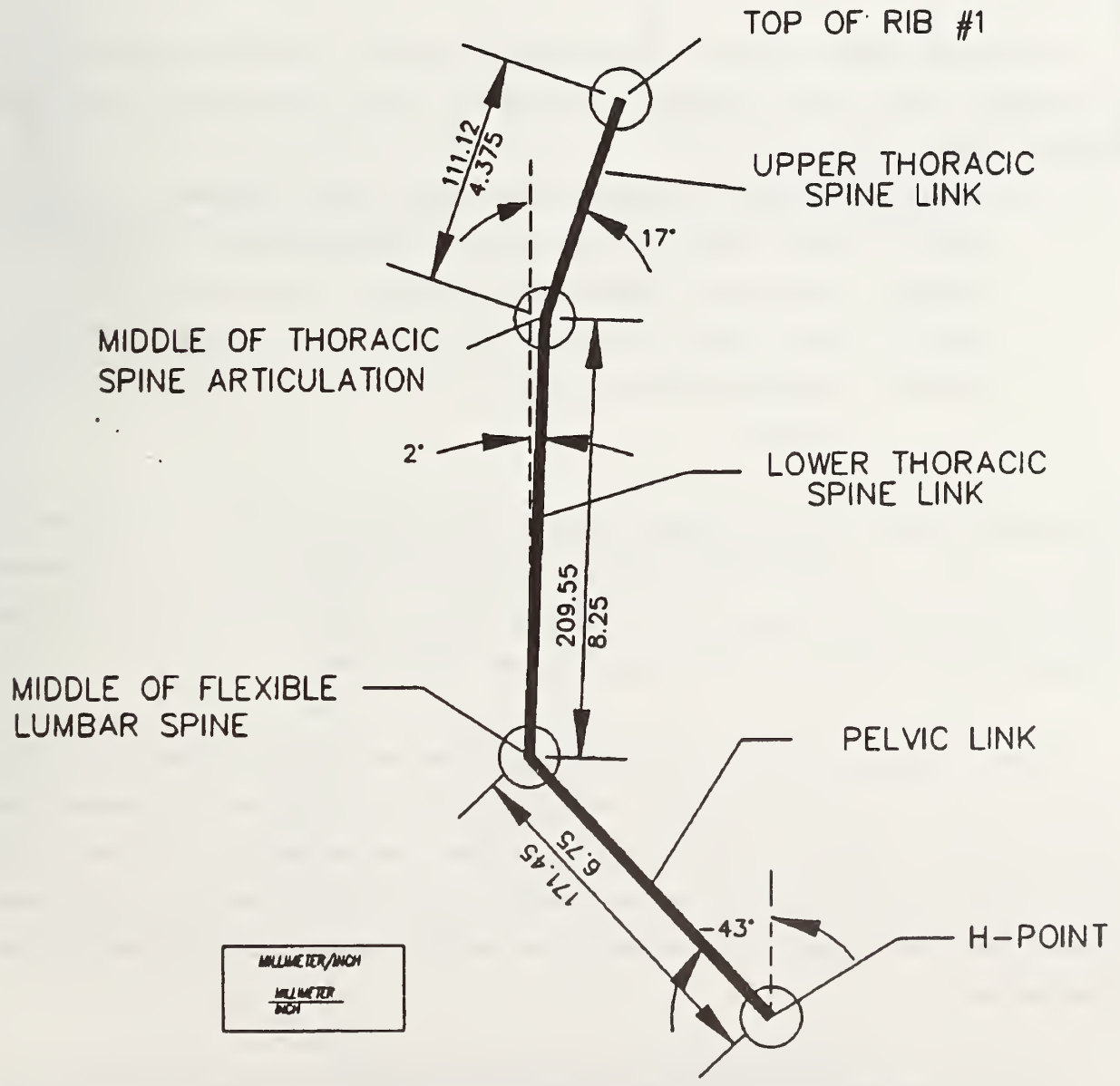

Figure 76. MHD "Stick Figure" Interpretation

Stick figures (Figures 77 - 79) are derived from the angular velocity sensors located at the upper spine, thoracic spine, and pelvis. The sensor locations are connected by the "sticks" in the figures (Figure 76). Integrating the MHD sensors provided the angular displacement associated with each sensor, which were then transformed into x and y coordinates for plotting. An extensive review of the MHD results will not be undertaken for all TAD tests. However, some interesting results will be pointed out for several tests.

The time histories for a three-point belt/ air bag test (test 472), a three-point belt test (test 475), and a lap belt/air bag test (test 478) appear in Figures 80 - 84. The following definitions correspond to Figures 80 - 84:

Figure 80. pelvis angle - angle between the pelvic link and the vertical

Figure 81. lumbar angle - angle between lower thoracic spine link and vertical

Figure 82. thoracic angle - angle between upper thoracic spine link and vertical

Figure 83. lumbar bending - angle between pelvic link and lower thoracic spine link

Figure 84. thoracic bending - angle between lower thoracic spine link and upper thoracic spine link.

The lap belt/air bag tests display the greatest degree of change in pelvic, lumbar, and thoracic angles (Figures 80 - 82). This occurs because the lap belt holds the pelvis and allows rotation of the thorax about the pelvis; it may also suggest pelvic rotation about the lap belt. The angles in these three figures correspond mostly to flexion in the TAD's upper and lower flexible spine.

When comparing results of three-point belt tests with and without air bags (tests 472 and 475, respectively), the test with the air bag displays less change in thoracic angle (Figure 82) compared to the same test condition without the air bag. The air bag apparently reduced bending at the upper thoracic spine, although as discussed earlier, it did not change the chest deflections very much. The thorax traveled further in tests without the air bag before it slowed down, caused either by the steering wheel or the seat belt.

Figure 83 illustrates the relative change of the angle between the pelvic link and the lower thoracic spine link. This angle relates directly to the amount of lumbar spine bending, and shows that the spine bent about 33° for the 3 point/air bag test compared to about 41° for the lap belt/air bag test.

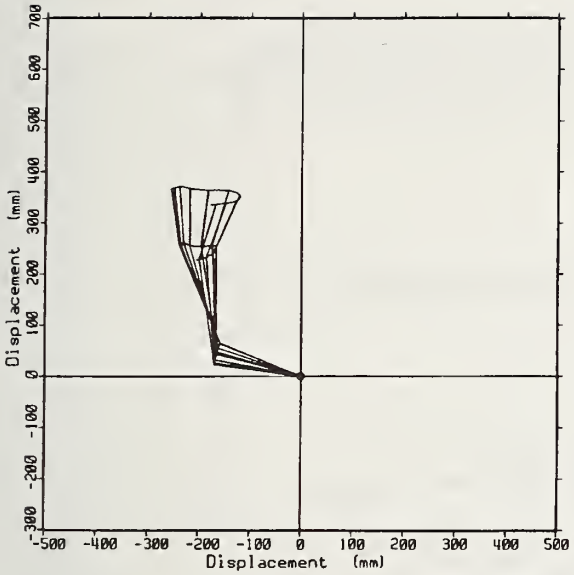

Figure 77. Stick Figure for TAD Test 472, a Three-Point Belt/Air Bag, 48 Kph Test

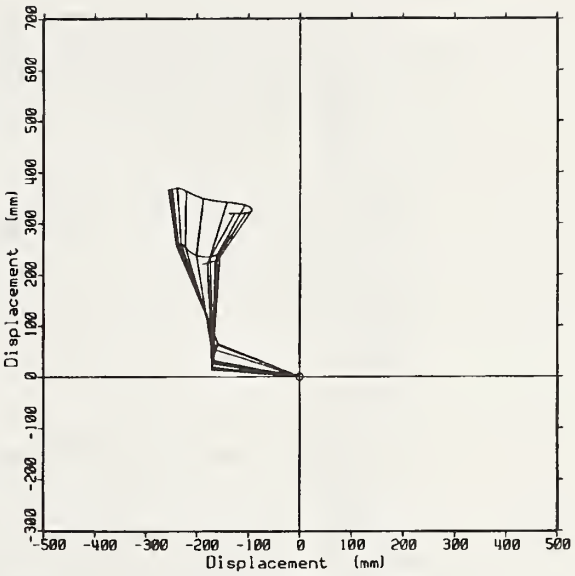

Figure 78. Stick Figure for TAD Test 475, a Three-Point Belt, 48 Kph Test

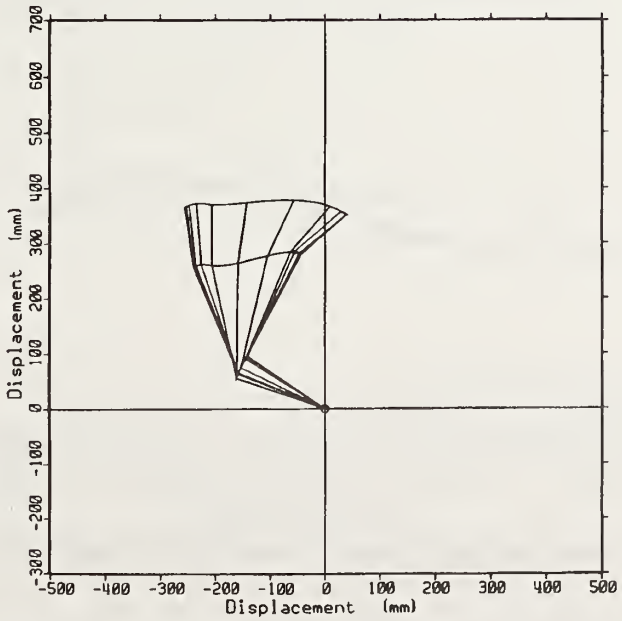

Figure 79. Stick Figure for TAD Test 478, a Lap Belt/Air Bag, 48 Kph Test

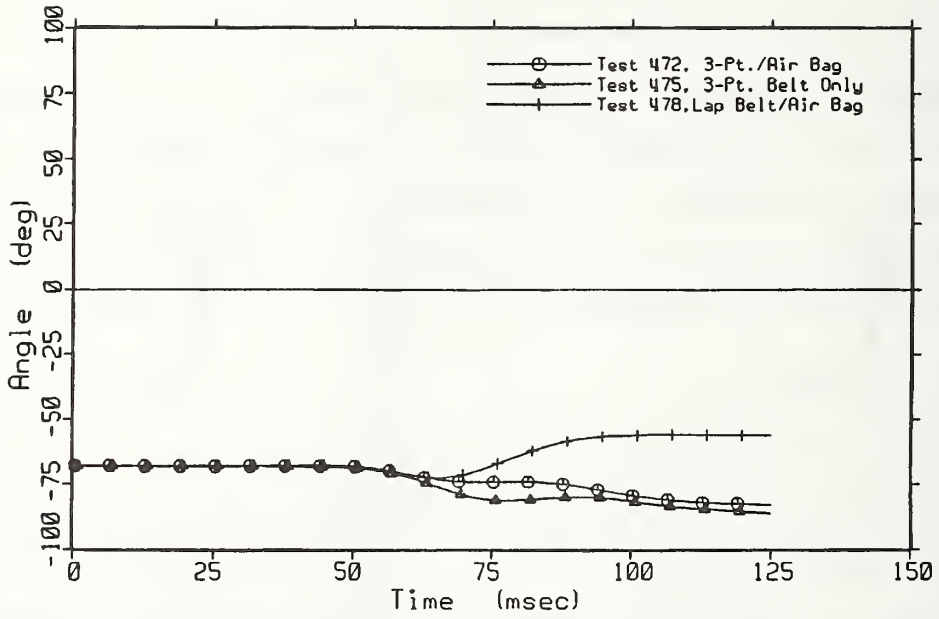

Figure 80. Pelvis Angles as Derived From MHD Analysis

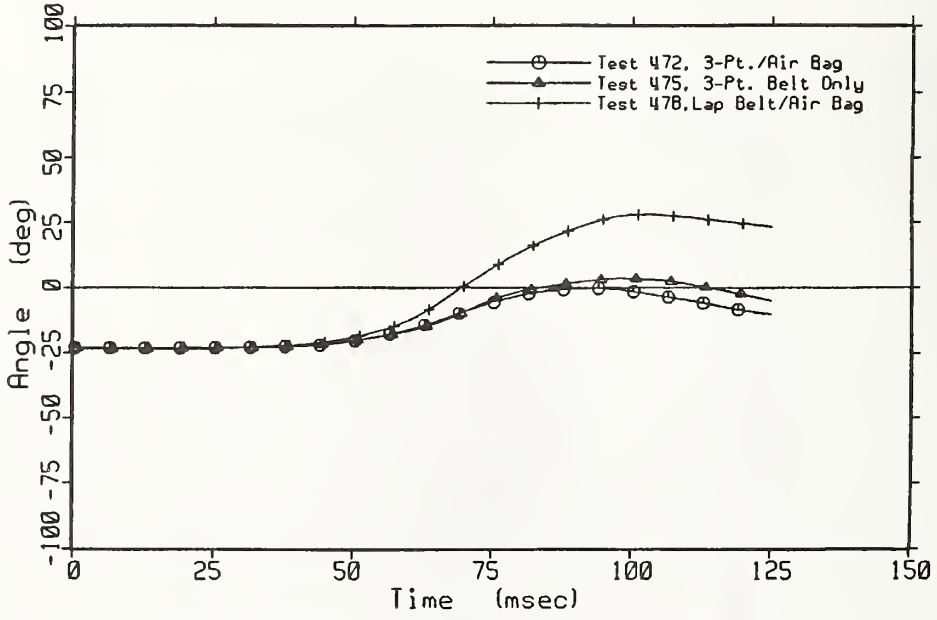

Figure 81. Lumbar Angles as Derived From MHD Analysis

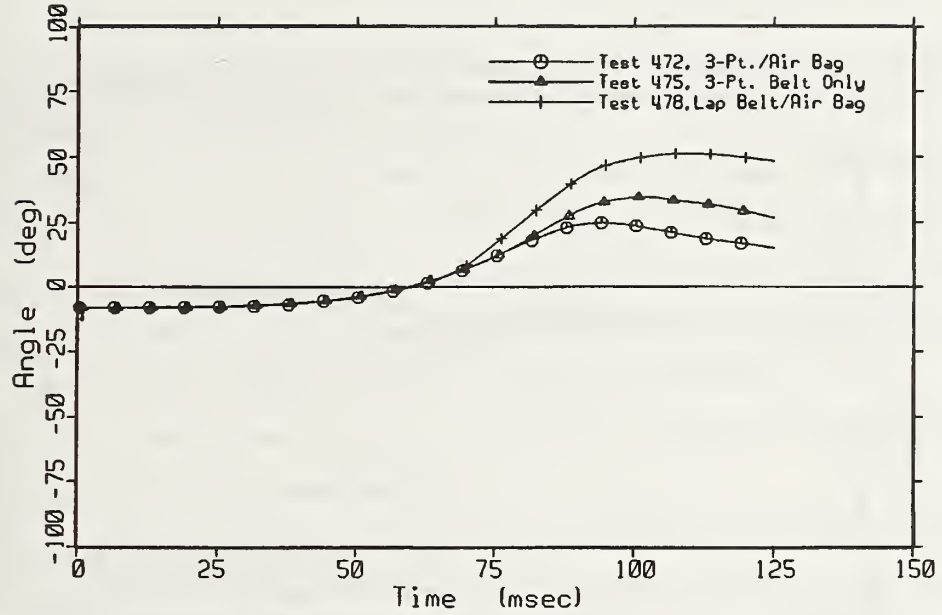

Figure 82. Thoracic Angles as Derived From MHD Angles

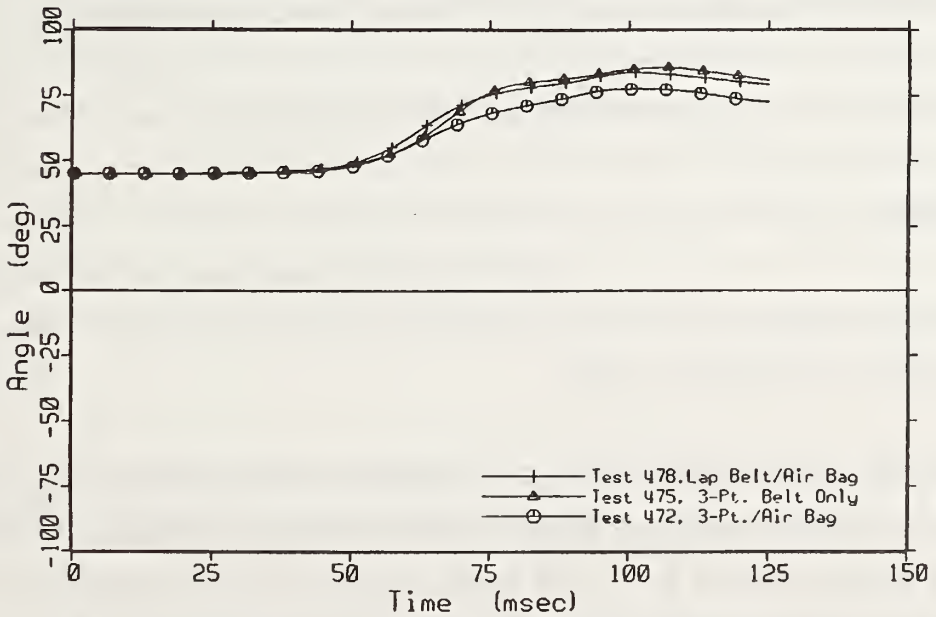

Figure 83. Lumbar Bending as Derived From MHD Analysis

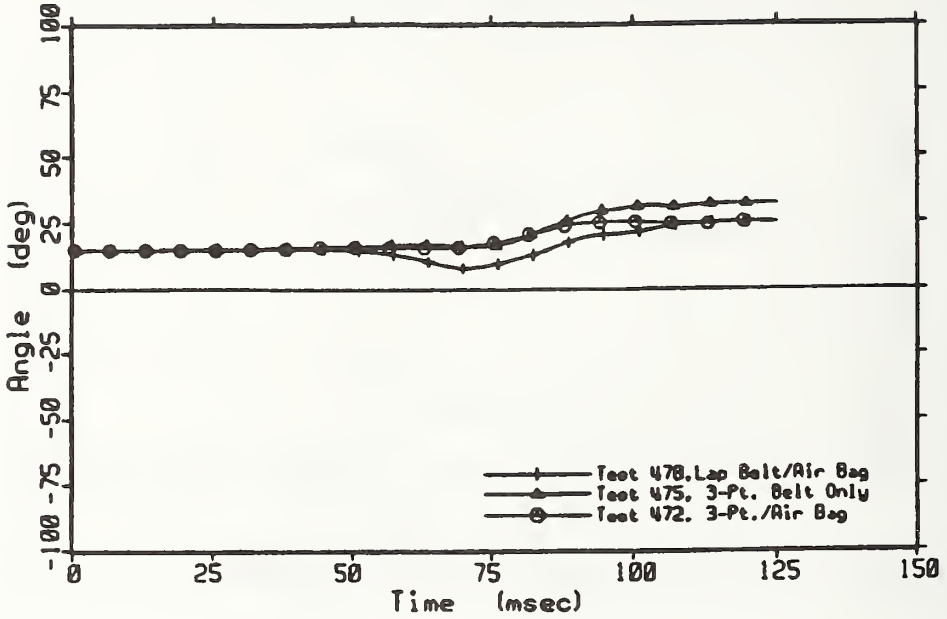

Figure 84. Thoracic Bending as Derived From MHD Analysis

Similarly, Figure 84 shows the relative change in angle of the upper and lower spine links and indicates the amount of bending that occurs in the articulated spine. This is about 10° for the 3 point/air bag and the lap belt/air bag tests and a maximum of about 17° for 3 point belt only test.

The stick figure plots for the remainder of the TAD sled tests appear in Appendix C.

CONCLUSIONS

Based on the results of this test series, the following conclusions can be drawn with regards to the performance of the TAD-50M thorax system:

1. The TAD thorax meets the desired Kroell pendulum corridors at the sternum at 6.7 m/s and Neathery provisional 4.3 m/s corridor at the lower ribcage. However, in a manner similar to the Hybrid III (6), the thorax falls short of the 4.3 m/s Kroell pendulum corridor at the sternum and may be somewhat stiff at low impact speeds.

2. The TAD thorax system can apparently discriminate the different types of restraint loading, asymmetry in restraint loading, and the intensity of local loading to the sternal region and lower ribcage. No assessment of the TAD response biofidelity under these conditions was made.

3. The TAD appears durable based on its extensive use in pendulum and sled tests without significant structural or functional failures.

4. When compared to the response of the Hybrid III tested in the same configuration, the TAD thorax responds in a more decoupled manner. The left and right sides of the thorax as well as the upper and lower ribs, were not constrained to act as a unit, but were able to move somewhat independently. In addition, the TAD's thorax design is such that it specifically allows for rib movement (and measurement) in the Z direction which the Hybrid III thorax does not address.

5. The MHD's located in the TAD spine provided useful information regarding the effect of various restraint systems on TAD's articulated spine.

6. Head excursion in the 48-kph, three-point belt test for the TAD indicates that the TAD's head traveled approximately 8 cm farther than the Hybrid III in similar test conditions. This may be partially attributed to the additional compliance of the TAD thorax and the contribution of the articulated spine. However, differences in posture between the two dummies accounted for an increased initial clearance between the wheel and the head of the TAD, thus allowing the TAD's head to travel approximately 8 cm more than the Hybrid III before wheel contact.

7. Both TAD and Hybrid III HIC's exceeded 1000 in all three-point belt tests conducted in this study. In the two comparable configurations, the TAD HIC's were slightly higher than the Hybrid III's. The largest HIC (2223) occurred in the TAD three-point belt/air bag test at 48-kph in the oblique configuration. HIC's were below 1000 in all other test conditions.

8. The highest resultant chest G's occurred in a TAD air bag test without belt restraint. Although chest G's were similar between the TAD and Hybrid III in the 48-kph three-point belt and three-point belt/air bag tests, the TAD was slightly higher (2 to 6 G's).

REFERENCES

1. Hagedorn, A.V., Haffner, M.P., and Schneider, L.W.,"Performance of an Advanced ATD Thorax System in Frontal Crash Environments," Proc. IRCOBI Conference, 1992.

2. Schneider, L.W., Salloum, M.J., Beebe, M.S., Rouhana, S.W., King, A.I., and Neathery, R.F.,"Design and Development of an Advanced ATD Thorax System for Frontal Crash Environments: Final Report; Volume I: Primary Concept Development," U.S. Department of Transportation, National Highway Traffic Safety Administration, 1992.

3. Kroell, C.K., Schneider, D.C., and Nahum,A.M., "Impact Tolerance and Response to the Human Thorax," Proc. 15th Stapp Car Crash Conference, p. 84-134, Society of Automotive Engineers, Warrendale, PA, 1971.

4. Kroell, C.K., Schneider, D.C., and Nahum,A.M., "Impact Tolerance and Response to the Human Thorax II," Proc. 18th Stapp Car Crash Conference, p. 383-457, Society of Automotive Engineers, Warrendale, PA, 1974.

5. Neathery, R.F., "Analysis of Chest Impact Response Data and Scaled Performance Recommendations," Proc. 18th Stapp Car Crash Conference, 1974.

6. Foster, J.K., Kortge, J.O., and Wolanin, M.J., "Hybrid III - a Biomechanically Based Crash Test Dummy," Proceedings of the Twenty-first Stapp Car Crash Conference, Paper No. 770938, Society of Automotive Engineers, Warrendale, PA, 1977.

7. Schneider, L.W., King, A.I., and Beebe, M.S., "Design Requirements and Specifications: Thorax - Abdomen Development Task. Interim Report. Trauma Assessment Device Development Program," Report DOT HS 807 511, U.S. Department of Transportation, National Highway Traffic Safety Administration, 1989.

8. Hagedorn, A.V., Eppinger, R.H., Morgan, R.M., Pritz, H.B., And Khaewpong, N., "Application of a Deformation Measurement System to Biomechanical Systems," Proc. IRCOBI Conference, 1991.

9. Hagedorn, A.V., "Evaluation of Chest Band Performance for Internal and External Chest Band Placement over the Hybrid III Thorax," Final Report in Preparation, U.S. Department of Transportation, National Highway Traffic Safety Administration, 1993.

10. Pritz, H.B., "Development and Evaluation of Hybrid III Multi-Point Thoracic Deflection Measurement Sensors," Report DOT HS 807 948, U.S. Department of Transportation, National Highway Traffic Safety Administration, 1990.

APPENDIX A

Sled Test Accelerations and Velocities

VRTC , TAD01
TAD TORSO EVALUATION
92057
SLDXG

FILTER = BLPP 100/ 250/ -16
MIN. MAX VALUES = -23.47 @ 50.00 , 0.65 @ 177.50

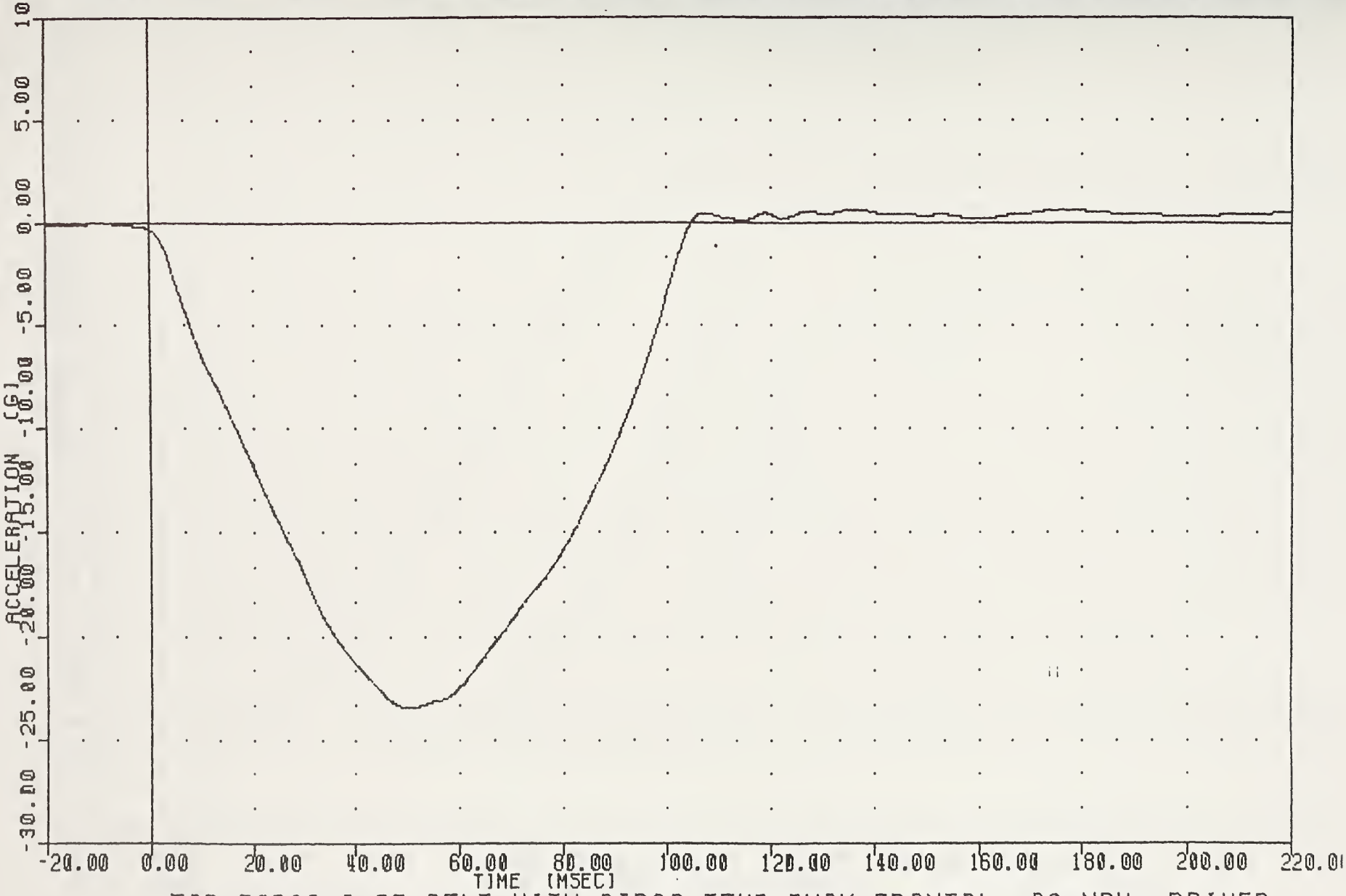

TAD TORSO;3 PT BELT WITH AIRAG;TEMP BUCK;FRONTAL; 30 MPH; DRIVER
SLED ACCELERATION X AXIS

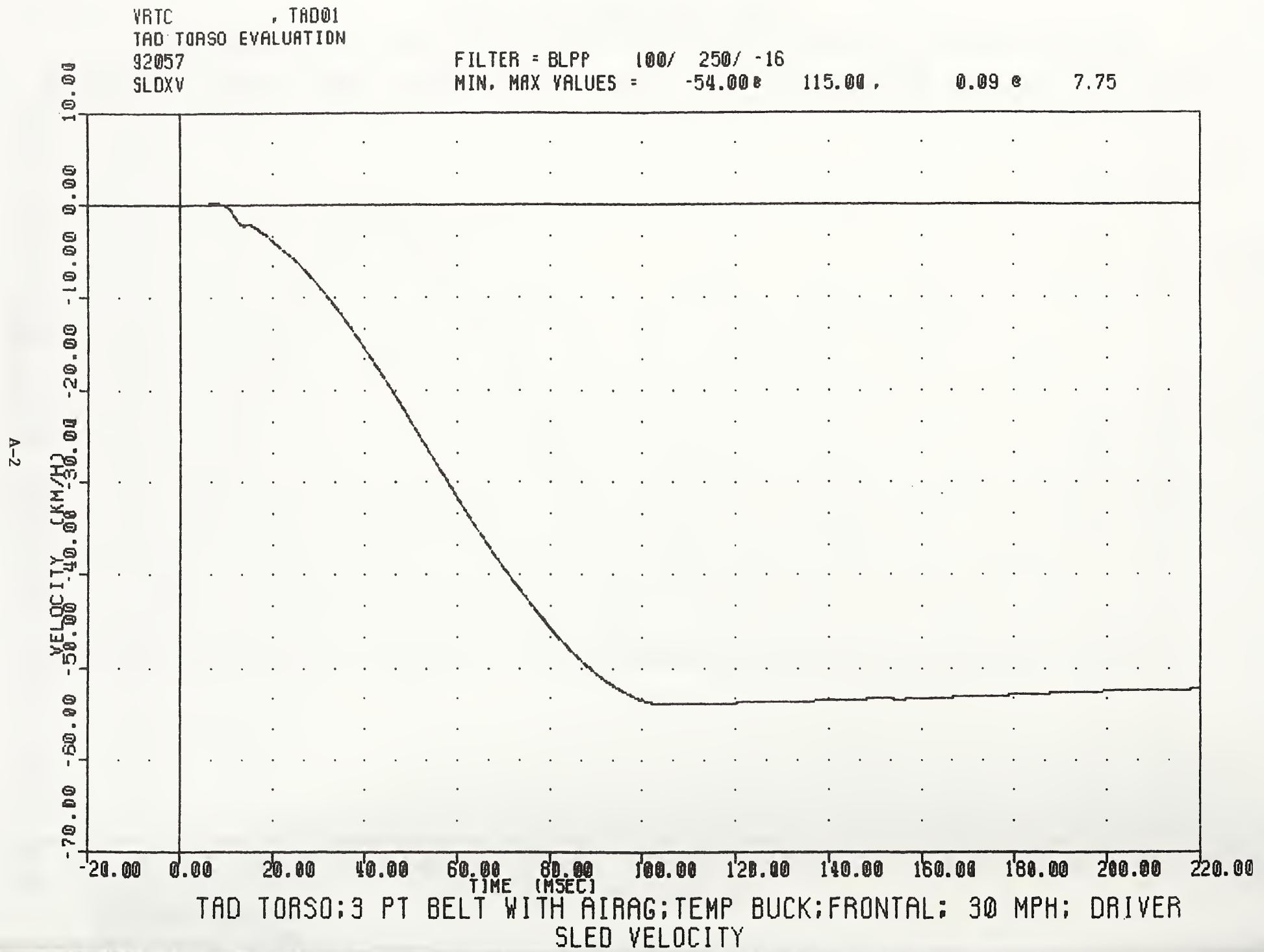

TAD TORSO;3 PT BELT WITH AIRAG;TEMP BUCK;FRONTAL; 30 MPH; DRIVER
SLED VELOCITY

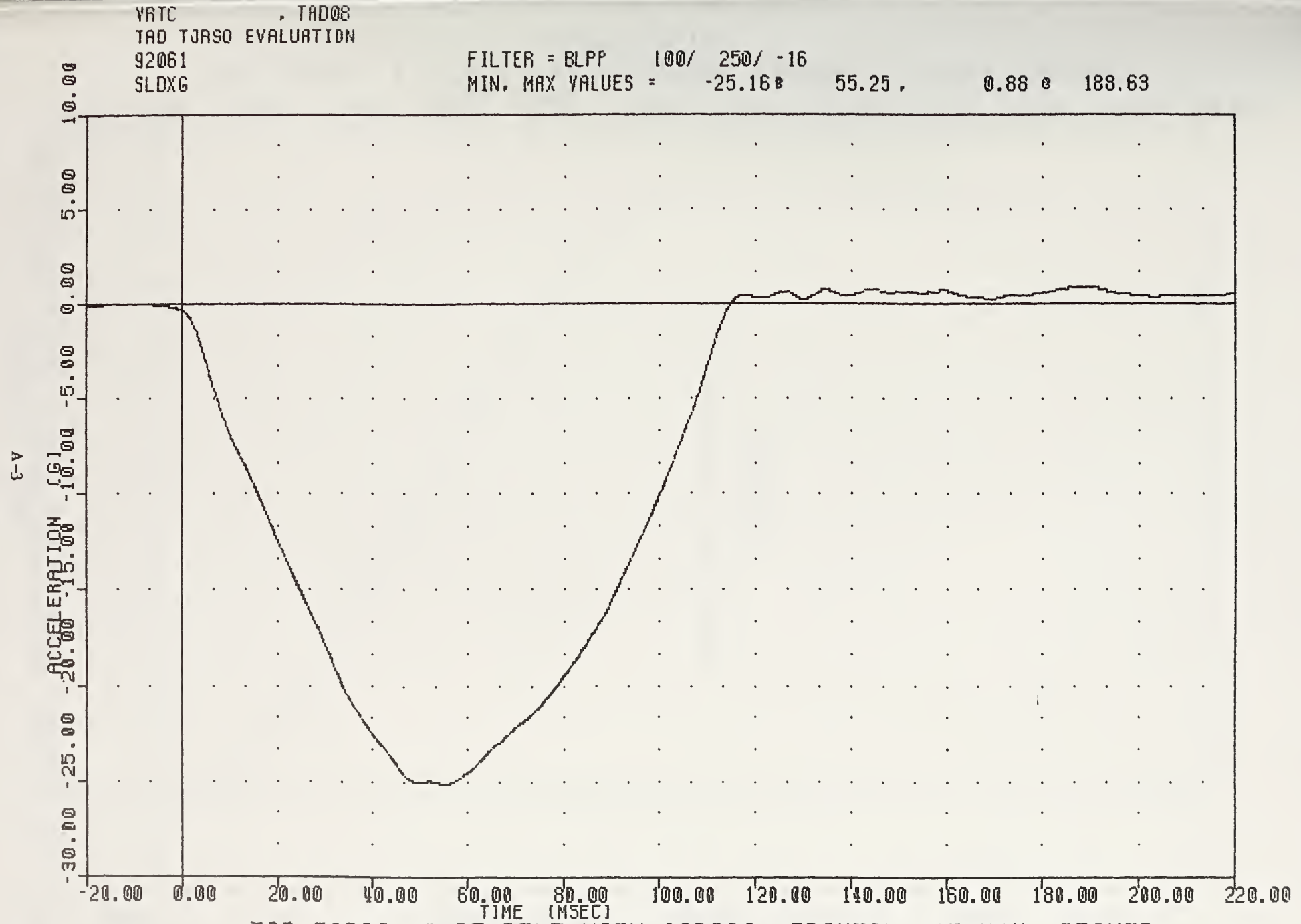

TAD TORSO; 3 PT BELT WITH AIRBAG; FRONTAL; 35 MPH; DRIVER
SLED ACCELERATION X AXIS

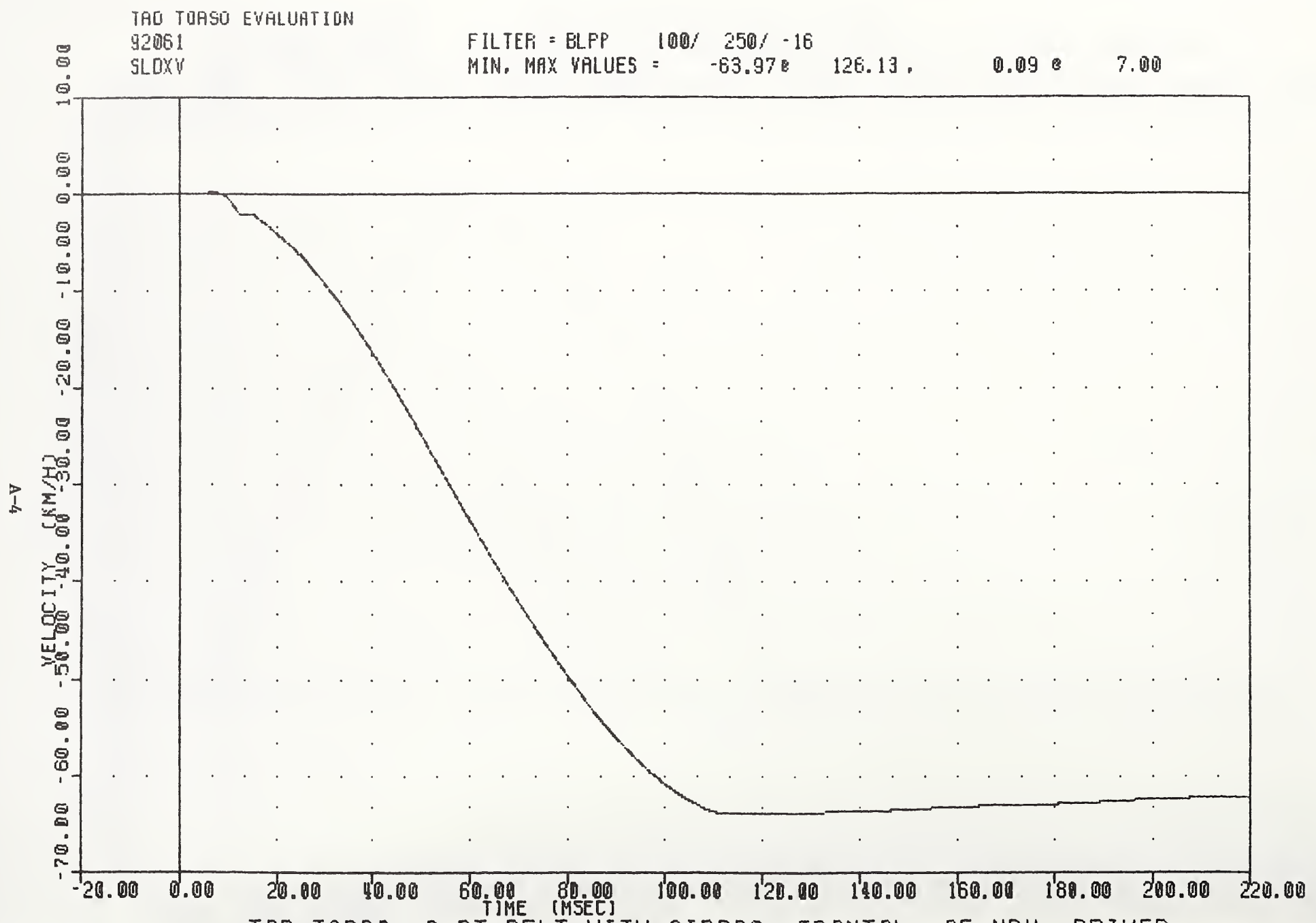

TAD TORSO; 3 PT BELT WITH AIRBAG; FRONTAL; 35 MPH; DRIVER
SLED VELOCITY

APPENDIX B

TAD Chest Band Plots: Selected Examples

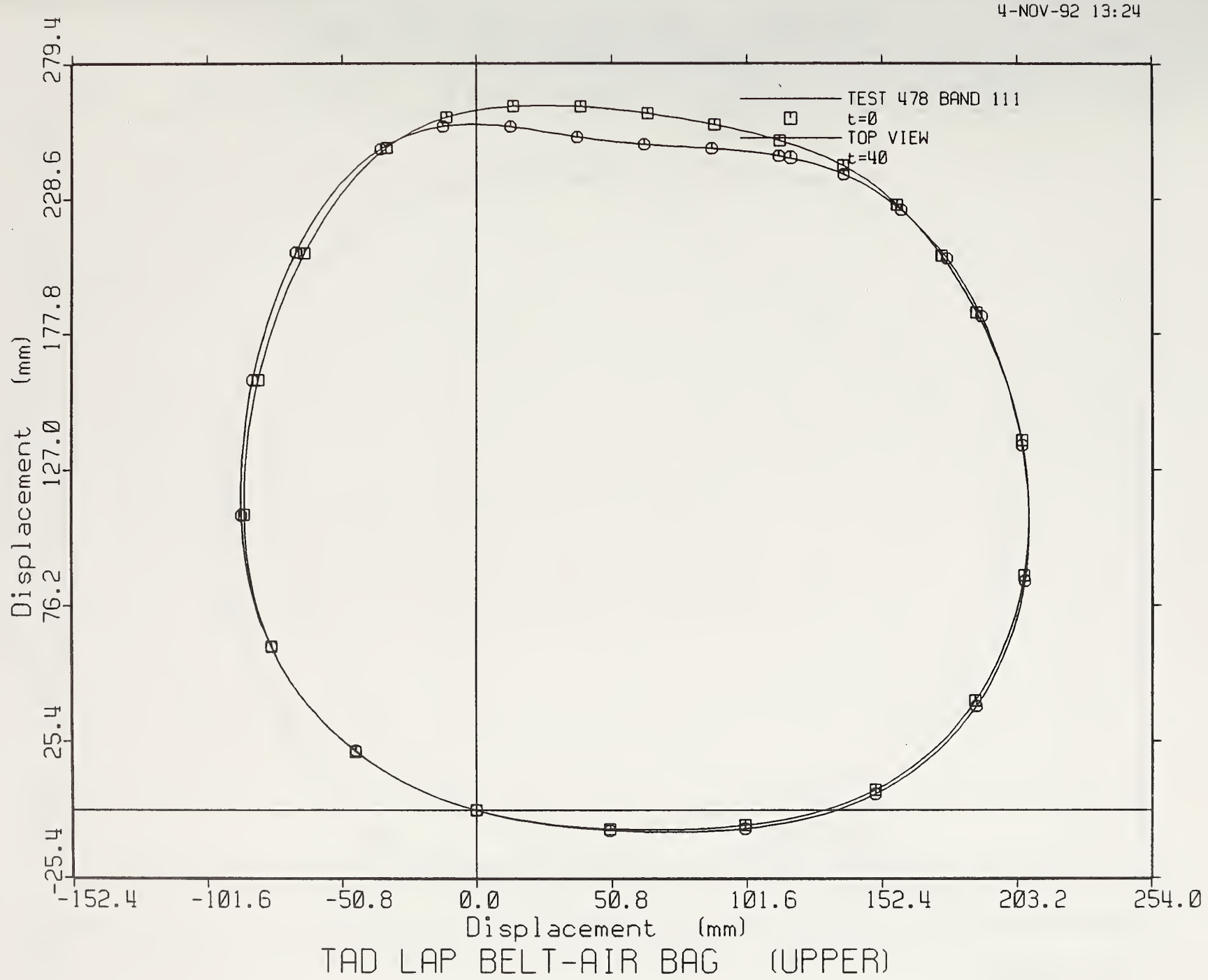
4-NOV-92 13:24
TEST 478 BAND 111
t=0
TOP VIEW
t=40
279.4
228.6
177.8
127.0
76.2
25.4
-25.4
Displacement (mm)
-152.4
-101.6
-50.8
0.0
50.8
101.6
152.4
203.2
254.0
Displacement (mm)
TAD LAP BELT-AIR BAG (UPPER)

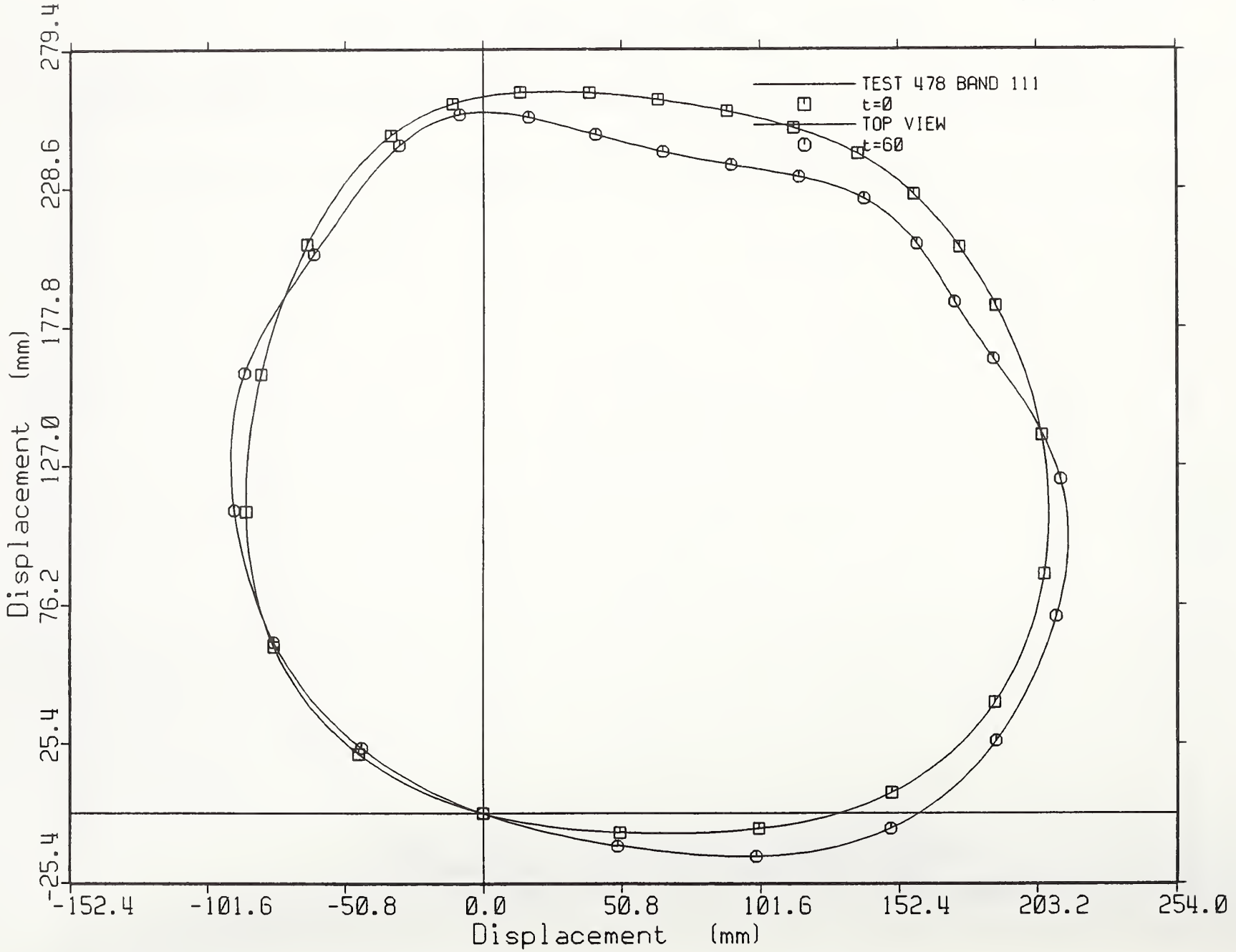

TAD LAP BELT-AIR BAG (UPPER)

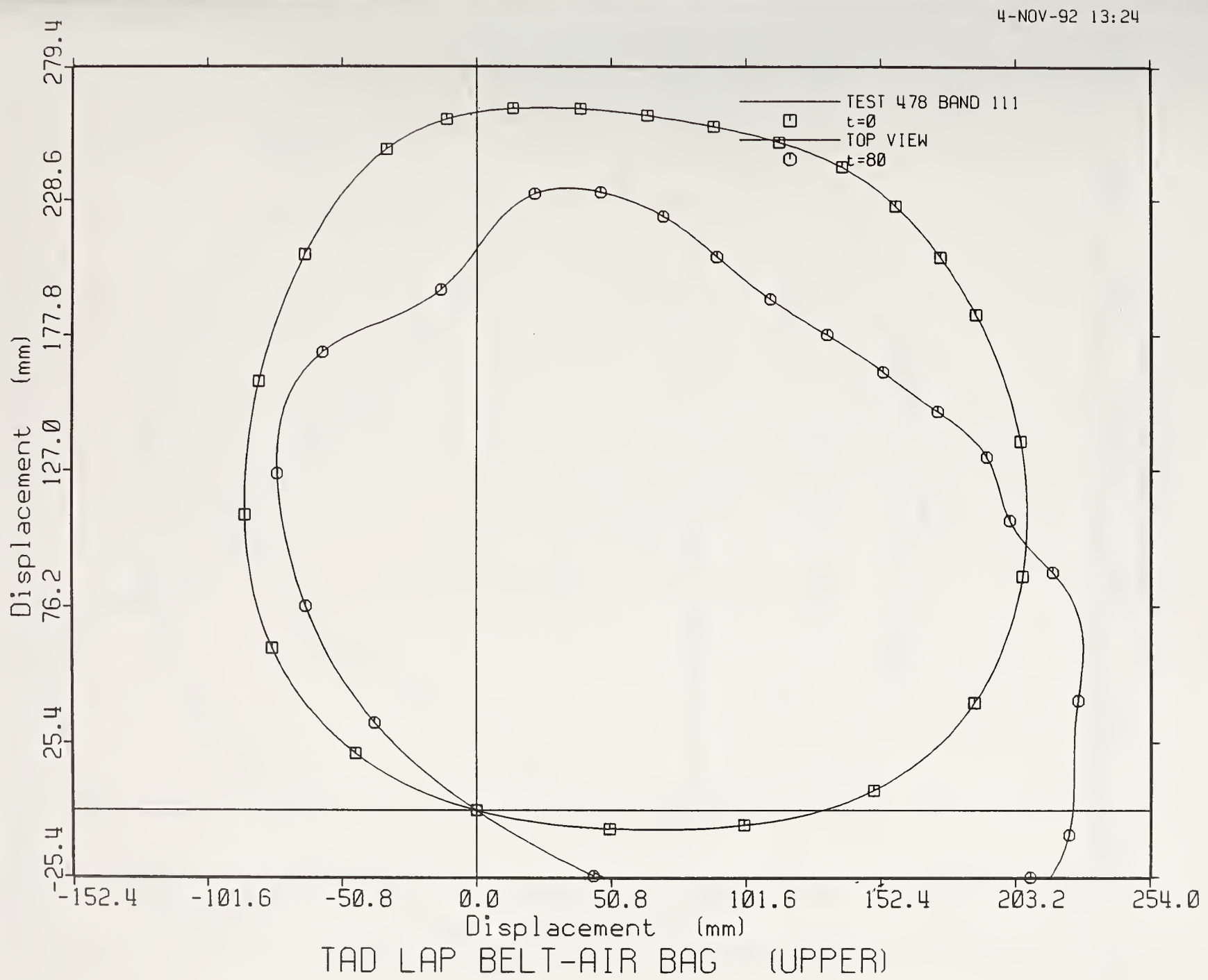
4-NOV-92 13:24
TEST 478 BAND 111
t=0
TOP VIEW
t=80
279.4
228.6
177.8
127.0
76.2
25.4
-25.4
Displacement (mm)
-152.4
-101.6
-50.8
0.0
50.8
101.6
152.4
203.2
254.0
Displacement (mm)
TAD LAP BELT-AIR BAG (UPPER)

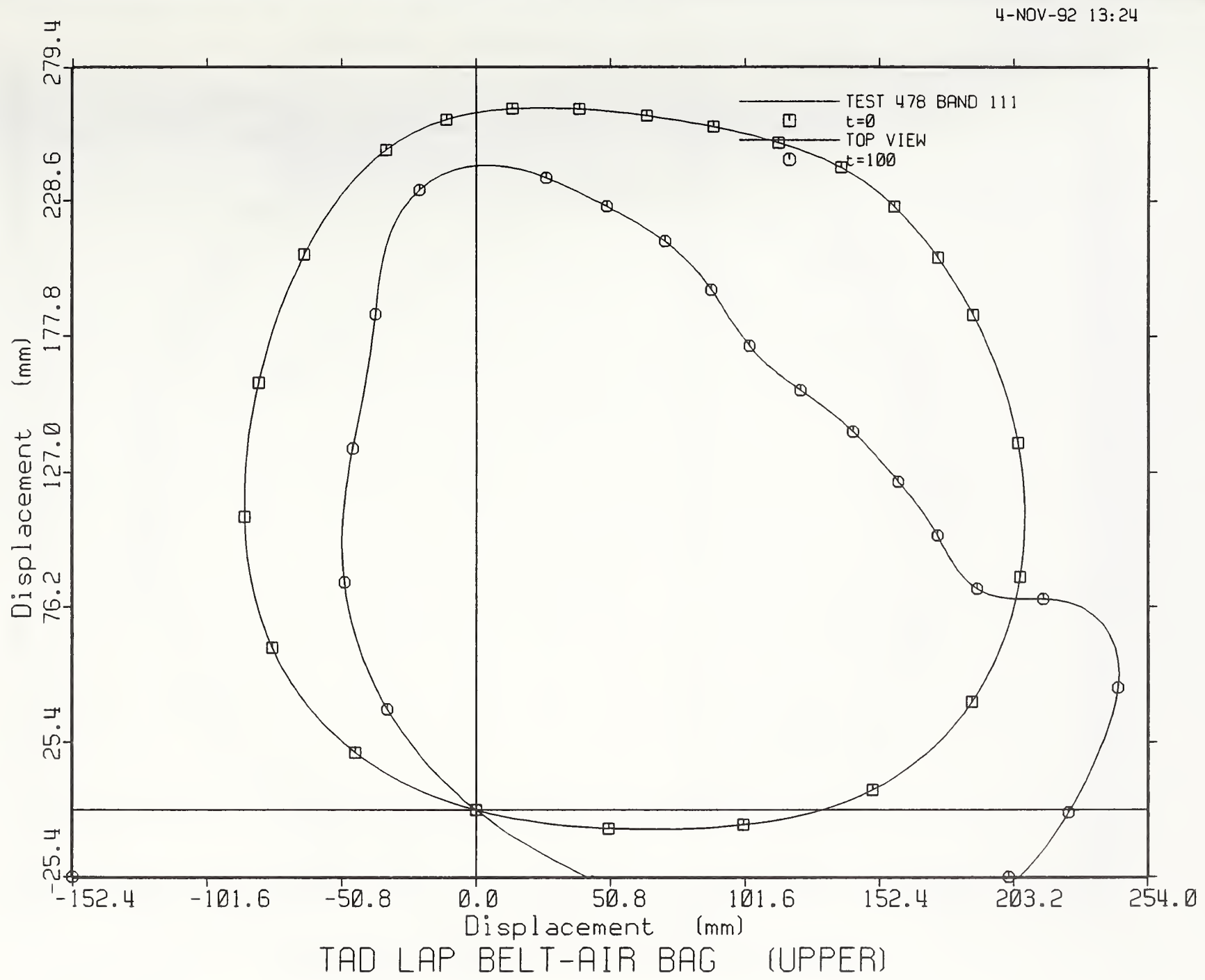
4-NOV-92 13:24
TEST 478 BAND 111
t=0
TOP VIEW
t=100
279.4
228.6
177.8
127.0
76.2
25.4
-25.4
Displacement (mm)
-152.4
-101.6
-50.8
0.0
50.8
101.6
152.4
203.2
254.0
Displacement (mm)
TAD LAP BELT-AIR BAG (UPPER)

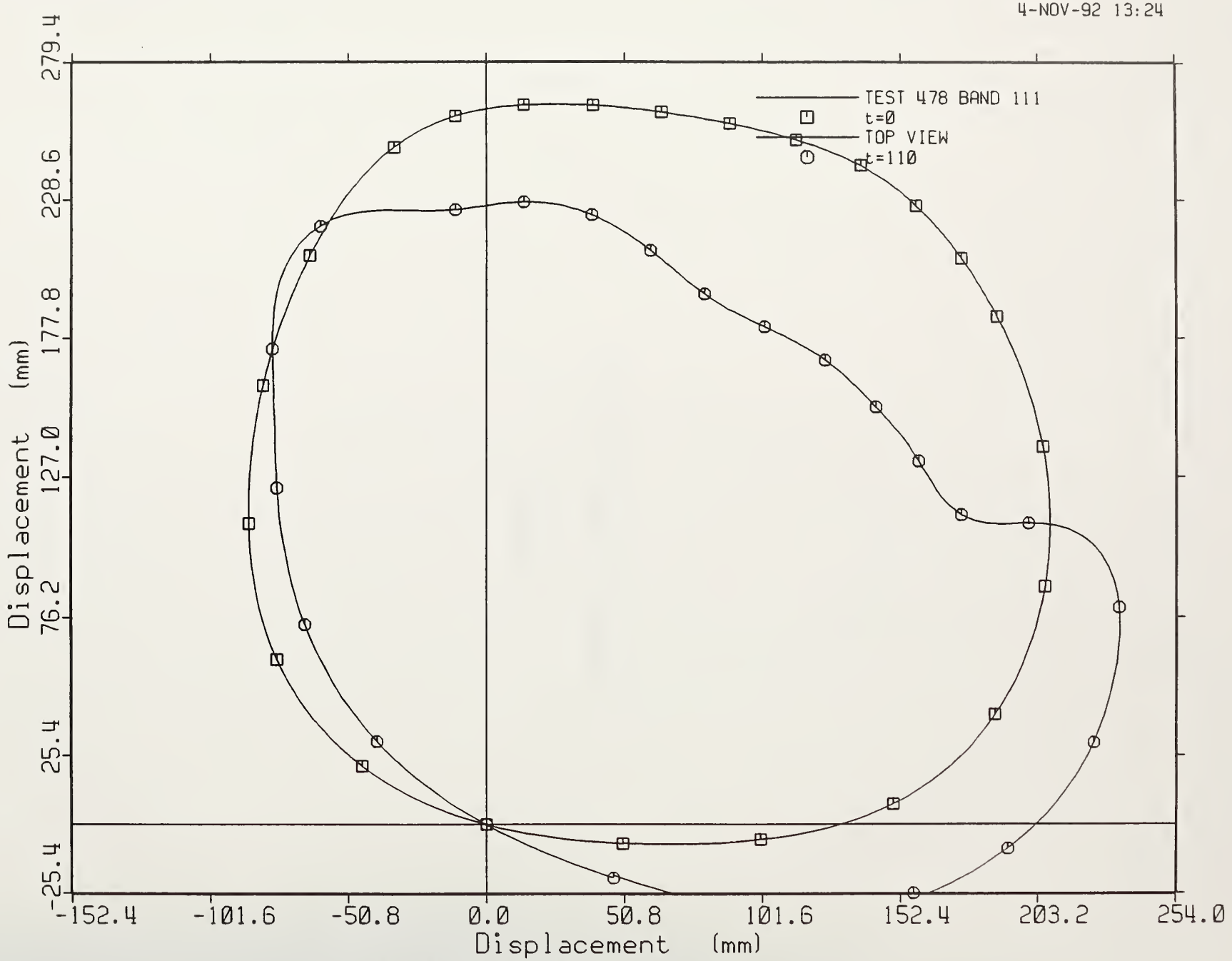

TAD LAP BELT-AIR BAG (UPPER)

APPENDIX C

TAD Sled Test MHD Plots (All Tests)

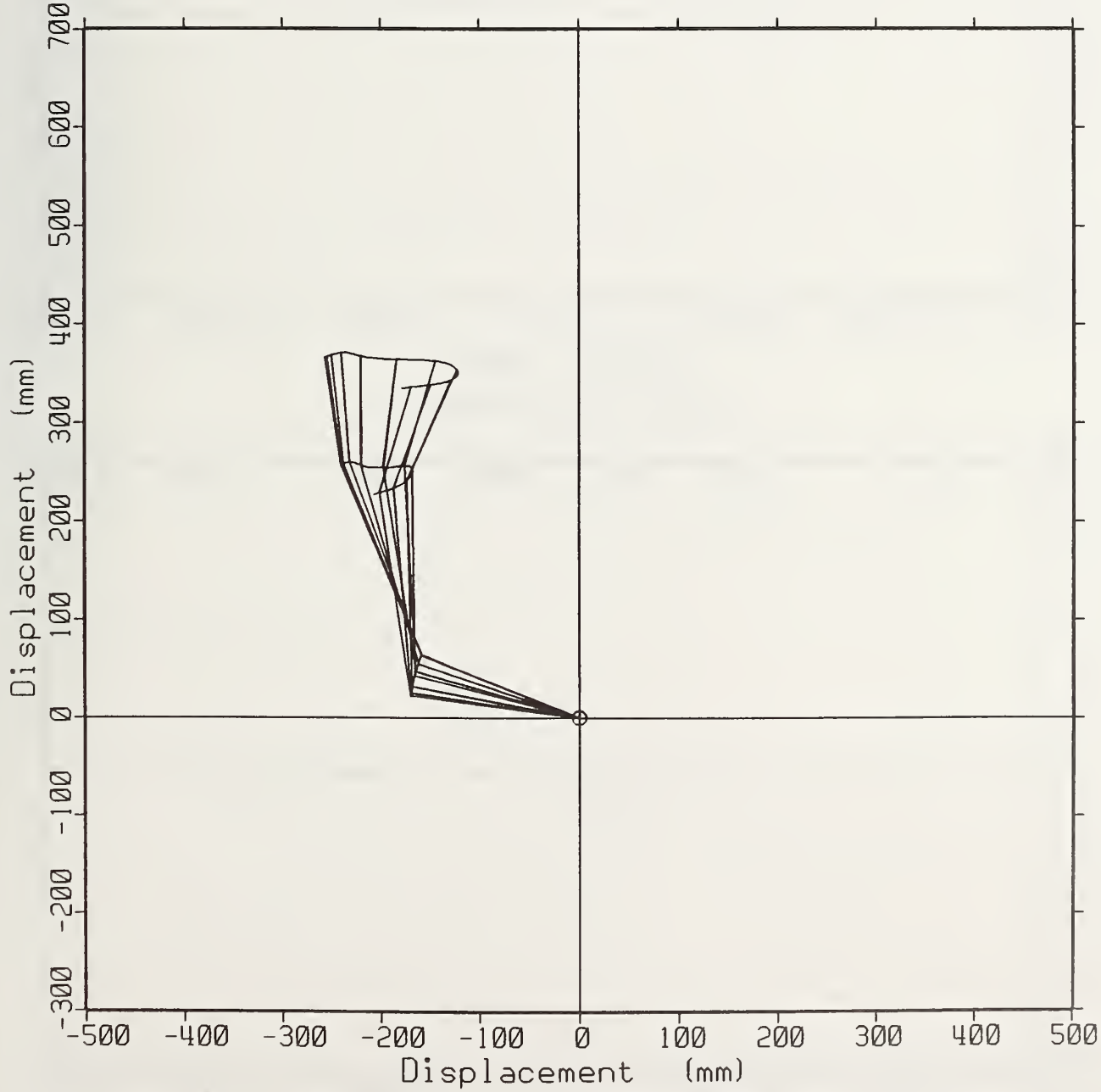

Spine Traj. SLED TEST 472 (3 PT/AB)

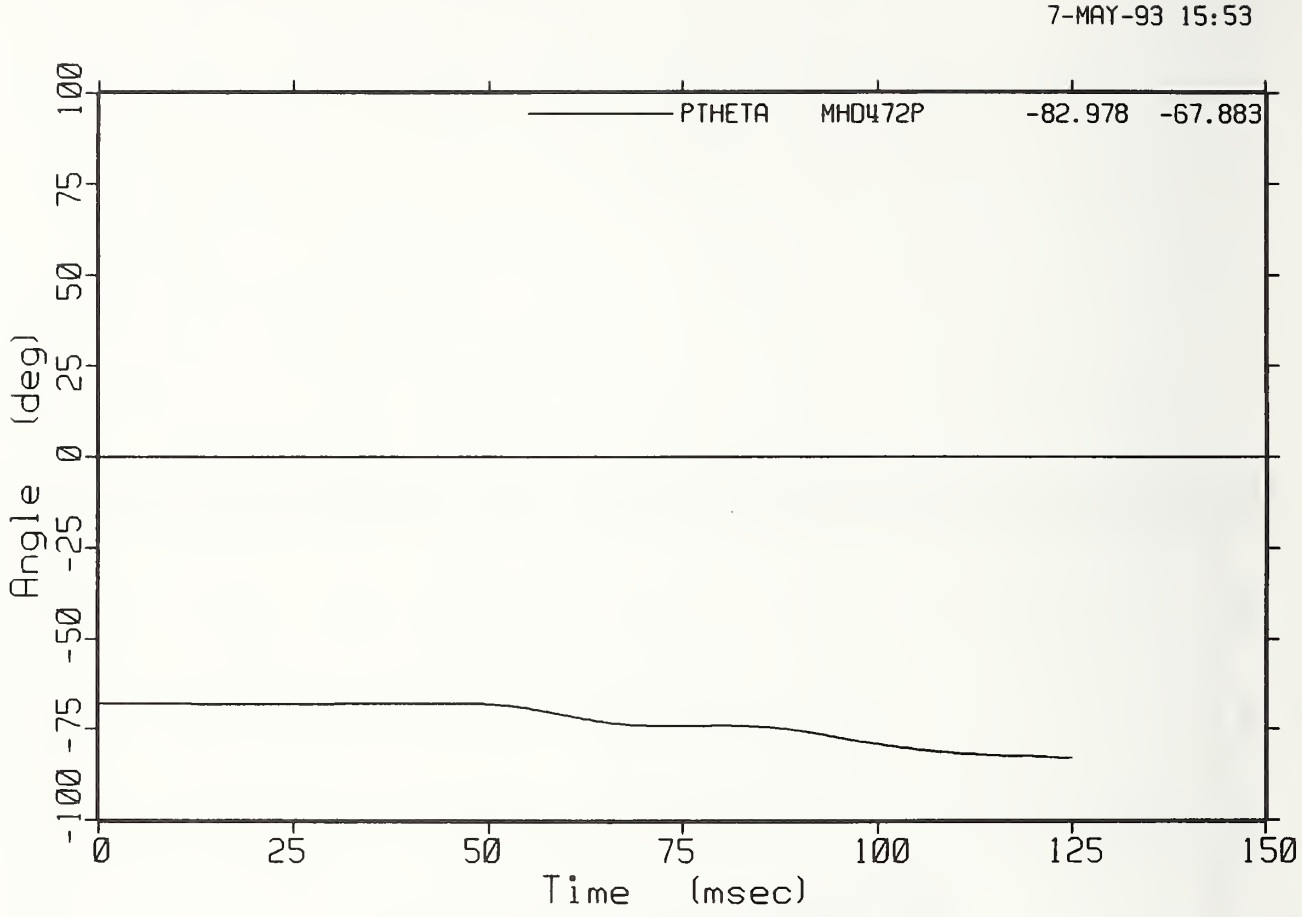

Pelvis angle

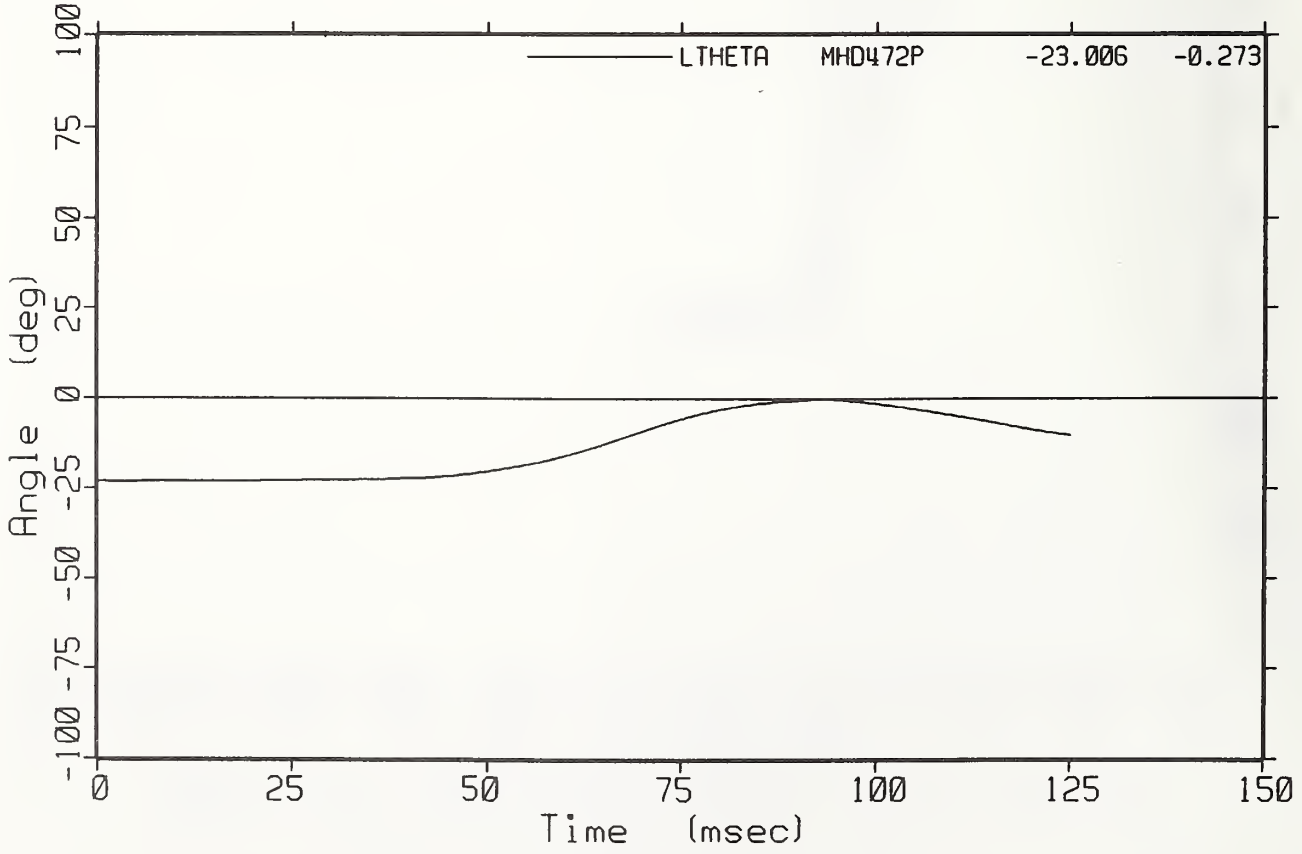

Lumbar angle

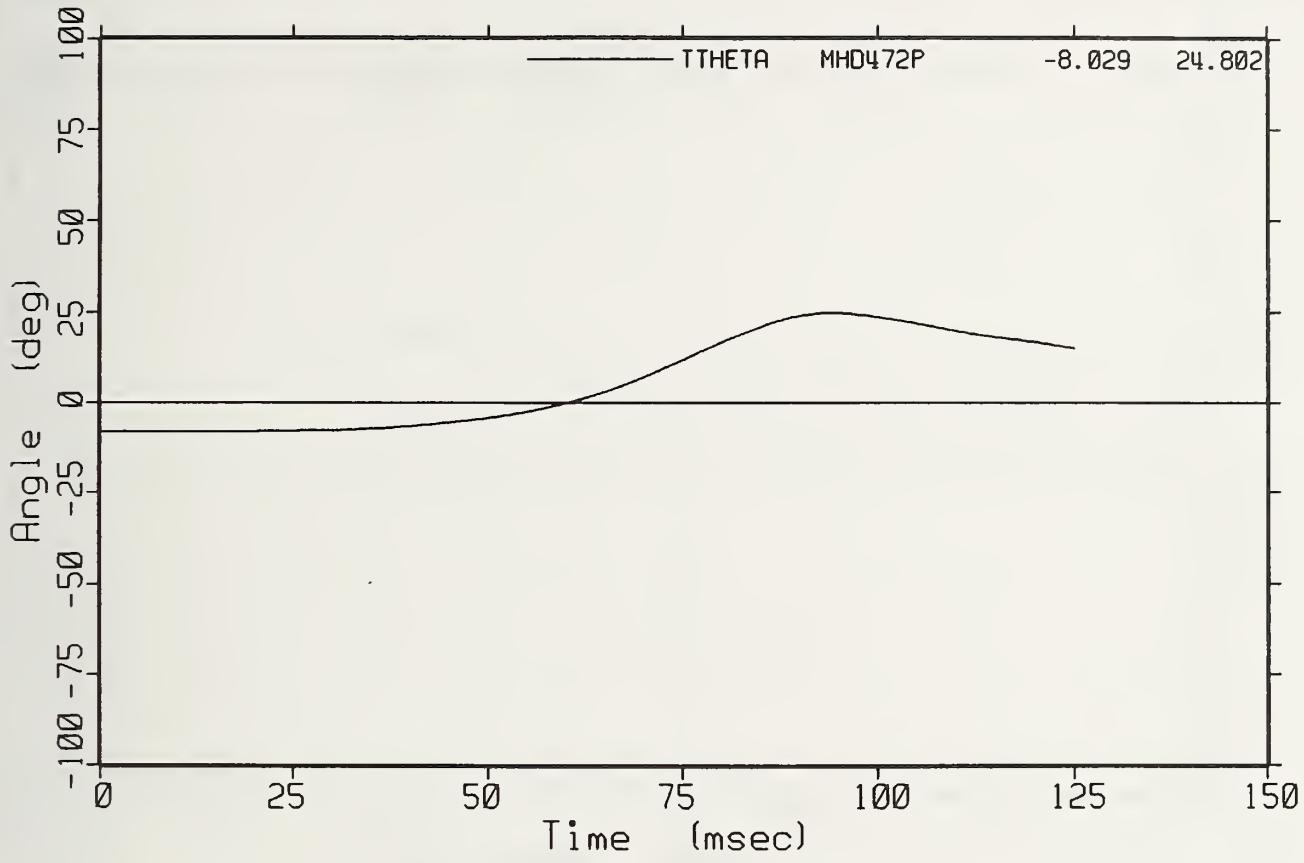

Thoracic angle

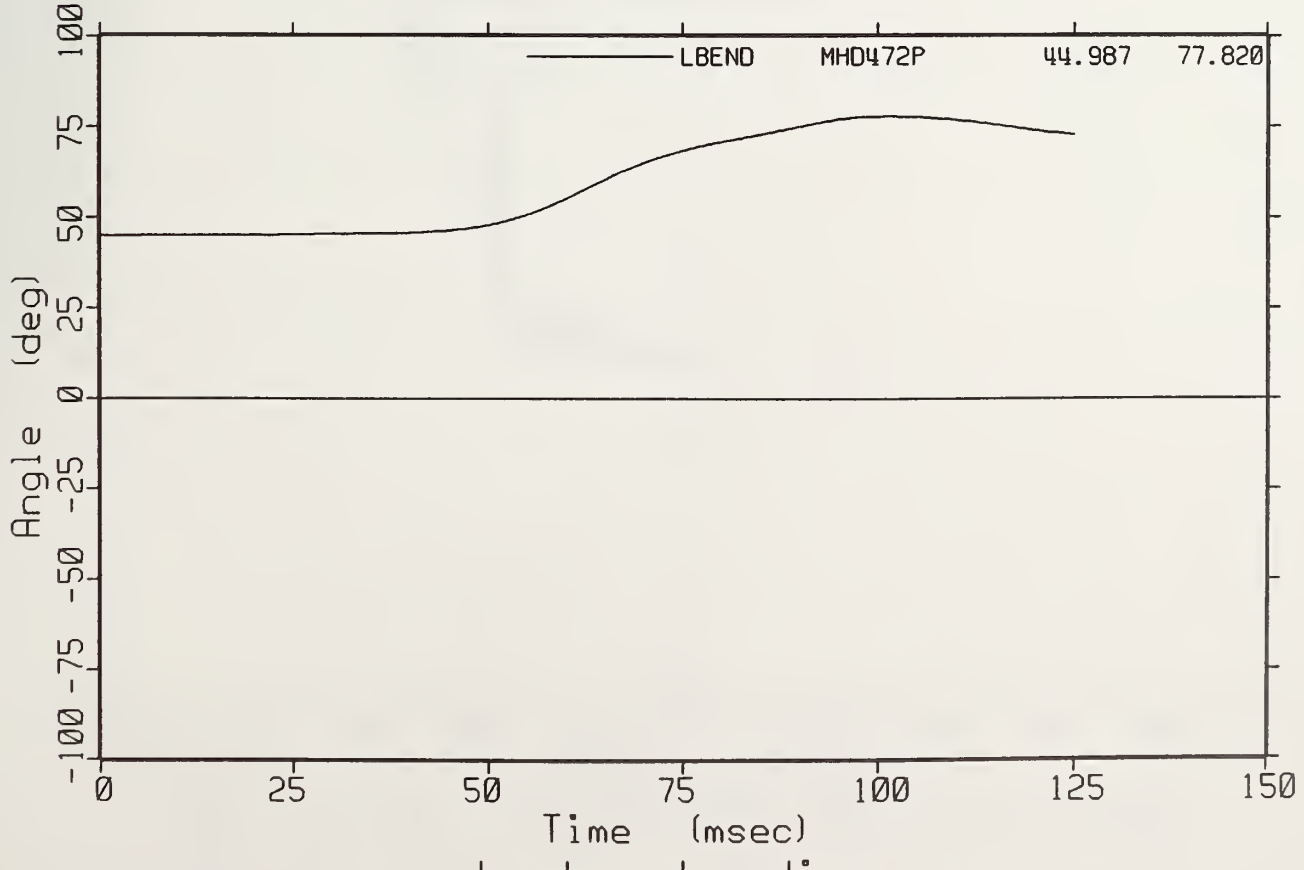

Lumbar bending

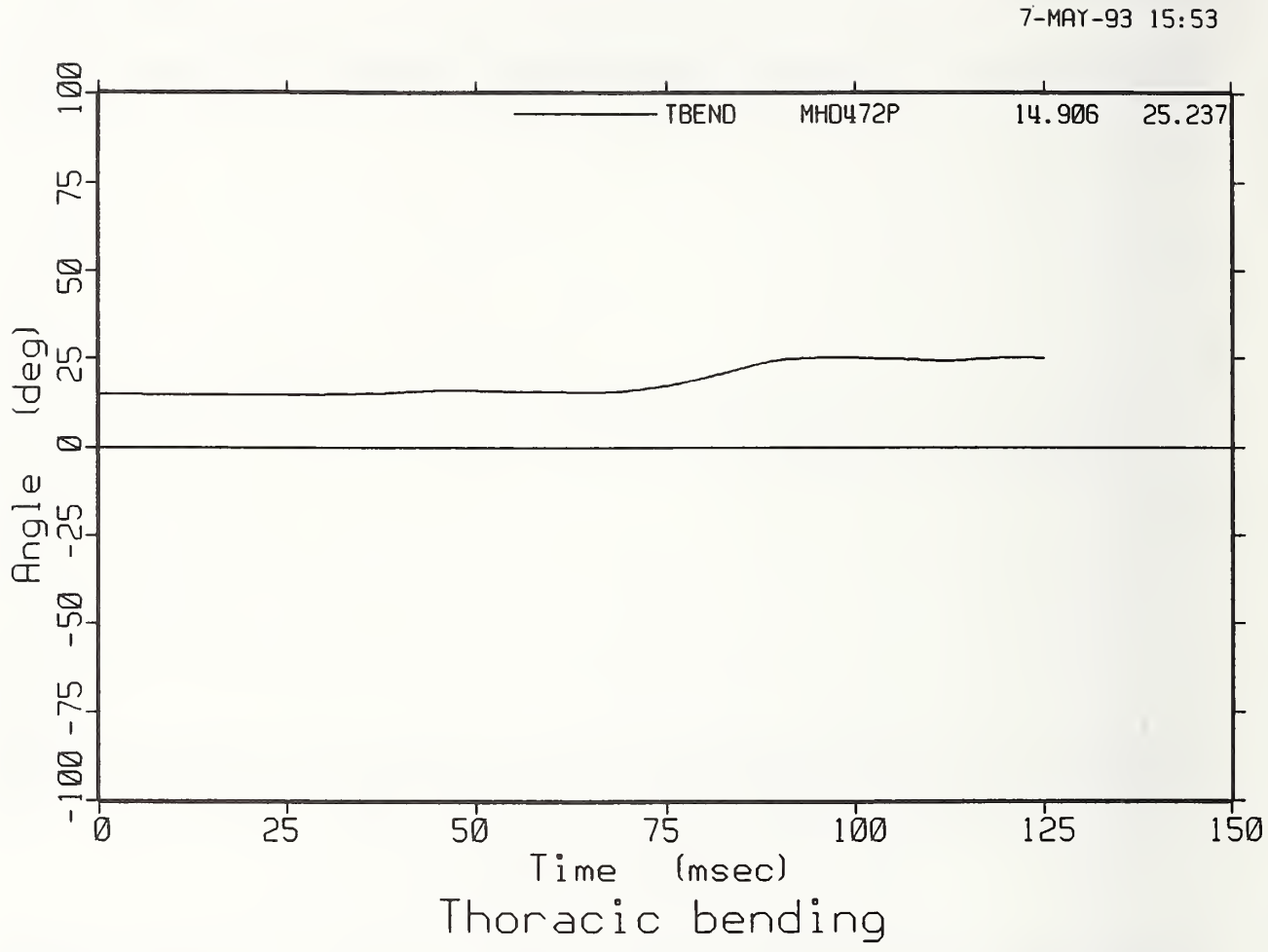

Thoracic bending

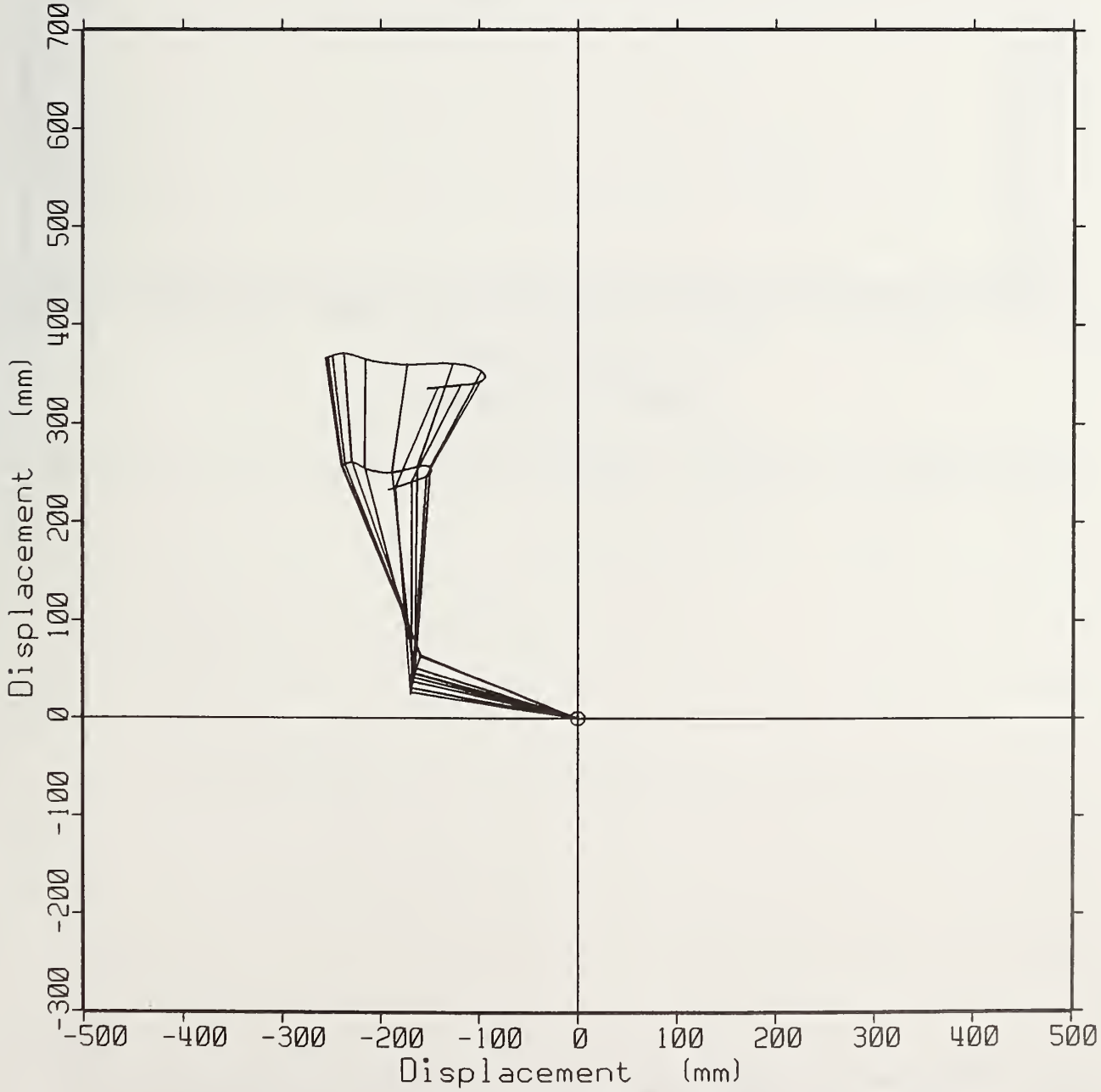

Spine Traj. SLED TEST 473 (3 PT/AB)

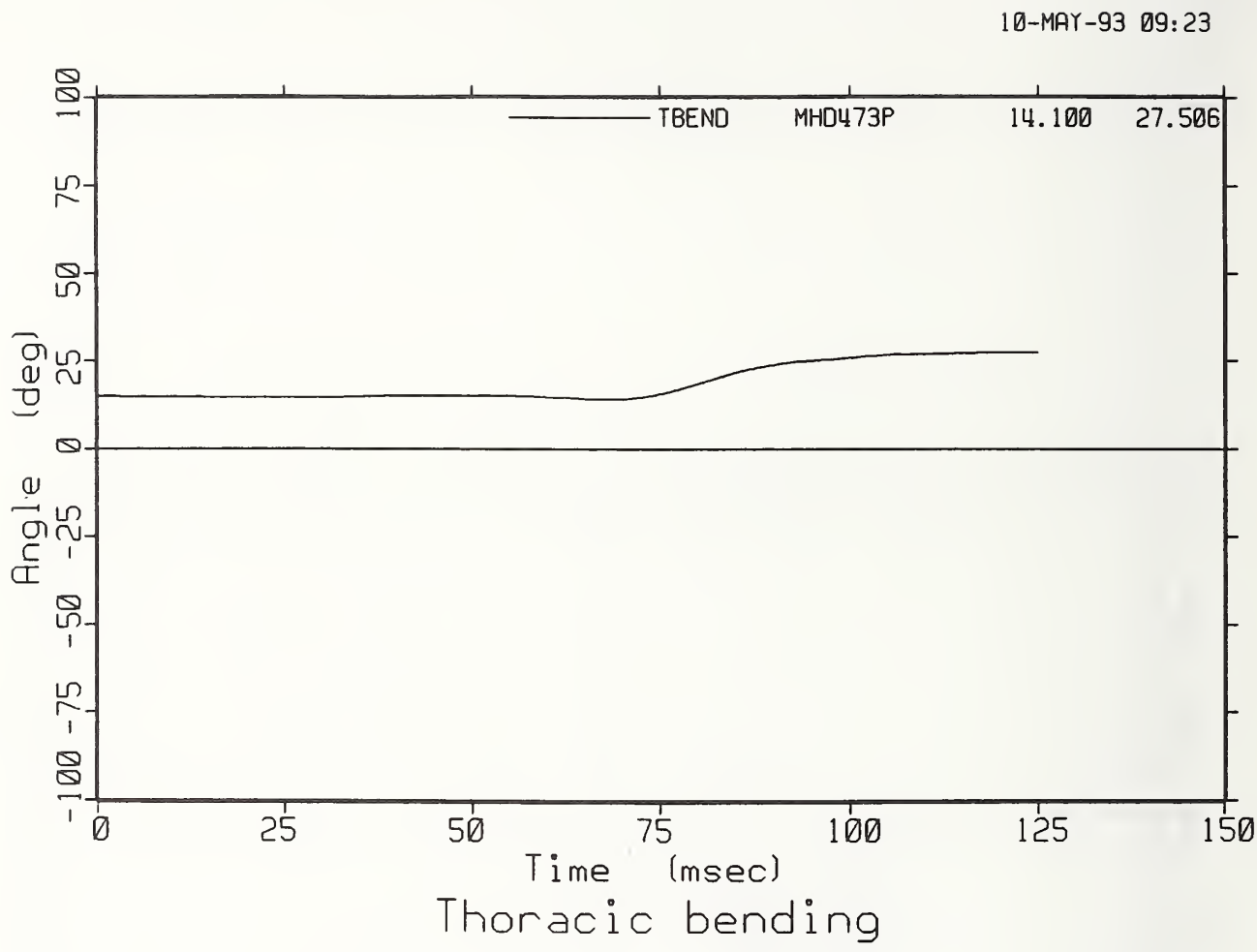

Thoracic bending

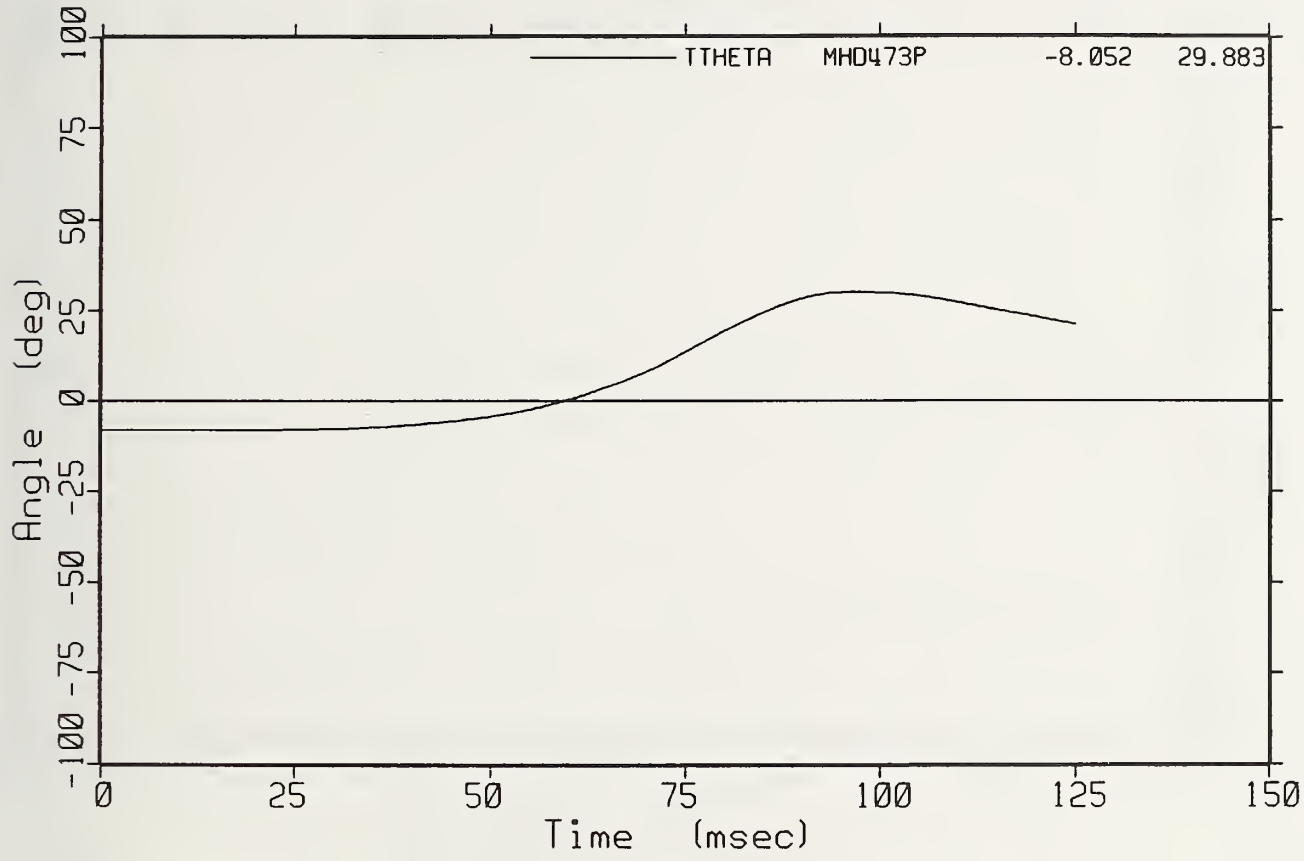

Thoracic angle

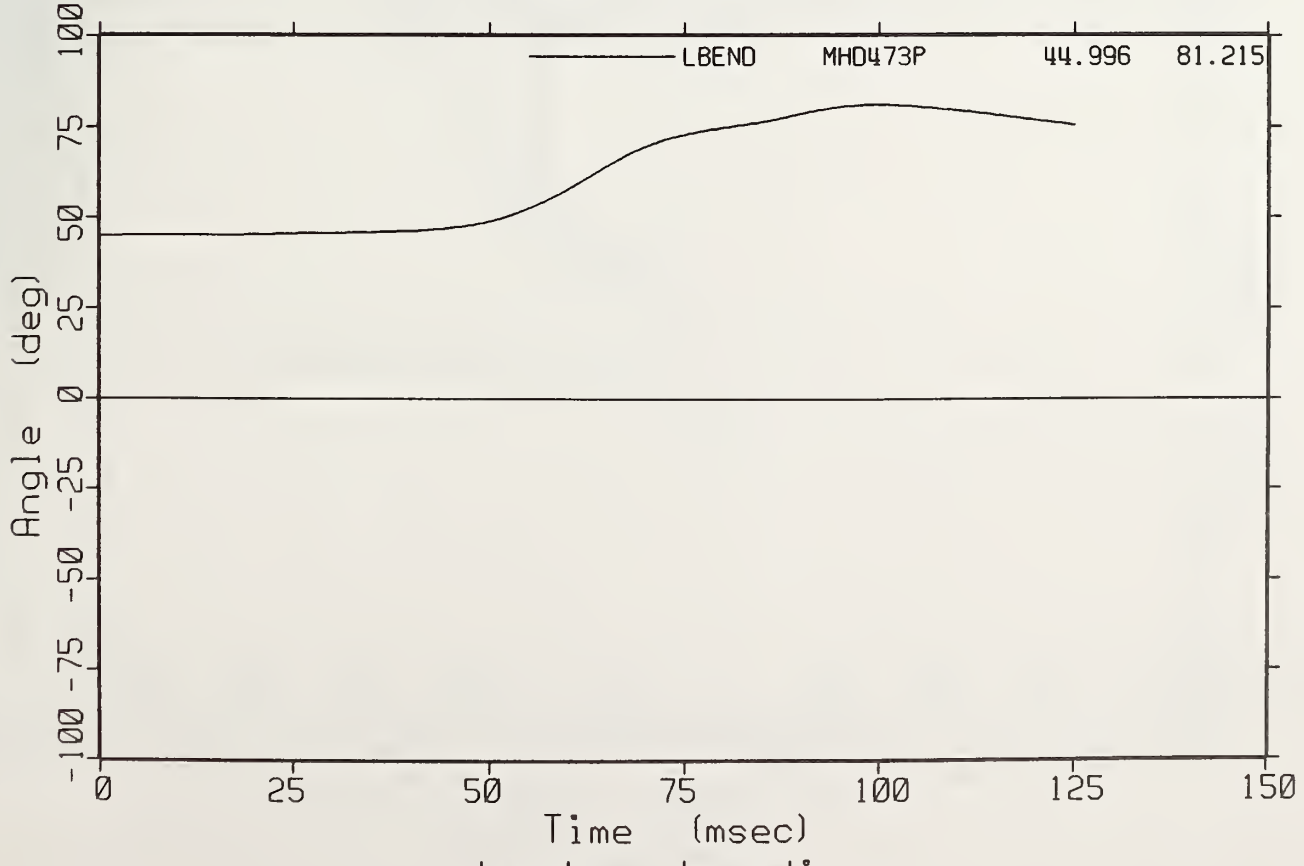

Lumbar bending

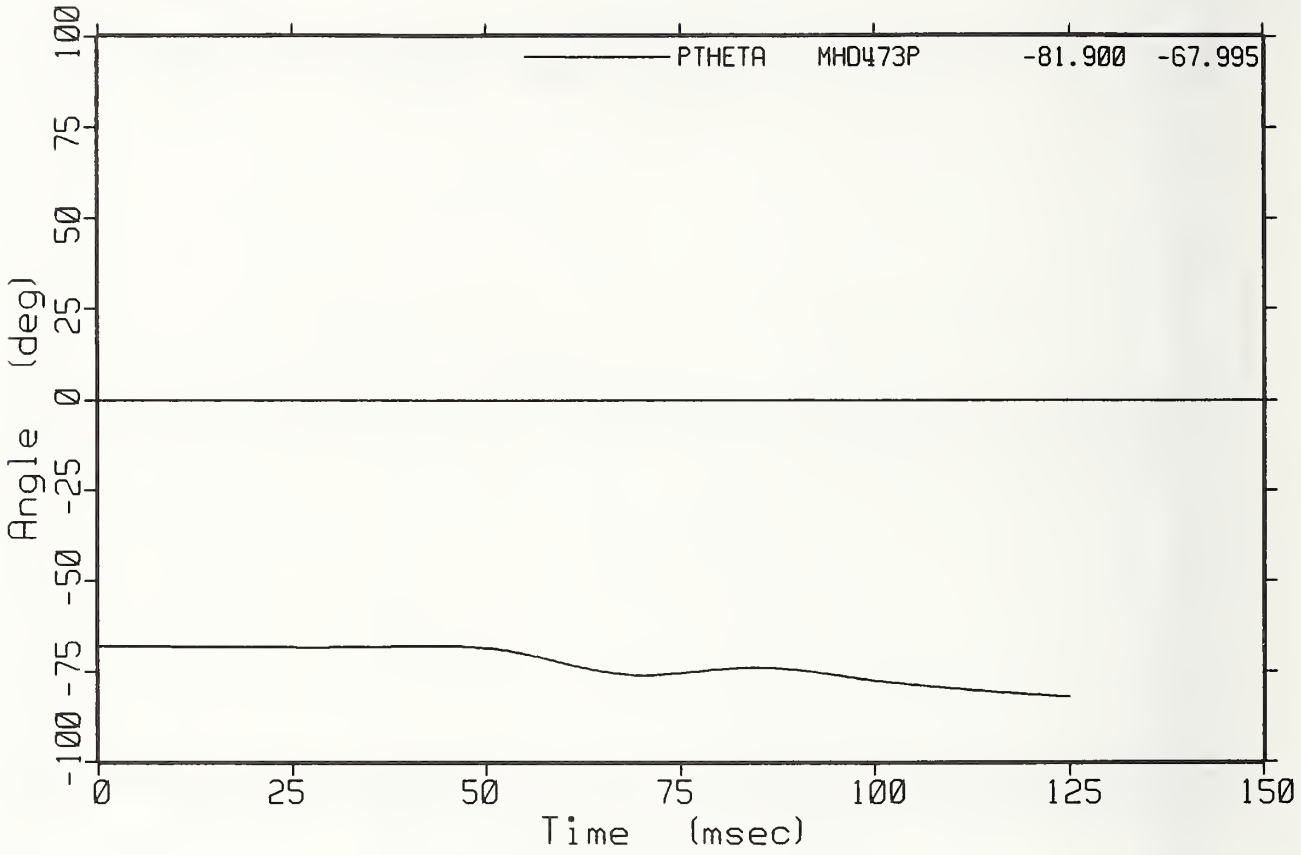

Pelvis angle

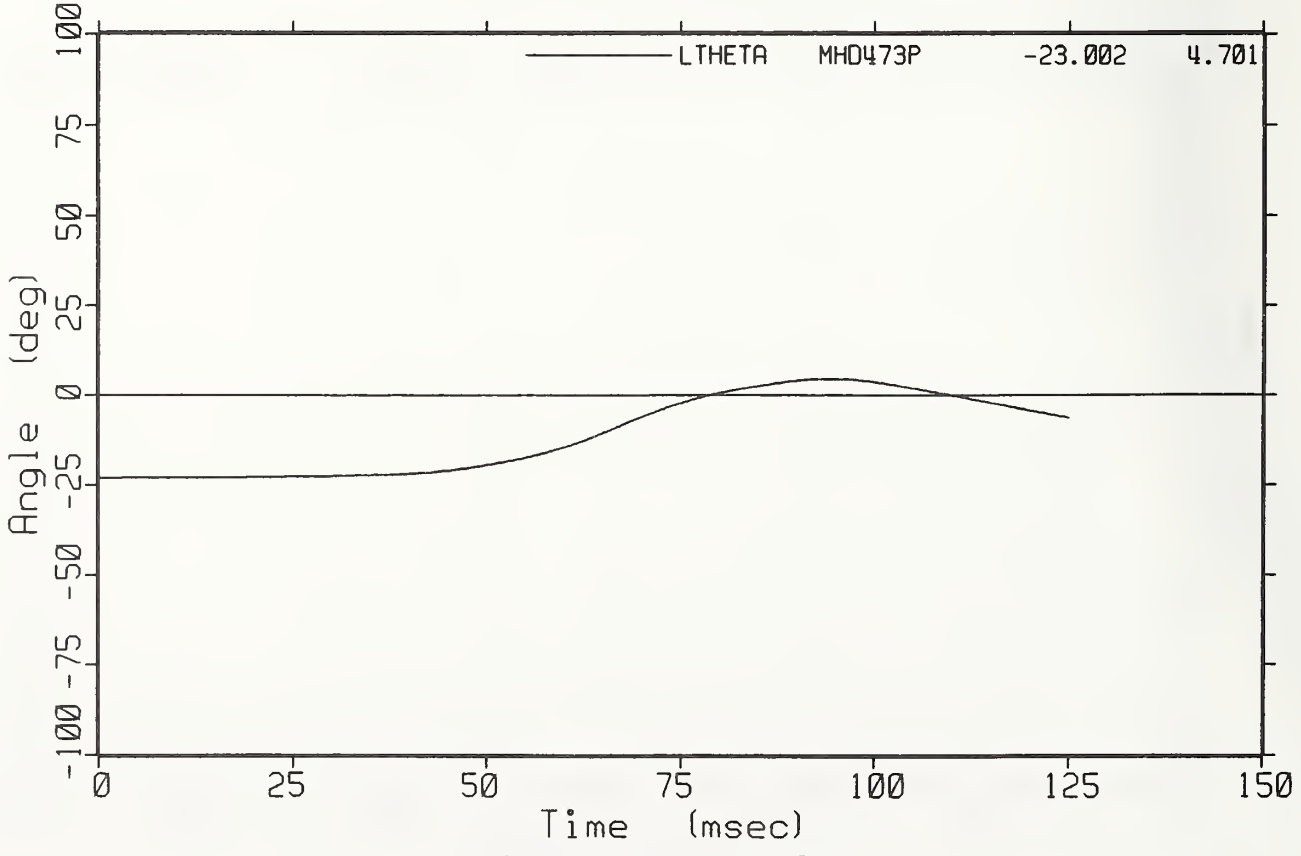

Lumbar angle

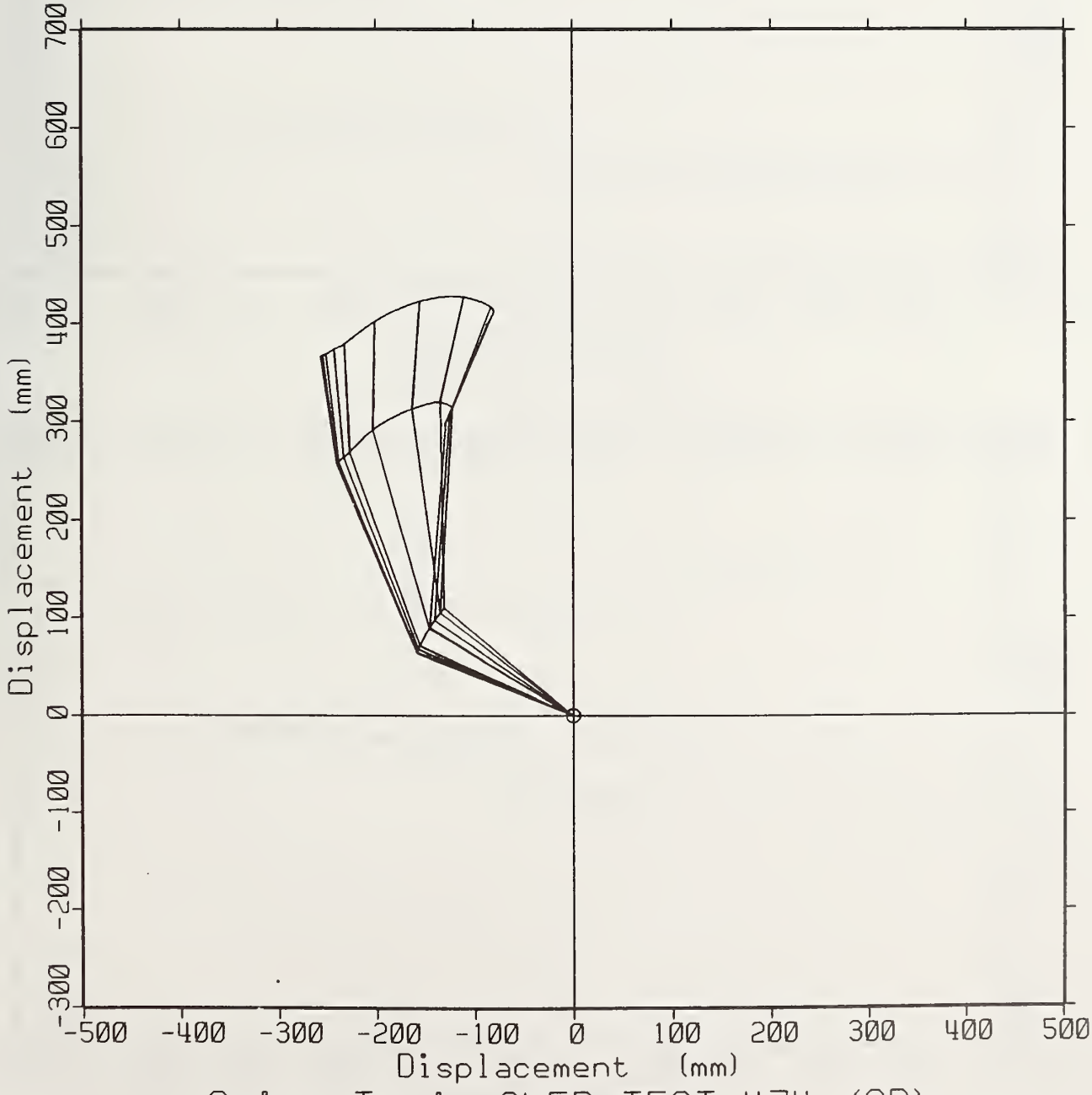

Spine Traj. SLED TEST 474 (AB)

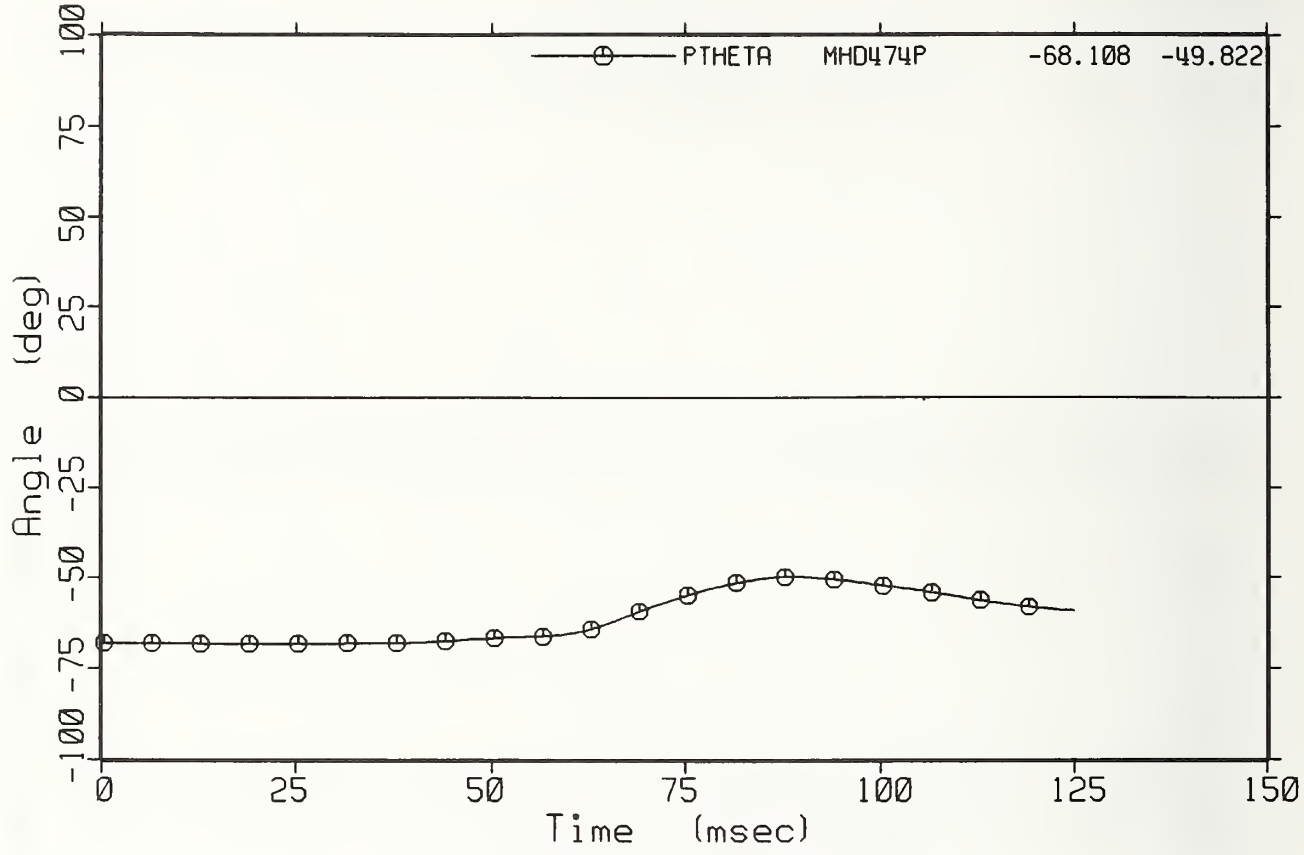

Pelvis angle

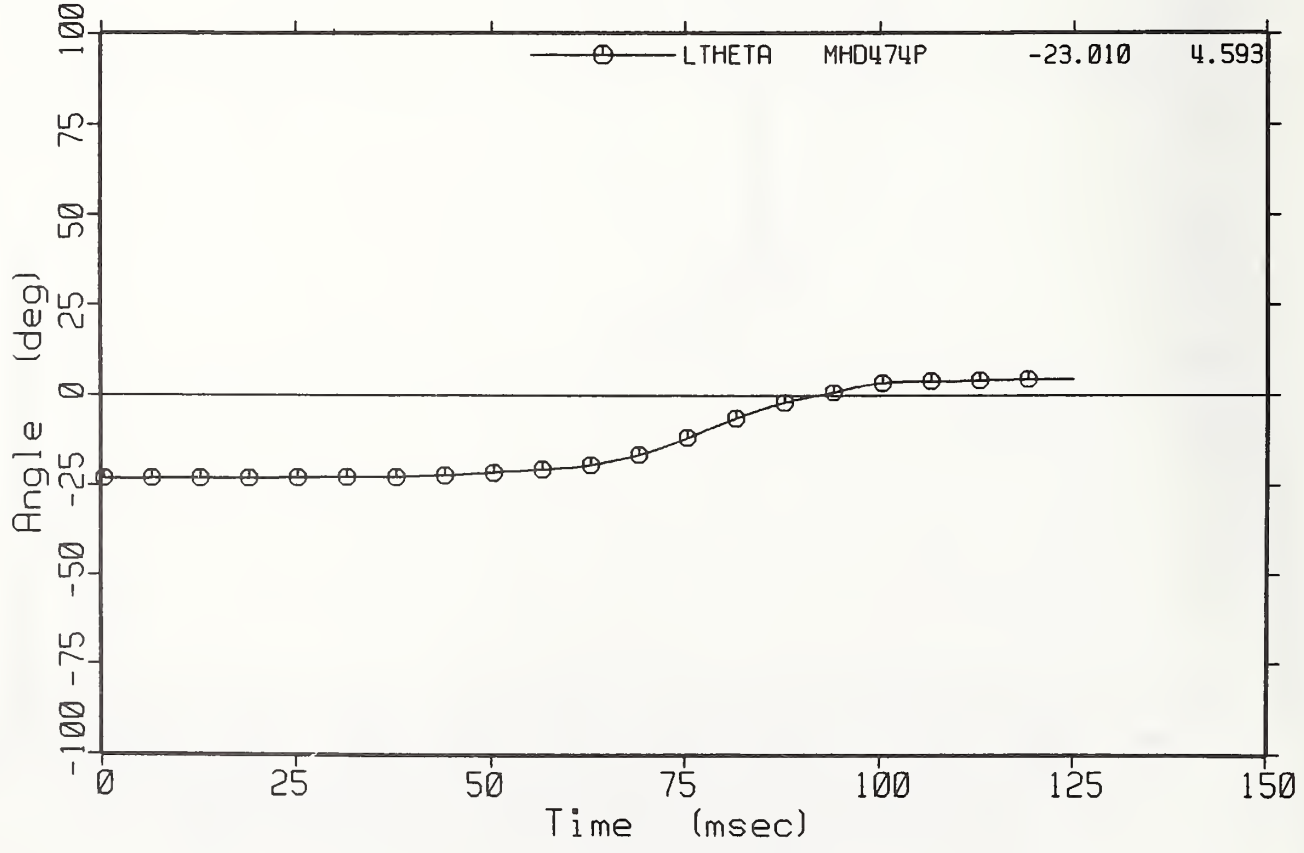

Lumbar angle

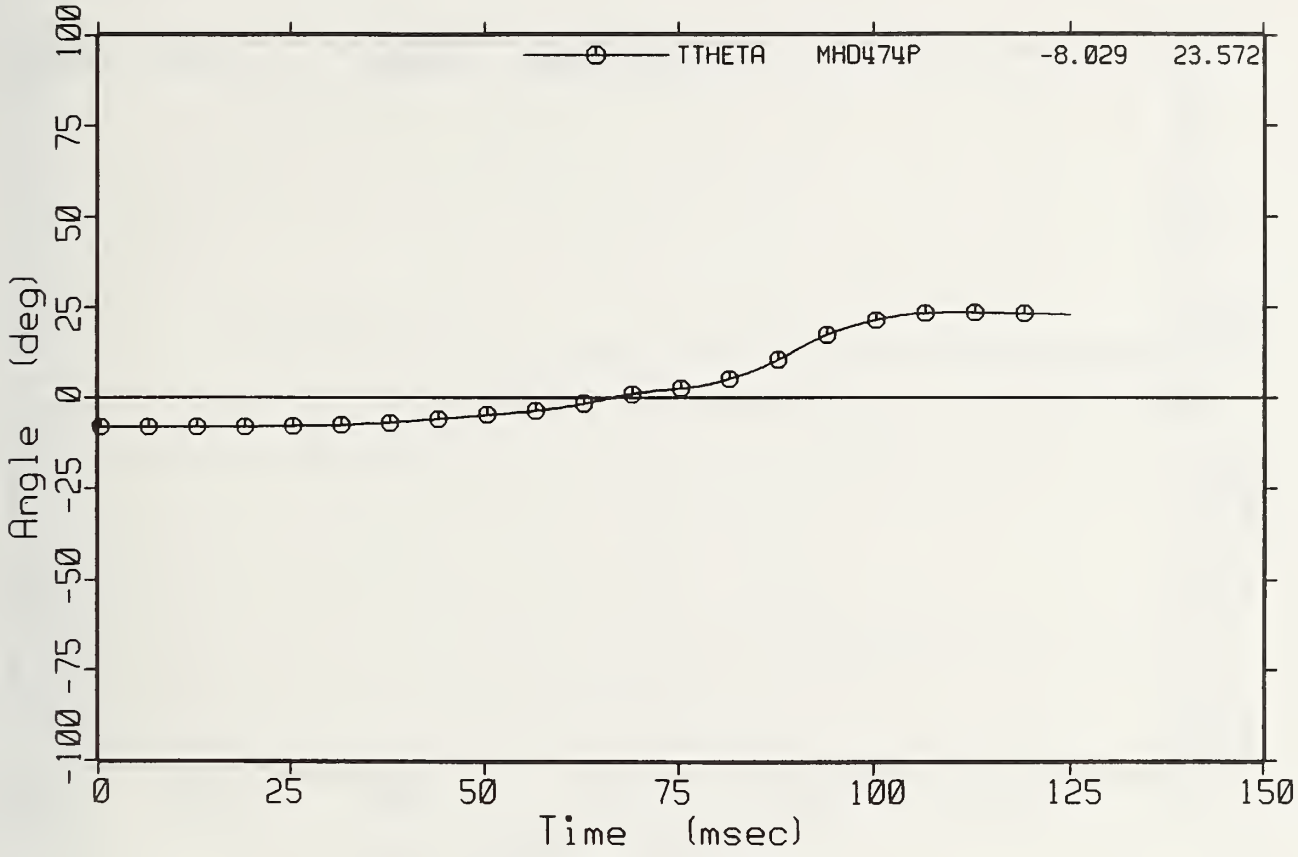

Thoracic angle

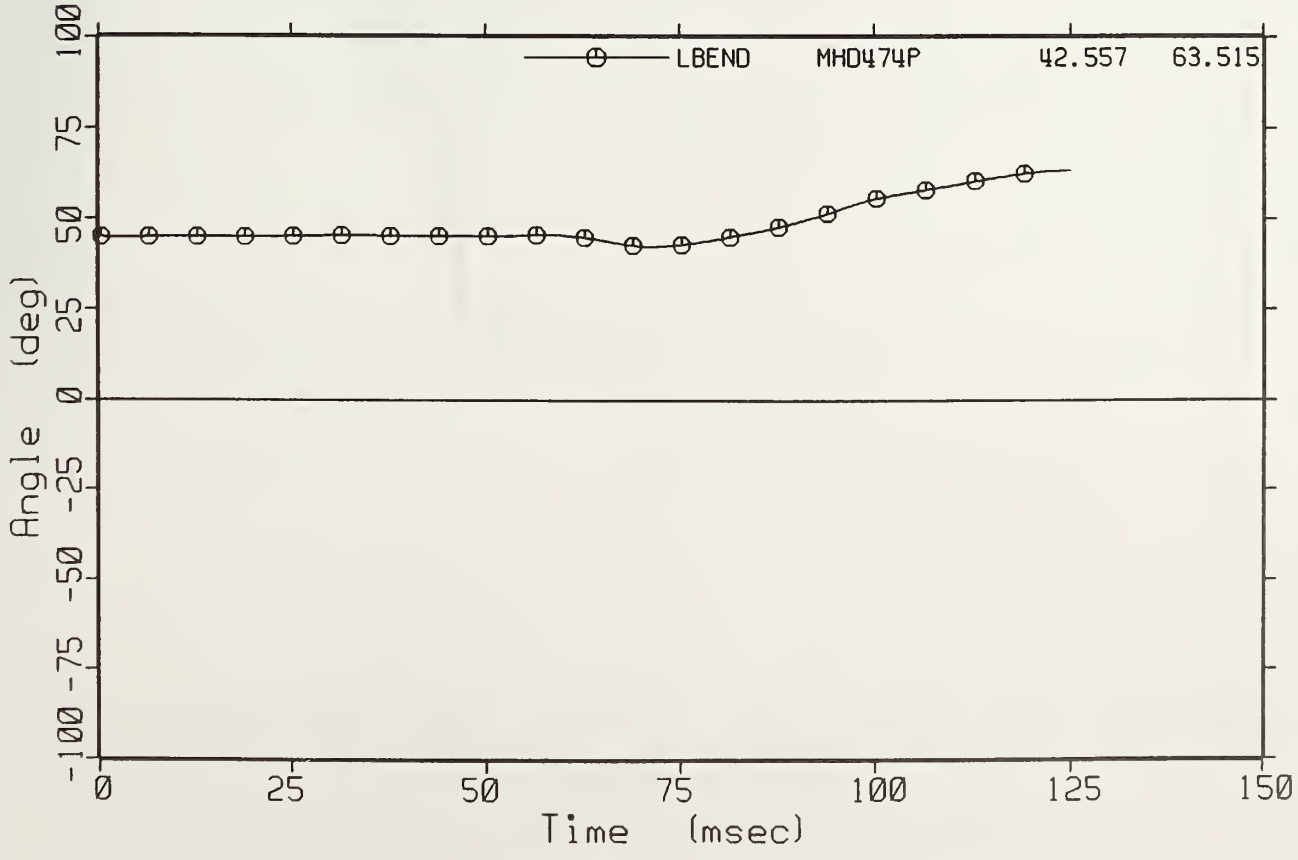

Lumbar bending

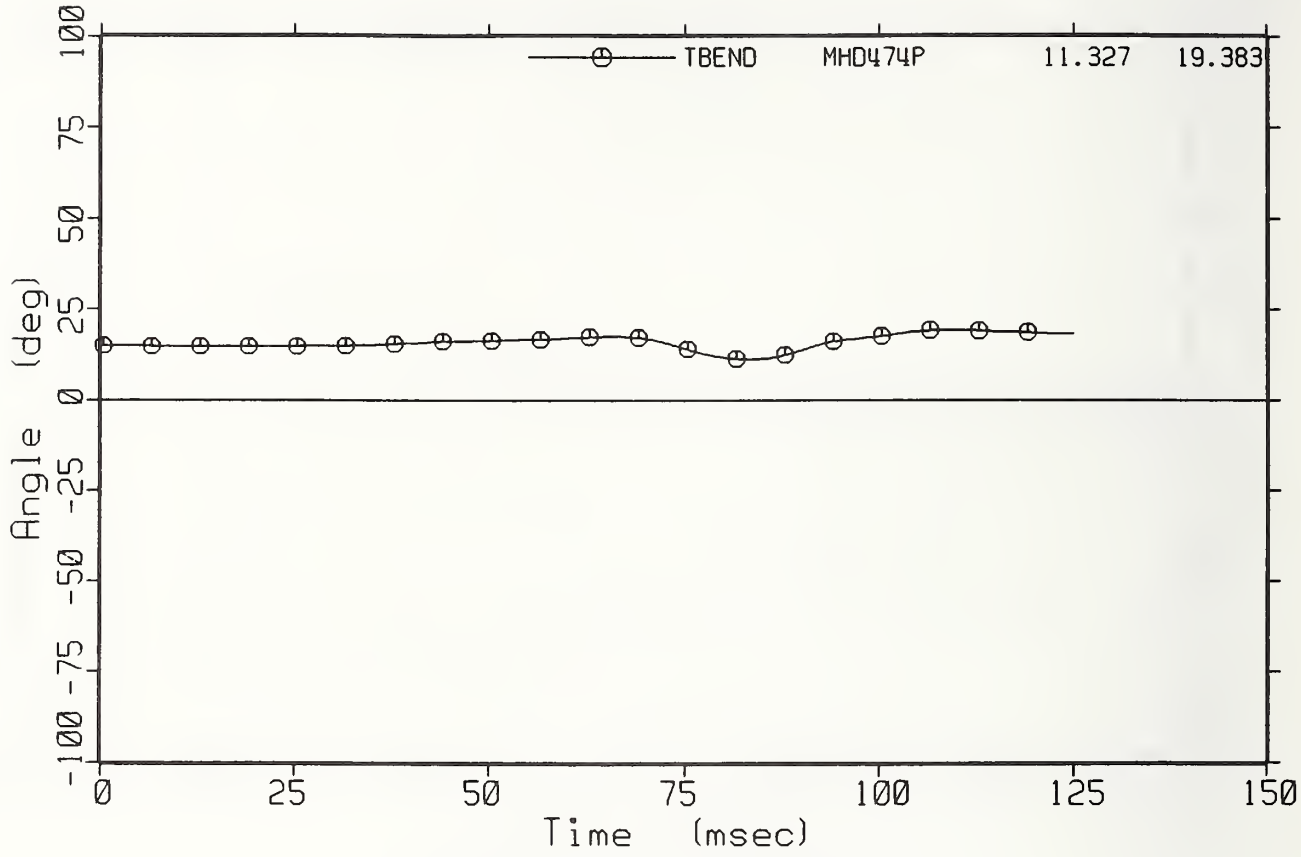

Thoracic bending

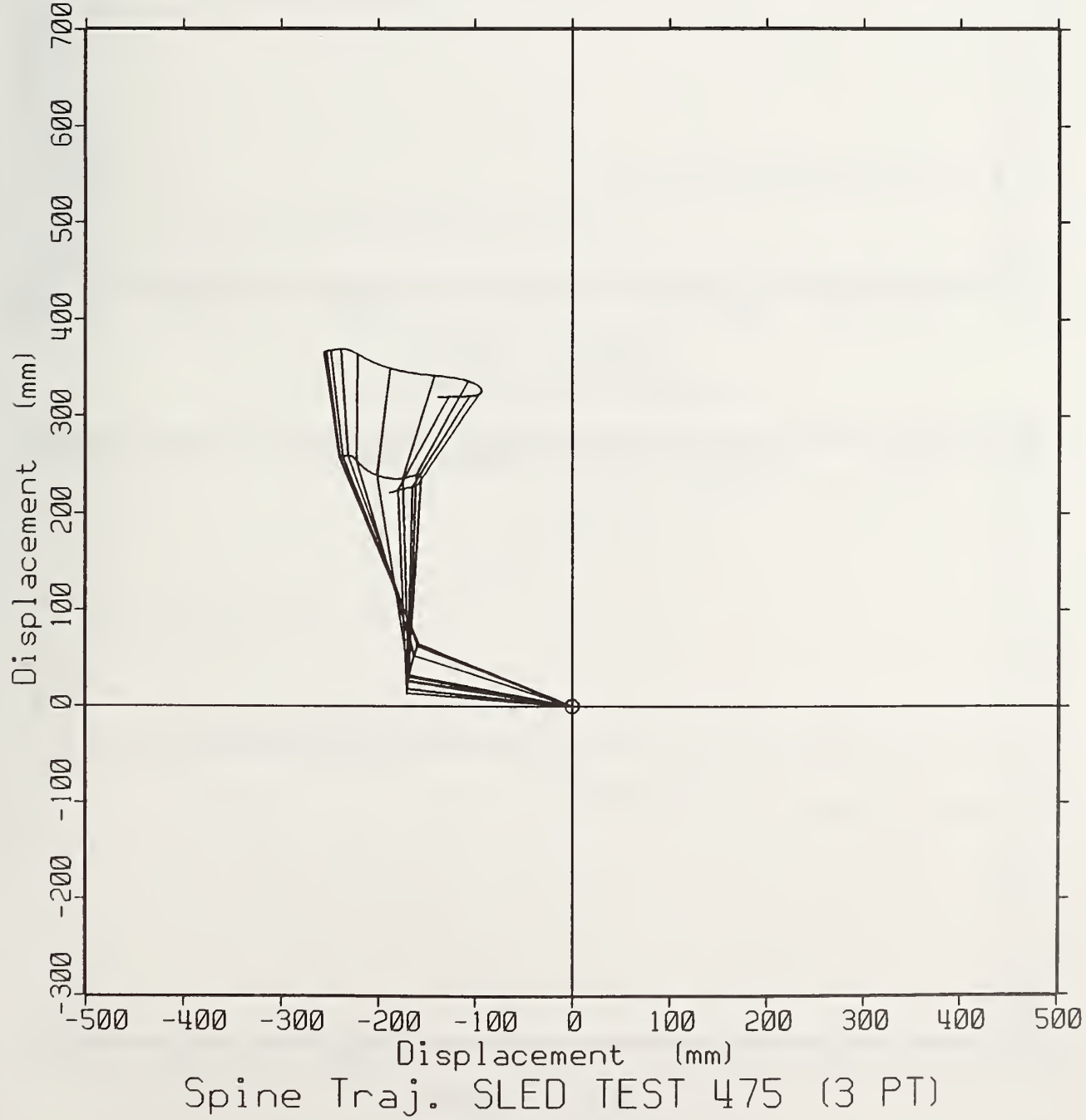

Spine Traj. SLED TEST 475 (3 PT)

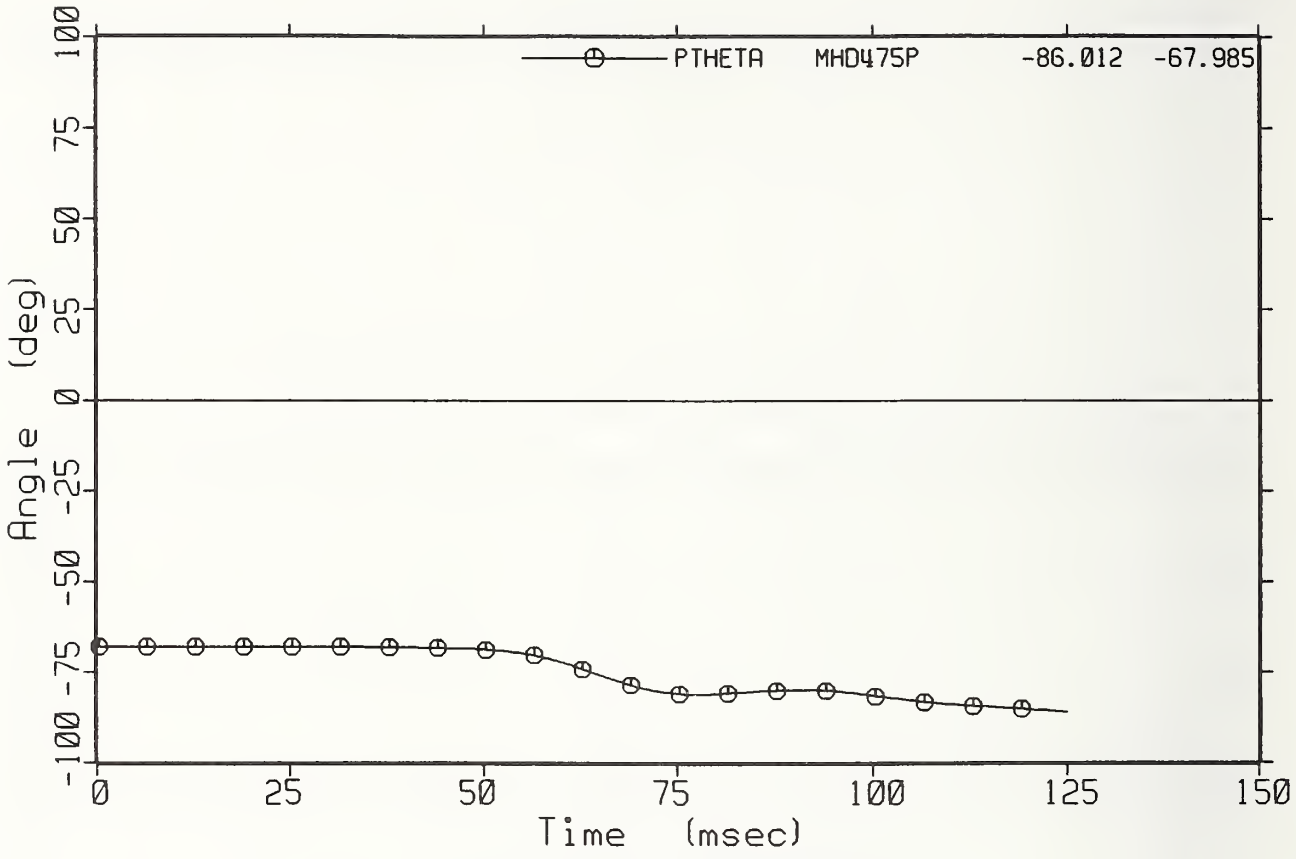

Pelvis angle

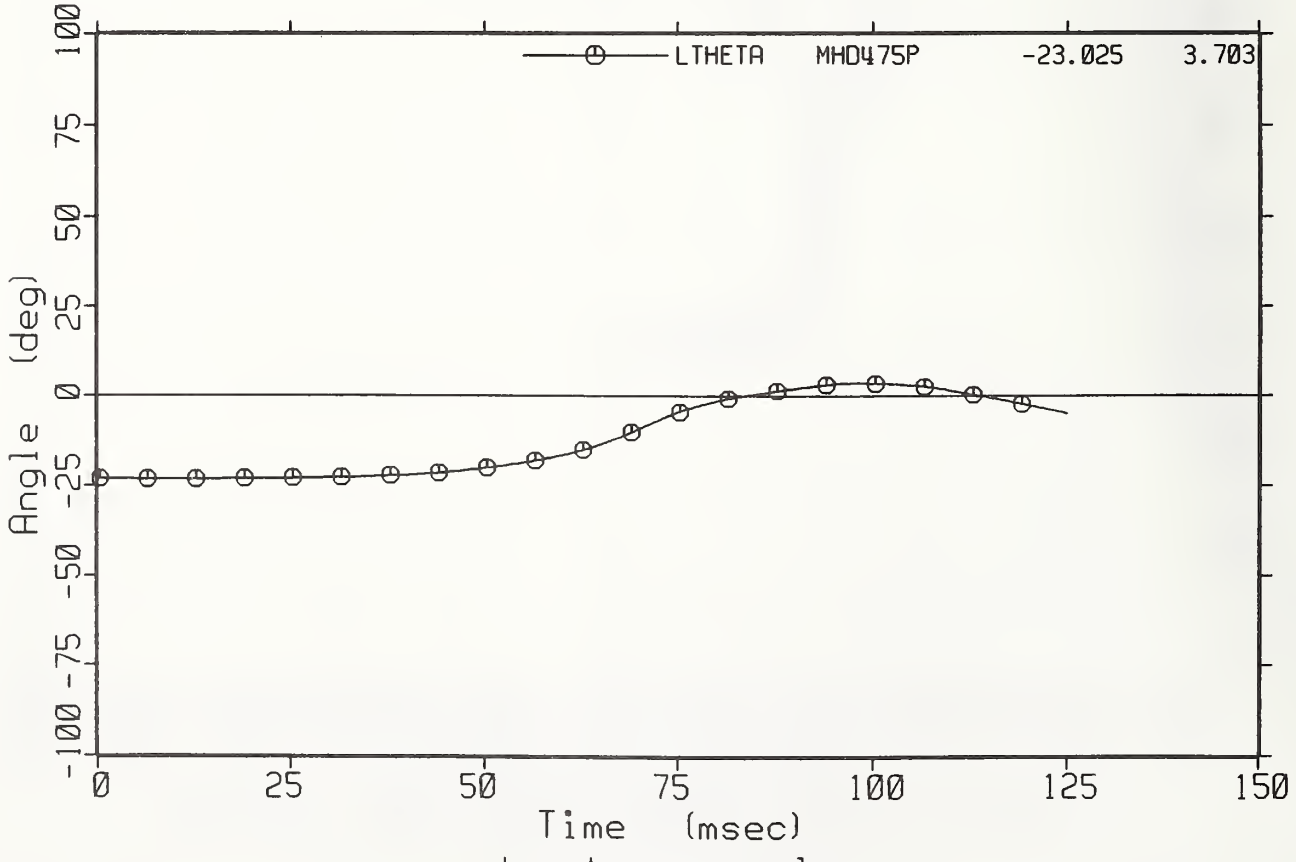

Lumbar angle

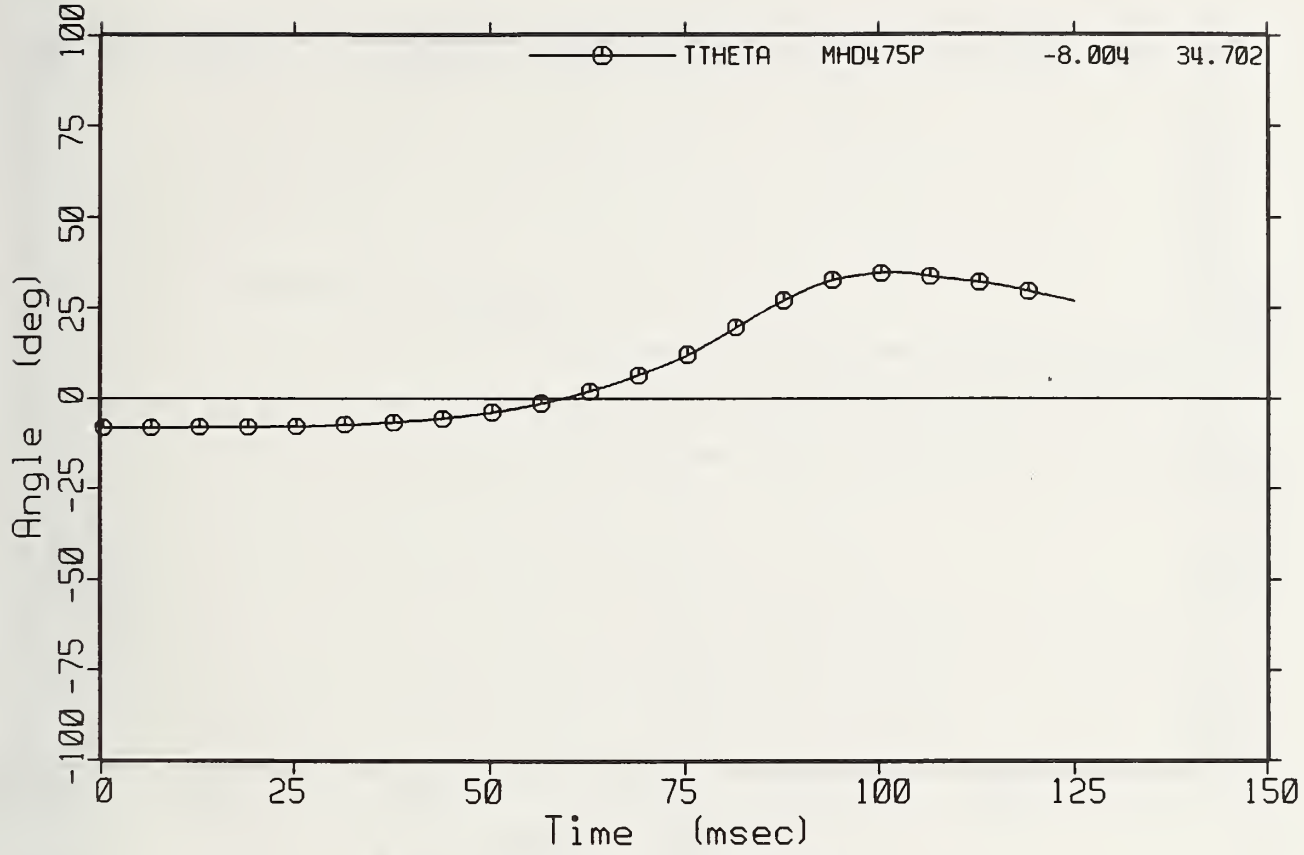

Thoracic angle

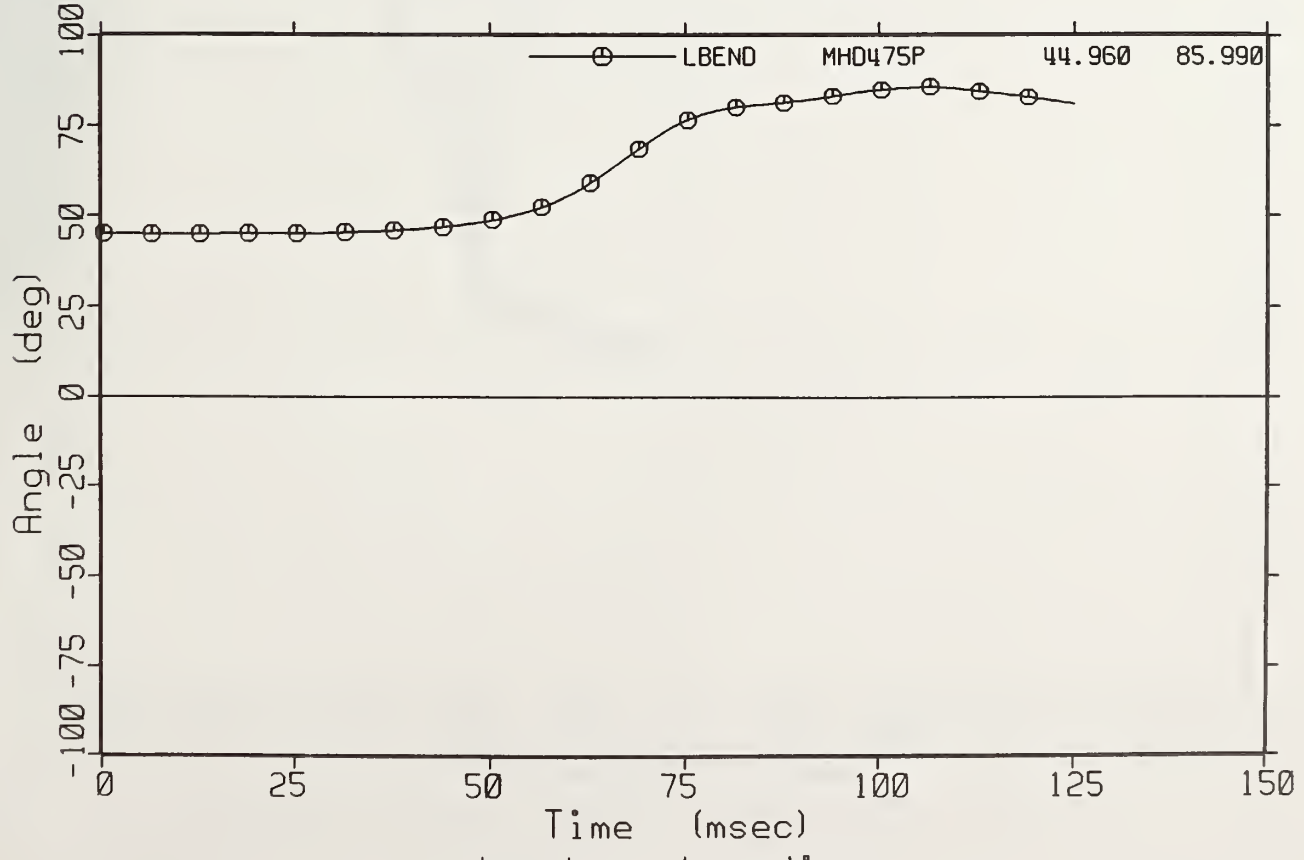

Lumbar bending

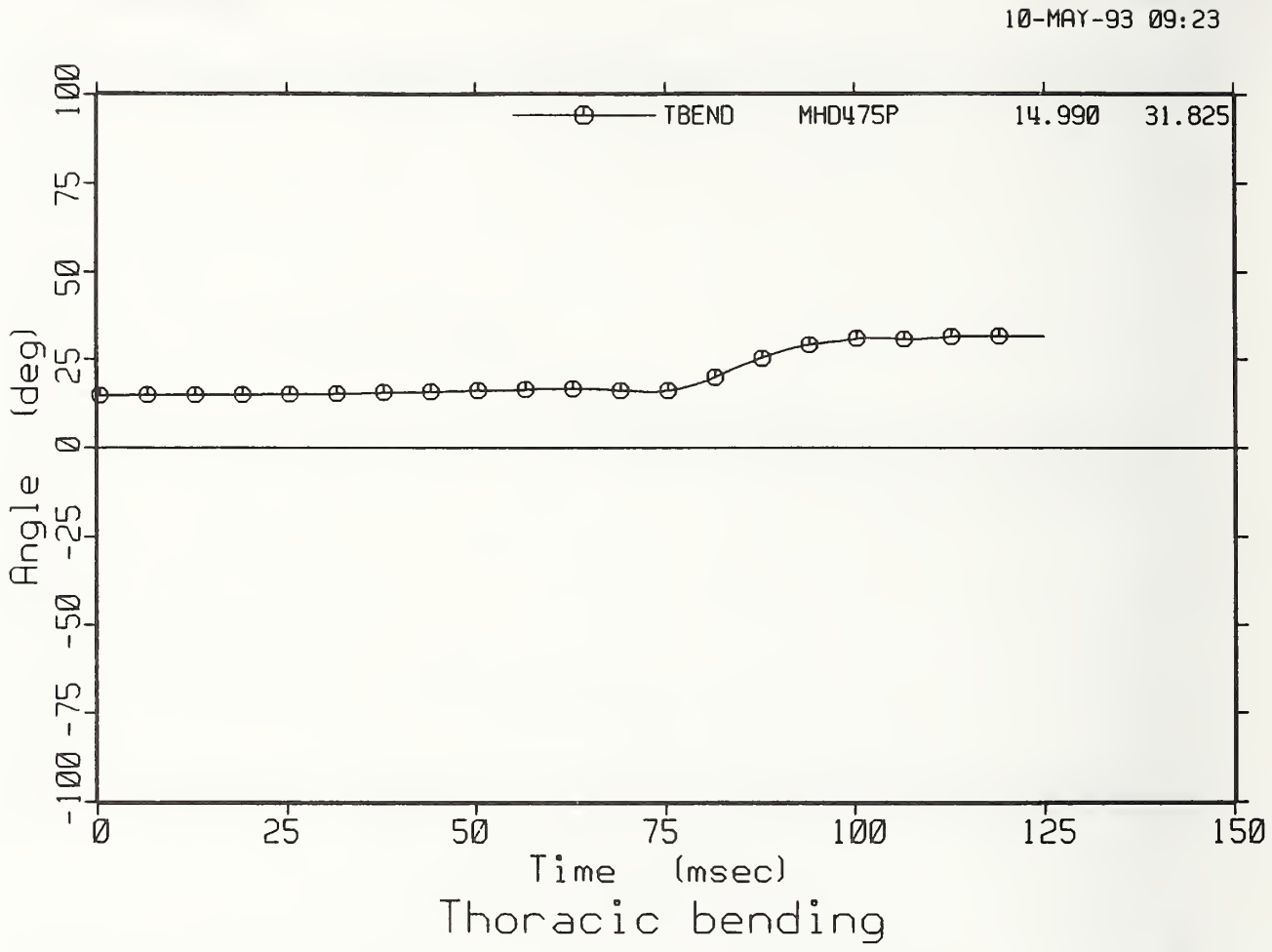
10-MAY-93 09:23
TBEND MHD475P 14.990 31.825
Angle (deg)
100
75
50
25
0
-25
-50
-75
-100
0
25
50
75
100
125
150
Time (msec)
Thoracic bending

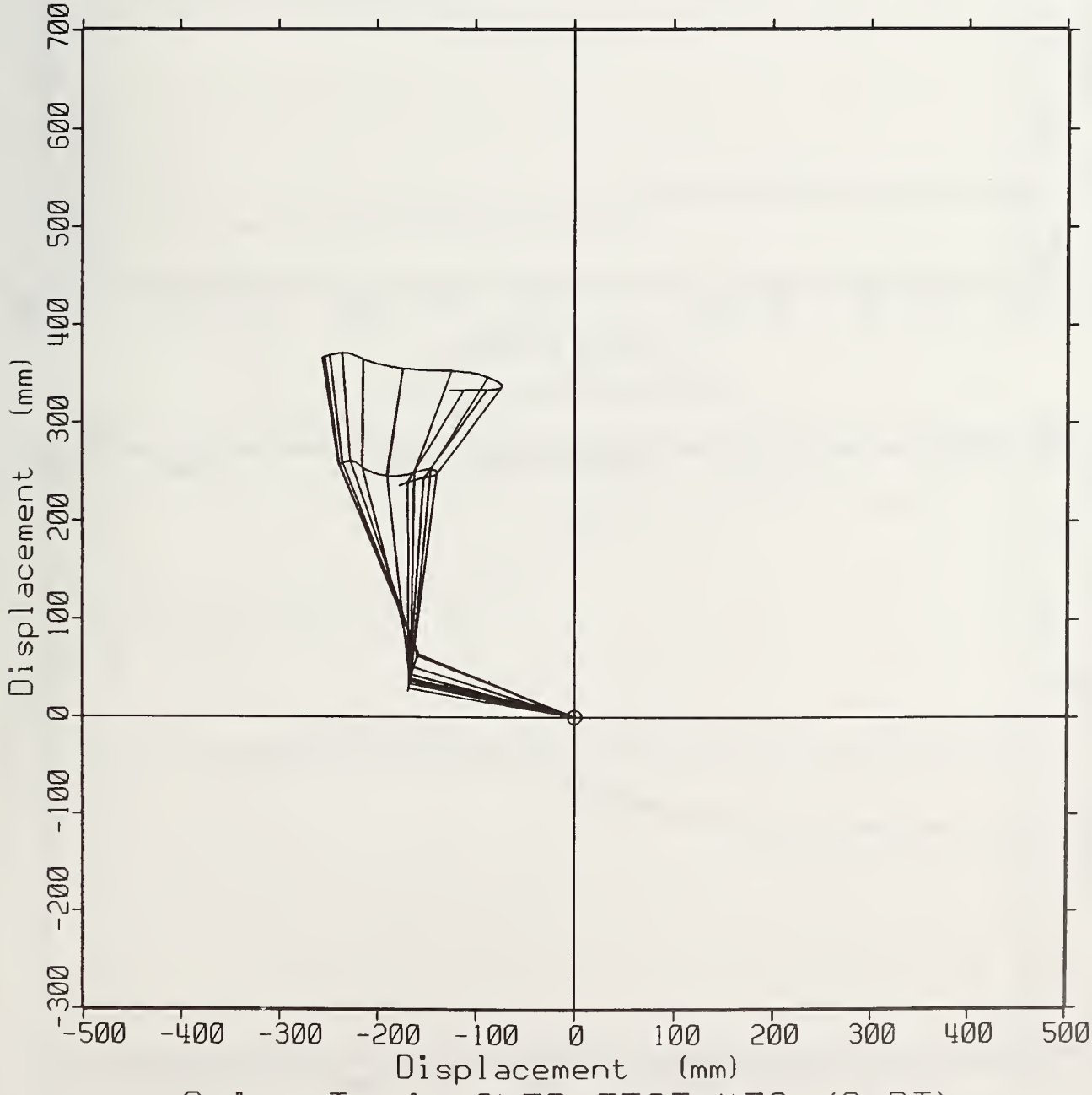

Spine Traj. SLED TEST 476 (3 PT)

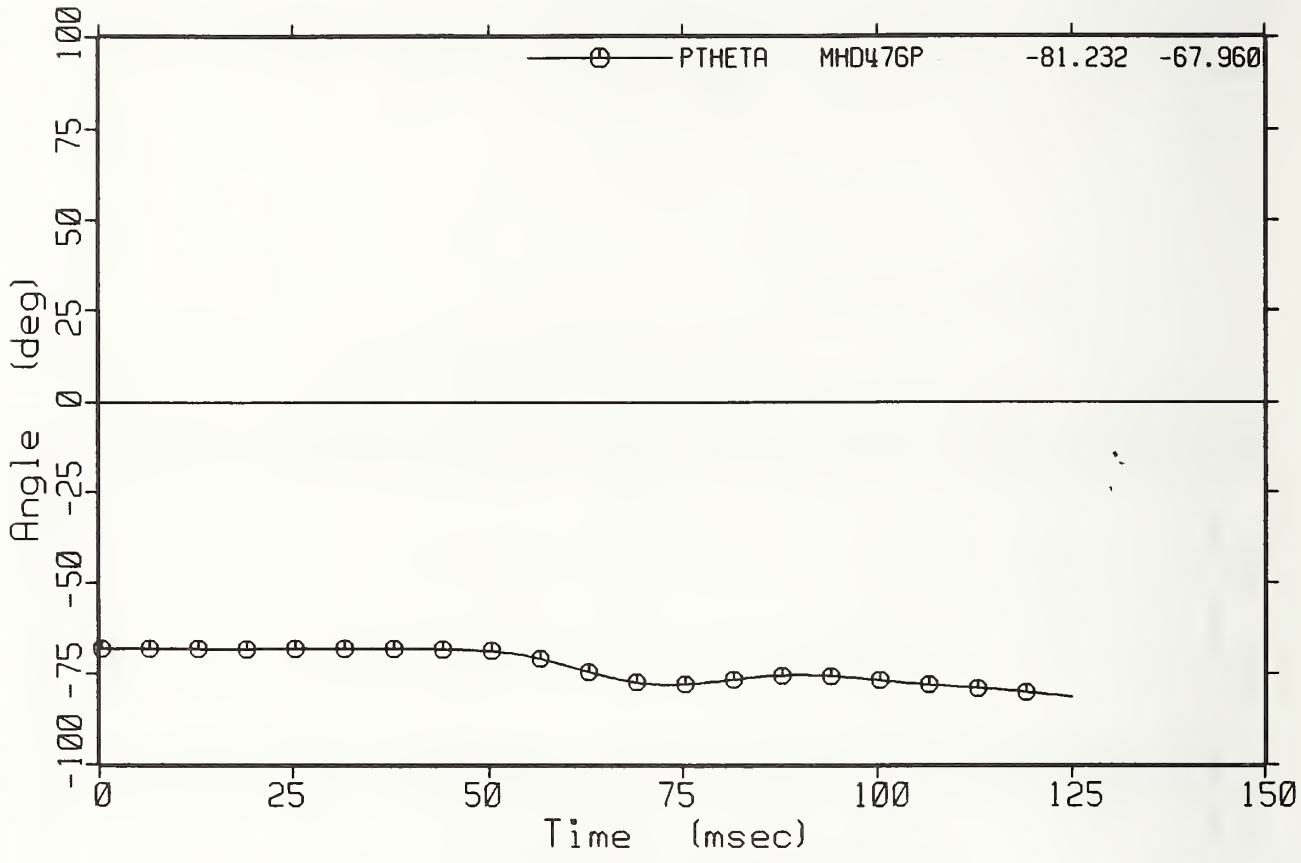

Pelvis angle

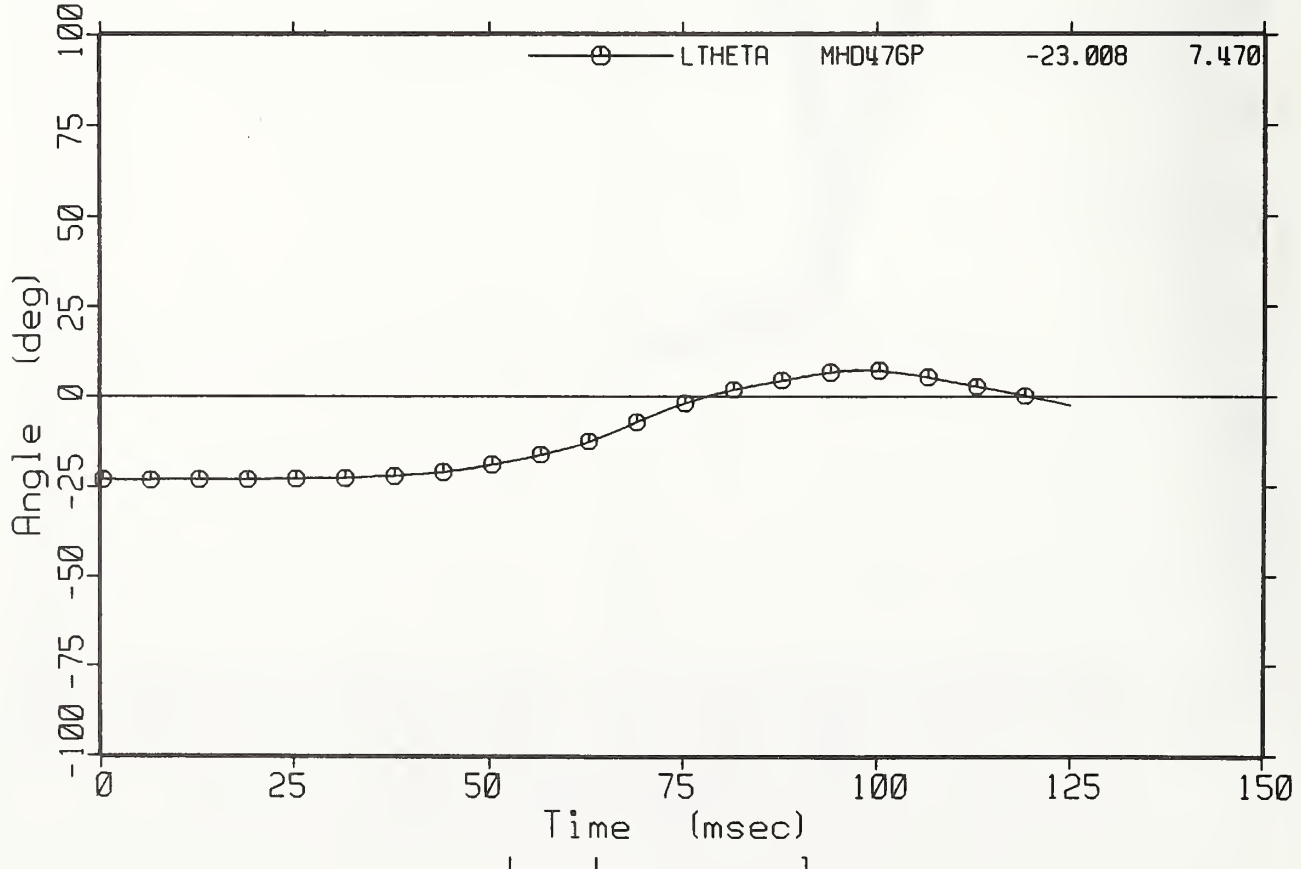

Lumbar angle

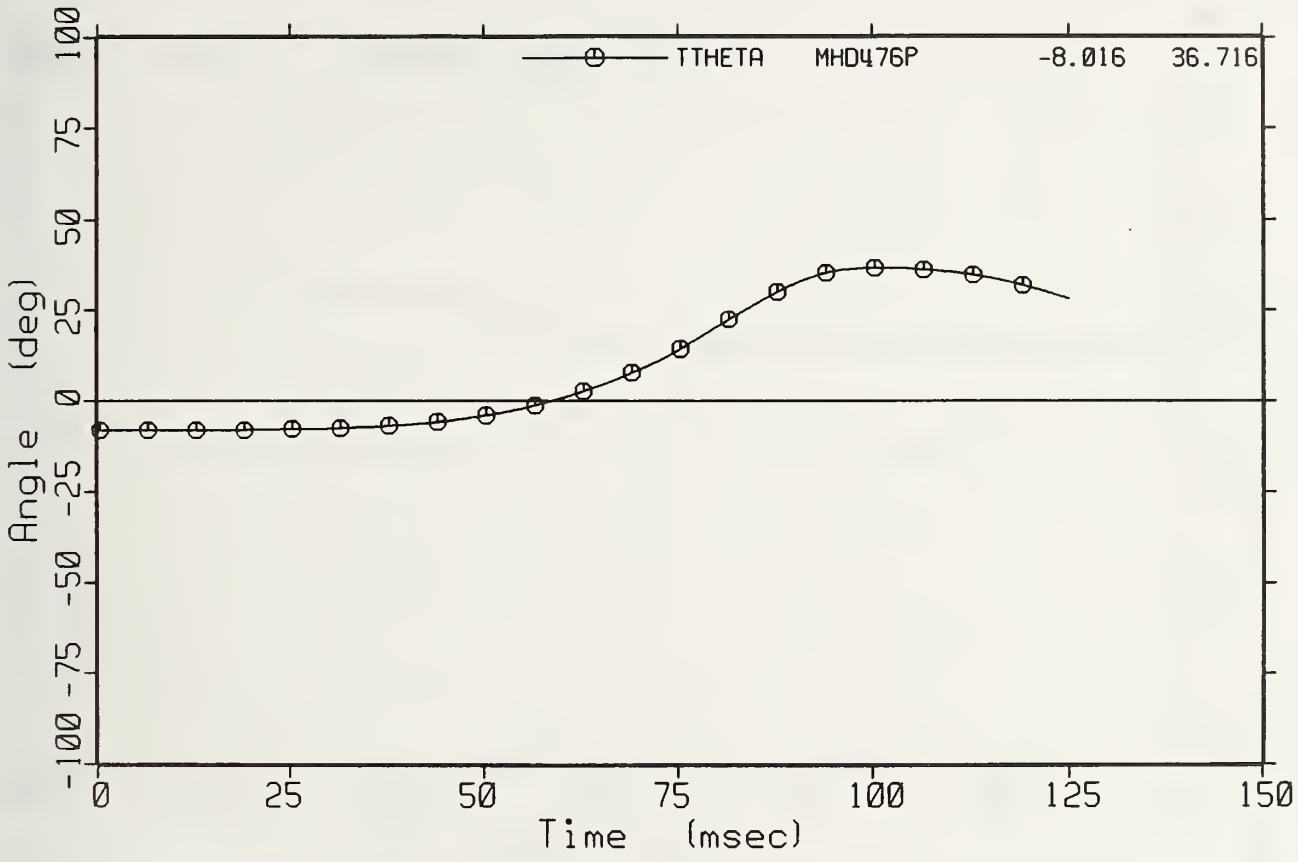

Thoracic angle

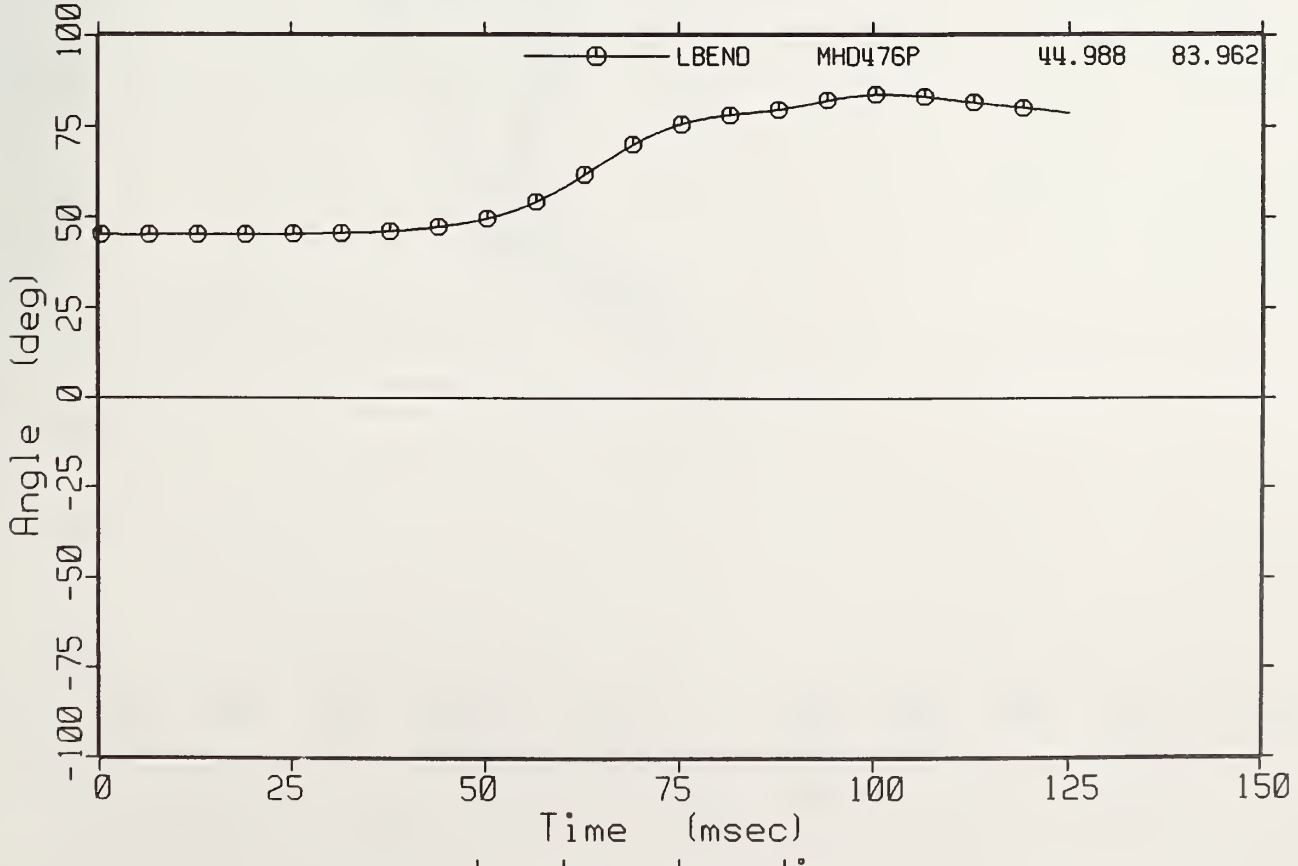

Lumbar bending

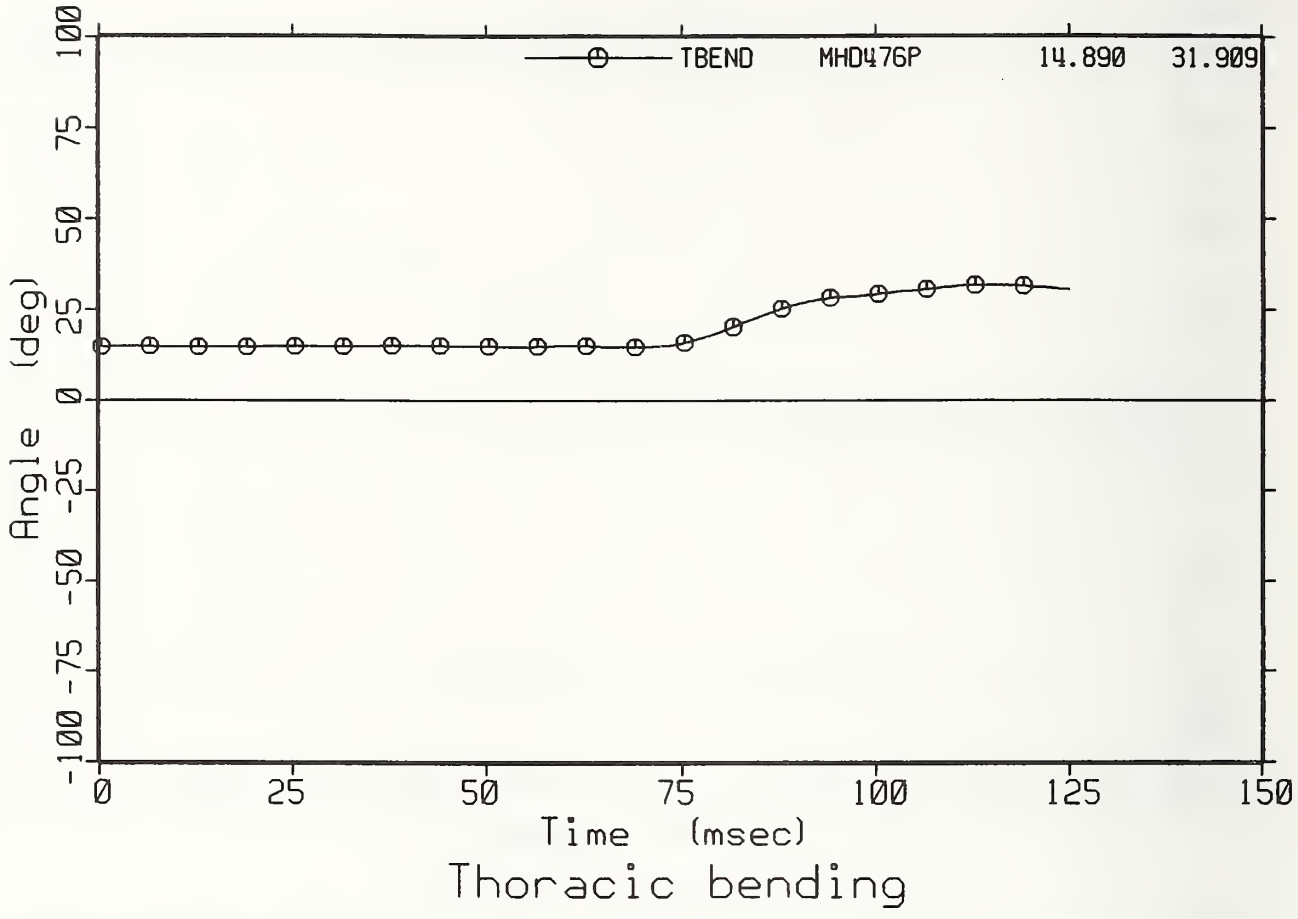

Thoracic bending

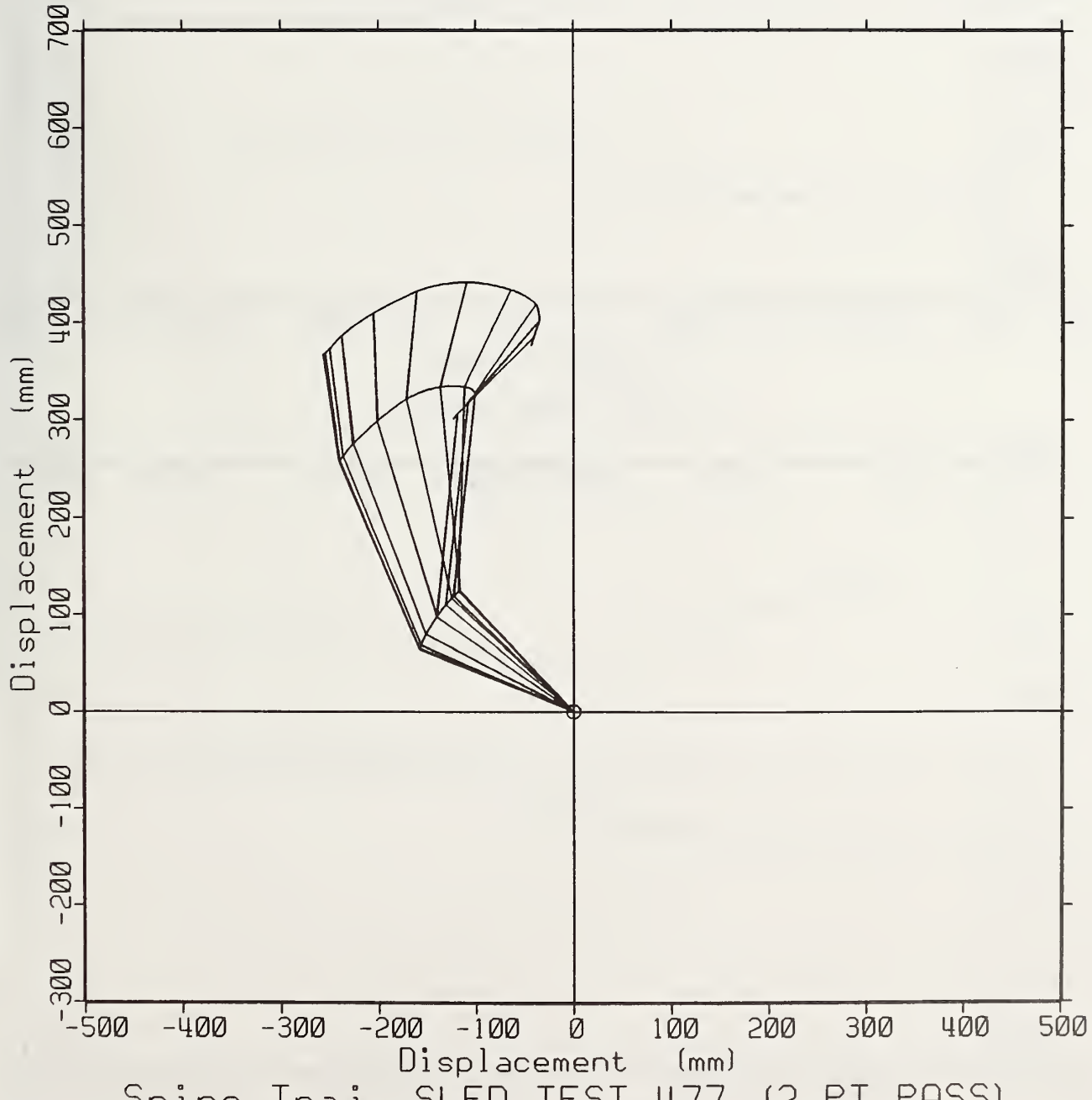

Spine Traj. SLED TEST 477 (2 PT PASS)

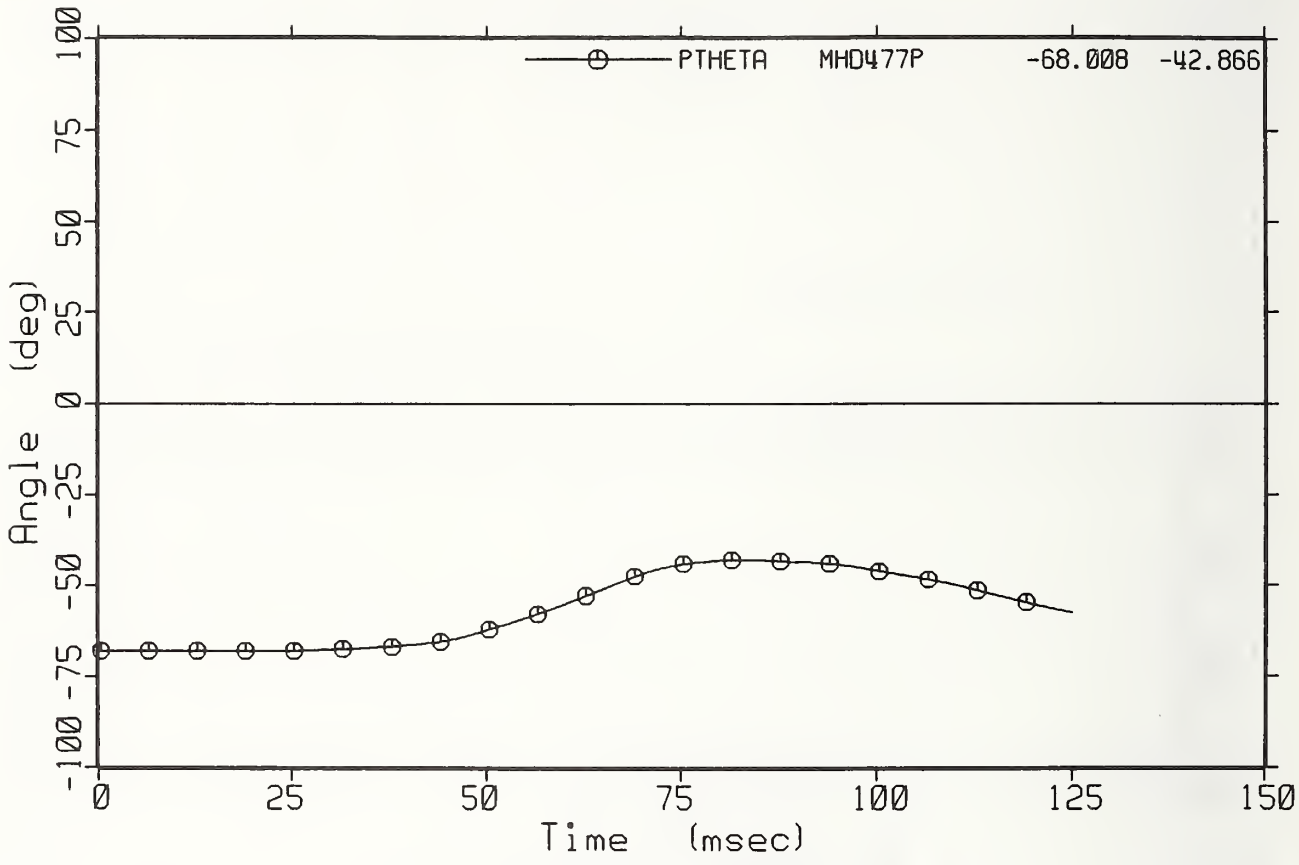

Pelvis angle

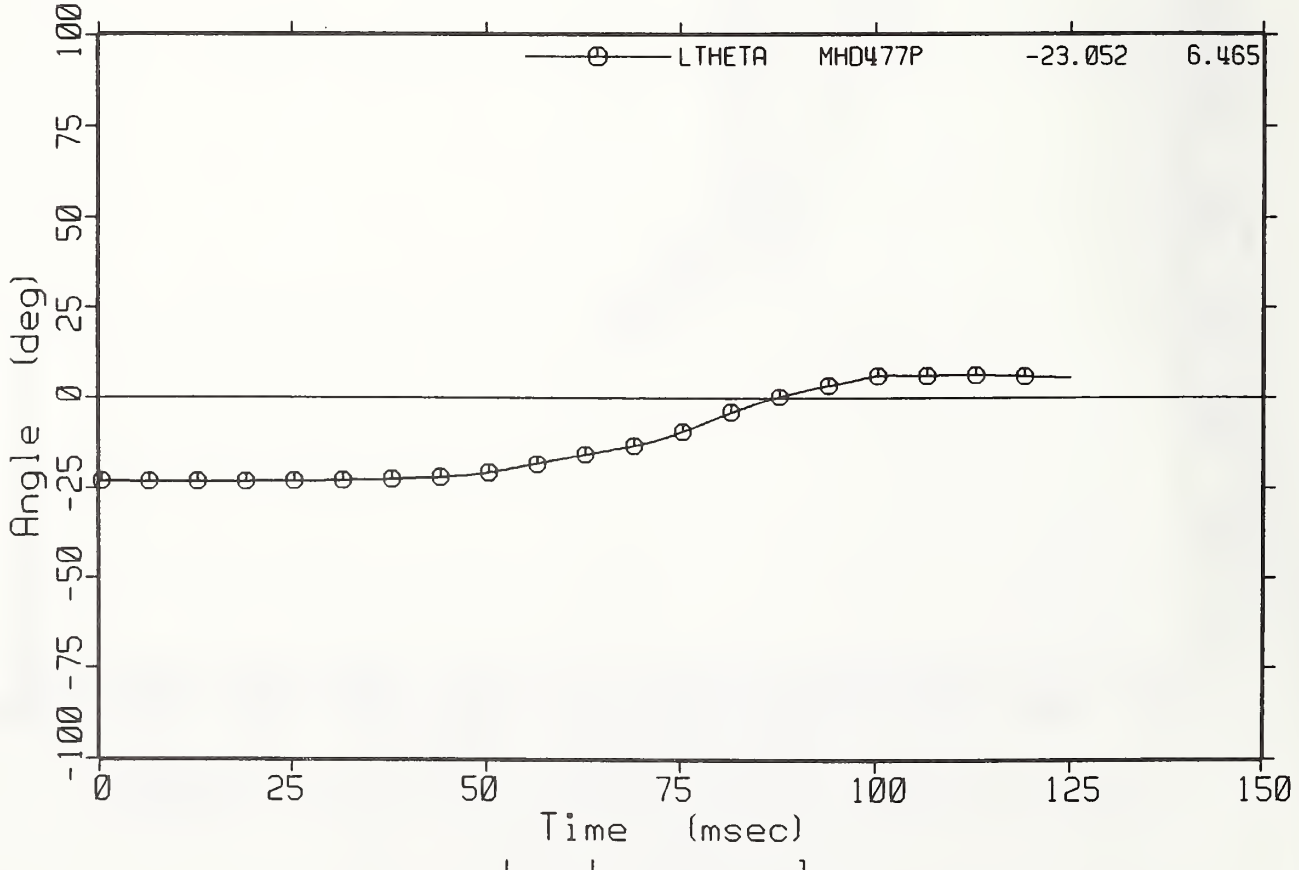

Lumbar angle

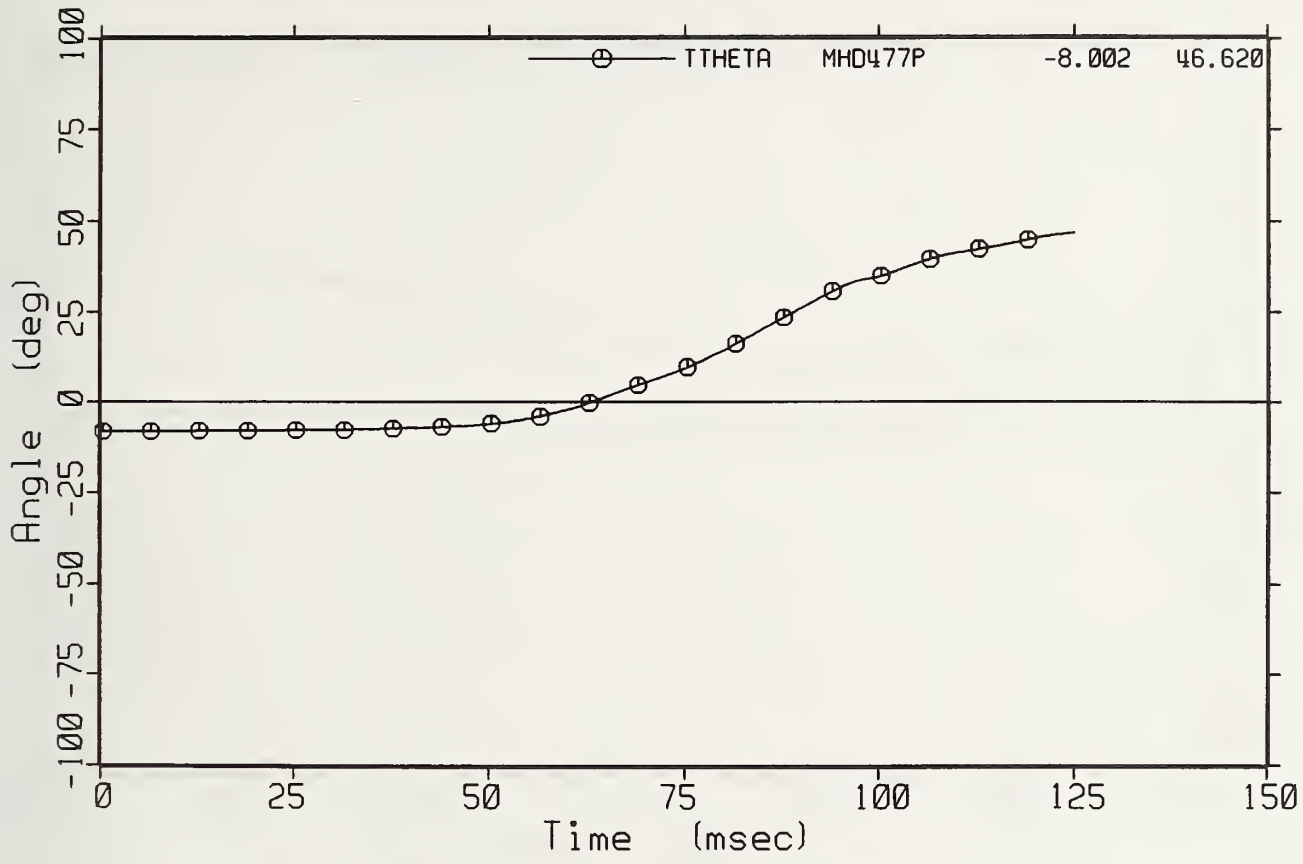

Thoracic angle

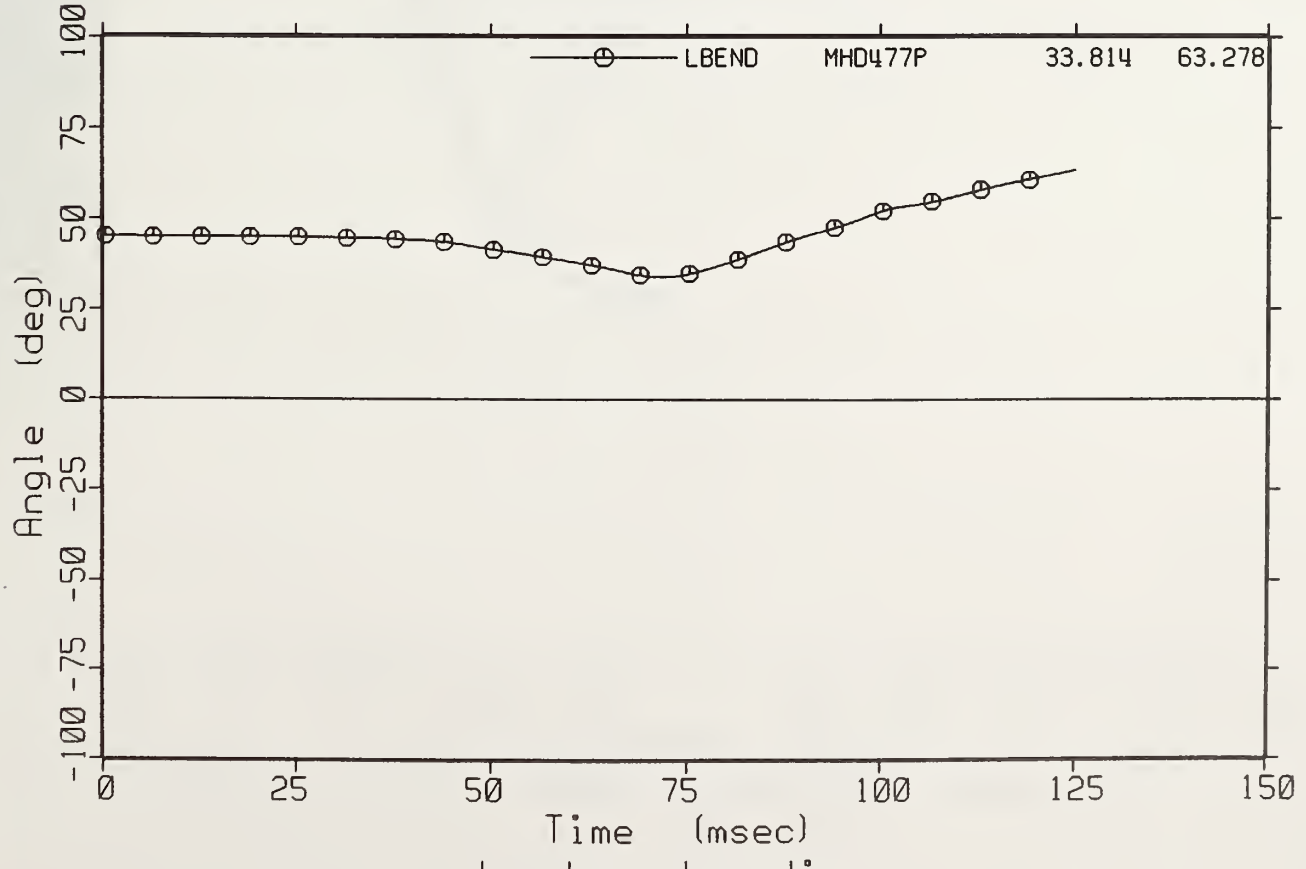

Lumbar bending

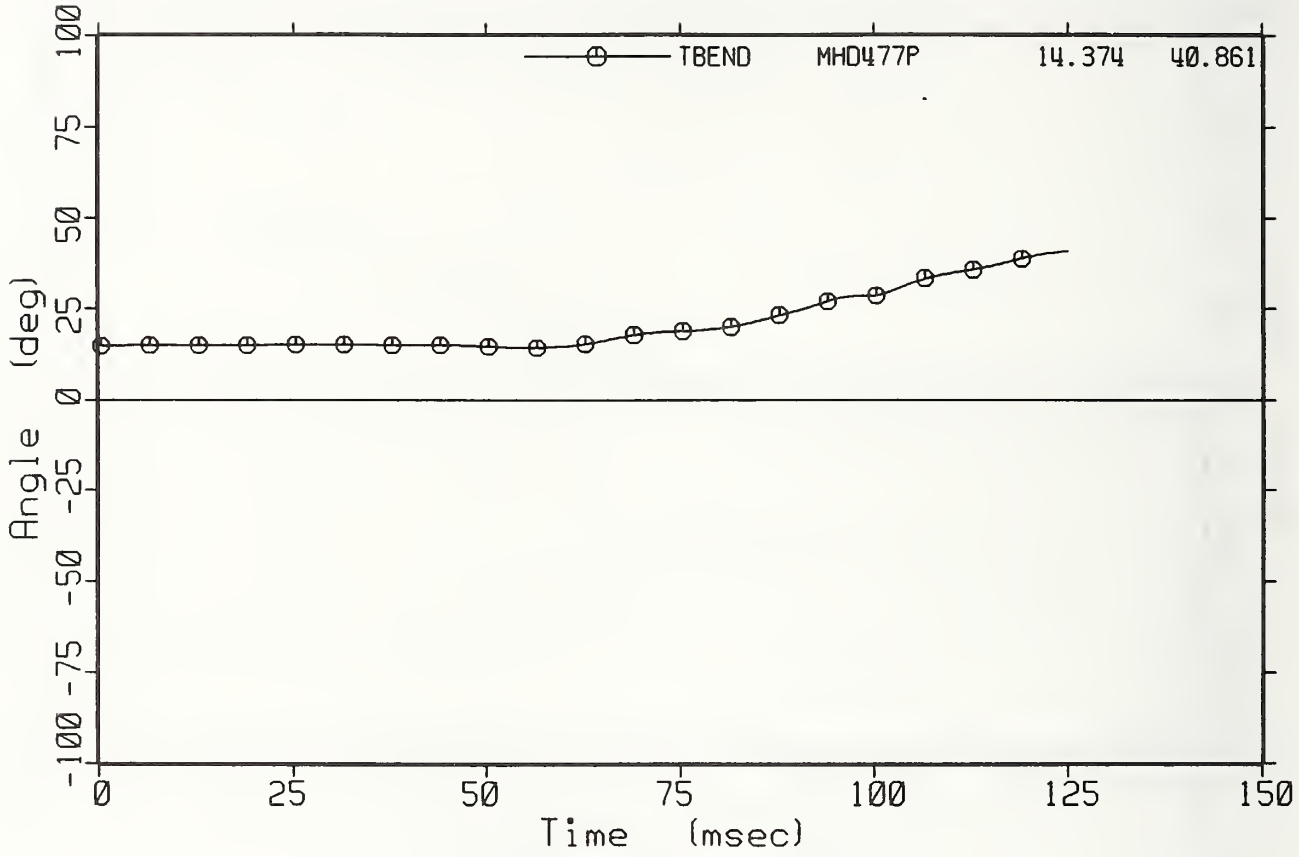

Thoracic bending

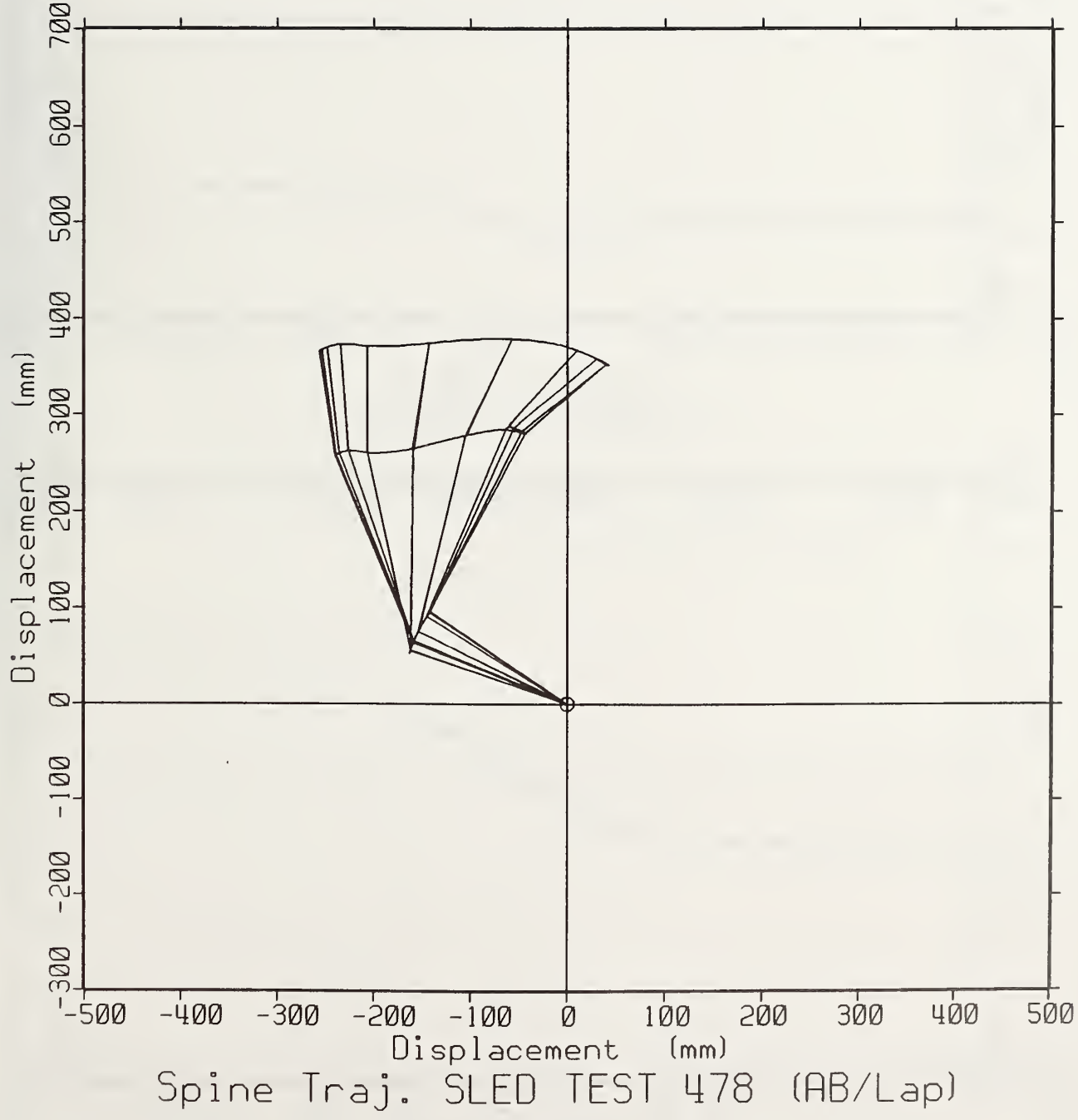

Spine Traj. SLED TEST 478 (AB/Lap)

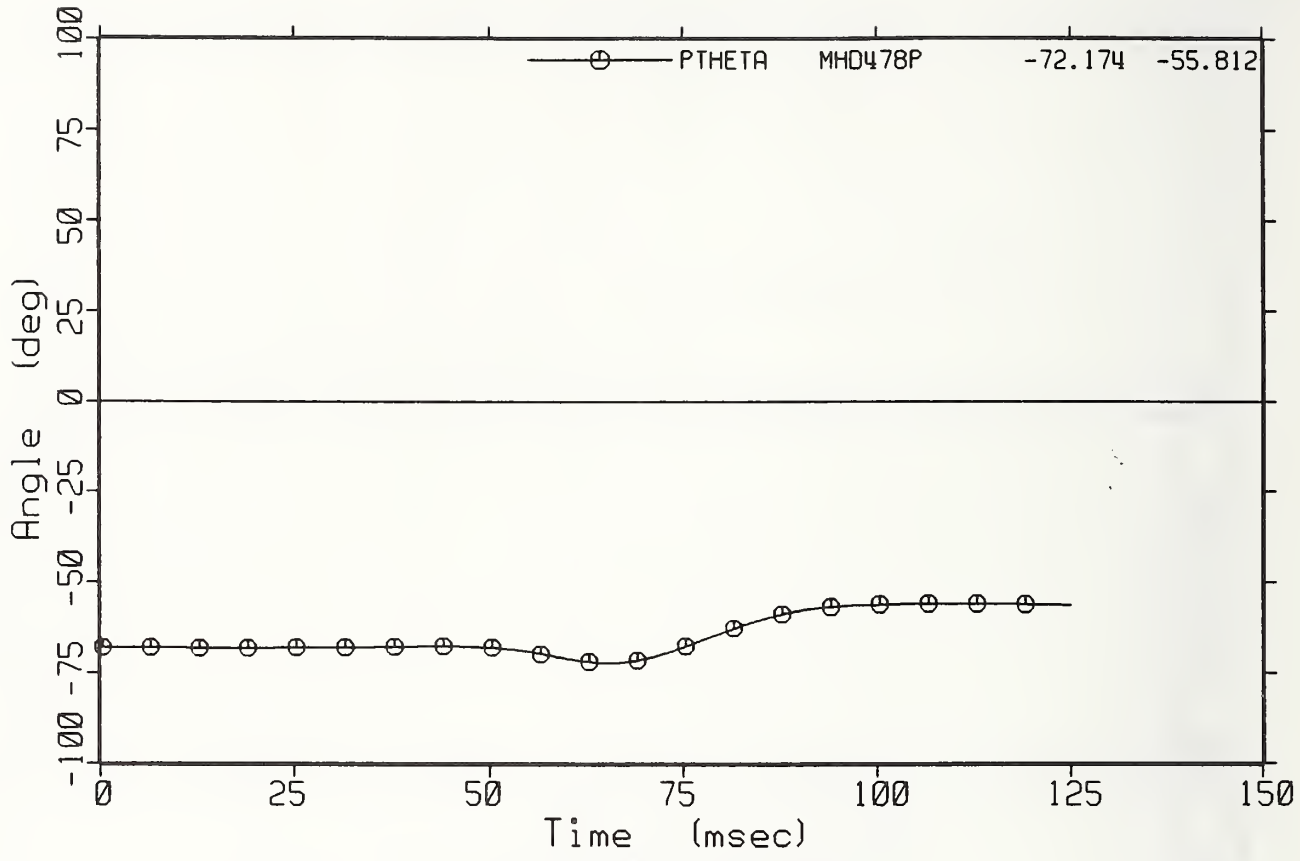

Pelvis angle

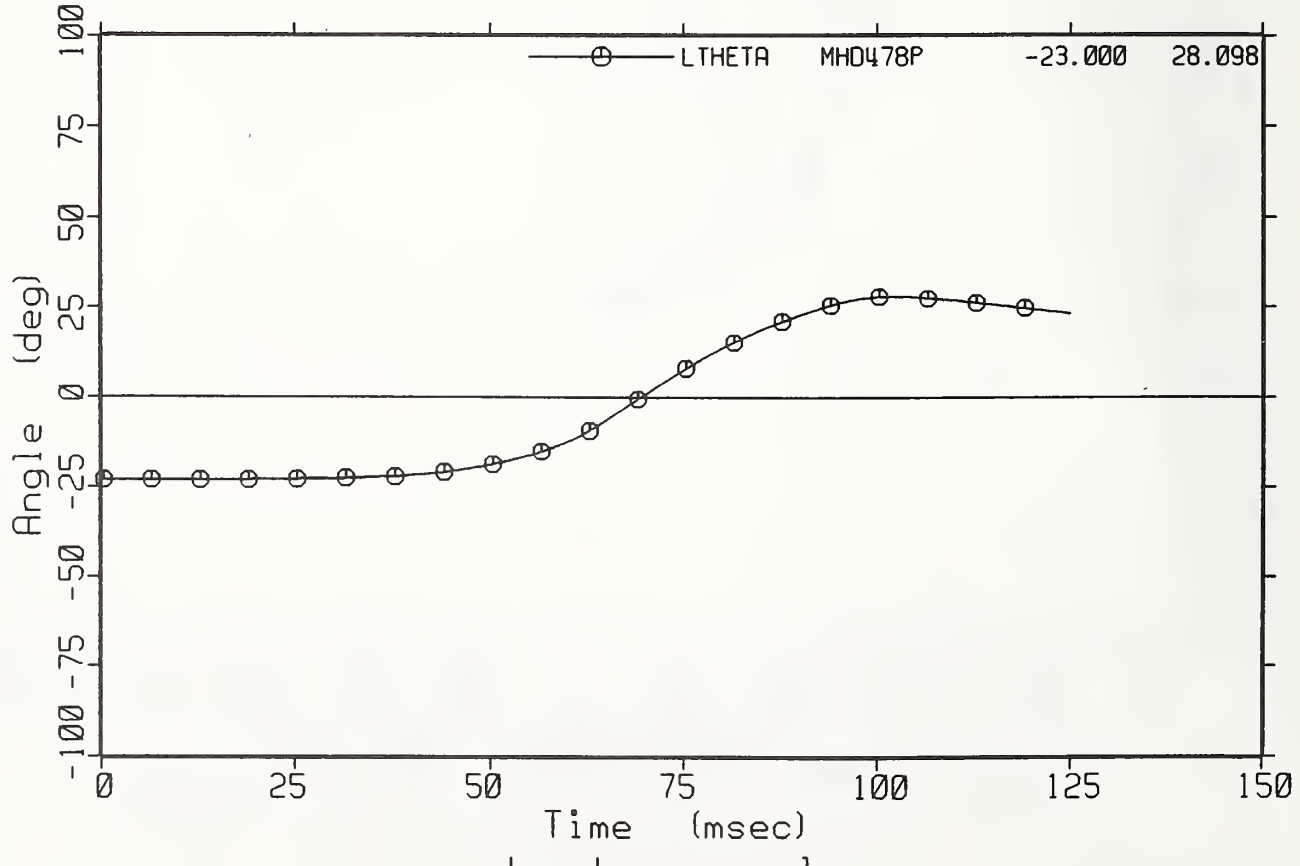

Lumbar angle

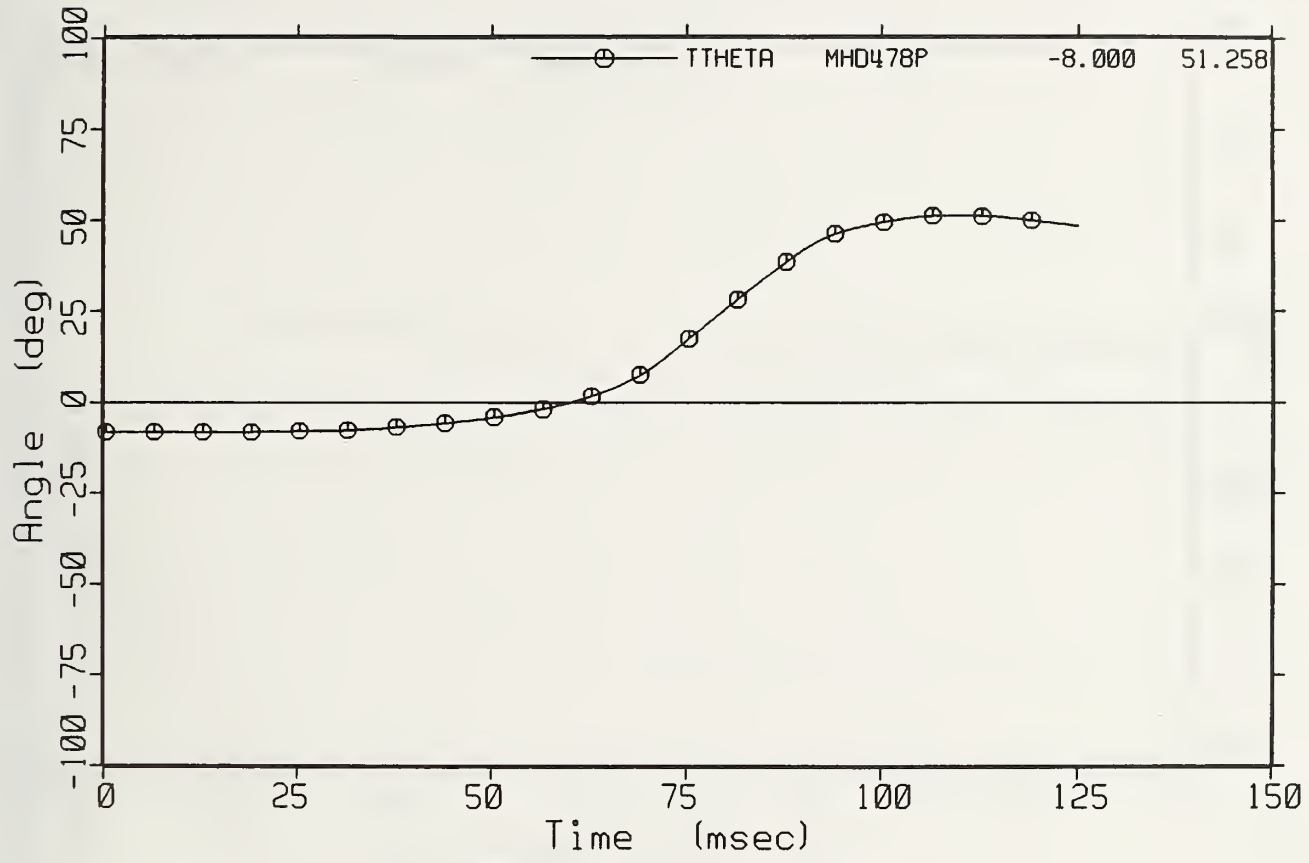

Thoracic angle

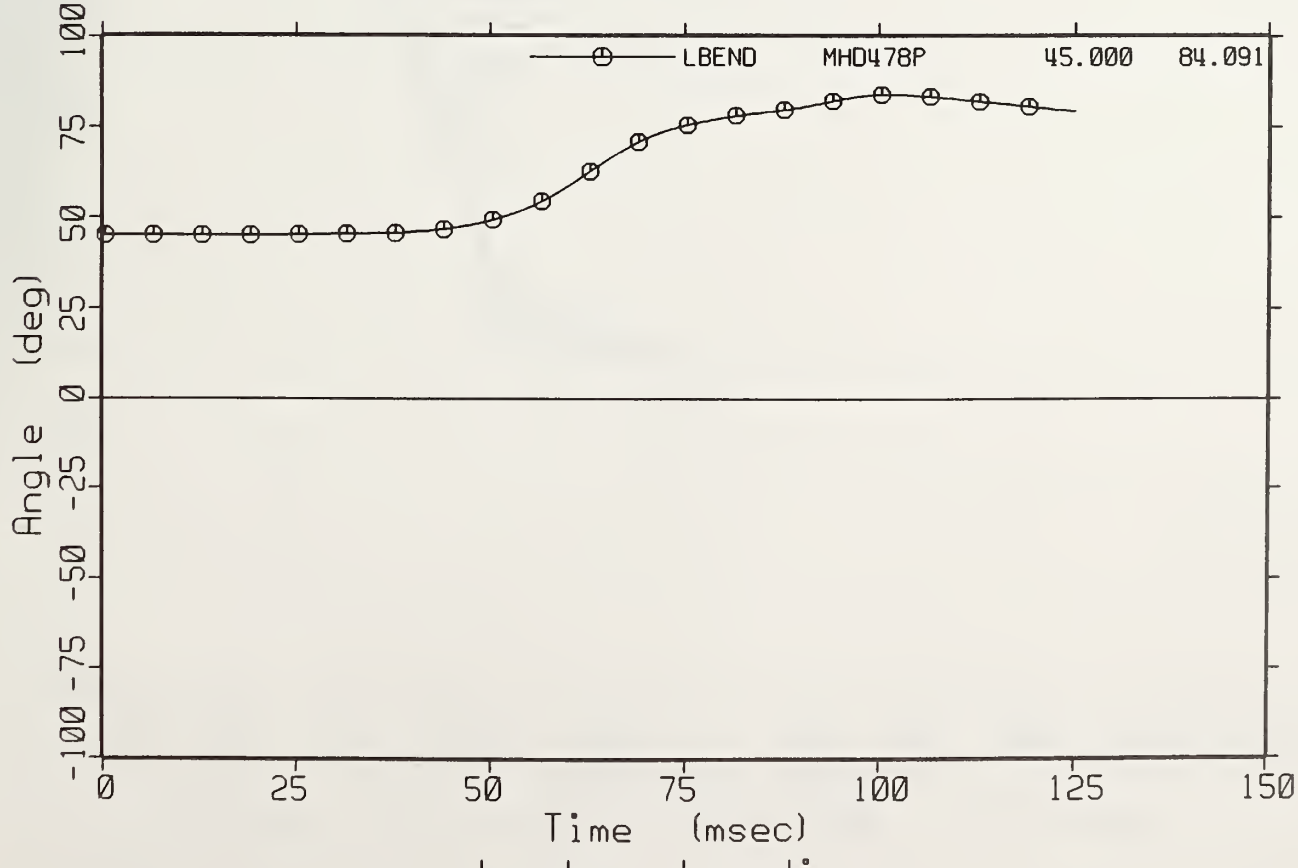

Lumbar bending

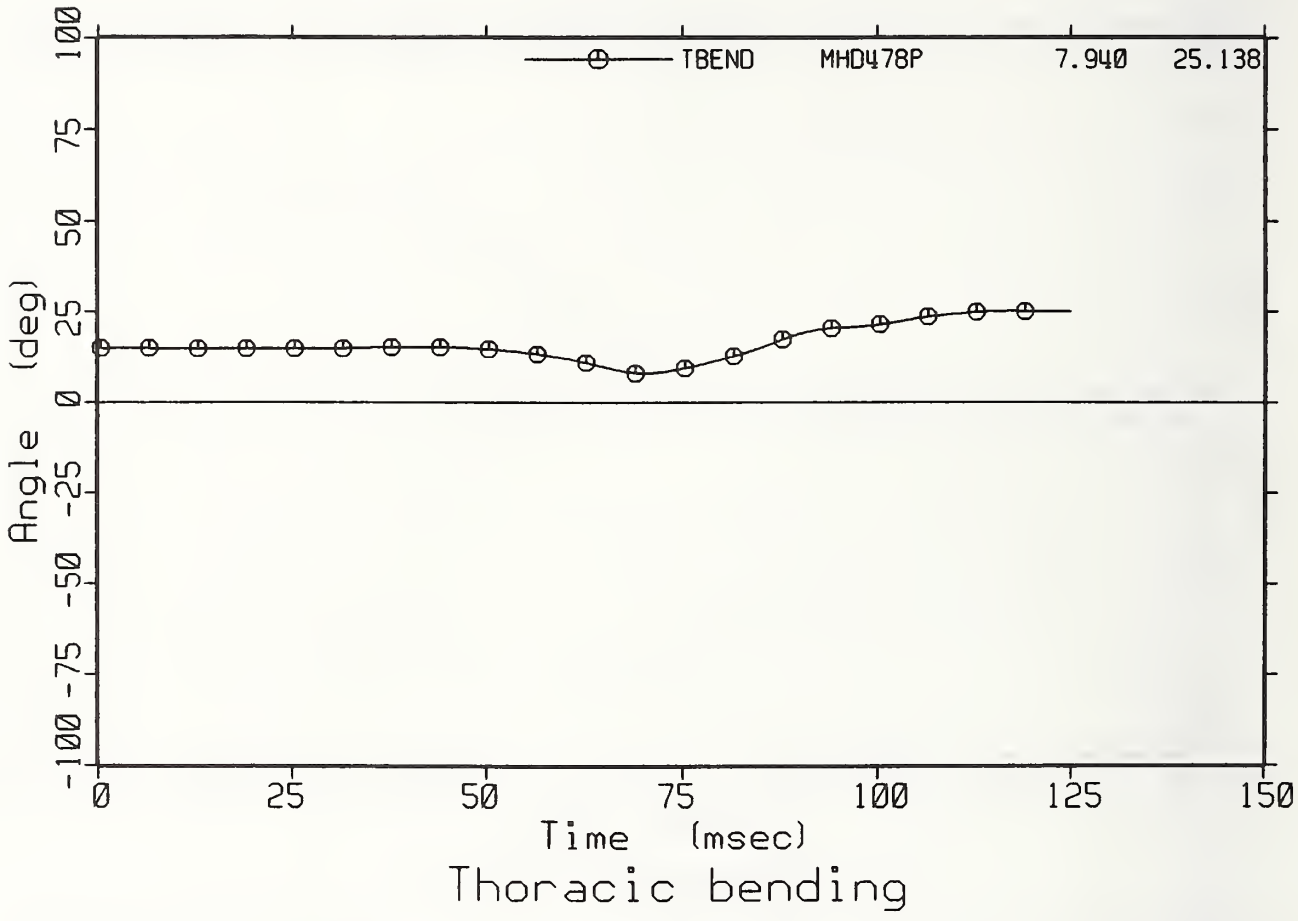

Thoracic bending

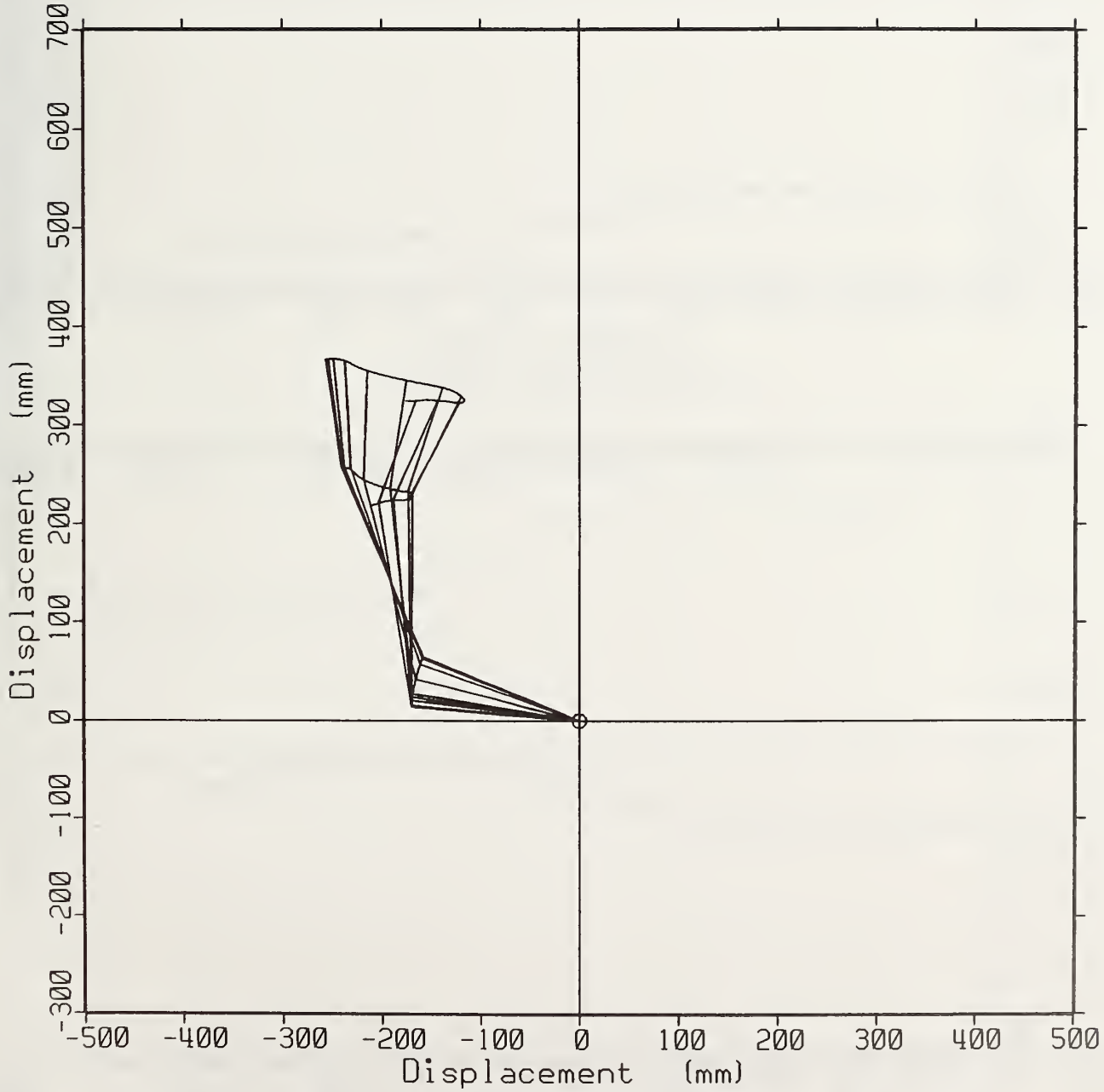

Spine Traj. SLED TEST 479 (3 PT/AB)

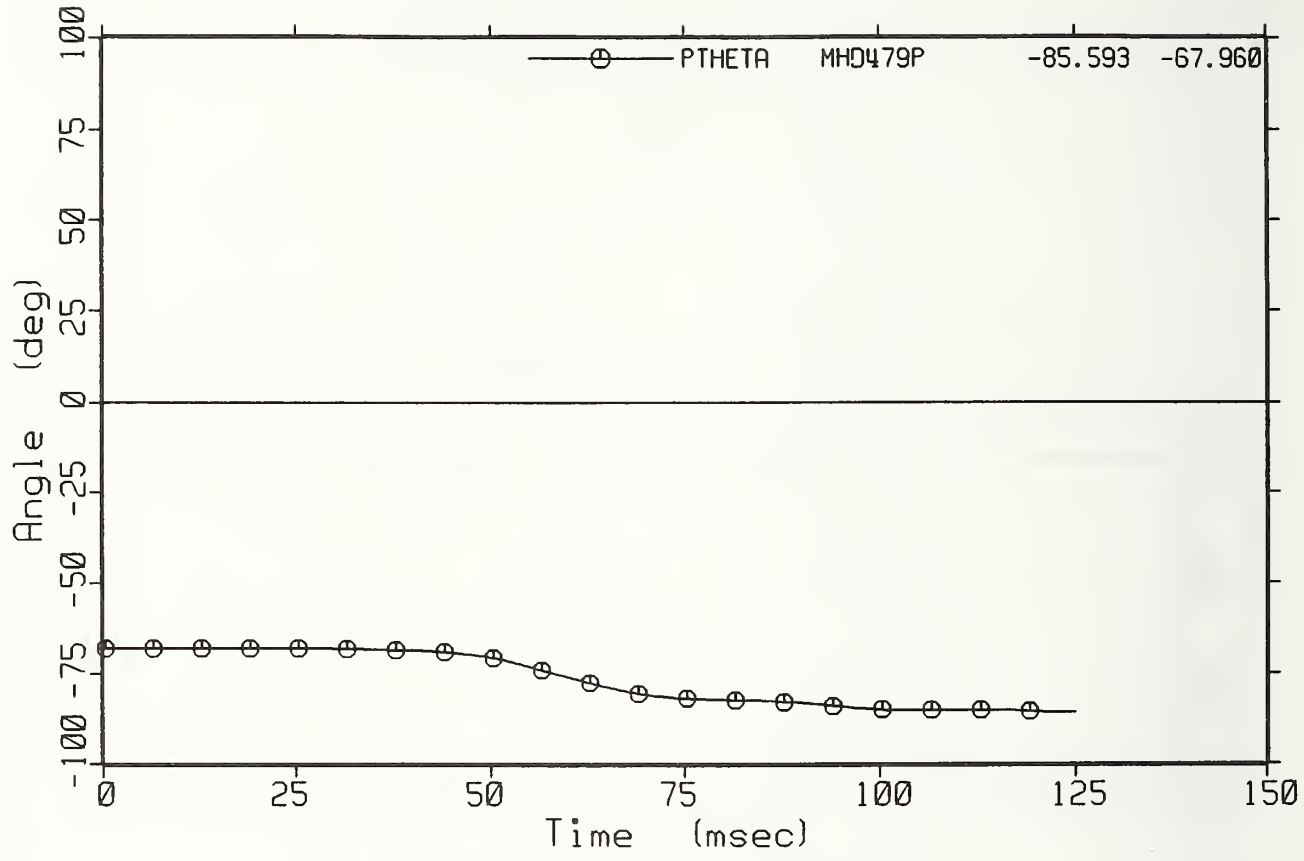

Pelvis angle

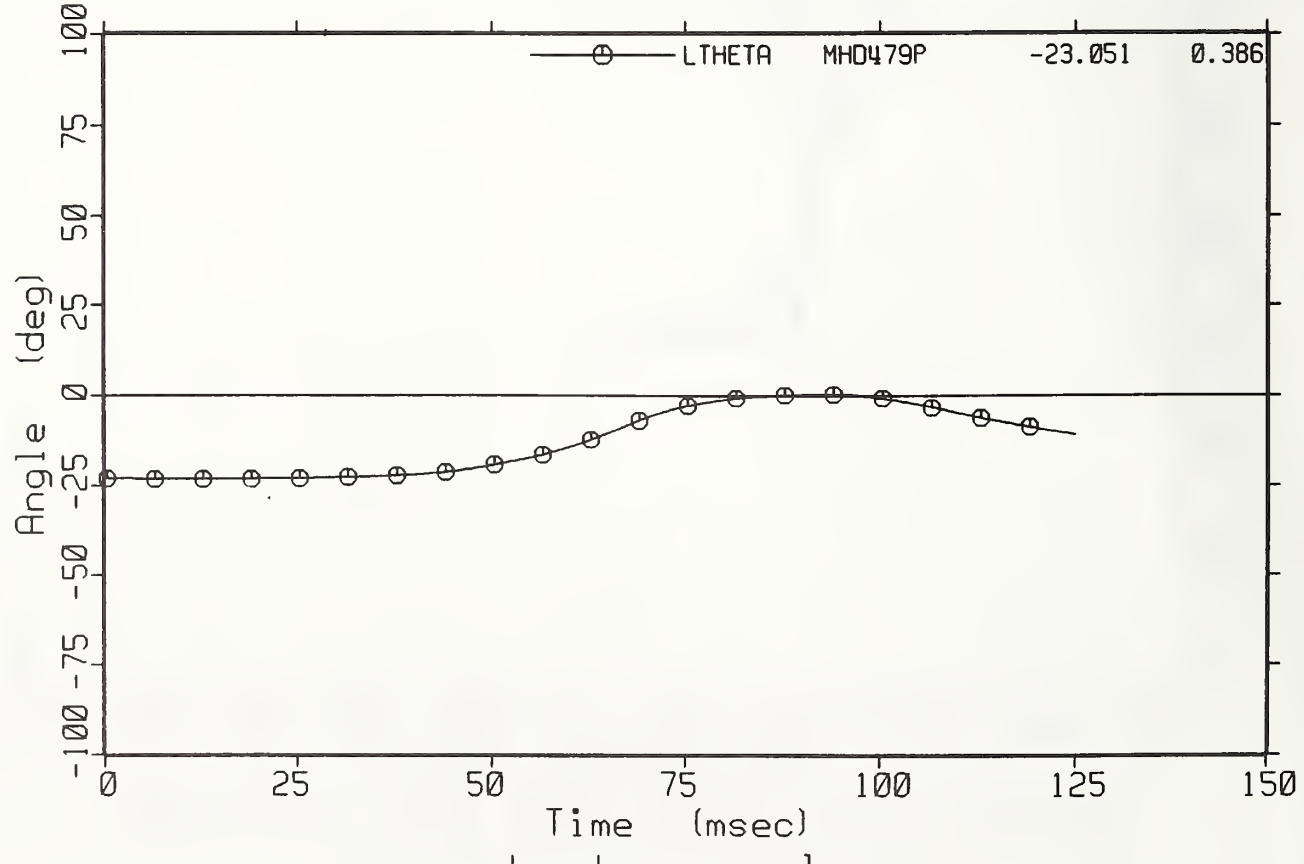

Lumbar angle

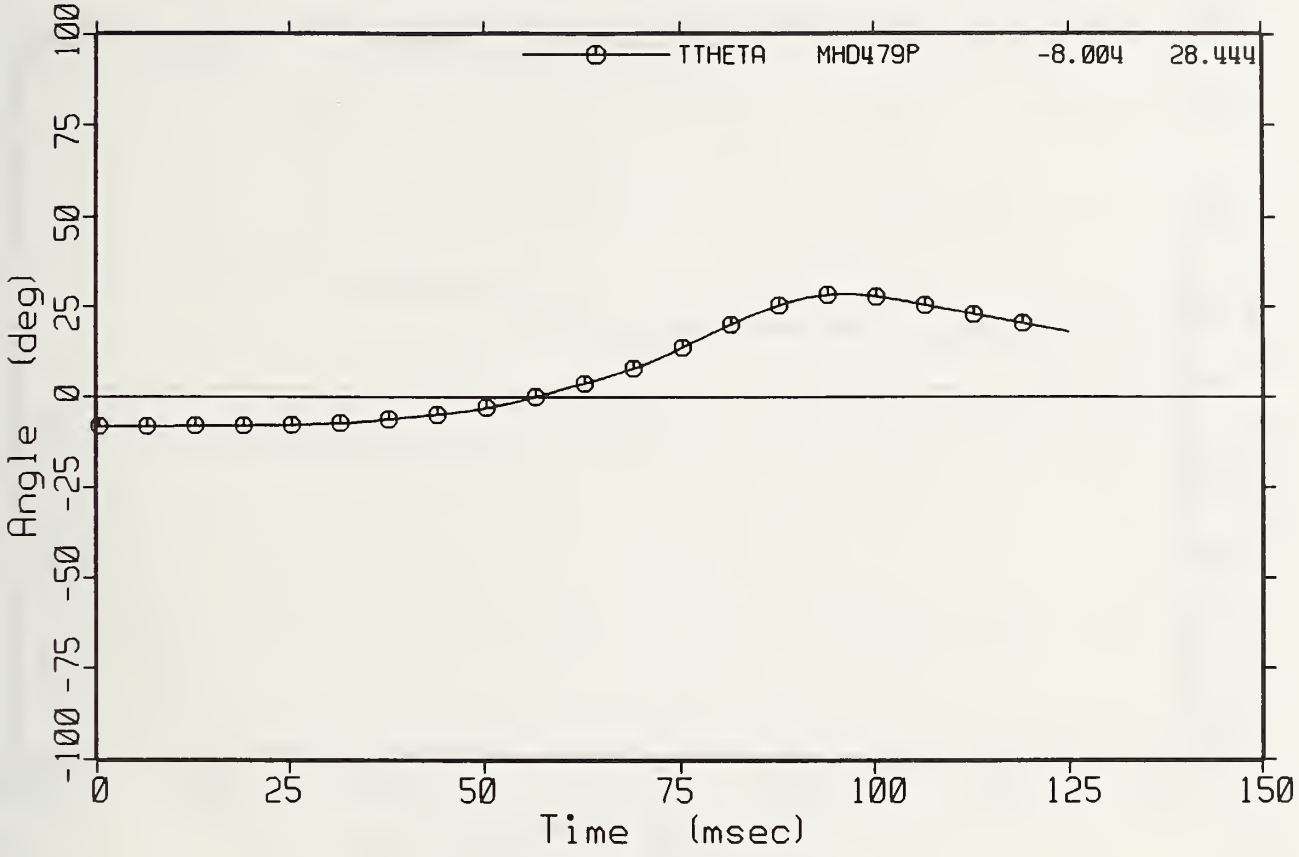

Thoracic angle

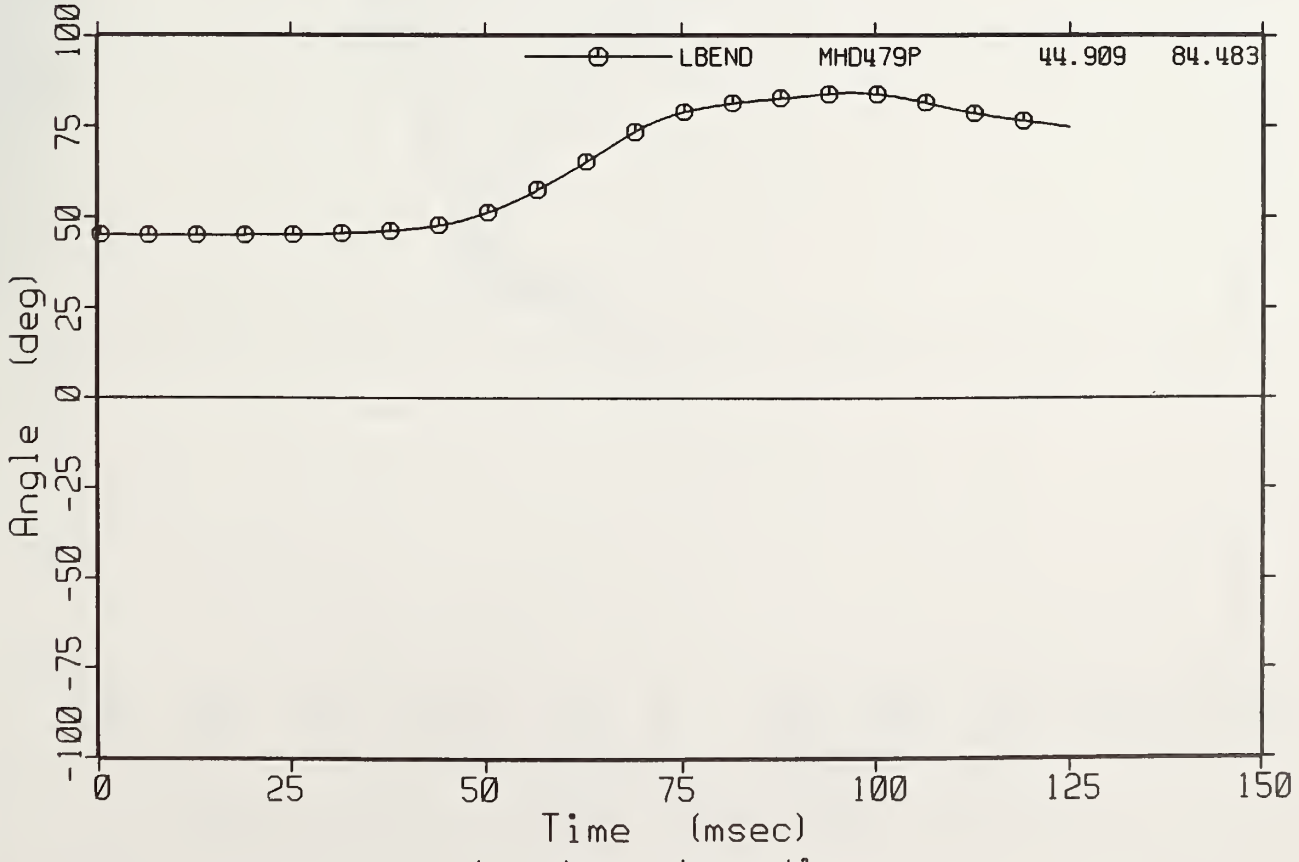

Lumbar bending

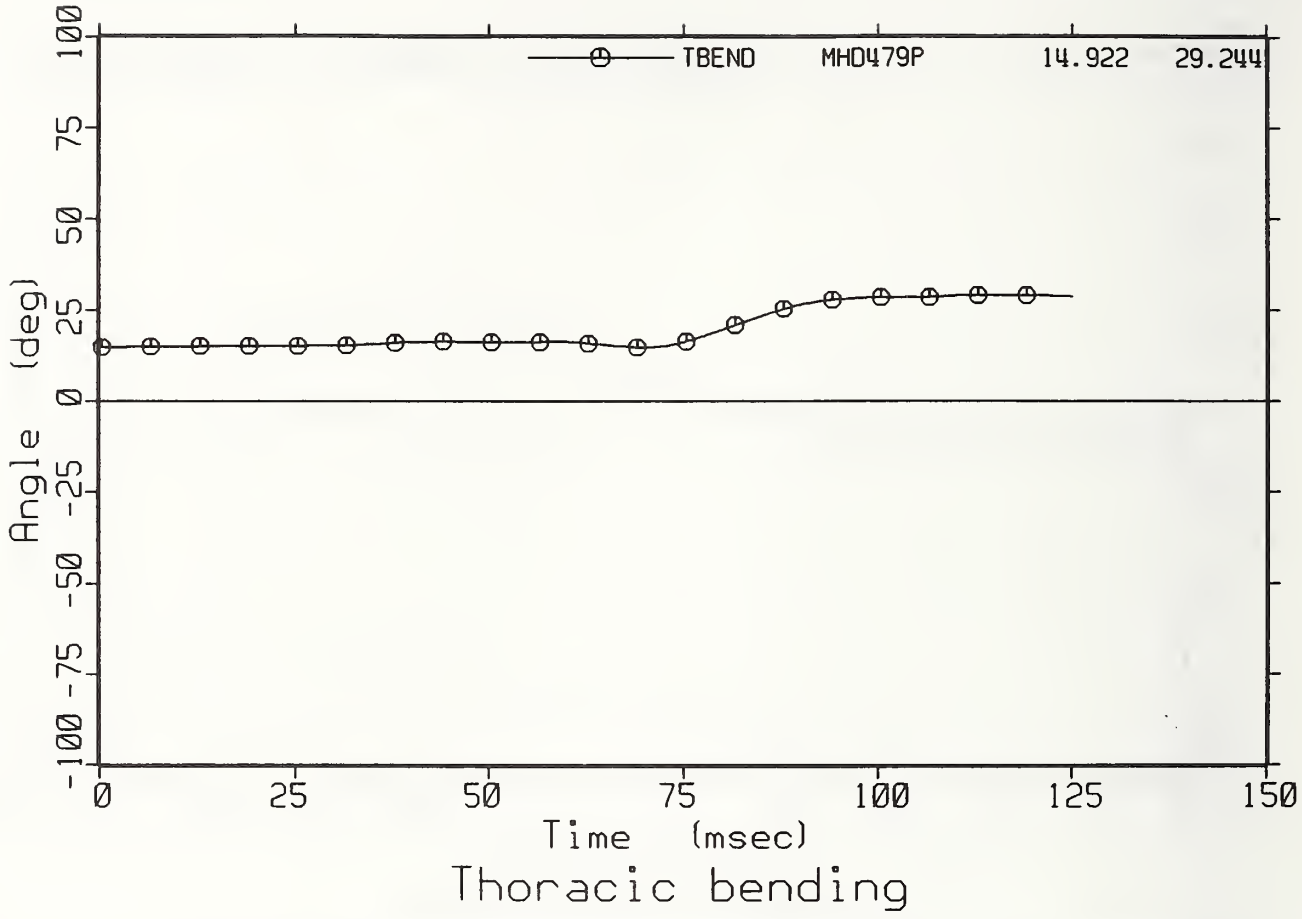

Thoracic bending

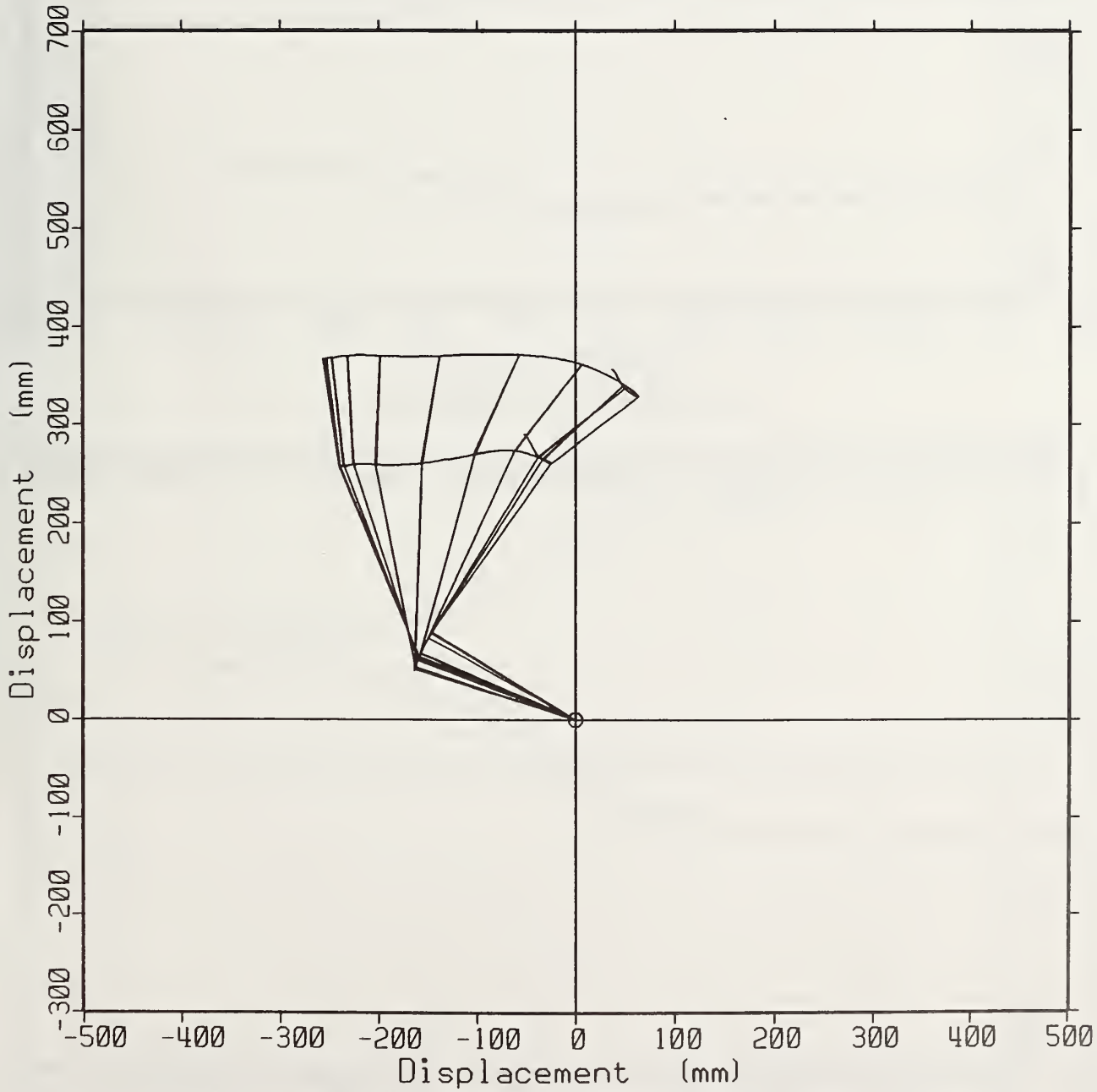

Spine Traj. SLED TEST 480 (AB/LAP)

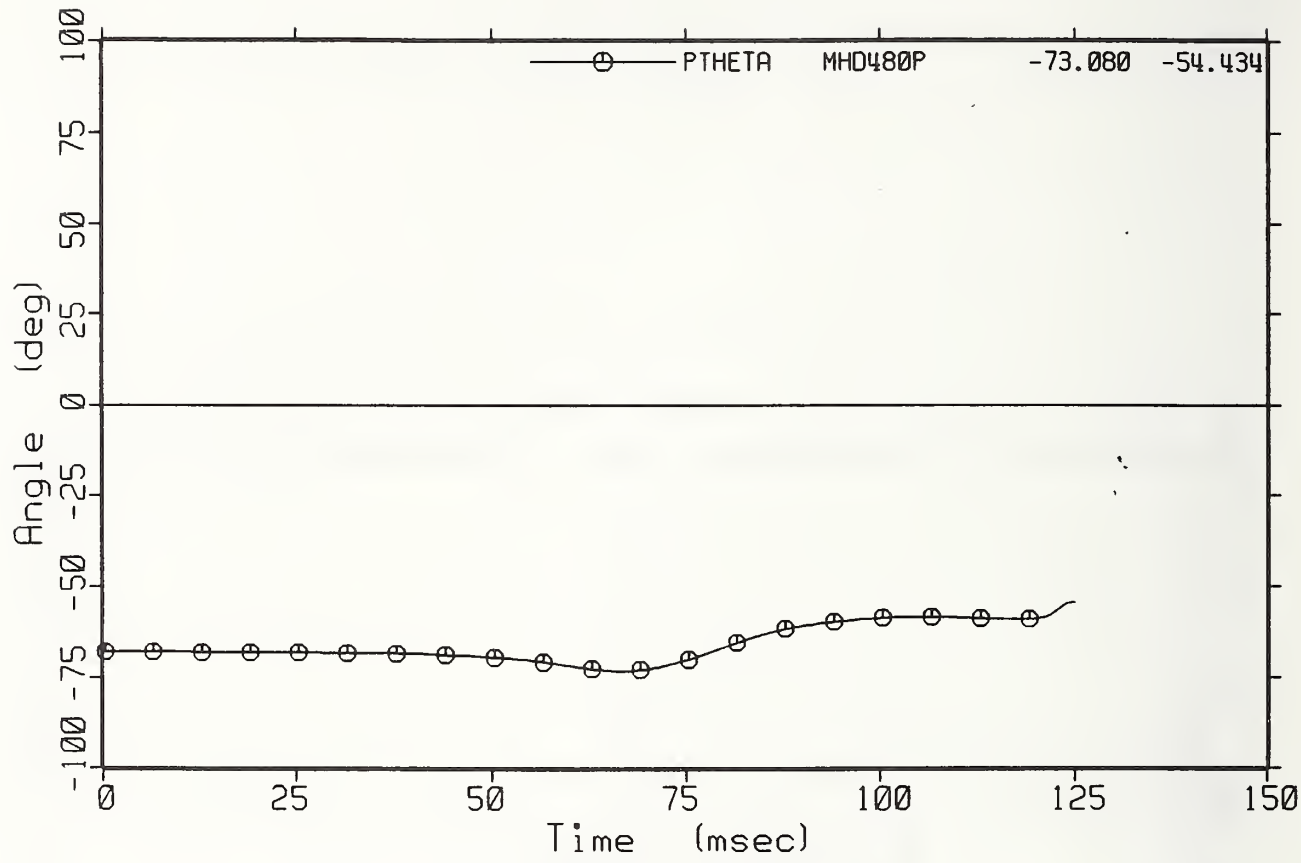

Pelvis angle

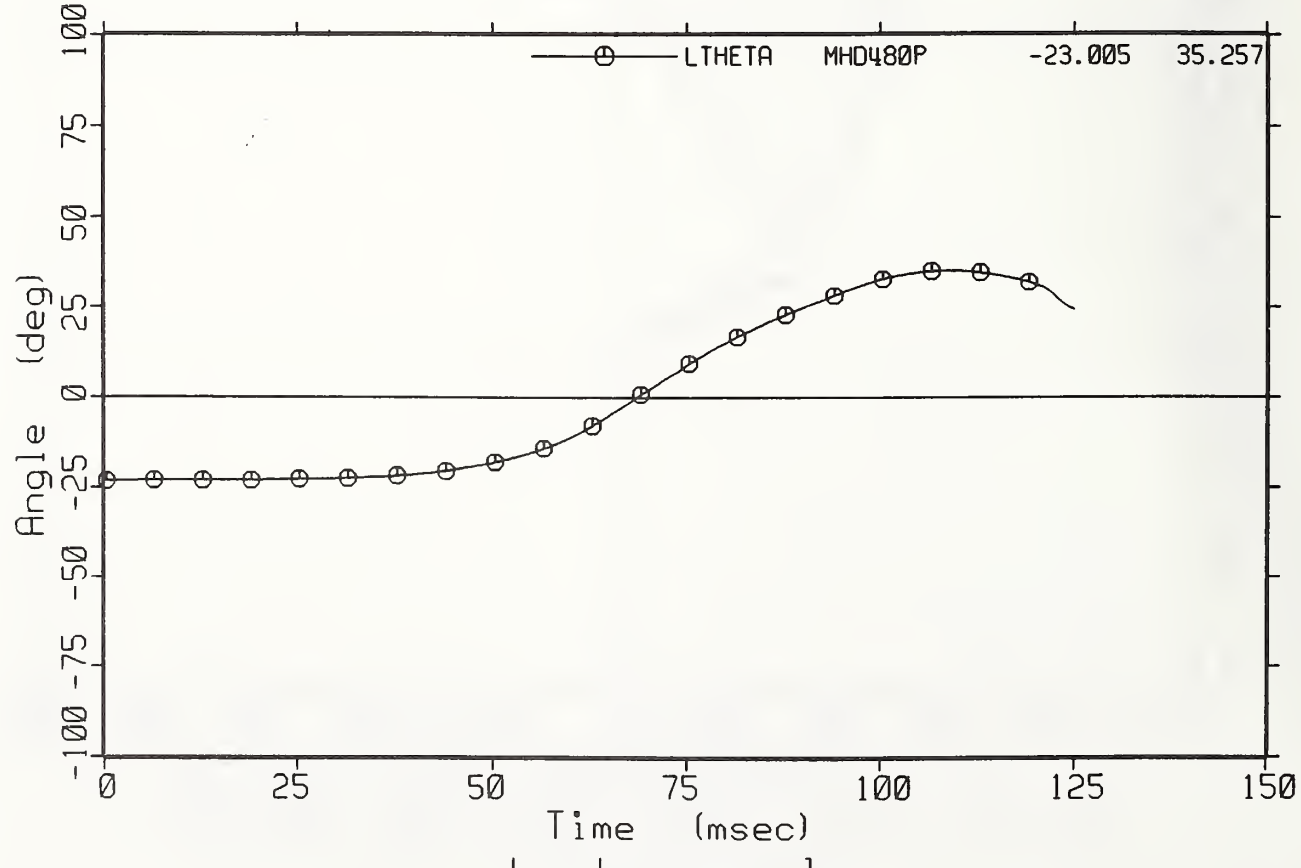

Lumbar angle

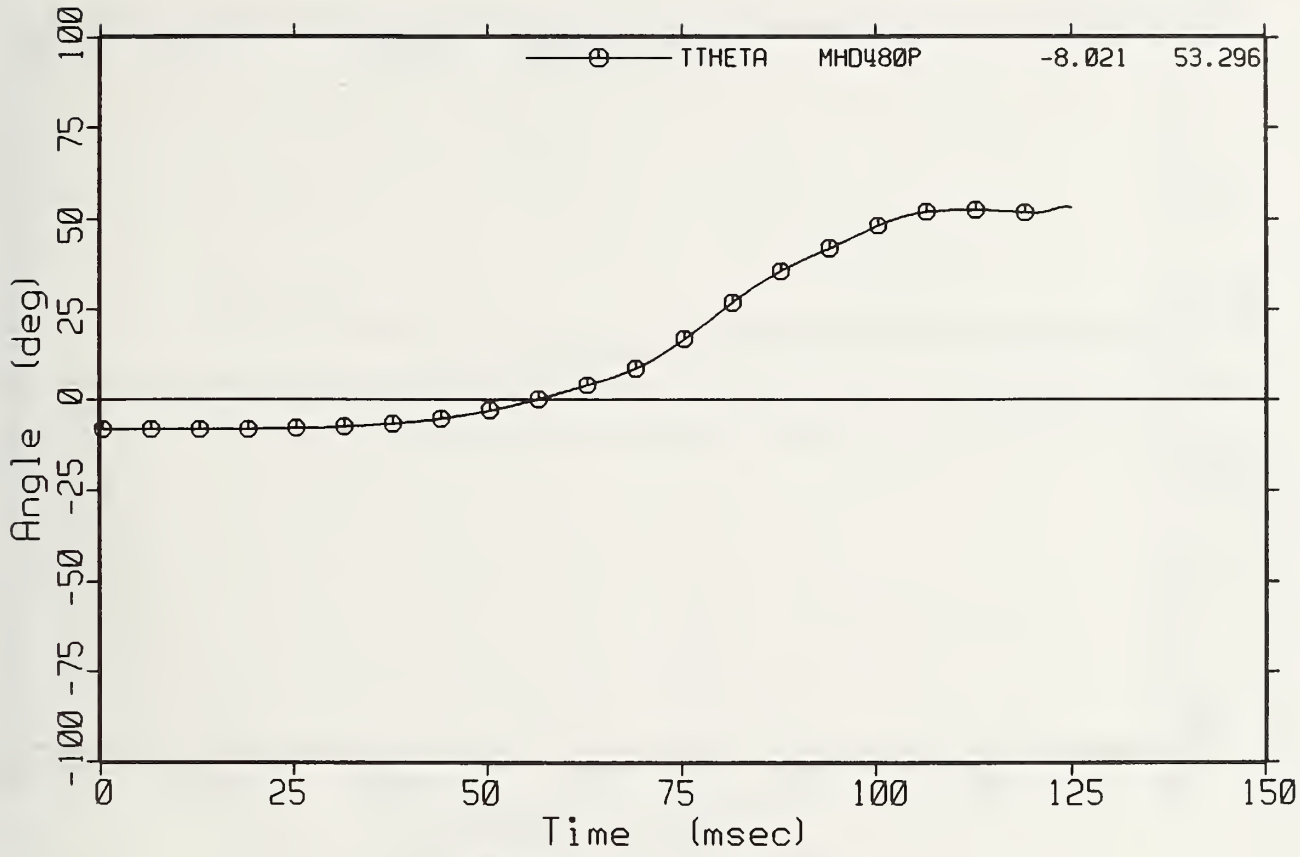

Thoracic angle

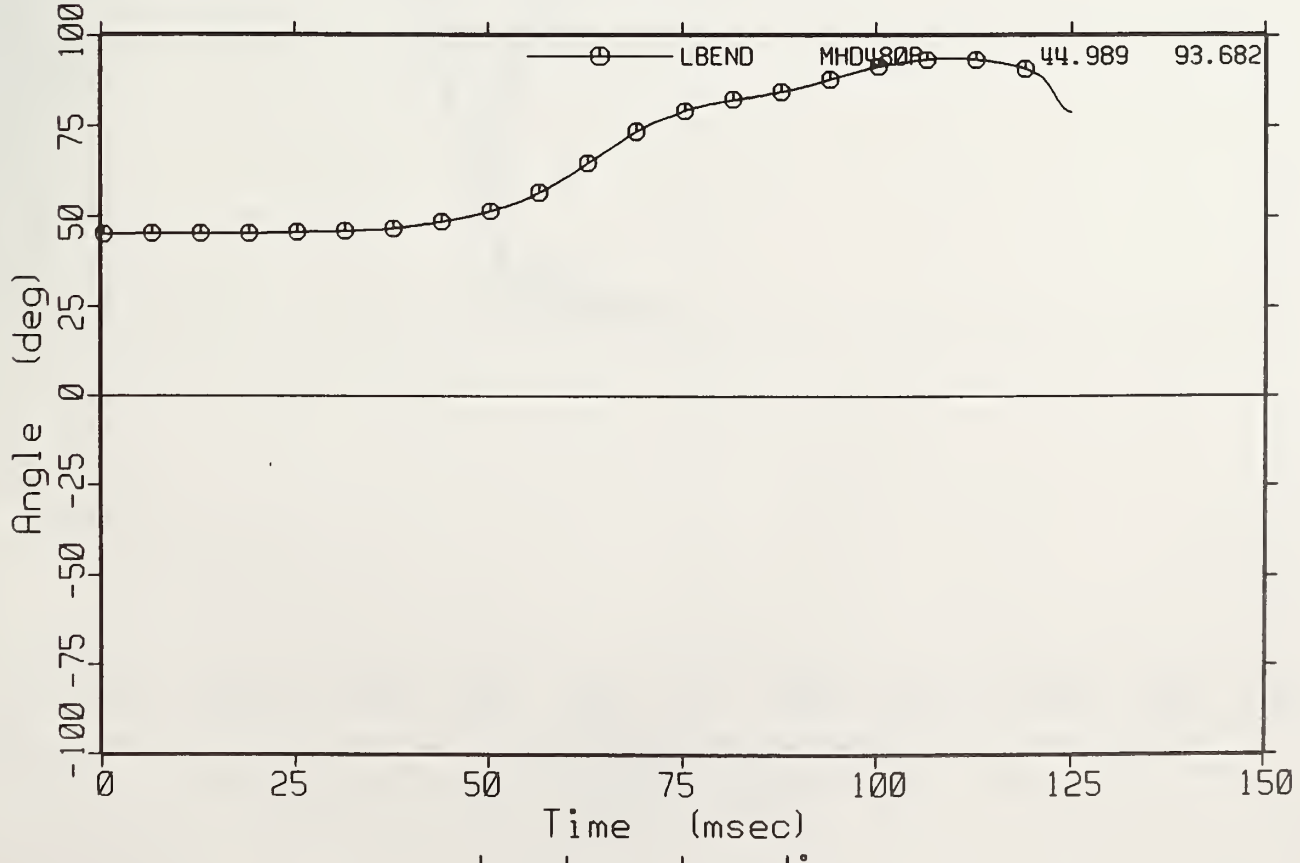

Lumbar bending

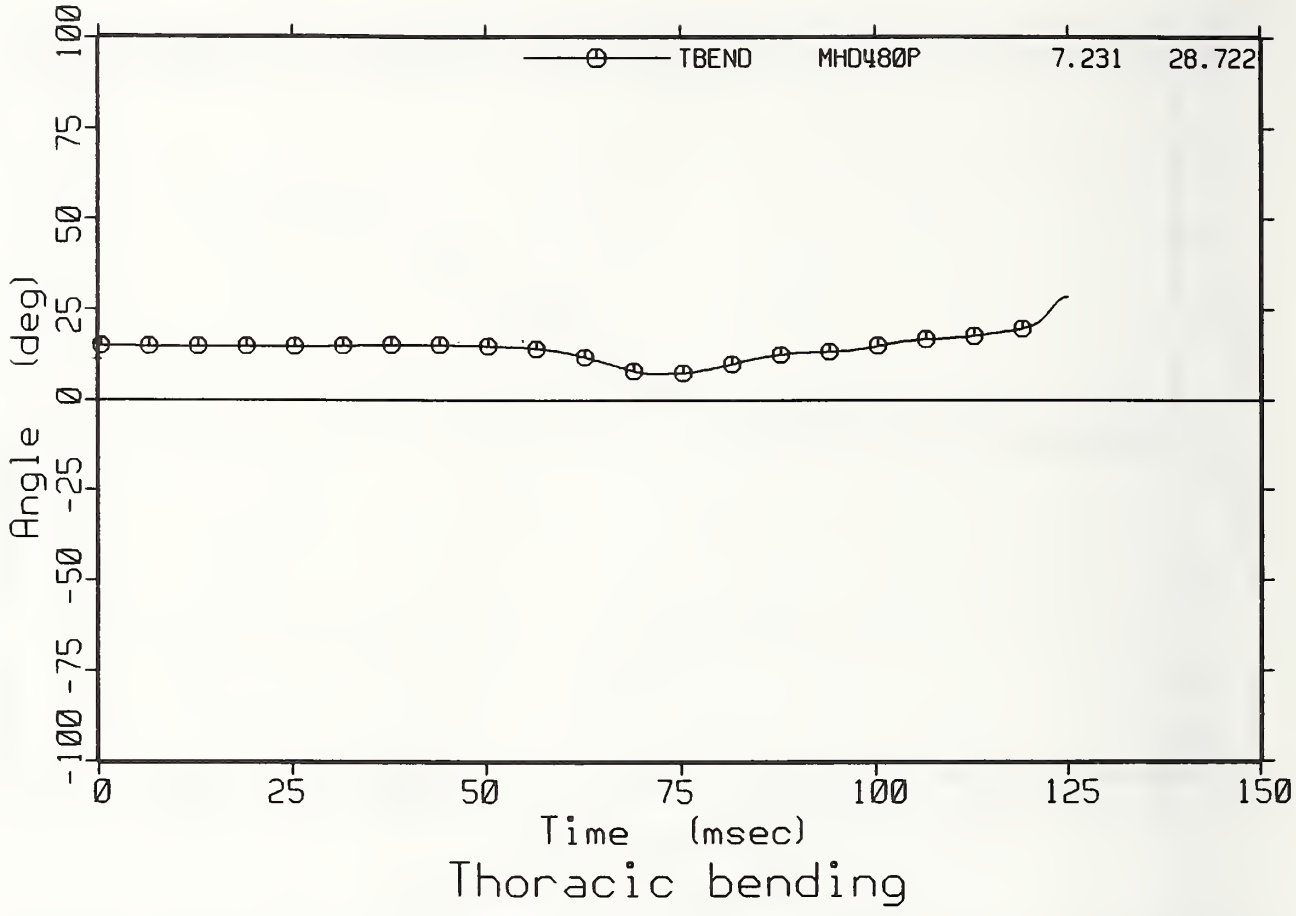

Thoracic bending

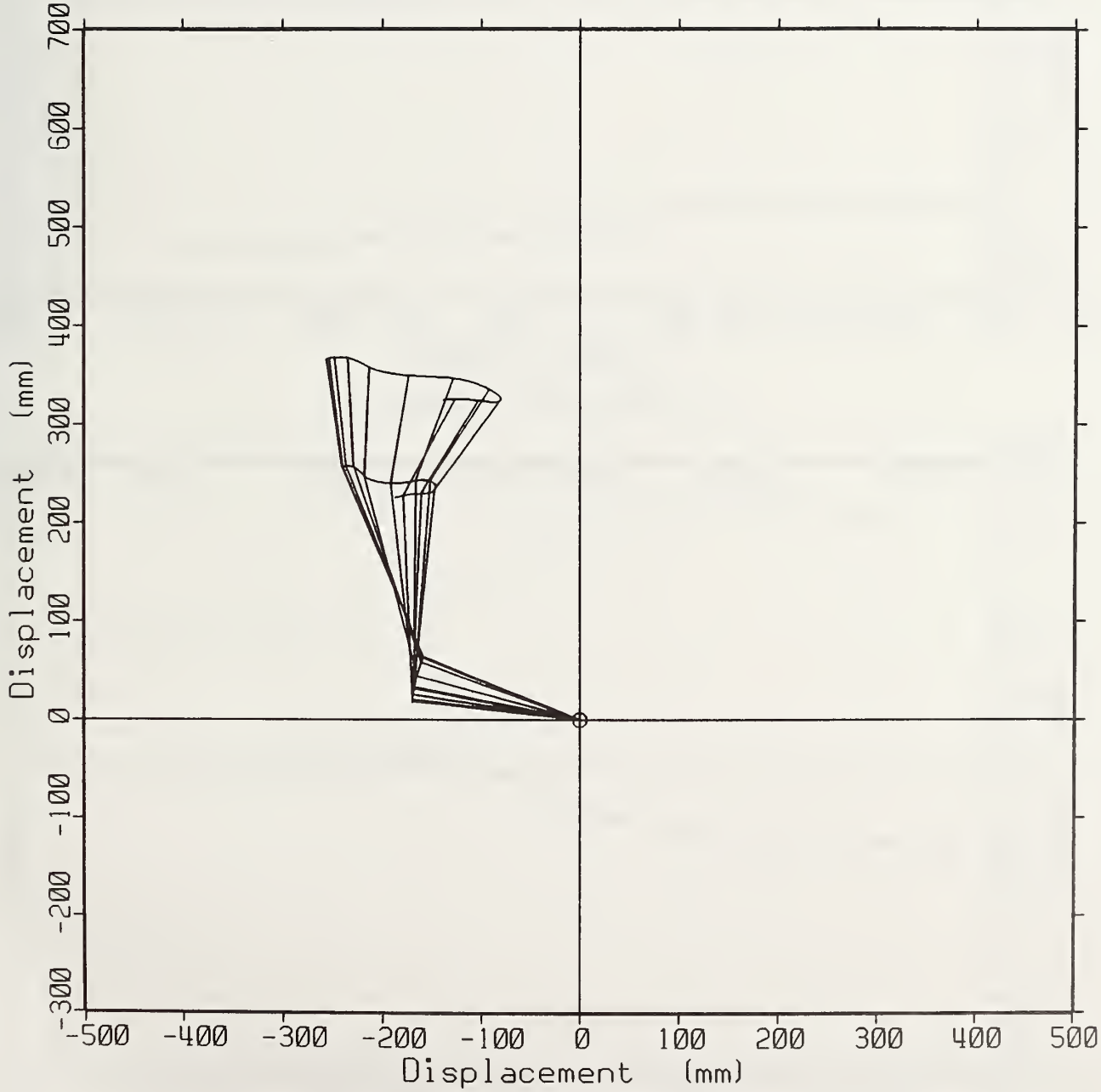

Spine Traj. SLED TEST 481 (3 PT)

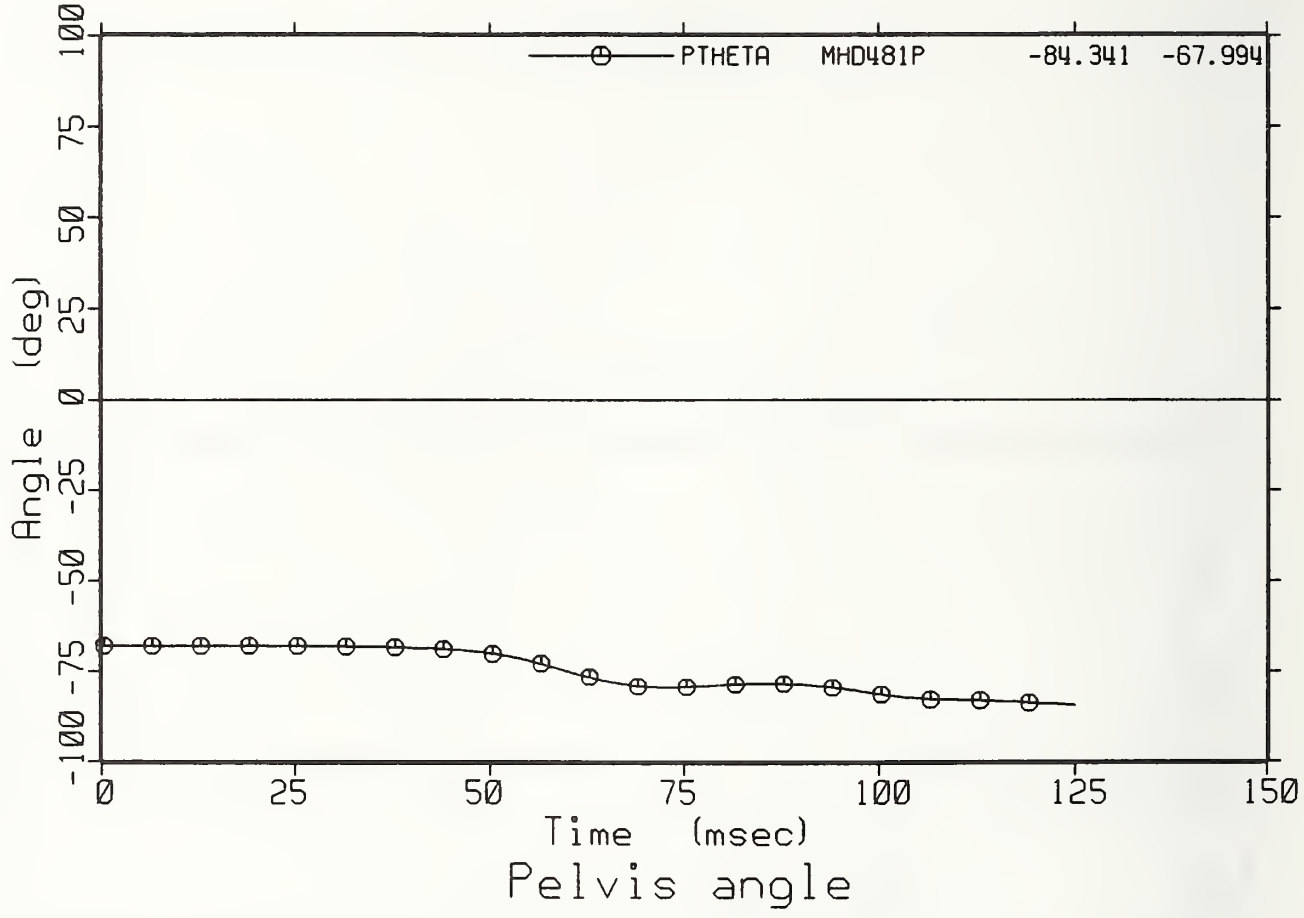

Pelvis angle

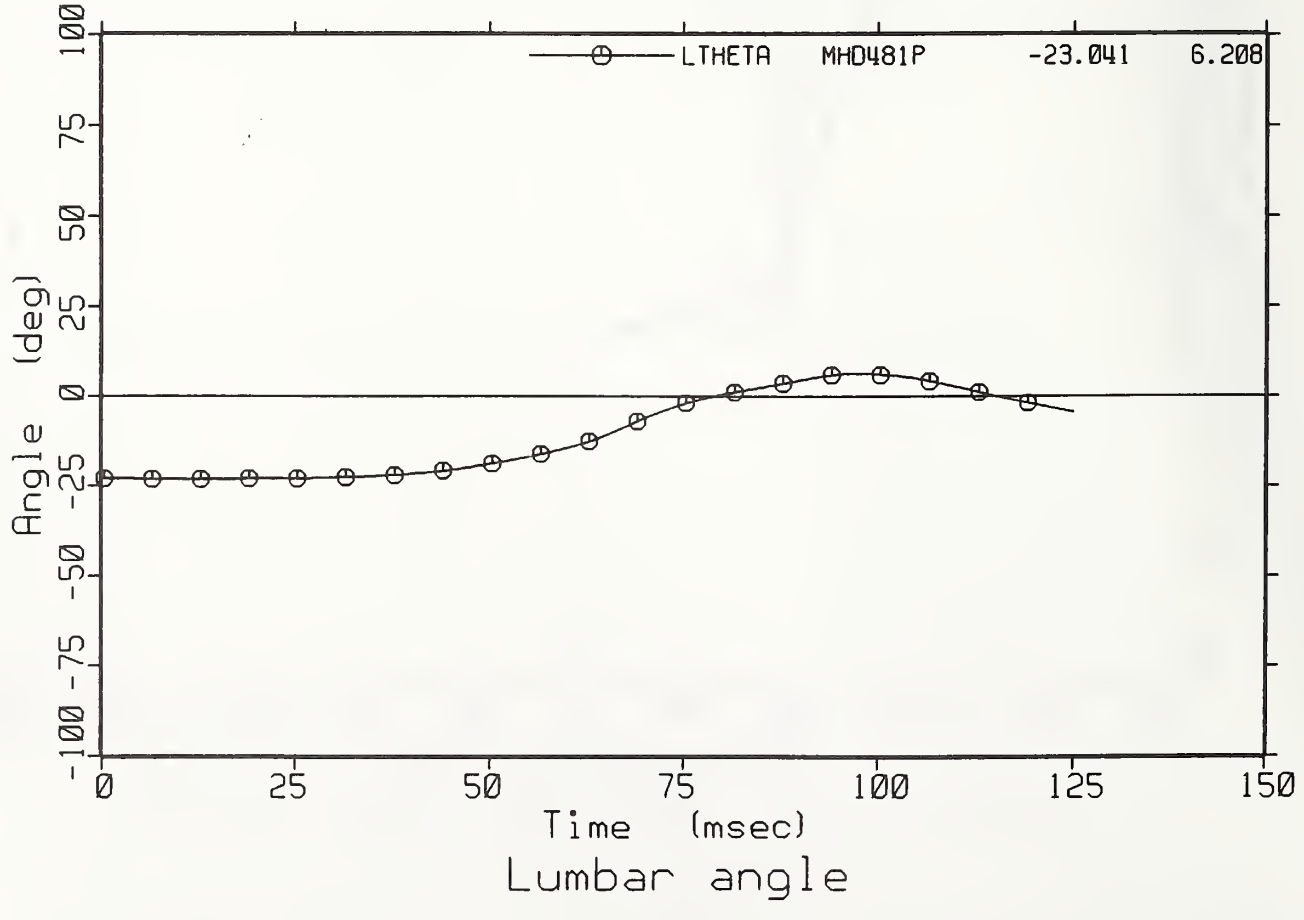

Lumbar angle

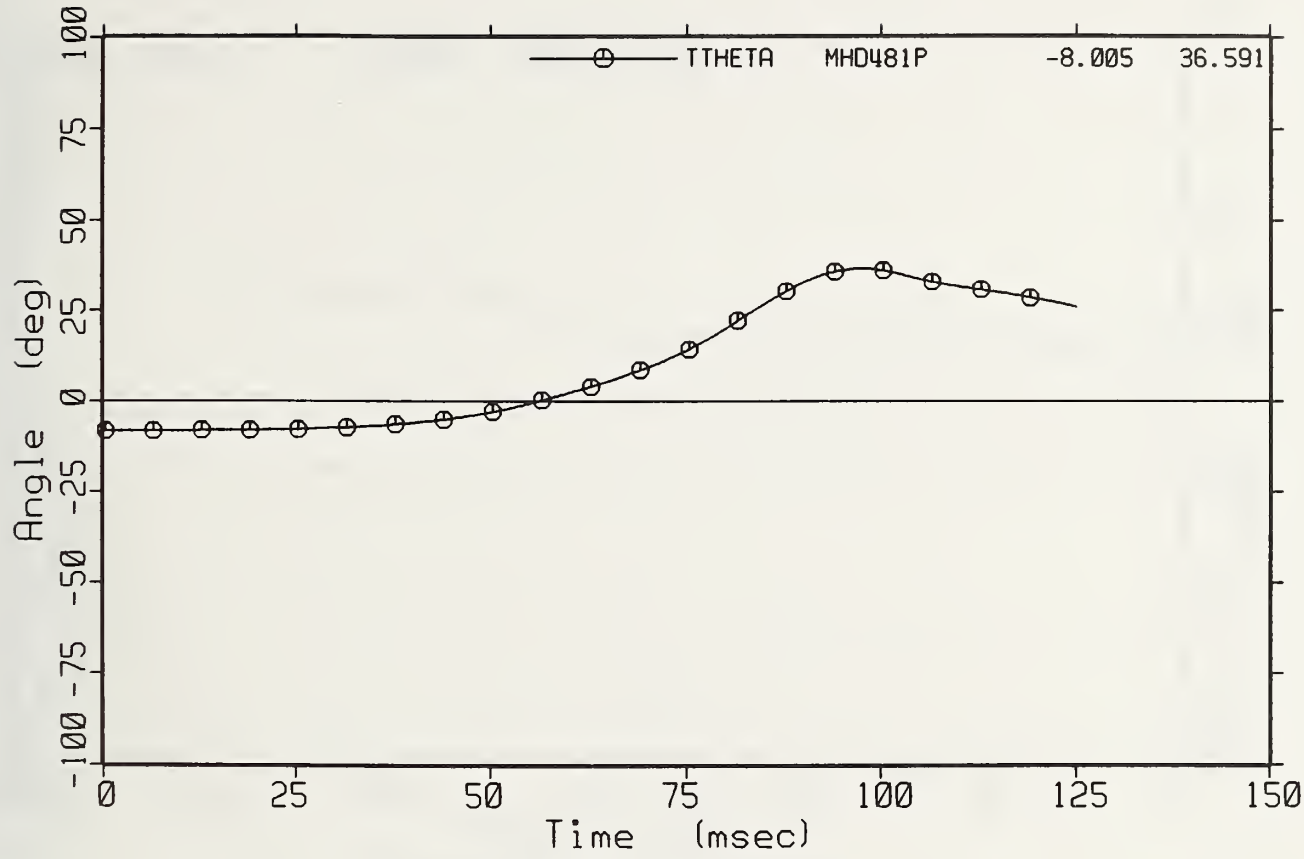

Thoracic angle

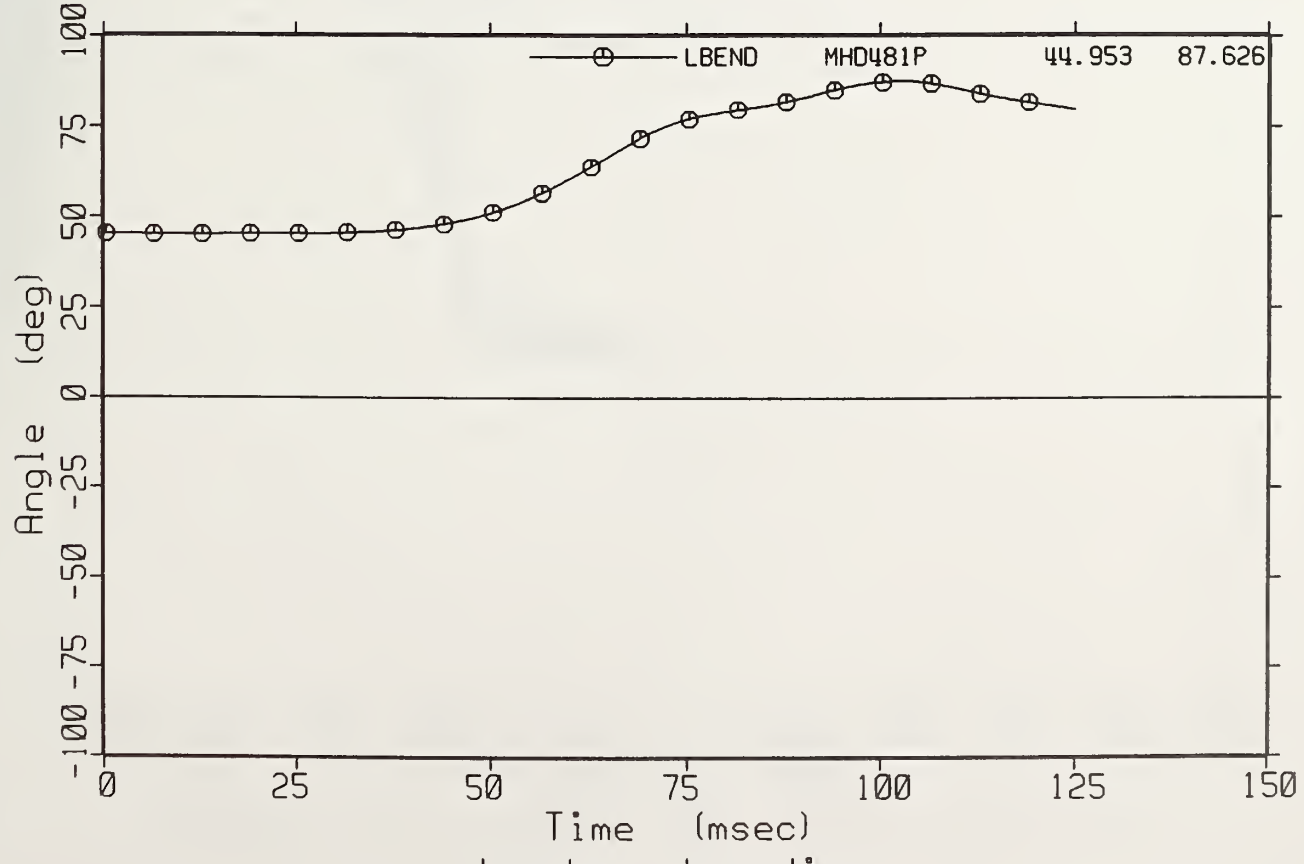

Lumbar bending

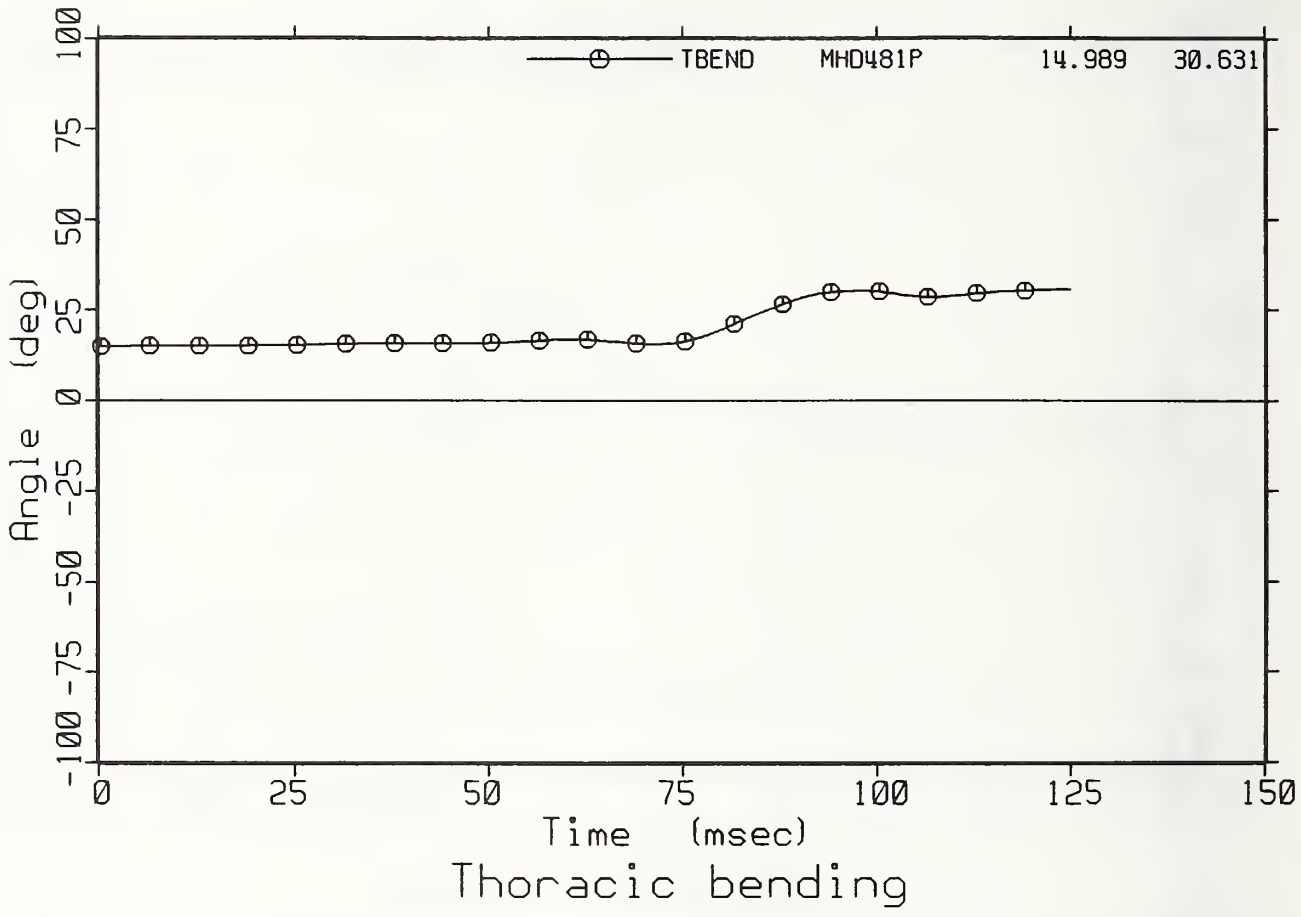

Thoracic bending

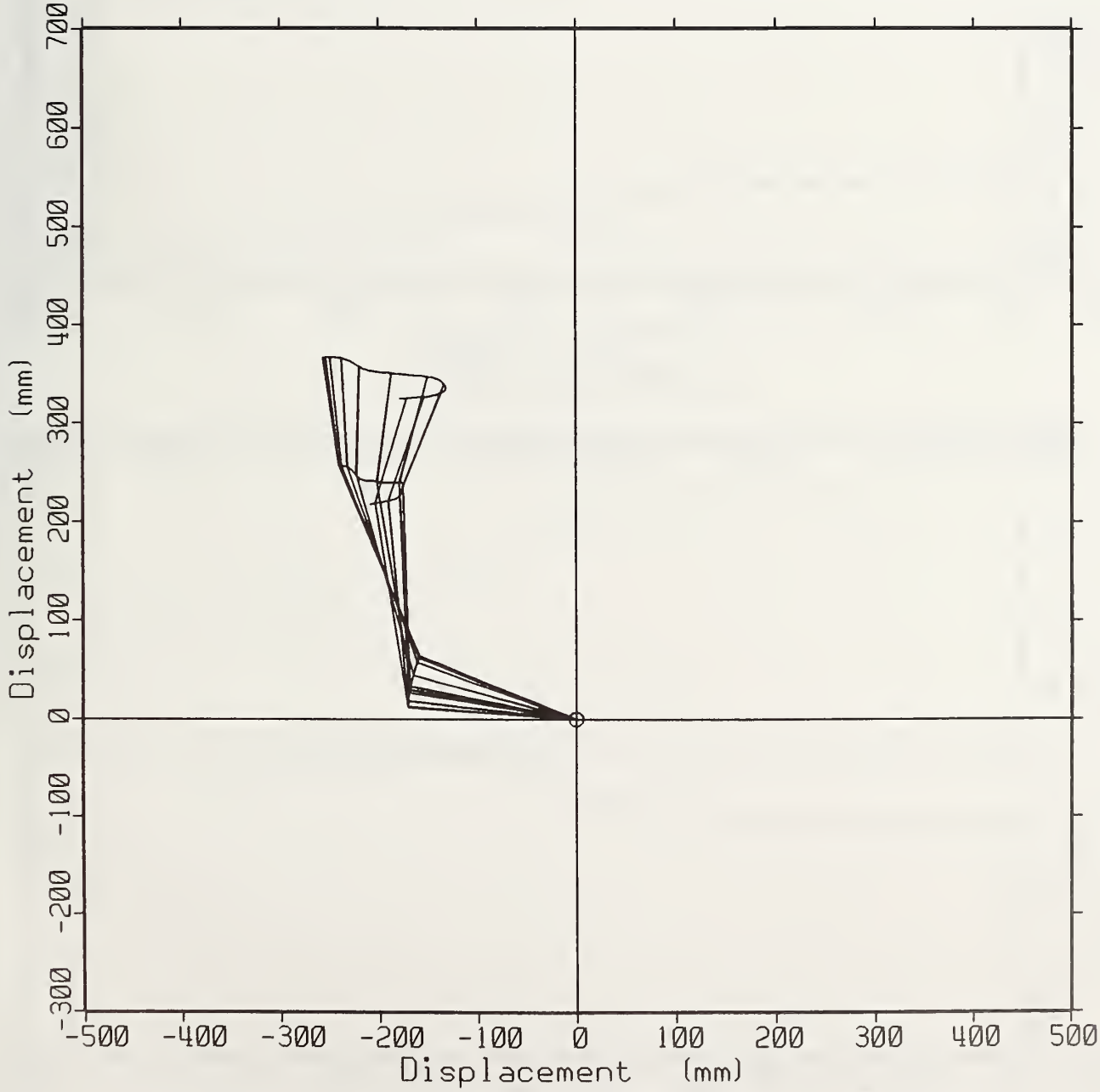

Spine Traj. SLED TEST 482 (3 PT/AB)

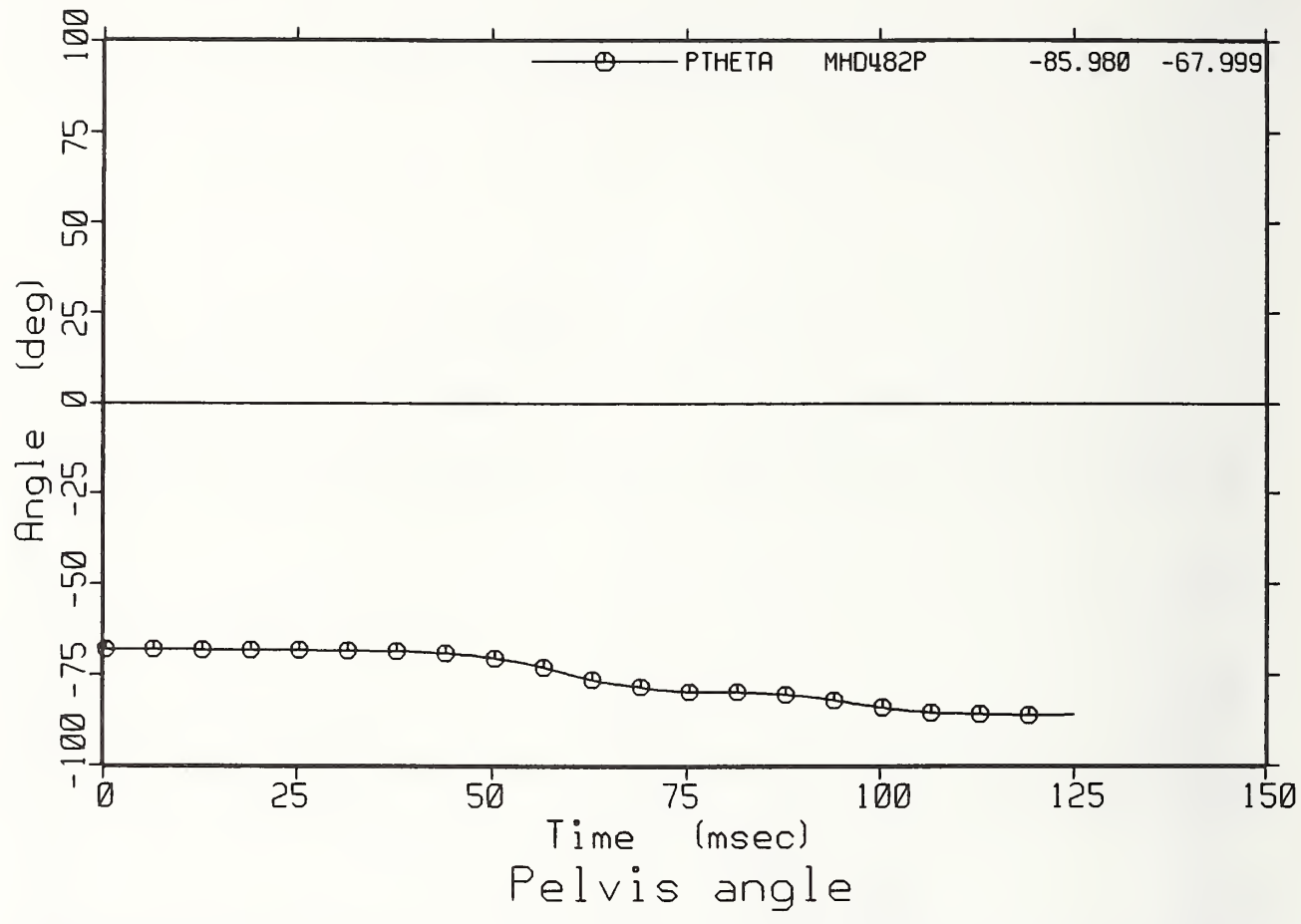

Pelvis angle

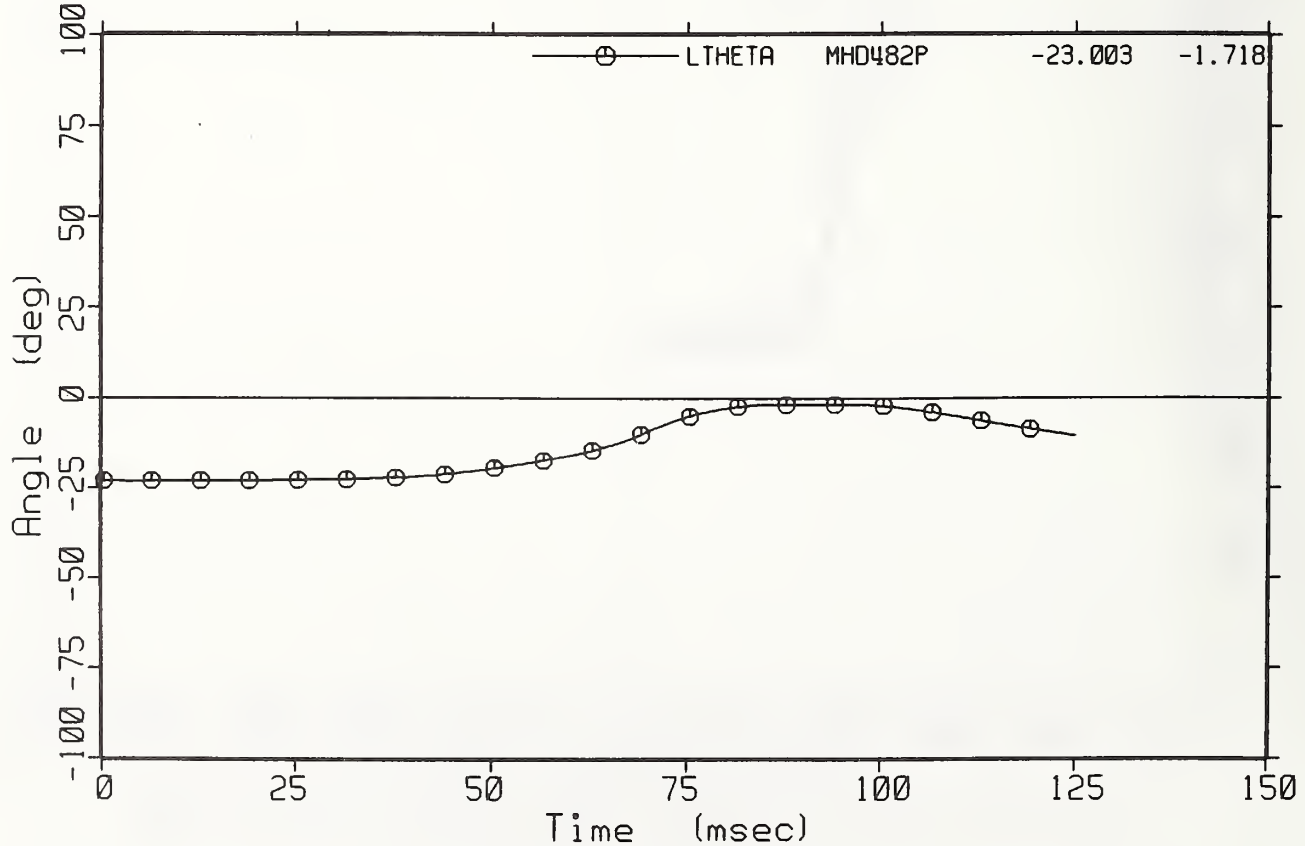

Lumbar angle

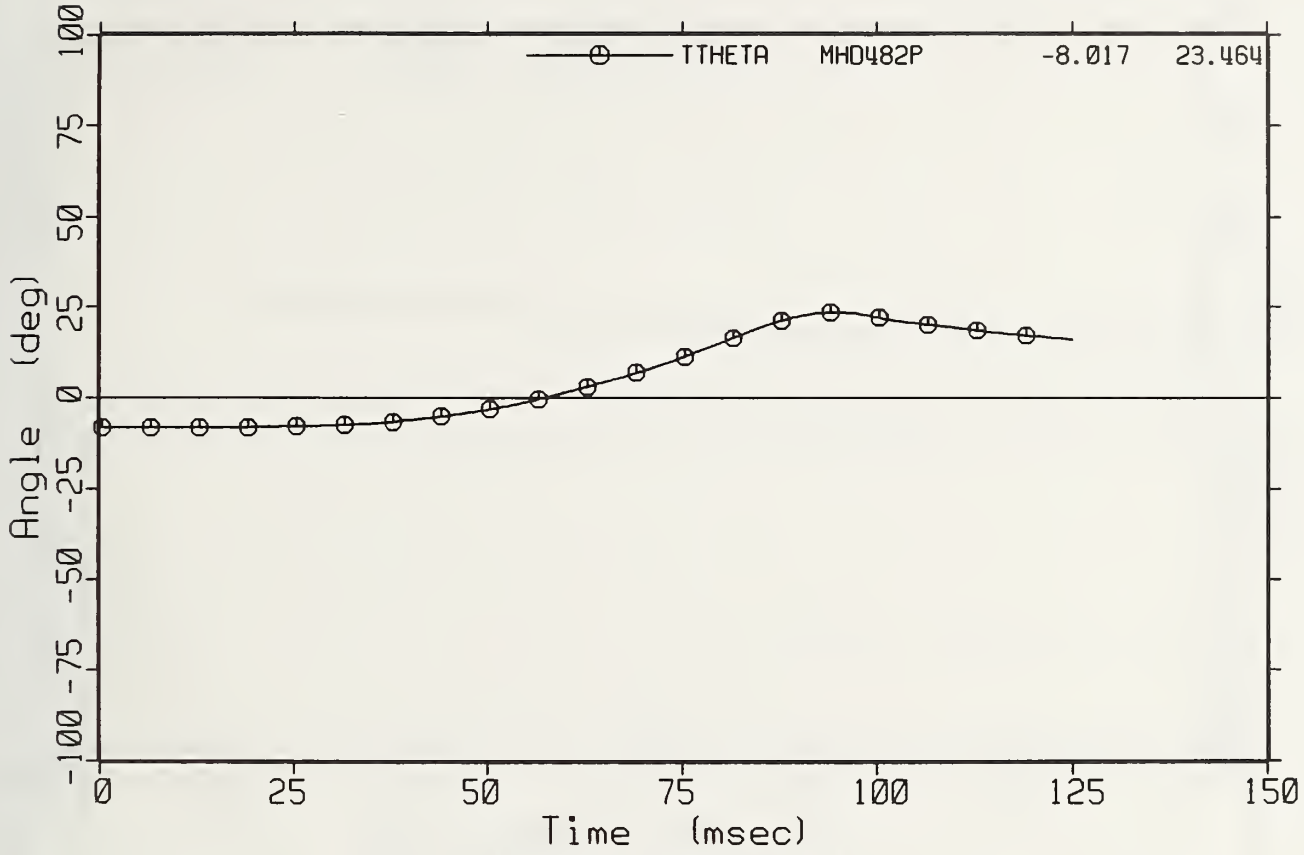

Thoracic angle

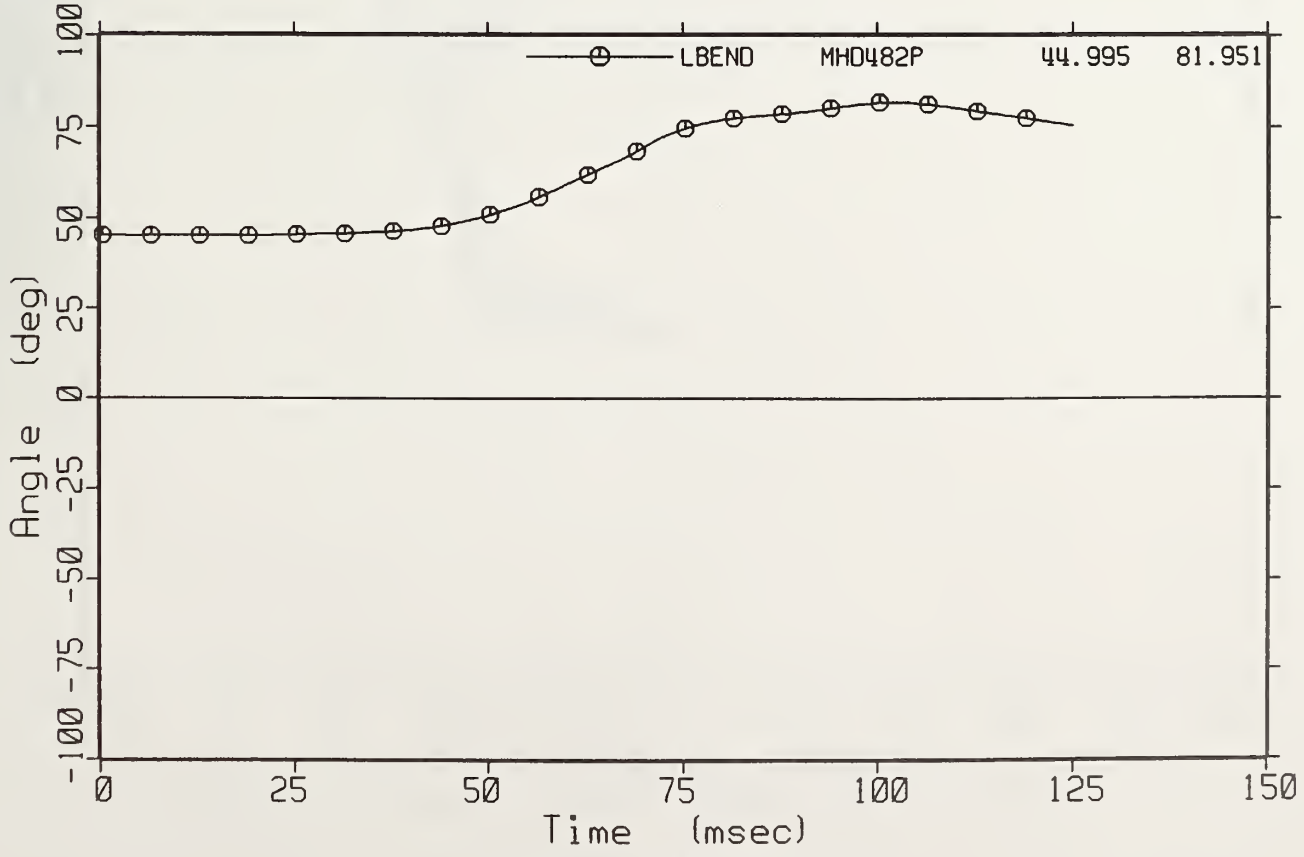

Lumbar bending

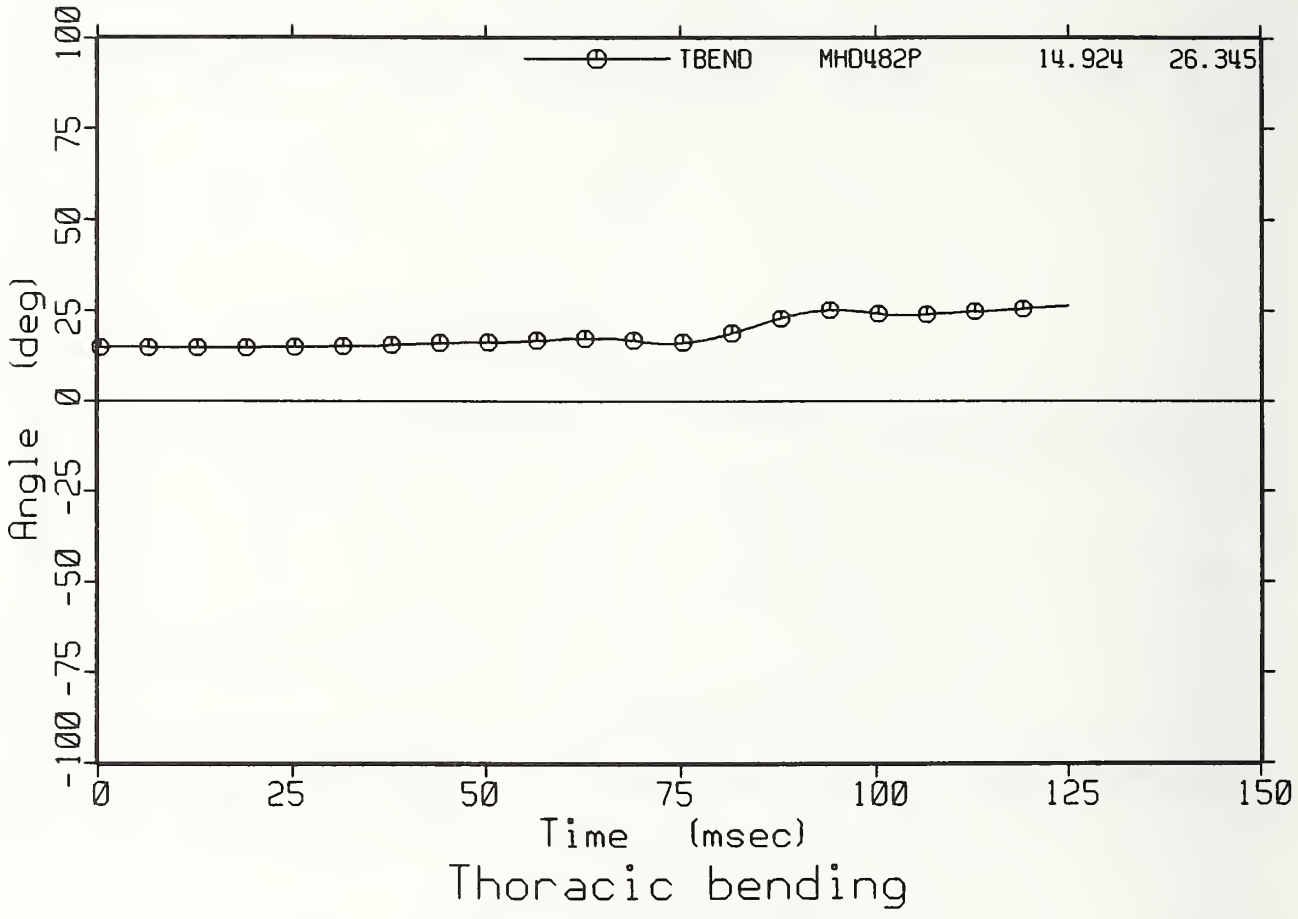

Thoracic bending

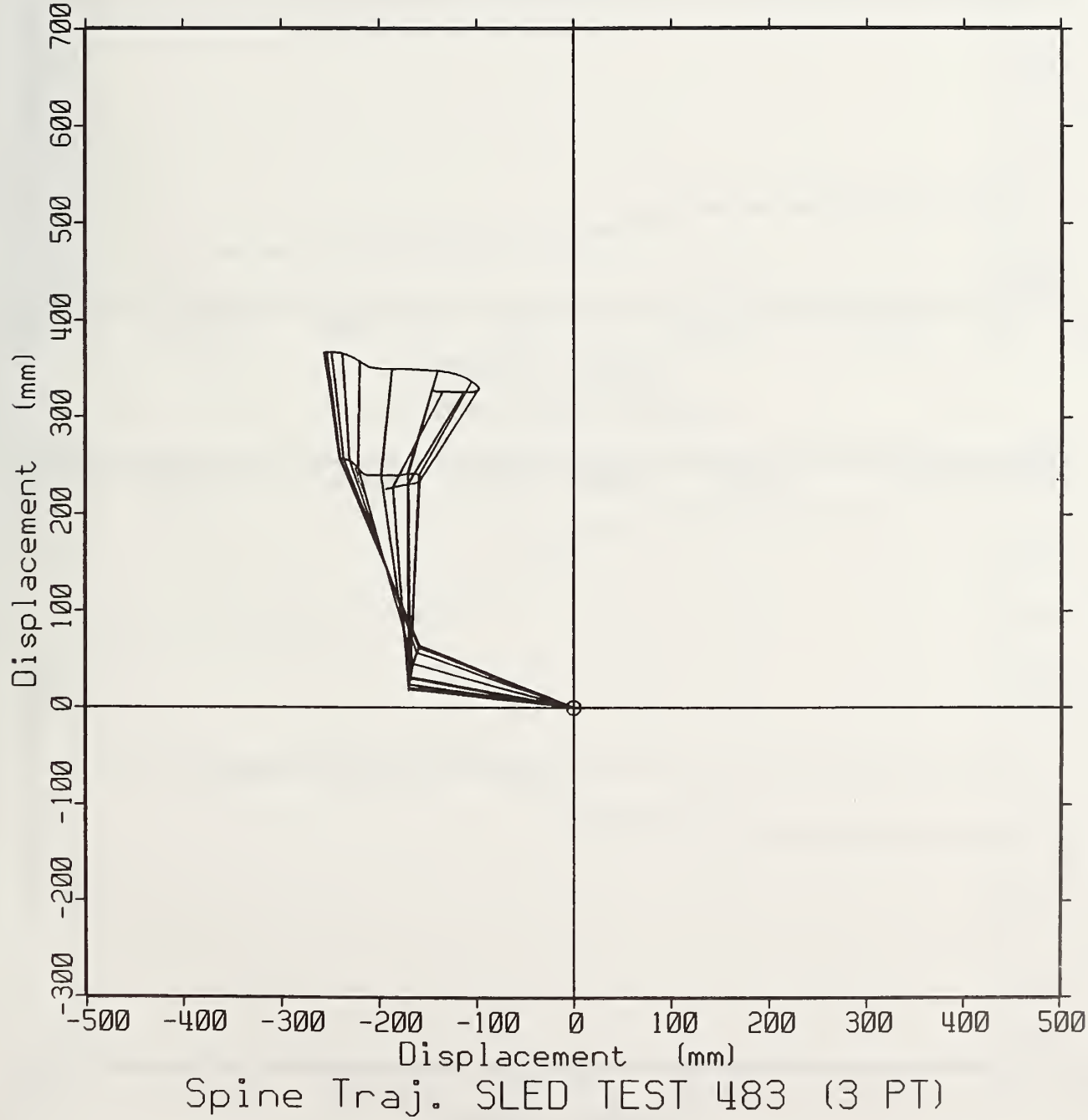

Spine Traj. SLED TEST 483 (3 PT)

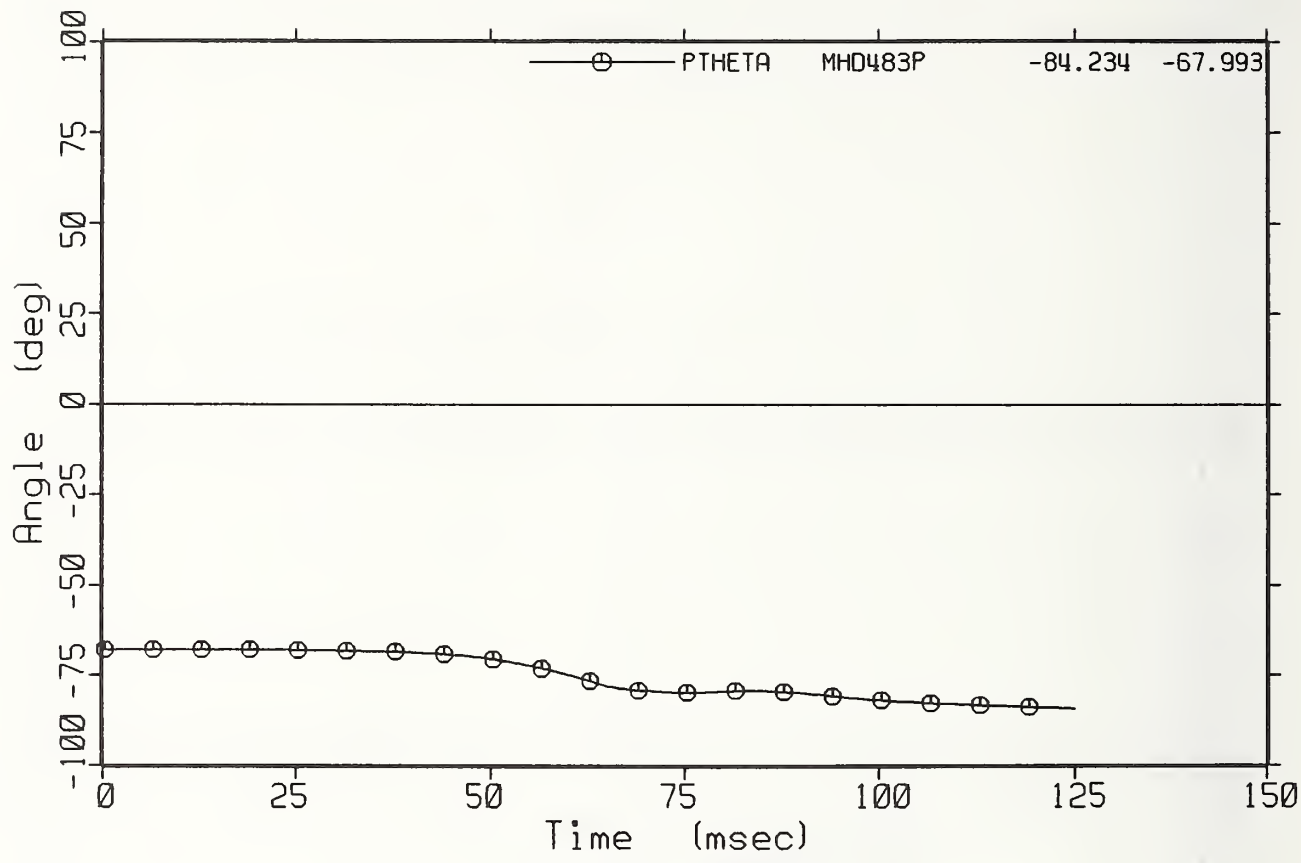

Pelvis angle

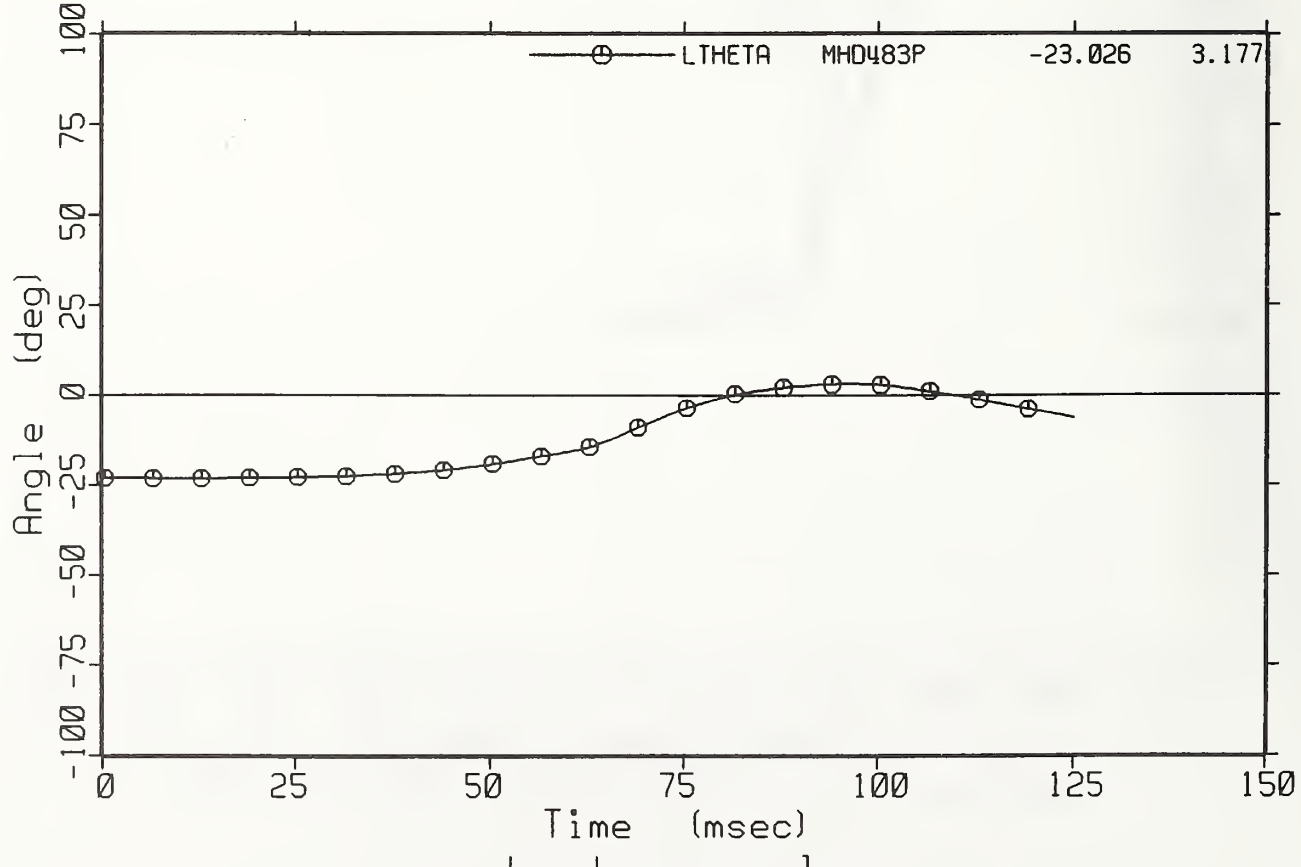

Lumbar angle

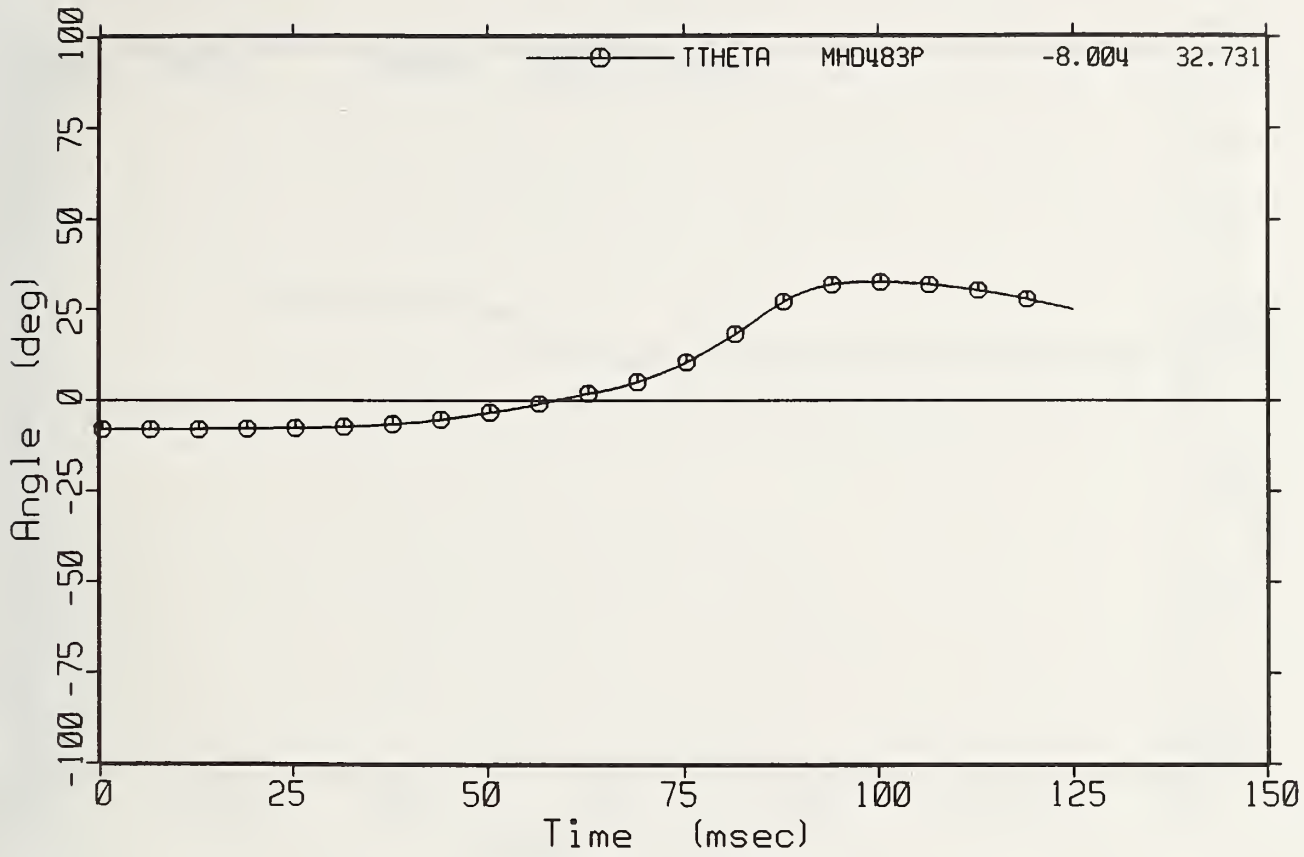

Thoracic angle

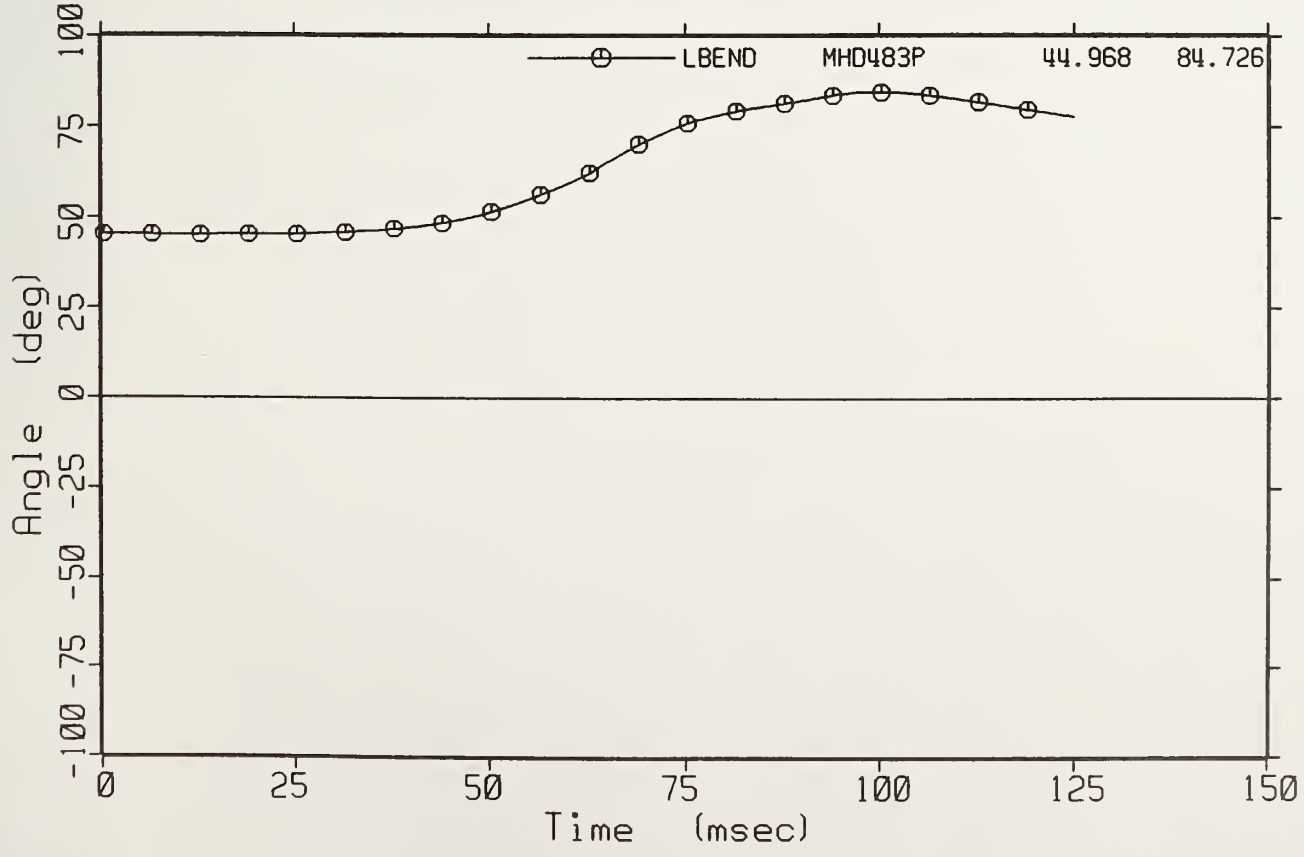

Lumbar bending

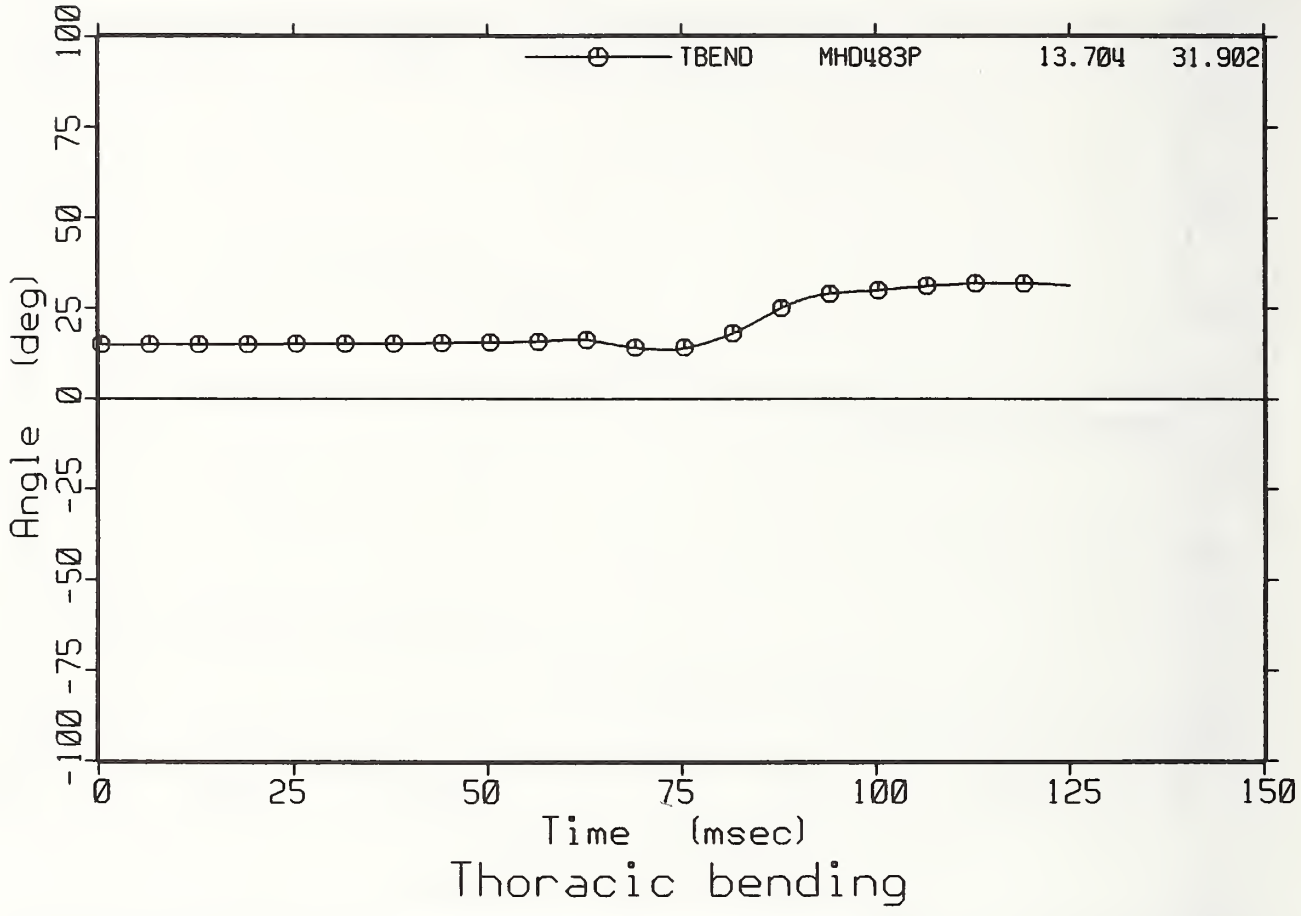

Thoracic bending